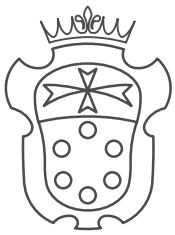

SCUOLA
NORMALE
SUPERIORE

Classe di Scienze

Corso di perfezionamento in
Metodi computazionali e modelli matematici per le scienze e la finanza

XXXV ciclo

Turbulence Enhancement of Coagulating Processes

Settore Scientifico Disciplinare **MAT/06**

Candidato
dr. Andrea Papini

Relatore
Prof. Franco Flandoli

Supervisione
Dott.ssa Alessandra Caraceni

Anno accademico 2022–2023

Abstract

We present and investigate the collision-coalescence process of particles in the presence of a fluid velocity field, examining the relationship between flow properties and enhanced coagulation. Our research focuses on two main aspects. Firstly, we propose a novel modeling approach for turbulent fluid at small scales, employing a Gaussian random field with non-trivial spatial covariance. Secondly, we derive rigorous partial differential equations (PDEs) and stochastic partial differential equations (SPDEs) from this model, capturing the physical characteristics of particles suspended in the fluid.

From an Eulerian perspective, we analyze a kinetic particle system subjected to environmental transport noise. Specifically, we rigorously study a modified version of Smoluchowski's coagulation equation, which incorporates velocity dependence akin to the Boltzmann equation. By utilizing techniques rooted in unbounded elliptic semigroup theory and weighted Sobolev space inequalities, we establish the existence and uniqueness of classical solutions for the case of a spatially homogeneous initial distribution.

Moreover, from a Lagrangian viewpoint, we employ this particle system to gain insights into the collision rate at a steady state for particles uniformly distributed within a medium. Considering a particle-fluid model, we perform two scaling limits. The first limit, involving the number of particles, yields a stochastic Smoluchowski-type system, with the turbulent velocity field still governed by a noise stochastic process. The second scaling limit pertains to the parameters of the noise, specifically targeting the direction associated with small-scale turbulence. This limit leads to a deterministic equation with eddy dissipation in the velocity variable. We conduct numerical simulations of this equation system and demonstrate the influence of turbulence on rain formation. Our qualitative findings reveal a steady increase in coagulation efficiency with escalating turbulent kinetic energy of the fluid. Additionally, we observe a power-law decay over time and in relation to the turbulence parameter. Furthermore, we recover fundamental laws governing the collision rate and relative velocity of moving particles in the high Stokes number regime.

Acknowledgement

Statement of originality

Hereby I declare that this thesis is my original authorial work, which I have worked out on my own. All sources, references, and literature used or excerpted during elaboration of this work are properly cited and listed in complete reference to the due source.

This thesis derived form three of my preprints and publications, namely:

- Franco, Flandoli, Ruojun Huang, and Andrea Papini. ”Smoluchowski coagulation equation with velocity dependence.” arXiv preprint arXiv:2211.06693;
- Andrea Papini, Ruojun Huang and Franco Flandoli. “Turbulence enhancement of raindrop formation: the role of eddy diffusion in velocity”.
  In: arXiv preprint arXiv:2209.14387. A;
  Accepted in Physica D: Non Linear Phenomena, Elsevier;
- Andrea Papini. “Coagulation dynamics under random field: turbulence effects on rain”. In: arXiv preprint arXiv:2111.12584.

While other preprints and publications were done during my doctoral studies, they did not found place here in this work, namely:

- Franco, Flandoli, Silvia Morlacchi and Andrea Papini. ”Effect of Transport Noise on Kelvin-Helmholtz instability”. In: arxiv.org/abs/2303.00033.
  Accepted in STUOD proceedings, Mathematics of Planet Earth, Springer;
- Franco, Flandoli, Francesco, Grotto, Andrea, Papini and Cristiano, Ricci. ”Epidemic Models as Scaling Limits of Individual Dynamics”. In: arxiv.org/abs/2007.05855;
- C.Metta, M.Fantozzi, A. Papini, M.Parton, F.Morandin, et all. ”Improving Performance in Neural Networks by Dendrites-Activated Connections”.
  In: arxiv.org/abs/2301.00924.

Pisa, September 12, 2023 In good faith, Andrea Papini 

Contents

List of Figures

List of Tables

Introduction

Coagulation processes permeate the natural world, spanning from cellular motion to atmospheric phenomena. Yet, comprehending them experimentally and mathematically poses a substantial challenge. Motivated by the key problem of clouds formation and rain precipitation, this thesis embarks on a quest to address and describe fundamental inquiries: Does a turbulent velocity field within the atmosphere amplify the coagulation of minuscule rain droplets, thereby promoting rainfall? Furthermore, if such enhancement occurs, how can we precisely quantify it, accounting for both Eulerian and Lagrangian dynamics of the fluid and particles?

Cloud formation and precipitation development are intricately intertwined processes influenced by both macro-scale and micro-scale phenomena. On the macro-scale, the fluid motion of air in relation to clouds plays a significant role, while on the micro-scale, processes such as condensation, stochastic coalescence, and evaporation of water droplets come into play. Hence, it can be inferred that cloud formation and precipitation development represent quintessential examples of multiscale-multiphysics phenomena.

Extensive literature in the field of physics has addressed this topic, with notable contributions dating back as early as the work of Saffman-Turner in the 1950s [78]. Additional studies by researchers such as [29, 75, 80], to name a few, have also provided substantial evidence supporting both the notion of coagulation enhancement and the selection of crucial quantities to measure the phenomena.

As shown in [88] and from seminal works of [52] and [80], we can boil down to three main contributions of a turbulent flow in the collision-coalescence process of droplets in a cloud. First, in localized regions of the flow where air streamlines experience significant curvature and change (e.g. areas with high vorticity), the distribution of droplets becomes nonuniform due to their finite inertia [25, 75]. Second, the unstable velocity field influences the relative velocity between colliding droplets, typically exceeding the terminal velocity due to gravitation observed in still air [1, 78]. Consequently, this nonuniform density and enhanced velocity difference may result in notably higher collision rates on average [64, 75, 90]. Lastly, turbulence also alters the hydrodynamic interactions and thus the collision efficiencies between droplets at a local level. This follows from the changes in both the relative distance between droplets and their distribution, influenced by the turbulent flow characteristics across different ranges of length and time scales, more so exceeding the one represented by the droplets themselves, see [88] and references therein.

Outline of the dissertation

The thesis will mostly concern the collision rate of coagulating particles and related statistics, as we investigate the impact of these flow fields on the relative velocity of inertial particles within an airflow. The study will rigorously examine their effect in the limiting regime of motion, while also providing heuristic insights for future advancements towards an extended unified theory. Additionally, we will explore the phenomenon of mass dislocation during the time evolution of the Eulerian system. Furthermore, we will assess the theoretical well-posedness of the derived equation governing the particles' density.

Chapter 1 serves as a preliminary to the dissertation, where we delve into the fundamental concept of collision rate and explore various modeling approaches known in the literature from both Lagrangian and Eulerian perspectives. We examine the behavior of particles in a flow, distinguishing between tracers and inertial particles. A novel modeling of fluid velocity is proposed, leading to a mean field equation for tracer particles akin to the classical Smoluchowski equation. One possible construction is explained in detail in Appendix A. However, we discover numerically that while this construction exhibits the anticipated enhancement diffusion and coagulation at the Lagrangian level with a hard sphere collision kernel, such effects are absent when transitioning to the density function of droplets. Consequently, without the use of averaged reasoning on the collision rate completely detached from the density equations, we realize the need for a change in perspective and employ a rigorous approach to derive the equation for particle density. To achieve this, as shown in Chapters 2 and 4, we shift our focus to inertial particles, which naturally capture these phenomena, and employ a heuristic construction of a scaling limit that yields a new Smoluchowski equation with velocity components featuring eddy diffusivity.

Building upon this reasoning, Chapter 2 details the development of a set of equations for particle density based on the aforementioned scaling limit. Within this system, we successfully recover the relative velocity of inertial particles in a turbulent fluid and the collision rate, assuming a uniform distribution of particles. Additionally, we conduct numerical investigations into the mass displacement during the temporal evolution, providing derivations for the steady state density, total system mass, and their dependence on the turbulent kinetic energy of the fluid.

In Chapter 3, we explore the potential for modifying our model to overcome limitations associated with the Stokes number regime of our particles, focusing on two-point motion statistics. This chapter presents preliminary results and conjectures regarding an effective formulation for the relative velocity and collision rate of inertial particles. Our aim is to develop an approach that not only satisfies the known limiting regime but also allows for the expression of dependence on the selected fluid model. Further exploration of this topic is expected in future works.

Lastly, in Chapter 4, we rigorously study the one-point motion system derived in Chapters 2 and 3, which specifically involves a homogeneous in space Smoluchowski equation with velocity components. However, it is important to note that while this equation bears resemblance to a multi-species Boltzmann equation, it lacks the same symmetry, boundedness, and conserved quantities. Consequently, the problem of establishing the existence and uniqueness of classical solutions becomes more complex. To address this

challenge, we employ a range of techniques from unbounded elliptic semigroup theory, ad hoc mollification and cancellation techniques in the uniqueness theorem and weighted Sobolev space inequality. These tools enable us to recover classical solutions for the equation and resolve the aforementioned issues.

Key quantities: two kind of particles

Rainfall is a vital component of the Earth's hydrological cycle, and understanding the processes that lead to the formation and growth of raindrops is of great importance in meteorology and atmospheric science. In the atmosphere, raindrops originate from tiny suspended particles called cloud droplets, which undergo a complex series of interactions and transformations to become precipitation. One key process involved in this transformation is coagulation, which refers to the collision and subsequent merging of cloud droplets to form larger raindrops. Coagulation plays a crucial role in the growth of raindrops within clouds. Understanding the coagulation rate, or the rate at which cloud droplets coalesce, is essential for predicting the growth and intensity of rainfall events, as well as for improving weather forecasting models.

Understanding the mechanisms by which turbulence enhances collision rates has made significant progress in recent years [25, 26, 64, 75, 90], yet a foundational construction of the quantities at play remains an open question.

In this chapter, we discuss mathematical concepts related to the formation and growth of raindrops, specifically focusing on the coagulation rate and the time of raindrop formation.

We start introducing two points of view that will be intertwined: a Lagrangian and a Eulerian modeling. Starting from a particle system approach we derive the construction of fundamental quantities and, from a new model for the continuum density a way to compute them and compare them, in a later Chapter, with classical results in the literature.

We start with defining an equation of motion for suspended particles in a flow, idealized as a spherical object with a density satisfying $\phi_p >> \phi_f$, where ϕ_p and ϕ_f are the densities of the particles and fluid respectively. In this regime, The Stokes Law describes the motion and we have

$$\dot{X}(t) = V(t), \quad \dot{V}(t) = \frac{1}{\tau_p}\left(u(t, X(t)) - V(t)\right) \tag{0.0.1}$$

where

$$\tau_p = \frac{2r^2\phi_p}{9\nu\phi_f},$$

is the particle relaxation time and X and V represent position and velocity of the particles. From this system, we derive the dimensionless parameter

$$St := \tau_p/\tau_U,$$

called Stokes number, where τ_U is the Kolmogorov response of the fluid, that completely characterizes the inertia of particles. We note that 0.0.1 reduces to a passive scalar model when $St \to 0$.

In principle, defining the concept of collision rate appears as a straightforward exercise in gas-kinetic theory, but in reality, it is a complex problem concerning the number of active variables and the complex dynamic of the system.

Imagining the particle as sphere-like objects, we describe the rate of collection for droplets moving in a flow, as in [25], by its fundamental unit: the collection kernel of two colliding particles

$$\Gamma = 4\pi R^2 |v_{r_1} - v_{r_2}| E(r_1, r_2),$$

where R is the sum of the droplets radii of the colliding pair r_1 and r_2, v_{r_1} and v_{r_2} are the velocity of each droplet, and E is the collection efficiency, which is the product of the collision efficiencies and the two-point correlation function. This general formulation is deduced considering the rate at which the separation line between the center of mass of the two particles crosses a disk of radius R, making the kernel proportional to the area of the spherical surface swept in a unit of time, hence the proportionality on the relative velocity of the particles.

In the classical theory, [87], reducing the active variable only to the mass m of the particles, we expect the collision rate $\mathcal{R}$ to be a function of just m, with a dimension of $[\mathcal{R}] = T^{-1}$, to be dependent on the collision kernel of two single droplets, where the relative velocity of the pair $|v_{r_1} - v_{r_2}|$ is approximated as a function of the radii, and proportional to the number density f_m of particles in the suspension.

In the discrete setting of masses being indexed by $\mathbb{N}$, we then obtain the classical rate of collision

$$\mathcal{R}_m := \sum_{n=1}^{\infty} \Gamma(m, n) f_n \tag{0.0.2}$$

where f_n is obtained as the mean field solution from the particle system 1.1.1, and is the classical solution of the Smoluchowski equation [83] with kernel Γ

$$\frac{\partial}{\partial t} f_m = \sum_{n=1}^{m-1} \Gamma(n, m-n) f_n f_{m-n} - 2 \sum_{n=1}^{\infty} \Gamma(m, n) f_m f_n, \quad m \in \mathbb{N}$$

In this setting, usually, Γ is obtained a priori with direct numerical simulation on particles moving into fluid, or with physical reasoning of dimensional analysis, in order to reduce the kernel to be a function of mass only. See [2, 81] and references therein for further details.

However, the classical Smoluchowski approach, [83], has limitations, especially when particles undergo runaway growth, such as in raindrop formation. To address this issue, alternative approaches have been developed, including direct numerical simulation (DNS) [81, 61] and the analysis of the Lyapunov exponent of the particle system's dynamics [89, 90]. From these results, the collision rate is expected to be composed of two independent components: collisions that occur when particles follow similar trajectories due to shearing motion in the flow, and collisions between particles that deviate from the fluid path lines and are influenced by small-scale turbulence. These mechanisms contribute differently and can be combined additively.

The focus of this work is on the latter, and the construction of an effective and rigorous theory for the collision rate in the presence of turbulence, where the folding of flow

lines and particle inertia play significant roles. Thus, under the hypothesis of a turbulent velocity field, in Section 1.4 and .1 we construct a time evolution for the density of particles $f_m(\xi)$ where ξ represents the active variables of the system, maintaining both position and velocity, instead of mass alone as in 0.0.2. Hence, defining our key quantity

$$\mathcal{R}_{turb} = \sum_{m=1}^{\infty} \int \Gamma(\xi, \xi) f_m(\xi)\, d\xi,$$

explained in detail in Section 1.4, for which we prove in Chapters 2 and 3 the derivation of the typical coagulation rate as in [1, 64]. More so, we study in Section 1.2 the time of formation of a raindrop, which declined as a loss of total mass in the truncated density evolution of particles with masses $m = 1, ..., M$, representing the typical raindrop mass.

$$\tau(f.) := \inf\{t \geq 0 \mid \sum_{i=1}^{M} \int f_i(t, \xi) d\xi \leq \mathcal{M}_0\},$$

where $\mathcal{M}_0$ is a reference threshold and ξ are the set of active variables for the particles' density proposing a prime example of dependence between the turbulence parameter of the fluid and the rain shower initialization. Under the assumption of a turbulent velocity field, a time evolution for the particle density is constructed, and the coagulation rate is expressed as an integral involving the collection kernel and the particle density.

To derive this construction, we first consider a system of N tracer particles in a turbulent fluid, i.e. $\phi_p \equiv \phi_f$.

$$\dot{X}(t) = \mathcal{U}(t) \tag{0.0.3}$$

Where, at the particles level, motivated by works of Boussinesq [15] and Majda [63], the large-scale turbulent flow $\mathcal{U}$ is modelled through its small scales as a common environmental transport noise:

$$\dot{\mathcal{U}}(t, x) = \sum_{k \in K} \sigma_k(x) \dot{W}_t^k \tag{0.0.4}$$

i.e. a white noise in time with non trivial spatial covariance where $\{\sigma_k(x)\}_{k \in K}$ countable divergence-free smooth vector fields, $\{W_t^k\}_{k \in K}$ independent 1-d Brownian motions. We define the covariance matrix $\mathcal{Q}(x, x) := \sum_{k \in K} \sigma_k(x) \otimes \sigma_k(x)$ derived by easy computation on the transport-type noise.

Under suitable and natural choice $\{\sigma_k\}_{k \in K}$, i.e Kraichnan type covariance [33, 58], we have $\mathcal{Q}(x, x) \equiv \kappa I_d$, for enhanced diffusion coefficient $\kappa > 0$ (see Chapter 2, and [35] with reference therein). These particles may coalesce in an instantaneous way as soon as they get in contact with each other and We investigate numerically the behavior of the discrete equivalent of first formation time of a raindrop in cloud, i.e.

$$\tau_f := \inf\{t \geq 0 | \exists i \in \mathcal{N}_t,\ R_t^i >= R_{rd}\}, \tag{0.0.5}$$

where R_t^i is the radius of the $i - th$ particle at time t and $R_{rd} := 4 \cdot 10^{-4}$ is the radius of the typical raindrop in our simulation. While $\mathcal{N}_t$ are the surviving particles at time t, with $\mathcal{N}_t \leq N$.

In Section 1.2.4, calling κ the parameters of the turbulent flow, we derive an explicit dependence for $\tau_f := \tau_f(\kappa)$ and we are able to argue a decay of the form

$$\mathbb{E}\left[\tau_f(\kappa)\right] \sim p(\kappa)^{-1}$$

where p is a polynomial of degree at most 2. The limiting case of $deq(p) = 2$ is obtained in the case of pure Brownian particles as shown in Section 1.2.2.

This toy numerical example has a natural downside: the setting of instantaneous coalescence presents a unique challenge in studying the probability density function (PDF) of the particles. Since the objective of the thesis is to produce a theoretical framework for the coagulating process of particles in a fluid, we had to approximate our process and pass to a probabilistic rate in the coagulating dynamics.

A such, following the work of [37] and given the difficulty associated with analyzing the PDF in such cases, we directed our focus towards a scaling limit approach. In this direction, one of the main results was provided by Hammond and his collaborator [46, 48, 47], extending rigorously the Smoluchowski equation to a PDE with space variable, as a scaling limit of a particle system undergoing pairwise coagulation (with an apriori rate, dependent only on the masses).

In particular, they provided a model of time evolution probability distribution $\{f_m(t,x)\}_{m=1}^{\infty}$ of diffusing particles of different sizes $m \in \mathbb{N}$. Particles undergo pairwise coagulation with coagulation rate $\alpha(m,n)$, and their resulting equation could be read as follows

$$\begin{aligned}\partial_t f_m(t,x) =& \kappa\Delta f_m(t,x) + \sum_{n=1}^{m-1} \alpha(n, m-n) f_n(t,x) f_{m-n}(t,x) \\ & -2\sum_{n=1}^{\infty} \alpha(m,n) f_m(t,x) f_n(t,x), \quad t > 0,\ x \in \mathbb{T}^d,\ m \in \mathbb{N}.\end{aligned}$$

In this setting, particles are moved independently and subjected to Brownian motions. Indeed, this is not enough to understand the behavior of particles moving into a fluid velocity flow.

This approach allows us to gain a deeper insight into the behavior of particles and their interactions, shedding light on the underlying mechanisms that govern coagulation processes, more so, finding what does not work in the standard modelling of tracer particles and how to pass to the kinetic system.

For this reason, as an analogous of the discrete formation time τ_f (0.0.5), defined in Section 1.2 equation 1.2.1, we define τ_κ which represent the first time the total density has put enough mass on effective raindrops:

$$\tau_\kappa(f.) := \inf\{t \geq 0 \mid \sum_{i=1}^{M} \int f_i(t,x)dx \leq \mathcal{M}_0\}, \tag{0.0.6}$$

with $\mathcal{M}_0$ a positive constant.

We know that $\mathbb{E}\tau_f \to 0$ as κ^{-2}, when $\kappa \to \infty$ in the discrete system with instantaneous collision. So the question we ask is: does $\tau_\kappa(f.)$ has a behavior akin to the one displayed by the tracer particles system?

Unfortunately, the numerical results produced for the quantity 0.0.6 in Section 1.3 show an increase for $\tau_\kappa(f.)$. Specifically:

$$\tau_\kappa(f.) \nearrow T, \text{ while } \tau_f(\kappa) \searrow 0$$

as $\kappa \to \infty$ in the time frame $[0, T]$, completely going against intuition, the toy model, and physical results from experiments.

The thesis aims to verify whether enhancing diffusion leads to coagulation enhancement, specifically the increase in probability densities for large masses and a rigorous construction of the key factor explaining the dynamics underneath the coagulating process. However, the first enrichment of the model used in the program results inadequate and unable to confirm coagulation enhancement through numerical simulations.

To overcome this challenge, it is necessary to consider all relevant factors from the beginning, even if it complicates the computational process. The coagulation kernel, which describes the probabilistic interaction of moving particles, should theoretically depend on the difference in velocity between particles. However, the current approximation of the kernel, based only on masses, neglects the complexities of kinetic evolution due to turbulence, hence making difficult to use the density evolution equation to derive meaningful result [65, 75]. This omission hinders the construction of a rigorous theory, particularly regarding the final density.

There are two mathematical models for the rate of coalescence between particles: deterministic and probability rates. In the deterministic model, two particles meeting result in the creation of a new particle with a mass equal to the sum of their masses and momentum conserved. In the probability rates model, particles within a certain distance from each other have a probability per unit of time to merge.

Deterministic models demonstrate that coalescence consistently occurs at a specific distance, regardless of the time spent in close proximity. However, when considering models based on probability rates, there is a limitation in connecting them to turbulence. Coalescence happens probabilistically over time, and as the duration of interaction decreases, the probability of coalescence diminishes.

This poses a contradiction: models based on probability rates in the space-mass framework favors coalescence with slow-moving particles, contradicting the practical understanding of turbulence. To resolve this issue, it is crucial to avoid bias toward slow motion in the modeling process.

As we have already pointed out, in the field of atmospheric physics [25], the coagulation of cloud particles is commonly analyzed using a rate proportional to the relative velocity between particles. However, this factor is usually studied separately and then applied to a Spatial Smoluchowski equation, making it impossible to derive accurate coagulation dynamics directly from the density. Additionally, this factor, when multiplied by the time spent in close proximity, remains relatively constant on average, ensuring a consistent probability of coalescence.

To address these limitations and incorporate both position and velocity variables, a new system of inertial particles is introduced in Sections 1.4 and .1.

From 0.0.1, we construct a particle system, indexed by the number of particles $N \in \mathbb{N}$. For each $N \in \mathbb{N}$, $T \in (0, \infty)$ and $m \in \{1, .., M\}$, we denote the process of empirical

measure on position and velocity of mass-m particles in the system by

$$\mu_t^{N,m}(dx,dv) := \frac{1}{N}\sum_{i\in\mathcal{N}(t)} \delta_{x_i^N(t)}(dx)\delta_{v_i^N(t)}(dv)1_{\{m_i^N(t)=m\}} \in \mathcal{M}_{1,+}(\mathbb{T}^d\times\mathbb{R}^d)$$

where $\mathcal{M}_{1,+} := \mathcal{M}_{1,+}(\mathbb{T}^d\times\mathbb{R}^d)$ denotes the space of sub probability measures on $\mathbb{T}^d\times\mathbb{R}^d$ equipped with weak topology while x_i and v_i denote position and velocity respectively of the ith particle.

Heuristically we show that the laws of the collection of $\mathcal{D}_T(\mathcal{M}_{1,+})^M$-valued random variables $\{\mu_t^{N,m} : t\in[0,T]\}_{m=1}^M$, $N\in\mathbb{N}$, is tight hence weakly relatively compact. Consider any weak subsequential limit

$$\{\mu_t^{N_\ell,m} : t\in[0,T]\}_{m=1}^M \overset{\ell\to\infty}{\to} \{\overline{\mu}_t^m : t\in[0,T]\}_{m=1}^M. \tag{0.0.7}$$

Where $\overline{\mu}_t^m$ solvers in the weak formulation the SPDE system

$$\begin{cases} df_m(t,x,v) = & \left(-v\cdot\nabla_x + c(m)\mathsf{div}_v\,(v\cdot) + \kappa c(m)^2\Delta_v\right) f_m(t,x,v)dt \\ & -c(m)\sum_{k\in K}\sigma_k(x)\cdot\nabla_v f_m(t,x,v)dW_t^k \\ & +\sum_{n=1}^{m-1}\int_{\{nw'+(m-n)w=mv\}} s(n,m-n)|w'-w| \\ & \qquad\times f_n(t,x,w')f_{m-n}(t,x,w)dwdw'dt \\ & -2\sum_{n=1}^M\int s(n,m)|v-w|f_m(t,x,v)f_n(t,x,w)dwdt \\ f_m(\cdot,x,v)|_{t=0} = & f_m^0, \quad m=1,...,M. \end{cases} \tag{0.0.8}$$

From this, in Chapter 2, we derive the deterministic Smoluchowski coagulation equation with both velocity and position as active variable. Now the enhanced diffusion due to the small scale turbulence of the fluid act on the coagulation process, giving a rigours construction, at least in the mono-disperse case, for the coagulation rate. In fact, limiting for clarity on mass of type 1, we get at the level of particles

$$\int_{t_0}^{t_0+\Delta t}\sum_{i\neq j}\lambda\left(X_t^i,X_t^j,V_t^i,V_t^j\right)\mathbb{1}_{\{m_t^i=1\}}\mathbb{1}_{\{m_t^j=1\}}\phi(X_t^i,X_t^j)ds \tag{0.0.9}$$

this is the number of collision of particle of mass $m=1$, in the volume Q (i.e. taking $\phi=\mathbb{1}_Q$) in the unit time Δt.

That reads out, for the density function as

$$\mathcal{R}_{turb}\sim\mathcal{N}_1(t_0)\int_{t_0}^{t_0+\Delta t}\iint\iint\lambda(x,y,v,w)\phi(x,y)f_t(x,v,y,w)\,dxdv\,dydw\,dt, \tag{0.0.10}$$

where the quantity $\mathcal{N}_1(t_0)$ is the number density of type 1.

This framework is the baseline to construct a rigorous theory that, from simple mathematical equation can naturally give rise to all the fundamental quantity of rain coalescence. As such, this will be the main system analyzed throughout the following Chapters.

Turbulence enhancement of coagulation

Following the discussion of Chapter 1, we have substantial clue to conclude that turbulence increases the relative velocity of particles suspended into a fluid, favours their collision and thus increases the collision rate. Motivated by the last result of the previous chapter, we investigate inertial particles and their density evolution under the action of an environmental noise capturing the turbulent kinetic energy of the fluid.

To this end, an identified key factor of the collision rate, precluded in the tracer modelling, is the average relative velocity between particles of mass m_1 and m_2:

$$R_{m_1,m_2} = \langle |\mathbf{v}_1 - \mathbf{v}_2| \rangle \,. \tag{0.0.11}$$

This quantity is of major importance since it relates the properties of particles and fluid to the intensity of the aggregation and thus it has been extensively investigated in several works, based on various arguments and models of turbulence, see for instance [1, 7, 19, 20, 25, 26, 45, 64, 73, 75, 76, 78, 81, 84, 88, 90, 93].

We propose a new modeling approach here. Many ingredients are classical, like the fact that we use an *inertial model* for particle motion (instead of a model when particles are transported). In particular, droplets in clouds or dust particles in gasses near young star have densities, ϕ_p, which are larger than the density of the fluid ϕ_f.

As such, in this thesis we analyze setting in which $\phi_p/\phi_f >> 1$. This way, the inertia of the particles is usually large enough to help them from not following exactly the flow' lines. In this regime [24], the dominant force acting on small particles is due to viscous drag, which causes the particle velocity to slow the motion in the same direction of the fluid velocity. Thus, the equations of motion for each of the small particles follow the Stokes' law

$$\frac{d\mathbf{x}}{dt} = \mathbf{v}, \qquad \frac{d\mathbf{v}}{dt} = \gamma \left(\mathbf{U}\left(t, \mathbf{x}\right) - \mathbf{v} \right) \tag{0.0.12}$$

(here γ is the damping coefficient and $\mathbf{U}\left(t, \mathbf{x}\right)$ is the fluid velocity).

We note here that in setting in which concentration of particle is too close to the fluid density, i.e. $\phi_p/\phi_f \sim 1$, we need to consider the history of the particles' motion, modifying the acting forces on the system and we postpone this analysis to future studies.

At the level of the density for different masses, following the reasoning on the scaling limit of the particle system showed in Chapter 1, we obtain a *Smoluchowski equation* with a kernel depending on the relative velocity $|\mathbf{v} - \mathbf{v}'|$ to describe macroscopically the system. The novelty is that we introduce a Boussinesq hypothesis, namely the fact that a small-scale turbulence acts on particles as a dissipation. And the key feature is that it acts as a *dissipation in the velocity component*, namely it spreads the distribution of particles in velocity (not or not only in space). This spread increases in a quantifiable way the value of R_{m_1,m_2} and thus the collision rate.

In order to describe the equations we use and the results, let us recall a few quantities associated to the particles and to the fluid. The damping coefficient γ appearing in equation (0.0.12) is given by Stokes' law $\frac{6\pi r\mu}{m}$ where r, m are the particle radius and mass and μ is the dynamic viscosity of the fluid. If we denote by τ_P and $\tau_{\mathbf{U}}$ the relaxation times of the particle and of the fluid respectively, we have $\gamma = \tau_P^{-1}$ and we define the Stokes number as $St = \tau_P/\tau_{\mathbf{U}} = 1/\left(\gamma\tau_{\mathbf{U}}\right)$. When we want to stress the dependence of the damping coefficient γ from the mass m, we write γ_m; and similarly for St_m. Two relevant

quantities of the fluid for our study are the turbulence kinetic energy $k_T = \frac{1}{2}\left|\overline{\mathbf{U}}\right|^2$ and the turbulent viscosity $\nu_T = \tau_{\mathbf{U}} k_T$. Our model, inspired by Kraichnan fundamental work [58], is based on the idealization that the turbulent small-scale fluid is white noise in time, space-homogeneous, with intensity σ (precisely, as a vector field, its space-covariance matrix $C(\mathbf{x})$ is assumed to have the auto-covariance $C(\mathbf{0})$ equal to $\sigma^2 I_d$, with d dimension of the spatial domain and I_d the identity matrix). As explained in all details in the Appendix .2, the link between these fluid quantities is

$$\frac{\sigma^2}{2} = \frac{2}{d}\tau_{\mathbf{U}} k_T = \frac{2}{d}\nu_T. \tag{0.0.13}$$

Indeed, in [1] the energy dissipation rate is expressed as $\varepsilon \sim k_T/\tau_{\mathbf{U}}$, clear from the energy balance of Navier-Stokes equation, and since all three quantities correspond to the turbulent fluid:

$$\frac{\partial}{\partial t}\left(\frac{1}{2}|\mathbf{U}|^2\right) = -\varepsilon + \text{lower order terms},$$

from which is possible to derive the link with our spatial covariance matrix.

The first main result of our work is that we derive the following Smoluchowski-type system for the particle densities of masses $m = 1, 2, ...$

$$\begin{aligned} &\frac{\partial f_m(t,\mathbf{x},\mathbf{v})}{\partial t} + \mathbf{v}\cdot\nabla_x f_m(t,\mathbf{x},\mathbf{v}) - \gamma_m \operatorname{div}_v\left(\mathbf{v} f_m(t,\mathbf{x},\mathbf{v})\right) \\ &- \frac{\gamma_m^2\sigma^2}{2}\Delta_v f_m(t,\mathbf{x},\mathbf{v}) = \left(\mathcal{Q}_m^+ - \mathcal{Q}_m^-\right)(\mathbf{f},\mathbf{f})(t,\mathbf{x},\mathbf{v}) \end{aligned} \tag{0.0.14}$$

where $\mathbf{f} := (f_1, f_2, ...)$, $\mathbf{x} \in \mathbb{T}^d$ (the d-dimensional torus), $\mathbf{v} \in \mathbb{R}^d$ and the collision kernels are given by

$$\begin{aligned} \mathcal{Q}_m^+(\mathbf{f},\mathbf{f})(t,\mathbf{x},\mathbf{v}) := \sum_{n=1}^{m-1} \iint_{\{n\mathbf{v}'+(m-n)\mathbf{v}''=m\mathbf{v}\}} s_{n,m-n} \\ \cdot|\mathbf{v}'-\mathbf{v}''| f_n(t,\mathbf{x},\mathbf{v}') f_{m-n}(t,\mathbf{x},\mathbf{v}'') d\mathbf{v}' d\mathbf{v}'', \end{aligned} \tag{0.0.15}$$

$$\begin{aligned} \mathcal{Q}_m^-(\mathbf{f},\mathbf{f})(t,\mathbf{x},\mathbf{v}) := 2 f_m(t,\mathbf{x},\mathbf{v}) \sum_{n=1}^{\infty} \int s_{n,m} \\ \cdot|\mathbf{v}-\mathbf{v}'| f_n\left(t,\mathbf{x},\mathbf{v}'\right) d\mathbf{v}' \end{aligned} \tag{0.0.16}$$

with $s_{n,m}$ defined in (2.2.1) below.

This equation proposes a change of viewpoint. In previous works, the central problem was determining the correct collision kernel which takes into account the fact that the fluid is turbulent. Here we use the original collision kernel depending on the relative velocity $|\mathbf{v}-\mathbf{v}'|$, without modifying its coefficients, but incorporate the presence of a small-scale turbulent background by adding the dissipative operator in the velocity variable. Collision and aggregation is not due to a stronger collision kernel, in this model, but to the spread-in-$\mathbf{v}$ of densities, produced by the additional diffusion term.

The derivation of this Smoluchowski-type system is explained in Sections 2.4 and 2.5 of this chapter, as well as in Chapter 1. This derivation is heuristic but reasonable in analogy with rigorous results proved recently for other models [35, 33, 42]. From the viewpoint

of the Physical validity of the result, let us stress that the rigorous proof would require very small $\tau_{\mathbf{U}}$, with γ_m having a finite limit. Therefore St must be large.

We analyze this new model both using approximate analytical computations and numerically. In Section 2.6 we prove, up to some approximation, the formula

$$R_{m_1,m_2} = \frac{2}{\sqrt{\pi}}\sqrt{\gamma_{m_1}+\gamma_{m_2}}\sigma = \frac{4}{\sqrt{3\pi}}\sqrt{\frac{k_T}{St_{m_1}}+\frac{k_T}{St_{m_2}}}, \tag{0.0.17}$$

in the physical dimension $d = 3$. In the large St regime, which is the regime of validity of our results, this formula confirms known results (see the discussion in [90]) and it is known as the gas-kinetic model, after [1]. Let us notice that it is obtained without any use of dimensional analysis; it is derived from basic equations, except for the stochastic model of the turbulent fluid.

In order to approximate analytically the average value $\langle|\mathbf{v}_1 - \mathbf{v}_2|\rangle$ of the relative velocity (0.0.11), we adopt the mean field viewpoint of Smoluchowski equations, where particles are independent. Therefore, if $p_m(\mathbf{v})$ is the normalized density $f_m(\mathbf{v}) / \int f_m(\mathbf{w})\, d\mathbf{w}$ of velocity of mass m, solution of Smoluchowski equation, we have

$$R_{m_1,m_2} = \iint |\mathbf{v}_1 - \mathbf{v}_2|\, p_{m_1}(\mathbf{v}_1)\, p_{m_2}(\mathbf{v}_2)\, d\mathbf{v}_1 d\mathbf{v}_2. \tag{0.0.18}$$

However, to avoid a dependence on the initial conditions, we consider, in the Smoluchowski system, the linear terms

$$\gamma_m \operatorname{div}_v(\mathbf{v} f_m(\mathbf{v})) + \frac{\gamma_m^2\sigma^2}{2}\Delta_v f_m(\mathbf{v})$$

associated with the transient phase that moves the initial distribution towards a certain limit shape. In this regime, the nonlinear terms (0.0.15) shift mass from lower to higher levels, but their impact on the modification of shape is minor.
Therefore we take, $f_m(\mathbf{v}) / \int f_m(\mathbf{w})\, d\mathbf{w}$ as the invariant distribution of the linear part, which is a centered Gaussian with covariance matrix $\frac{1}{2}\gamma_m\sigma^2 I_d$ (I_d is the identity matrix), which lead us to the fundamental formula (0.0.17). This founding are also supported with numerical result on the steady state solution of the Smoluchowski system, as shown in 2.7.

We stress here that it is not immediately clear if we may modify our approach to incorporate the concentration effects related to singularities described in [25, 64, 90] directly in the relative velocity (0.0.11), or if this effect must be study in relation to the particle density and, as such, the full collection kernel.

In Section 2.7, finally, we investigate numerically the Smoluchowski equations, quantifying in various ways the efficiency of aggregation of the turbulence model.

To this end, we define

$$\mathcal{M}_1^{\sigma}(t) := \sum_{m=1}^{M} m \int f_m(t,\mathbf{v})\, d\mathbf{v}\,, \tag{0.0.19}$$

which we also call “total mass” for simplicity.

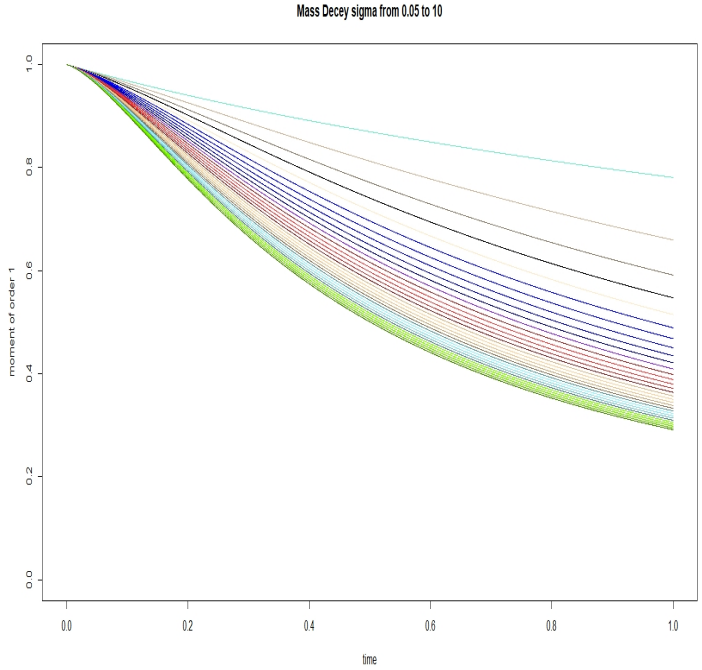

Figure 1: Decay of $\mathcal{M}_1^\sigma(t)$ for $t \in [0,1]$, with $M = 3$, initial density $f_1(0,\mathbf{v})$ for $m = 1$ concentrated on the set $\mathbf{v} \in [-1/2, 1/2]$. Parameter σ^2 ranges in the set 0.05 to 10 (around 30 points). A visible increase in coagulation is present at the increase of σ^2.

This function represents the total mass present in the system, at a given time t, respect to a threshold $M > 0$ representing the mass level in which particles leave the system, i.e. fall out of the cloud as rain. Indeed, analyzing the non linearity of our PDE, we notice that

$$\sum_{m=1}^{M} \int m(\mathcal{Q}_m^+ - \mathcal{Q}_m^-)\, d\mathbf{v} \leq 0, \quad \forall t \tag{0.0.20}$$

implying that $d\mathcal{M}_1^\sigma(t)/dt \leq 0$ and so (0.0.19) is non-increasing in time. Notice that for the infinite system $M = \infty$, equality is achieved in (0.0.20), hence the mass deficiency in the finite system is not lost at all and it is simply sent to higher order of mass-type densities that are not analyzed in the closed system and thus can be interpreted as rain precipitation.

With a semi implicit method we solve numerically equation (0.0.14). Thanks to results on fast decay at infinity, showed in Chapter 4, we compute the total mass showing enhancement coagulation in Figure 1.

The second quantity we consider is closely linked to the enhanced coagulation due to turbulence that we will establish with the "total mass" and gives more quantitative information. Specifically, let

$$m_0^T := \inf_{t\in[0,T]} \mathcal{M}_1^0(t)$$

and define a sequence of "barrier exit times" $(\tau_\sigma)_{\sigma\geq 0}$

$$\tau_\sigma := \inf\left\{t \geq 0,\, \mathcal{M}_1^\sigma(t) \leq m_0^T\right\} \wedge T. \tag{0.0.21}$$

Since $t \mapsto \mathcal{M}_1^0(t)$ is decreasing, we have that $\tau_0 = T$. This exit time represents the first moment in which the total mass $\mathcal{M}_1^\sigma(t)$ drops below a certain level respect the turbulence parameter σ. Since $\mathcal{M}_1^\sigma(t)$ is expected to decay faster as σ increases, $\sigma \mapsto \tau_\sigma$ should be decreasing, as shown in Figure 2.

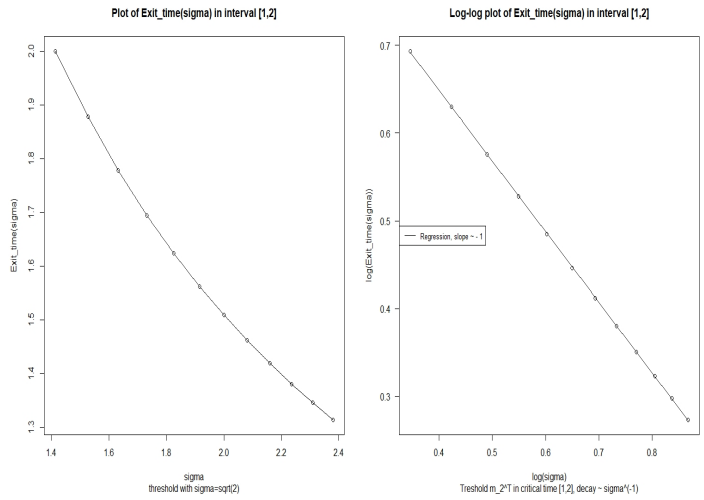

Figure 2: $M = 1$; A plot of the barrier exit time τ_σ with respect to the turbulence parameter σ, and the corresponding log-log regression in the time window $[0, 2]$, taking into consideration only those exit times in the interval $[1, 2]$, yields $\tau_\sigma \propto \sigma^{-1}$.

We conjecture that the function (0.0.19) can be expressed as (for t suitably large, say $t > 1$ in our simulations)

$$\mathcal{M}_1^\sigma(t) \sim \frac{1}{A_d(\sigma)t + \mathcal{M}_1^\sigma(0)^{-1}}, \tag{0.0.22}$$

for some function A_d that depends on dimension d, and that $A_1(\sigma) \propto \sigma$, the turbulent kinetic energy of the fluid.

A rough explanation of the numerical findings exploring different M and initial conditions, is the following one. When $M = 1$, the density $f(t, \mathbf{v})$ of the unique level $m = 1$ satisfies the identity

$$\frac{d}{dt}\int f(t,\mathbf{v})\, d\mathbf{v} = -\iint \left|\mathbf{v} - \mathbf{v}'\right| f(t,\mathbf{v})\, f\left(t,\mathbf{v}'\right) d\mathbf{v}d\mathbf{v}'$$

because the differential terms cancel by integration by parts. Up to a small approximation, near the steady state of the linear operator,

$$f(t,\mathbf{v}) \sim \alpha(t)\, f_0(\mathbf{v})$$

namely the decay of $f(t, \mathbf{v})$ is self-similar [23]. Then $\alpha' = -\sigma_0\alpha^2$ where

$$\sigma_0 = \iint \left|\mathbf{w} - \mathbf{w}'\right| f_0(\mathbf{w})\, f_0\left(\mathbf{w}'\right) d\mathbf{w}d\mathbf{w}'$$

is an average variation of velocity under f_0, namely

$$\alpha(t) \sim \frac{1}{\sigma_0 t + C}$$

after an initial transient period. Moreover, under this hypothesis the standard deviation of f_0 near the steady state is σ (since the dispersion produced by the linear differential operator is proportional to σ), we expect that σ_0 increases linearly with σ, the turbulent kinetic energy. As for the behavior in time, since this computation can be carried out for every $d > 1$, we believe that the decay in time is dimension-independent.

Future directions: a unified theory

In Chapter 2 a Smoluchowski-type equation is derived to study the collision rate of inertial particles in a high Stokes number regime under the effect of a turbulent fluid.

While this regime is of interest in the astrophysical context, it has less impact on atmospheric physics, in which particles have, usually, low to moderate $\mathbf{St}$ numbers. In particular, the regime we have recovered is the same as Abrahamson [1], which is a limiting behavior of coagulating particles akin to gas-kinetic theory.

Motivated by this, we are trying to study heavy (with respect to fluid density) inertial particles in a turbulent environment with a two-point statistic approach. This way, dependence on radius and relative distance of particles are still present in the computation of the PDF and, hopefully, all ranges of $\mathbf{St}$ could be investigated.

This problem will be formalized in the following chapter, leaving different comments, heuristics and proofs, more so open questions to be answered.

Main achievement of the chapter is the complete formulation for the average relative velocity of two particles advected by a turbulent fluid, i.e.

$$\langle \mathbf{v} \rangle \sim \sqrt{\langle \mathbf{v}^2 \rangle} \sim \sqrt{\frac{k_T}{St}} \sqrt{1 - q\left(\frac{v_p St}{\sqrt{2k_T}}\right)}.$$

where $\mathbf{St}$ is the Stokes number, $\mathbf{k_T}$ the turbulent kinetic energy and q is a function that helps modelling the fluctuating structure of the fluid.

We discuss the consequences of this formula depending on the choice of the modelling of $\mathbf{U}(\mathbf{x}, t)$ fluid velocity and its link with others given in the literature.

In a similar fashion to Chapters 1 and 2 and stochastic modelling via transport noise, we are considering the noise to be turbulent and fluctuating, i.e.

$$U(\mathbf{x}) = \sigma \sum_k e_k(\mathbf{x}) W_k'(t).$$

As shown in .2, we can still give meaning to the quantity σ as the product of the turbulent kinetic energy, k_T, and relaxation time of the fluid, τ_f.

With the same reasoning, we obtain at the level of the SPDE for the joint density of the two-point motion: $f_t(\mathbf{x_1}, \mathbf{x_2}, \mathbf{v_1}, \mathbf{v_2})$, i.e.

$$\partial_t f + \operatorname{div}_{x_1}(v_1 f) + \operatorname{div}_{x_2}(v_2 f) - \frac{1}{\tau_p} \operatorname{div}_{v_1}(v_1 f) - \frac{1}{\tau_p} \operatorname{div}_{v_2}(v_2 f) =$$

$$= \frac{\sigma}{\tau_p} \sum_k e_k(\mathbf{x_1}) \cdot \nabla_{v_1} f \circ dW_k(t) + \frac{\sigma}{\tau_p} \sum_k e_k(\mathbf{x_2}) \cdot \nabla_{v_2} f \circ dW_k(t) \quad (0.0.23)$$

Writing the Ito-Stratonovich corrector in (0.0.23) we obtain a second order elliptic operator that depends on the covariance matrix of the noise. Call Q such matrix we have:

$$Q(x_i, x_l) = \sigma^2 \sum_k e_k(x_i) \otimes e_k(x_l).$$

and computing the Ito formula and the corrector, we get mixed derivatives in the $\mathbf{v} = (\mathbf{v_1}, \mathbf{v_2})$ variables, giving the following second order operator (we assume for simplicity $Q(\mathbf{x_1}, \mathbf{x_2}) = Q(\mathbf{x_2}, \mathbf{x_1})$):

$$\begin{aligned}\mathcal{D}f =& \frac{\sigma^2}{2\tau_p^2} div_{v_1}(Q(\mathbf{x_1}, \mathbf{x_1})\nabla_{v_1} f) + \frac{\sigma^2}{2\tau_p^2} div_{v_2}(Q(\mathbf{x_2}, \mathbf{x_2})\nabla_{v_2} f) \\ &+ \frac{\sigma^2}{\tau_p^2} div_{v_1}(Q(\mathbf{x_1}, \mathbf{x_2})\nabla_{v_2} f).\end{aligned}$$

Under suitable conditions, we show the proximity of such an equation with the transient PDE or Galeati limit. In particular, we estimate the difference between the two solutions:

$$\mathbb{E}\left[\left\langle f - \overline{f}, \phi \right\rangle^2\right] \leq C \|\mathbb{Q}\|_{L^2 \to L^2} \|f_0\|_{L^2},$$

refining this estimate as much as possible, and as such supporting the fact that we transition from the SPDE to the PDE, due to their proximity. For $\overline{f}$ we obtain the PDE for the density of the two-point statistics.

$$\partial_t \overline{f} + \mathrm{div}_{x_1}\left(v_1 \overline{f}\right) + \mathrm{div}_{x_2}\left(v_2 \overline{f}\right) - \frac{1}{\tau_p}\mathrm{div}_{v_1}\left(v_1 \overline{f}\right) - \frac{1}{\tau_p}\mathrm{div}_{v_2}\left(v_2 \overline{f}\right) = \mathcal{D}\overline{f} \quad (0.0.24)$$

Note that under the same assumption of Chapter 2, we recover the equation for the single-particle density, hence showing that this is indeed a consistent extension of the developed theory. Indeed, this can be done by integrating in the desired variable and using the divergence theorem and the symmetry of the covariance matrix, then Q is basically independent on the position and the only contribution is given by $\sigma^2 \sim k_T$.
Here, instead, the position is essential and changes the behavior of the relative velocity.

To compute the mean velocity we need to investigate the density function of the two-point motion. Since we are interested in obtaining an average value that is independent from the initial condition, we focus on the steady-state solution of the PDE (0.0.24). Following similar ideas from [10, 75, 90, 89] and others, we note that is the distance of the two particles the meaningful quantity. We search solution of the form:

$$f(\mathbf{x_1}, \mathbf{x_2}, \mathbf{v_1}, \mathbf{v_2}) = \widetilde{f}(\mathbf{x_1} - \mathbf{x_2}, \mathbf{v_1}, \mathbf{v_2})$$

Call $\mathbf{r} := \mathbf{x_1} - \mathbf{x_2}$, the function $\widetilde{f} = \widetilde{f}(\mathbf{r}, \mathbf{v_1}, \mathbf{v_2})$ satisfy the PDE:

$$-\frac{1}{\tau_p}\mathrm{div}_{v_1}\left(v_1 \widetilde{f}\right) - \frac{1}{\tau_p}\mathrm{div}_{v_2}\left(v_2 \widetilde{f}\right) = \mathcal{D}\widetilde{f}$$

$$\mathcal{D}\widetilde{f} = \frac{\sigma^2}{2\tau_p^2}\left(\Delta_{v_1}\widetilde{f} + \Delta_{v_2}\widetilde{f}\right) + \frac{\sigma^2}{\tau_p^2} div_{v_1}\left(Q(\mathbf{r})\nabla_{v_2}\widetilde{f}\right) \tag{0.0.25}$$

this equation is the adiabatic formulation, i.e. constant in space, of the steady state equation of (0.0.24), where we impose:

$$\mathrm{div}_{x_1}\left(v_1\widetilde{f}\left(x_1 - x_2, v_1, v_2\right)\right) + \mathrm{div}_{x_2}\left(v_2\widetilde{f}\left(x_1 - x_2, v_1, v_2\right)\right) = 0. \tag{0.0.26}$$

We show, in Section 3.7, through numerical simulations that solution of such equations are close, respect to the problem of finding the relative velocity of particles, to steady-state solutions of Equation (0.0.24).

This makes the task of finding a solution for (0.0.25) feasible: given any $\mathbf{r}$, we can find solution pdf $\theta_{\mathbf{r}}\left(\mathbf{v_1}, \mathbf{v_2}\right)$ which satisfies equation (0.0.25). We have, for each fixed $\mathbf{r}$,

$$\int\int \theta_x\left(v_1, v_2\right) dv_1 dv_2 = 1, \quad f\left(\mathbf{r}, \mathbf{v_1}, \mathbf{v_2}\right) := \theta_{\mathbf{r}}\left(\mathbf{v_1}, \mathbf{v_2}\right) \tag{0.0.27}$$

up to constant depending on the space domain we are working on.

The important consequence is that, following from classical theory of both stochastic processes and elliptic equation, we have

$$\theta_{\mathbf{r}}\left(\cdot\right) \sim N\left(0, C_{\mathbf{r}}\right)$$

with a known $C_{\mathbf{r}}$ which will depend on our choice of $Q(\mathbf{r})$ covariance of our noisy fluid modelling.

The structure function that we want to compute is the average relative velocity between two particles considering all the inertial range of the particles in the fluid, i.e.

$$\mathbb{E}\left[|\mathbf{V_1} - \mathbf{V_2}|\right]$$

this is the average difference of velocities between particles in the portion of space that has a length scale of the order of the Kolmogorov length ℓ_k.

Using the equilibrium probability density (0.0.25) of pairs of particles and calling $\|\mathbf{r}\| \sim \ell_{\mathbf{p}}$ the typical length scale of colliding particles, in the unitary torus, we have:

$$\begin{aligned}
\mathbb{E}\left[|\mathbf{V_1} - \mathbf{V_2}|\right] &= \frac{\int\int |\mathbf{v_1} - \mathbf{v_2}| f\left(\ell_{\mathbf{p}}, \mathbf{v_1}, \mathbf{v_2}\right) d\mathbf{v_1} d\mathbf{v_2}}{\int\int f\left(\ell_{\mathbf{p}}, \mathbf{v_1}, \mathbf{v_2}\right) d\mathbf{v_1} d\mathbf{v_2}} \\
&= \int\int |\mathbf{v_1} - \mathbf{v_2}| \theta_{\ell_{\mathbf{p}}}\left(\mathbf{v_1}, \mathbf{v_2}\right) d\mathbf{v_1} d\mathbf{v_2} \\
&\sim \sqrt{C^{11}_{\ell_{\mathbf{p}}} + C^{22}_{\ell_{\mathbf{p}}} - 2C^{12}_{\ell_{\mathbf{p}}}}.
\end{aligned}$$

Hence, the main objective of the following section is to give fair assumptions on $Q(\mathbf{r})$ to compute $C_{\mathbf{r}}$ from which we'll derive: $C^{11}_{\ell_{\mathbf{p}}}$, $C^{22}_{\ell_{\mathbf{p}}}$, $C^{12}_{\ell_{\mathbf{p}}}$ and as such the relative velocity.

For this reason, consider a scalar function $q(r)$ dependent on the magnitude of the relative distance.

$$\begin{cases} Q\left(\mathbf{x}, \mathbf{y}\right) & = Q\left(\mathbf{x} - \mathbf{y}\right) = \sigma q\left(\frac{\mathbf{x}-\mathbf{y}}{\ell_{\mathbf{f}}}\right) Id \\ q\left(0\right) & = 1 \end{cases}$$

(Note that we can always assume $q(0) = 1$ since we can always modify σ with a dimensionless constant dependent only on the domain).

Thus the matrix C_r is linked to $q\left(\frac{r}{\ell_f}\right)$. From the elliptic equation we obtain with usual computation on invariant measure the covariance matrix

$$C_r = \frac{\sigma^2}{\tau_p} \begin{pmatrix} Id & q\left(\frac{r}{\ell_f}\right) Id \\ q\left(\frac{r}{\ell_f}\right) Id & Id \end{pmatrix}$$

Using the results of previous section and the computation on C_r, we can obtain for the structure function the following closed form:

$$\mathbb{E}\left[|\mathbf{V_1} - \mathbf{V_2}|\right] \sim \frac{\sigma}{\sqrt{\tau_p}} \sqrt{1 - q\left(\frac{\ell_p}{\ell_f}\right)}.$$

Different covariance models from Gaussian decay to Kraichnan and Kolmogorov scaling are proposed and studied. Hence, recovering the known limiting regime for the relative velocity as in [1, 14, 72].

Concerning the collision rate $\mathcal{R}$, we propose in the chapter some explanation on how to connect our result with the literature and what is still missing to complete the puzzle and have a closed formulation and a unified theory for particle colliding in fluid flow. In the physics community, there is now a general consensus [90, 89, 75, 10, 11, 26, 25] that the coagulation rate, introduced in Chapter 1, has a natural splitting in two main components

$$\mathcal{R} = \mathcal{R}_{adv} + \mathcal{R}_{tur}.$$

These two uncorrelated main components are: $\mathcal{R}_{adv}$, the coagulation due to advection, and $\mathcal{R}_{tur}$, due to the turbulent flow.

The advecting part $\mathcal{R}_{adv}$ is estimated for low Stokes regime with a uniform density of almost tracer particles in [78], that read as

$$R_a := \sqrt{\frac{8\pi}{15}} n_0 \left(2\mathbf{r}\right)^2 {\tau_\mathbf{f}}^{-1},$$

where n_0 is the density and $\mathbf{r}$ the radius of the particles. This last term $\mathcal{R}_T$ is obtained independently from two different computations both from Falkovich [26, 25] and Mehlig [90, 89], while it is being considered in the works of Bec [11, 10] and Pumir [75]. This is called *the sling effect* or *caustic effect*, which proposes a correction due to the fluid turbulence that creates singularity on the gradient of the particles' velocity and then modifies their density.

Both of these effects are obtained considering the usual collision kernel when turbulent flow is involved,

$$\mathcal{R}_{kin} \sim \langle |\mathbf{v}_1 - \mathbf{v}_2| \rangle ,$$

is mostly dependent on the relative velocity of the particles. They propose a correction due to the fluid turbulence that creates singularity on the gradient of the particles' velocity and then modify their density.

For this reason, if we have a statistically uniform spatial distribution of particles, call such density n_0, then we have the relation between the turbulent collision rate, $\mathcal{R}_{tur}$, and the relative velocity, i.e.

$$\mathcal{R}_{tur} \sim n_0 \left\langle |\mathbf{v}_1 - \mathbf{v}_2| \right\rangle .$$

Unfortunately, under this hypothesis, we fail to capture in fullness the turbulent part of the turbulent coagulation rate described by the Sling Effect. It can be argued, considering the derivation of the relative velocity and the heuristics proposed in Chapter 1, Section 1.4, and seminal paper such as [12, 41, 25], that the assumption of statistically uniform spatial distribution in the limit for $St \to 0$ is not what we are really working with. In particular, all of our assumption in the computation of the structure function needs to work in the steady state regime, as such, also the density must be taken at is steady limit after the turbulence of the fluid has taken effect on the trajectories of the particles. More so, since in our equation velocity is an active variable, this must be carried on, as a Maxwellian-like average for the particle and to be computed in a domain as big as two colliding particles. The first reasonable guess, e.g. [59], is to consider the collision rate in the following form:

$$\mathcal{R} \sim n_0 g(\mathbf{r}, \mathbf{v}) \left\langle |\mathbf{v}_1(\mathbf{r}) - \mathbf{v}_2(\mathbf{r})| \right\rangle$$

where $g(\mathbf{r}, \mathbf{v})$ is somewhat analogous to a radial density function of the particles, but now depending on the relative distance, radius and velocities of the particles.

In analogy with Maxwell-Boltzmann-Arrhenius density, we expect to multiply the relative velocity $\langle |\mathbf{v}| \rangle$ with the number density of particles able to collide at a certain length distance with their related averaged velocity $\mathbf{v}_p$ obtained from the Maxwellian, derived from the single point statistics in Section 2.5, representing the activation kinetic energy due to the particles respect to the fluid $\mathbf{k_T}$. If we call h this new factor, then:

$$h := \exp\left(-\frac{1}{2} m_p \frac{\left\langle |\mathbf{v}|^2 \right\rangle}{\mathbf{k_T}}\right) \sim \exp\left(-\frac{1}{2} m_p \frac{\mathbf{v}_p^2 \tau_\mathbf{p}}{\sigma^2}\right)$$

This is closely related to Maxwell distribution in which we have

$$h \sim \exp\left(-\frac{E}{T}\right)$$

where E is the energy and T is the temperature and, in our case, the turbulent intensity of the fluid, given by $\sigma^2/\tau_\mathbf{p}$. In particular, we can argue that this h is not an artificial factor, but nothing more than the steady state solution of the modified Smoluchowski, which is a type of Vlasov-Fokker-Plank equation.

Under this assumption and our Gaussian covariance hypothesis we get:

$$\mathcal{R}_{tur}(\mathbf{m}_p) \sim n_0 \exp\left(-\frac{m_p}{2} \frac{\ell_p^2}{{\ell_\mathbf{f}}^2} \frac{1}{\mathbf{St}}\right) \sqrt{\frac{\mathbf{k_T}}{\mathbf{St}}} \sqrt{1 - \exp\left(-\left(\frac{\mathbf{v_p}}{\sqrt{\mathbf{2k_T}}} \mathbf{St}\right)^2\right)}.$$

This leaves us with a final formulation that agrees with Falkovich's [26, 25] and Mehlig's [64] analytic formula. This factor well represents the activation aspect of the turbulent energy with respect to the fluid trajectories and the fast decay as $\mathbf{St} \to 0$, but, albeit essential, it is formulated with a reasoning due to kinetic theory and energy balance. For this reason, it is still fundamental to understand how can we capture this from the particle system at play, as shown in Sections 1.4 and 1.5, and, in a rigorous way, from the limiting equation 3.2.2. This would be the primary work for future development of this theory.

Smoluchowski equation with velocity

In previous chapters we took a kinetic viewpoint to obtain our equations for the density of particles in a turbulent fluid, obtaining numerical and rigorous theoretical results on the effect of such field on the coagulation process both for tracer and inertial particles.

In Chapter 4 we undertake the complex task of study rigorously such variant of Smoluchowski's coagulation equation with velocity dependence that is akin to Boltzmann equation. As explained, it arises as the scaling limit of a system of second-order (microscopic) coagulating particles, modelling the interactions of rain droplets in the clouds, which are subjected to a common noise of transport type. Such a noise, constructed in recent mathematical works [42, 35], possesses several characteristics of real turbulence, such as it enhances diffusion of passive scalars. We focus on the existence, uniqueness and regularity of this new PDE, after briefly introducing its origin.

Smoluchowski's classical equation [83] provides a first model for the time evolution of the probability distribution $\{f_m(t,x)\}_{m=1}^{\infty}$ of diffusing particles of different sizes (or masses) $m \in \mathbb{N}$, say in $\mathbb{T}^d := (\mathbb{R}/\mathbb{Z})^d$, when they undergo pairwise coagulation with certain coagulation rate $\alpha(m,n)$:

$$\begin{aligned}\partial_t f_m(t,x) = \Delta f_m(t,x) &+ \sum_{n=1}^{m-1} \alpha(n,m-n) f_n(t,x) f_{m-n}(t,x) \\ &-2\sum_{n=1}^{\infty} \alpha(m,n) f_m(t,x) f_n(t,x), \quad t>0,\, x\in\mathbb{T}^d,\, m\in\mathbb{N}.\end{aligned}$$

The non linearity has two parts, a gain term and a loss term. Such a system of equations has been derived from scaling limits of Brownian particle systems by Hammond-Rezakhanlou [48, 46]. To model the influence of a large-scale turbulent flow, it is natural to introduce a common noise. If we adopt a transport noise of the type in [35]

$$\dot{\mathcal{W}}(t,x) = \sum_{k\in K} \sigma_k(x) \dot{W}_t^k$$

where $\{\sigma_k(x)\}_{k\in K}$ is a countable collection of divergence-free smooth vector fields and $\{W_t^k\}_{k\in K}$ independent one-dimensional Brownian motions, then we get a stochastic version of Smoluchowski's equation (an SPDE)

$$\begin{aligned}df_m(t,x) =& \Delta f_m(t,x)dt + \sum_{n=1}^{m-1} \alpha(n,m-n) f_n(t,x) f_{m-n}(t,x)dt \\ &-2\sum_{n=1}^{\infty} \alpha(m,n) f_m(t,x) f_n(t,x)dt - \sum_{k\in K} \nabla f_m(t,x)\cdot\sigma_k(x)\, dW_t^k \\ &+ \operatorname{div}\left(\mathcal{Q}(x,x)\nabla f_m(t,x)\right), \quad m\in\mathbb{N}\end{aligned} \tag{0.0.28}$$

where $\mathcal{Q}(x,x) := \sum_{k\in K} \sigma_k(x)\otimes\sigma_k(x)$ coming from the transport-type noise. Under specific choice of $\{\sigma_k\}_{k\in K}$, we can have that $\mathcal{Q}(x,x)\equiv \kappa I_d$, for an enhanced diffusion coefficient $\kappa > 0$, the so-called "eddy diffusion" [15]. This picture, in its special case of finitely many mass levels $m = 1,2,...,M$ and unit coagulation rate $\alpha(m,n)\equiv 1$, has

been derived from particle systems in [30]. Another version of the SPDE with continuous mass variables $m \in \mathbb{R}$ has also been derived from particle systems with mean-field interactions in [73].

However, conceptually and mathematically, the most difficult step in this program is to verify that diffusion enhancement leads to coagulation enhancement, namely, the fast increase of probability densities f_m for $m \gg 1$ (large masses) for large diffusion coefficient case. In fact, the model (0.0.28) turns out to be too crude, and even numerically we cannot verify a coagulation enhancement.

The problem lies in the fact that quick diffusion of masses may not lead to enhanced collision unless the coagulation rate depends on the velocity variable. Otherwise, the masses merely move around. We introduce a new system with both position and velocity variables. In the atmospheric physics literature, e.g. [25, 75, 80, 45], it is also common to consider cloud particles coagulate with a rate that is proportional to (when $d = 3$)

$$\alpha(m_1, m_2) := |v_1 - v_2|(r_1 + r_2)^2$$

where v_i, $i = 1, 2$ are the velocities of two colliding rain droplets and $r_i := m_i^{1/3}$, $i = 1, 2$ their respective radius. Under certain simplifications, it leads to the following kinetic version of Smoluchowski's equation (cf. Chapter 1, Section 1.5)

$$\begin{cases} \partial_t f_m(t,x,v) = -v \cdot \nabla_x f_m + c(m)\mathsf{div}_v\,(v f_m) + \kappa c(m)^2 \Delta_v f_m + Q_m(f,f) \\ f_m|_{t=0} = f_m^0(x,v), \quad m = 1, ..., M, \end{cases} \tag{0.0.29}$$

where $(t, x, v) \in [0, T] \times \mathbb{T}^d \times \mathbb{R}^d$, and

$$\begin{aligned} &Q_m(f,f)(t,x,v) := \\ &= \sum_{n=1}^{m-1} \iint_{\{nw'+(m-n)w=mv\}} s(n, m-n) f_n(t,x,w') f_{m-n}(t,x,w)|w - w'|dwdw' \\ &\quad - 2\sum_{n=1}^{M} \int s(n,m) f_m(t,x,v) f_n(t,x,w)|v - w|dw, \end{aligned} \tag{0.0.30}$$

where

$$c(m) := \alpha m^{(1-d)/d}, \quad s(n,m) := (n^{1/d} + m^{1/d})^{d-1}. \tag{0.0.31}$$

In Chapter 1, Section 1.5, we sketched the proof of the scaling limit from a coagulating microscopic particle system subjected to a common noise, to an SPDE that eventually gives rise to this PDE. Although it is not fully rigorous, it should justify the interest of this equation. Here again, turbulence contributes to large κ versus small κ when no turbulence. The eddy diffusion occurs now in the velocity variable.

The aim of our research is two-fold. Theoretically, we are interested in proving the well-posedness of the PDE and associated SPDE cf. (0.0.8), as well as the passage from the one to the other. Then, both theoretically and numerically we aim to demonstrate that the larger the κ, i.e. the more intense is the turbulence, the faster masses coagulate. See

[31] and Chapter 2 and 3 for a first theoretical and numerical study in this direction. In the present article, we focus on the PDE system (0.0.29) in the spatially-homogeneous case, i.e. by considering the initial conditions f_0^m constant in x for every m, we can reduce (0.0.29) to

$$\begin{cases} \partial_t f_m(t,v) = c(m)\mathrm{div}_v\left(v f_m(t,v)\right) + \kappa c(m)^2 \Delta_v f_m(t,v) + Q_m(f,f)(t,v) \\ f_m|_{t=0} = f_m^0(v), \quad m = 1,...,M, \end{cases} \tag{0.0.32}$$

where $(t,v) \in [0,T] \times \mathbb{R}^d$ and $Q_m(f,f)$ is as in (0.0.30) but without the x-dependence, and we prove existence, uniqueness and regularity of the solutions of (0.0.32), for every fixed $\kappa > 0$.

Denote a weighted L^p space

$$L^p_k(\mathbb{R}^d) := \left\{ f : \mathbb{R}^d \to \mathbb{R} \text{ s.t. } f\langle v\rangle^k \in L^p(\mathbb{R}^d) \right\}, \quad p \in [1,\infty],\ k \in \mathbb{N}, \tag{0.0.33}$$

where

$$\langle v\rangle := \sqrt{1+|v|^2}$$

and a weighted Sobolev space

$$H^n_k(\mathbb{R}^d) := \left\{ f \in L^2_k \text{ s.t. } \nabla^\ell f \in L^2_k(\mathbb{R}^d),\ \forall 1 \le \ell \le n \right\}. \tag{0.0.34}$$

The main result of this article is as follows.

Theorem 0.0.1. *Fix any finite T and $\kappa > 0$. Suppose that initial conditions $f_m^0(v) \in (L^2 \cap L^1_2)(\mathbb{R}^d)$ and nonnegative, for every $m = 1,...,M$, then there exists at least one nonnegative solution in the class $L^\infty\left([0,T]; L^1_2(\mathbb{R}^d)\right)^{\otimes M}$.*

If the initial conditions $f_m^0(v) \in (H^1_1 \cap L^1_2)(\mathbb{R}^d)$ and nonnegative, then there exists a unique nonnegative solution, and in this case $f_m(t) \in C^\infty_b(\mathbb{R}^d)$ for any $t > 0$.

The most difficult part in our opinion is uniqueness, due mainly to the presence of $|w - w'|$ in the nonlinear term, and the fact that the velocity variable $v \in \mathbb{R}^d$ is unbounded, hence in the presence of Laplacian, $f_m(t,v)$ is never compactly supported even if starting with so. These together with the fact that we have a system rather than just one equation, cause a severe difficulty in closing a Gronwall inequality for uniqueness. As far as we are able, the weighted L^1 space is the only one in which a Gronwall argument can work, even if one is willing to assume that solutions are Schwartz functions. (The problem is related to integrability rather than smoothness.) Indeed, with weighted L^1 we can find certain cancellations that remove those terms with higher weights brought by the kernel, and this seems not achievable with other spaces such as weighted L^2. Equally essential to this cancellation is considering the sum over the norms of all the densities $f_m, m = 1,..,M$, rather than treating them individually. Indeed, this is already essential to derive various apriori estimates.

Consider for this the set of equation solved by $h_m(t,v) := f_m(t,v) - g_m(t,v)$, $\forall m = 1,...,M$ and call $H_m(t,v) := f_m(t,v) + g_m(t,v)$, where f_m, g_m are two solution with

the same initial condition. Then:

$$\begin{cases} \partial_t h_m(t,v) = \Delta h_m + \mathsf{div}(v h_m) + \frac{1}{2}\left(Q_m(h,H) + Q_m(H,h)\right) \\ h_m|_{t=0} = 0 \end{cases} \tag{0.0.35}$$

where we denote

$$\begin{aligned} Q_m(h,H) &:= \sum_{n=1}^{m-1} \int \left(\frac{m}{n}\right)^2 h_n(\varphi(v,w)) H_{m-n}(w)|v-w|dw \\ &\quad - 2\sum_{m=1}^{M} h_m(v) \int H_n(w)|v-w|dw, \\ Q_m(H,h) &:= \sum_{n=1}^{m-1} \int \left(\frac{m}{n}\right)^2 H_n(\varphi(v,w)) h_{m-n}(w)|v-w|dw \\ &\quad - 2\sum_{m=1}^{M} H_m(v) \int h_n(w)|v-w|dw. \end{aligned}$$

We consider now the function $\psi_\varepsilon(x)$ an approximation of the function $\mathsf{sgn}(x)$ such that

$$\psi_\varepsilon(x) := \begin{cases} -1, & x \le -\varepsilon \\ x/\varepsilon, & -\varepsilon < x < \varepsilon \\ 1, & x \ge \varepsilon \end{cases}$$

We consider the weight $\langle v\rangle^2 := 1+|v|^2$ and thus the function $\Psi_\varepsilon(h_m, v) := \psi_\varepsilon(h_m)\langle v\rangle^2$, multiplying it to the equations (4.2.2) solved by $h_m, \forall m$ and integrating by part. Defining also

$$\chi_\varepsilon(x) := \begin{cases} 1, \text{ if } |x| < \varepsilon \\ 0, \text{ otherwise}, \end{cases}$$

we obtain:

$$\partial_t \int h_m \psi_\varepsilon(h_m)\langle v\rangle^2 dv = \int (\partial_t h_m)\psi_\varepsilon(h_m)\langle v\rangle^2 dv + \frac{1}{\varepsilon}\int (\partial_t h_m)\chi_\varepsilon(h_m) h_m \langle v\rangle^2 dv \tag{0.0.36}$$

This two term can now be computed independently using both the regularity of the solution and the cancellation property of the sgn function that make possible to discharge the weight of the non linearity Q_m to the function H_m sum of the two solutions, leaving h_m, the difference, untouched, hence, closing the Gronwall lemma and proving uniqueness.

On the other hand, existence is proved by constructing a family of approximating equations each corresponding to a truncation of the kernel $|w-w'|$ in the nonlinearity. These approximating problems are more amenable to study since the difficulty related to the kernel is no longer severe, for each fixed truncation parameter.

When $f_m^0 \ge 0, \ \forall\ m = 1,..,M$, the solution of (4.3.1) is nonnegative and regular enough and has a fast decay at infinity, then we have for the nonlinear term:

$$\chi_R(v) \int f_n\Big(t, \varphi(v,w)\Big) f_{m-n}(t,w)|v-w|\chi_R(w)dw$$

$$\leq \int f_n\Big(t, \varphi(v,w)\Big) f_{m-n}(t,w)|v-w|dw$$

And thus we can recover the same a priori estimate in both the full and approximated system. Luckily, we can define a map Γ from $X_T \to X_T$, given by

$$\Gamma(f) := P_{\cdot} f^0 + \int_0^{\cdot} P_{\cdot - s}(df - Q^R(f,f))ds, \ f \in X_T.$$

where $X_T = C([0,T], \mathbb{L}^2)$ is a suitable functional space in which a semigroup associated to the following unbounded operator on function defined on $\mathbb{R}^d$:

$$\mathcal{L}f := \Delta f + v \cdot \nabla f,$$

guarantees adequate gain in regularity for the truncated solution, [66]. This, joint with suitably weighted embedding in Sobolev space, gives us the desired solutions.

There is an unexpected connection to the vast area of Boltzmann equations [86]. Our (0.0.29) may be viewed as a Boltzmann-type equation with perfectly inelastic collision, rather than the classical elastic collision. Indeed, it is derived from particles undergoing pairwise coagulation, hence two particles merge into one based on the principle of conservation of momentum (and not energy). It is also local in nature in that the nonlinearity acts on the velocity variable, per (t,x). The closest works in the Boltzmann literature seem to be the ones on excited granular media, see [43] and references therein, and on multi-species Boltzmann equations, see [17] and references therein. In a sense our equation combines the features of both of them. From a technical point of view, the aforementioned difficulties with uniqueness are also present in [67, 43] and some references therein, and we have learned from these sources. On the other hand, there are various differences that set our model apart from these references. Since $M < \infty$, we do not have the conservation of mass and momentum, and we do not expect nontrivial stationary solutions – indeed all $f_m(t)$ should decay to zero as $t \to \infty$ (i.e. eventually all masses are transferred out of the system). In general, our nonlinearity $Q_m(f,f)$ does not enjoy any particular kind of symmetry. Our derivation of the apriori estimates is also quite different, in particular, we need not invoke entropy estimates and Povzner-type inequalities, as are standard in the Boltzmann literature.

Chapter 1

Key quantities: two kind of particles

Although clouds play a crucial role in atmospheric phenomena, the effect of turbulence in cloud formation is not well established up to the present.

Two processes mutually affecting each other characterize the cloud formation and precipitation development: macro-scale processes such as the fluid motion of air associated with clouds and the micro-scale processes such as condensation, stochastic coalescence, and evaporation of water droplets. Thus we can say that cloud formation and precipitation development are typical multiscale-multiphysics phenomena.

Motivated by the numerical studies for Lagrangian particles, [81], in which the authors propose a novel algorithm to compute the stochastic coalescence of large number of droplet; and [61], in which the problem of the role of turbulence in the cloud droplet growth is treated with simulation of density equations in the spirit of Fokker-Planck and Smoluchowski; we investigate the time of first formation of a raindrop, the rate of collision and the displacement of mass through time, for the space, time and velocity density of particles with different masses in a cloud during rain formation, under different turbulent settings and inertial regime, to explore the role of turbulent flow in the aggregation of small droplets in clouds.

1.1 Introduction

Objective and main interest of this thesis is in the study of transported particles in fluid flow and the property of collision and mixing of such particles when the flow itself is in a turbulent regime.

The presence of suspended particles, such as dust, droplets, or ice crystals in natural fluids like the atmosphere and the sea, affects their behavior. For example, the interaction of water droplets in clouds, through the absorption of solar and terrestrial radiation, play a role in the planet's energy forecast and atmospheric dynamics. Understanding the distribution of particle sizes in suspensions is essential for comprehending these processes.

More so, the stability of suspended particles in large fluid bodies is also significant. Raindrop formation from the coalescence of microscopic water droplets in clouds is a central question in cloud microphysics. The formation of planets is similarly dependent on the collision and coalescence of dust grains in the atmosphere around young stars. Explaining weather phenomena and the habitability of our planet relies on understanding

the behavior of aerosol suspensions and their susceptibility to collisions.

However, developing a quantitative theory for rain initiation and planet formation encounters difficulties. The collision rates of atmospheric aerosol particles, caused by differential settling rates or Brownian motion, mostly relies on direct numerical simulations and appear inadequate to explain the rapid onset of rain or planet formation. Turbulence offers a possible solution to these problems.

Turbulent motion is a prevalent phenomenon in fluid dynamics, and it is known that small particles disperse much faster in turbulent environments compared to molecular diffusion. This suggests that turbulence could significantly enhance collision rates and play a crucial role in particle coagulation.

Understanding the mechanisms by which turbulence enhances collision rates has made significant progress in recent years [25, 26, 64, 75, 90], yet a foundational construction of the quantities at play remains an open question.

1.1.1 Two points of view

To do so we'll consider two, interconnected, points of view: a Lagrangian and Eulerian vision of such systems. The first one deal with the understanding of trajectories $X(t)$ of particles given the velocity field $u(t, X(t))$ of the flow in which they are embedded. While the second tries to understand the property of the field, or density, of such particles, as a continuous function $f_t(x)$, given the same velocity field $u(t, x)$.

This two theory can answer different questions: one, in a sense, is more local in nature, while the other one is more akin to a mean field description and as such are the property that can be retrieved. Even so, the two methods of study are linked together and one usually can be derived from the other. A standard example, in this direction, is the motion of passive scalar in a velocity field subjected to a random noise, i.e.

$$\frac{d}{dt}X(t) = u(t, X(t)) + \sqrt{2D_0}\dot{W}(t)$$

where $D_0 \in \mathbb{R}$ and $\dot{W}(t)$ is a white noise. This equation for particles has a natural counterpart, when considering the mean field limit of such particle system, as an evolution equation for the continuous field $f(t, x)$, i.e.

$$\partial_t f + u \cdot \nabla f = D_0 \Delta f$$

More so we have that the law of the particle is indeed a solution of such a system. While this link is classical and detail can be found in [54], we have presented it here to show how studying particle trajectories is thus relevant also to understand the transport of fields.

While this example is fundamental in understanding our idea of moving back and forth between a mean field and a particles description to understand our problem of mixing and collision, we first need to add some richness in our particles and describe two main regime of motion, one of which will be the center of this dissertation.

Call ϕ_p the density of the particles and ϕ_f the density of the fluid, then we can distinguish to behavior:

- $\phi_p = \phi_f$: the particles can be approximated as point-like object and move with the same velocity of the fluid. In this case they are essentially like fluid elements and

we call them *tracer particles*. Their equation of motion usually looks like

$$\dot{X}(t) = u(t, X(t)) \, (:= V(t));$$

- $\phi_p \neq \phi_f$: the particles are now finite size object and are subjected to inertia and other external forces that can change the velocity of the particles drastically and making it no more adherent to the fluid streamline. In this case, kinetic equation are more suited to describe this *inertial particles* motion and we have:

$$\dot{X}(t) = V(t), \quad \dot{V} = F(V(t), u(t, X(t), \phi_p, \phi_f, ...).$$

Note that in either case we'll focus on passive particles, i.e. the velocity field is not modified by their presence. Since we are interested in coagulating processes, we attach to each one of them a quantity that represent the mass m, which we link to the radius r under the assumption of each particles to be spherical.

Even with this settled framework, describing the motion of particles in simple flow configurations is a difficult task. For this reason, the equation of motion are determined by the simple Stokes' formula

$$\dot{X}(t) = V(t), \quad \dot{V} = \frac{1}{\tau_p} \left(u(t, X(t)) - V(t) \right) + \mathbf{g}. \tag{1.1.1}$$

where

$$\tau_p = \frac{2r^2 \phi_p}{9\nu\phi_f},$$

is the particle relaxation time. This constant is usually determined from the Stokes' formal for the drag on a moving sphere. ν is the kinematic viscosity, $\mathbf{g}$ is the gravity.

More so, compering the Kolmogorov time τ_f of the fluid and the typical time of the particle τ_p, we obtain a way to quantify the effect of inertia. As such, we define

$$St := \frac{\tau_f}{\tau_p}$$

the Stokes number for a particle of mass m_p, where τ_f is the typical fluid relaxation time, dependent on its kinetic viscosity an density.

For $St << 1$ the fluid advect the particles and most of the phenomena are the results of shear of relative motion. While for $St >> 1$ the particles are allowed to move freely relatively to the fluid motion, but still be affected by its velocity, leading to entirely different phenomena.

Thus, the Stokes number could be regarded as the unique dimensionless parameter necessary to understand the different physical regime of collision and growth. For this reason, this quantity would be central in measuring both the inertia and understanding the collision behavior of suspended particles.

Note that this equations are valid only in the limit when the suspended particles are small and dense, i.e. $\phi_p/\phi_f >> 1$. When the opposite happens the history forces became important and the model must be changed. For this reason we focus on framework in which the reduce model of Stokes' formula holds.

1.1.2 Effect of turbulence: key quantities

Now that we have the ideas on how to model particles motion and densities evolution, to understand the processes that lead to the formation and growth of raindrops, we need to discuss few mathematical objects that can characterize such dynamics: the coagulation rate and the time of raindrop formation.

In the atmosphere, raindrops originate from tiny suspended particles called cloud droplets, which undergo a complex series of interactions and transformations to become precipitation. One key process involved in this transformation is coagulation, which refers to the collision and subsequent merging of cloud droplets to form larger raindrops. As cloud droplets collide and coalesce, they combine their volumes and increase in size, eventually reaching a critical threshold at which they become large enough to overcome the air resistance and fall as rain.

Understanding the coagulation rate, or the rate at which cloud droplets coalesce and the time of formation of particles, is essential for predicting the growth and intensity of rainfall events, as well as for improving weather forecasting models.

Coagulation rate

In principle, defining the concept of collision rate appears as a straightforward exercise in gas-kinetic theory, but in reality it is a complex problem concerning the number active variables and the complex dynamic of the system.

Imagining the particle as sphere-like objects, we can describe the rate of collection for droplets moving in a flow, as in [25], by the collection kernel of two colliding particles

$$\Gamma = 4\pi R^2 |v_{r_1} - v_{r_2}| E(r_1, r_2),$$

where R is the sum of the droplets radii of the colliding pair r_1 and r_2 , v_{r_1} and v_{r_2} are the velocity of each droplet, and E is the collection efficiency, which is the product of the collision efficiencies and two-point correlation function. This general formulation is deduced considering the rate at which the separation line between the center of mass of the two particles cross a disk of radius R, making the kernel proportional to the area of the spherical surface swept in a unit of time, hence the proportionality on the relative velocity of the particles.

In the classical theory, [87], reducing the active variable only to the mass m of the particles, we expect the collision rate $\mathcal{R}$ to be a function of just m, with a dimension of $[\mathcal{R}] = T^{-1}$, to be dependent on the collision kernel of two single droplet, where the relative velocity of the pair $|v_{r_1} - v_{r_2}|$ is approximated as a function of the radii, and proportional to the number density f_m of particles in the suspension.

In the discrete setting of masses being indexed by $\mathbb{N}$, we then obtain the classical rate of collision

$$\mathcal{R}_m := \sum_{n=1}^{\infty} \Gamma(m, n) f_n \tag{1.1.2}$$

where f_n is obtain again as the mean field solution from the particle system 1.1.1, and is

the classical solution of the Smoluchowski equation [83] with kernel Γ

$$\frac{\partial}{\partial t} f_m = \sum_{n=1}^{m-1} \Gamma(n, m-n) f_n f_{m-n} - 2 \sum_{n=1}^{\infty} \Gamma(m, n) f_m f_n, \quad m \in \mathbb{N}$$

In this setting, usually, Γ is obtained a priori with direct numerical simulation on particles moving into fluid, or with physical reasoning of dimensional analysis, in order to reduce the kernel to be a function of mass only. See [2, 81] and references therein for further details. In analogy to the passive scalar example, this equation is obtained with different degree of idealization, for this reason the Smoluchowski ODE framework, which employs a mean-field approximation, has several limitations.

When particles grow in size, such as droplets in a cloud, the collision rate escalates rapidly, leading to runaway growth observed in raindrop formation, known as gelation in polymer physics. Surprisingly, modeling gelation with the Smoluchowski equation suggests an instantaneous transition with zero time required, which is physically unrealistic. Consequently, this mean-field descriptions based on the classical Smoluchowski approach is not enough to obtain a rigorous construction of the collision rate [75].

To solve this issue, extensive physical literature has been produced [90, 89, 75, 10, 11, 26, 25], in which derivations of coagulation rate, analogous to 1.1.2, are obtained via direct numerical simulation (DNS) or thorough the analysis of Lyapunov exponent of the dynamical system of particles [65].

From Saffman and Turner [78], to Falkovich [26], the main concept is that the collision rate can be divided into two independent components in first approximation. Some collisions occur when particles follow similar trajectories for an extended period and eventually come into contact due to shearing motion in the flow. This mechanism is dominant at low Stokes numbers, or more generally for tracer trajectories, when particles precisely follow the flow. The collision rate resulting from this mechanism depends on the local shear rate and the local particle concentration. On the other hand, collisions between particles that deviate from the fluid path lines and the turbulence at small scale, contribute differently, contributing not only as a "rate of strain". A significant difference between the two contributions lies in their dependence on the typical time of a the particle τ_p and the relation with the Kolmogorov response τ_f. These mechanisms operate independently, and their contributions can be combined additively.

For this reason, we focus our work on the construction of an effective and rigorous theory for $\mathcal{R}_{turb}$, when the folding of the flow line and the inertia of the particles became meaningful in the interplay of the collision process. In doing so, under the hypothesis of a turbulent velocity field, we construct a time evolution for the density of particles $f_m(\xi)$ where ξ represent the active variables of the system, containing both position and velocity. Hence, defining our key quantity

$$\mathcal{R}_{turb} = \sum_{m=1}^{\infty} \int \Gamma(\xi, \xi) f_m(\xi) \, d\xi,$$

explained in detail in Section 1.4, for which we prove in Chapter 2 and 3 the derivation of the typical coagulation rate as in [1, 64].

Time to rainfall

Rainfall often starts suddenly from cumulus clouds, which form when the atmosphere is convecting. In contrast, rainfall from stratiform clouds in a stable atmosphere has a much slower onset. Interestingly, this can occur even when none of the cloud's parts are below freezing point. The disparity between convecting and stable clouds is believed to stem from the fact that convection generates small-scale turbulent motion. This turbulence facilitates the merging of microscopic water droplets (referred to as "visible moisture") into raindrops.

The concept of convective clouds aiding in raindrop formation has a long history, with [78] being a significant contribution that includes references to earlier works. However, a comprehensive theory explaining this phenomenon has proven elusive, making it a subject of extensive ongoing research as recently reviewed in [80].

In this direction we study in Section 1.2 and Chapter 2 the time of formation of rain drop, declined as a loss of total mass in the truncated density evolution of particles with masses $m = 1, ..., M$, representing the typical raindrop mass.

$$\tau(f.) := \inf\{t \geq 0 \mid \sum_{i=1}^{M} \int f_i(t, \xi) d\xi \leq \mathcal{M}_0\},$$

where $\mathcal{M}_0$ is a reference threshold and ξ are the set of active variables for the particles' density. The relation to the small scale turbulence, derived in Chapter 2, propose a prime example of dependence between the turbulence parameter of the fluid and the rain shower initialization.

1.2 Tracer particles: a simple numerical study

Even though our goal is to understand the theoretical formulation of collision rate for inertial particles in a turbulent fluid, from particle system to a PDE formulation of the problem, we start our journey a little far back.

We first consider a system of tracer particles in a turbulent fluid, i.e. $\phi_p \equiv \phi_f$. For this system theoretical results on the limiting equation of the density and the structure of the collision rate due to the advection of the fluid, in the case of probabilistic rate of collision, are derived in [37] and Appendix A.

In this section we propose, as a motivating example, a small numerical study on the time of coagulation of tracer particles subjected to two different velocity field modelling a fluid in which they are embedded.

In the first case we suppose that the field act independently on each particle akin to a Brownian motion, while in the second case we propose a modelling of the fluid in which the particles are embedded motivated by works of Majda [63], Flandoli and his collaborator [32, 34, 33].

The reason for such experiments is to understand the effect of turbulence on the coagulation of particles in the simplified context of tracer particles with a hard sphere collision, i.e. collision happens as soon as there is a contact between particles, motivating the study of a rigours theoretical definition, via density function, of the coagulation rate,

other meaningful quantities or, alternatively, the direction in which a suitable system can be constructed to investigate the aformationed properties.

1.2.1 Numerical Simulation: First Time Rain Generation

We focus our study on the behavior of the first formation time of a raindrop in cloud, i.e.

$$\tau_f := \inf\{t \geq 0 | \exists i \in \mathcal{N}_t,\ R_t^i >= R_{rd}\}, \tag{1.2.1}$$

where R_t^i is the radius of the $i-th$ particle at time t and $R_{rd} := 4 \cdot 10^{-4}$ is the radius of the typical raindrop in our simulation. While $\mathcal{N}_t$ are the surviving particles at time t, with $\mathcal{N}_t \leq N$.

Main result of this computation is the production of decay estimates, numerical and theoretical, in the formation time of droplet respect to the different turbulence parameter identified in the modelling of the fluid.

The complete setting we are going to consider for our tracer particles is the following

$$dX_t^i = \varepsilon_{rf} \sum_{k \in K} \sigma_k(X_t^i) \xi_t^k dt + \varepsilon_{bm} \sigma dB_t^i, \tag{1.2.2}$$

for $i = 1, ..., \mathcal{N}_t,\ \mathcal{N}_0 = N \in \mathbb{N},\ \sigma \in \mathbb{R}$, simulated with an Euler-Maruyama scheme.

The parameter $\varepsilon_{bm},\ \varepsilon_{rf} \in \{0, 1\}$ select the setting in which we investigate the formation time τ_f: a pure Brownian case or a random field driving the particles.

The domain in which we have done our simulation is the due dimensional torus $\mathbb{T}^2 = [-2, 2]^2/\sim$, adimensional, with periodic condition on the border. The intuition is to represent a zoom in inside the cloud and we assume that as the particles move they are replaced with probability one with particles of almost the same size.

Concerning the random velocity field in which the particles moves, it is defined as the stochastic process $\mathcal{U}(t, x)$ with the following form

$$\mathcal{U}(t, x) = \sum_{k \in K} \sigma_k(x) \xi_t^k \tag{1.2.3}$$

$$\sigma_k(x) = \frac{1}{2\pi} \frac{(x - x_k)^\perp}{|x - x_k|^2},\ (a, b)^\perp = (b, -a)$$

where points x_k are fixed and selected with a uniform distribution over the considered domain. This choice represent small vortex patch akin to the vorticity of the turbulent flow in which the droplet are submerged, [33]. We regularize the field with the following: $\sigma_k(x_k) = 0$.

The real-valued stochastic processes ξ_t^k are Ornstein-Uhlenbech that satisfy:

$$d\xi_t^k = -\lambda \xi_t^k dt + \lambda dB_t^k,\quad \xi_0^k = 0,\ k = 1, ..., K.$$

which we have also simulated with an Eulero-Murayama scheme and used the result to compute 1.2.2.

To every particle X^i we associate a volume and, assuming as usual the raindrops to be spherical, we represent the radius and the volume in a bijection, i.e.

$$\forall i = 1, ..., N,\ V_t^i \sim \frac{4}{3}\pi (R_t^i)^3.$$

The initial condition of the particle, X_0^i, are sampled from a uniform distribution over the domain, while the initial volumes $V_0^i > 0$ are selected uniformly in the range of large droplet $\sim [10^{-5}, 10^{-4}]$.

On the rule of collision

Two real-droplets may collide and coalesce completely into one big real-droplet and this process is responsible for precipitation development.

Even though the coalescence process can be described in a probabilistic way, here we simplify our model and we put ourself in a setting of deterministic hard sphere: what we expect is that our $V_t^{i,N}$, of the $i-th$ particle, changes not in a continuous way, but with jumps proportional to the particle that i interact with.

Meaning that, when two particle interact with each other, they merge into one single particle. So that the volume of a particle increase only when collide with other rain droplets in a linear way. To state it clearly this is how our coalescence works:

1. Let $x_i,\ i = 1, ..., N$ the particles of the system, and denote R_i their radius;
2. For every couple (i, j) such that $|x_i - x_j| \leq R_i + R_j$ the coalescence happens in the following way:
   - If $V_t^{i,N} \geq V_t^{j,N}$ then
     - $V_t^{i,N} = V_t^{i,N} + V_t^{j,N}$;
     - $V_t^{j,N} = 0$ and the particle j is removed from the system.
   - Vice versa if $V_t^{j,N} > V_t^{i,N}$.

At last, concerning the number of particles, we performed our simulation with $N = 10^3$. Finding the right time step was challenging, since the position of the particle is discrete and as such we could lose interaction between particle in the motion of the rain droplets, causing numerical error and inconsistency in the behaviour of the formation time. After few trials we set our parameter $\Delta t = 10^{-4}$ to have a second order error and a control on the collision.

1.2.2 Pure Brownian Movement

In this small section we analyze the particle system under the action of independent Brownian motion attached to the droplets. We set $\varepsilon_{rf} = 0, \varepsilon_{bm} = 1$ in 1.2.2 and we reduce the model to the motion equation given by:

$$dX_t^i = \sigma dB_t^i,$$

where X_0^i are drawn from a uniform distribution over $\mathbb{T}^2$ and $\sigma \in \mathbb{R}$.

The radius of the particles are selected in such a way that a raindrop is created as soon as the value it the threshold

$$R_t^i \sim 4 \cdot 10^{-4},$$

and the radius R_0^i of the starting volume of the rain droplets are drawn from a uniform distribution between values 10^{-5} and 10^{-4} smaller than a real raindrop.

We wan to analyze the formation time τ_f dependent on the intensity σ of the independent Brownian motions. To do so, for each parameter, we have simulated 200 times the particle system, collecting the time formation in a time series from which we extract the mean time. In detail we have, calling N_r the number of repetition, T_f^i the formation time of the $i-th$ simulation, the following:

$$N_r = 200, \;\; T_{mean} = \mathbb{E}[T_f] \sim \frac{1}{N_r}\sum_{i=1}^{N_r} T_f^i, \forall \sigma \in \Sigma.$$

Where $\Sigma := \{0.1, 0.2, 0.3, 0.4, 0.5, 0.6, 0.7, 0.8, 0.9, 1\}$, is a partition of the reasonable interval, $[0, 1]$, for the intensity of a realistic Brownian motion.

We selected $dt \sim 10^{-4}$ through the simulations.

A simplified theoretical reasoning

Before showing the numerical result, we show a theoretical reasoning on a simplified model that can explain the expected result in such a model.
Let us consider two particles moving subjected to independent Brownian motion with different initial condition: $\sigma W_t^1 + x_1$, $\sigma W_t^2 + x_2$ on the unitary Torus.
Call $x_0 = x_1 - x_2$ and define the random time

$$\tau_{\sigma,x_0} := \inf\{t \geq 0 : |\sigma W_t^1 - \sigma W_t^2 + x_0| \leq \varepsilon\}$$

which is linked to our formation time, since coalescence happens when two raindrops are near depending on a set threshold.
Then we ask the question: how σ impact the collision time of particles?
This quantity cannot be independent from σ, indeed call $B_t = W_t^1 - W_t^2$, this is a new Brownian motion, with intensity dependent from the dimension (but fixed), so without loss of generality we fixed it at 1.
Thus we consider the quantity τ_{σ,x_0}:

$$\begin{aligned}\tau_{\sigma,x_0} :&= \inf\{t \geq 0 : |\sigma B_t + x_0| \leq \varepsilon\} \\ &= \inf\{t \geq 0 : |\sigma B_{\sigma^2 t/\sigma^2} + x_0| \leq \varepsilon\} \\ &= \inf\{t \geq 0 : |W_{\sigma^2 t} + x_0| \leq \varepsilon\} \\ &= \tau_{1,x_0}/\sigma^2.\end{aligned}$$

Here we have used the auto-similarity of the Brownian motion.
What we recover is that there is an inverse quadratic dependence of the formation time with the intensity of the Brownian motion moving the particles. That we can express in a compact form as

$$\mathbb{E}\left[\tau_{\sigma,x_0}\right] \sim \sigma^{-2}.$$

Results on Regression

Let's start showing the result table 1.1 of the mean formation time and the standard deviation, in dependence of Brownian intensity $\sigma \in \Sigma$, of the simulated system. Note that we express the result in iteration, to obtain the simulation's time we need to multiply the epoch with the time step Δt.

Following the theoretical background, not only we expect that at the increase of the fluctuation our formation time decrease, but we also expect to find a quadratic inverse dependence with the intensity of the diffusion, i.e.

$$\mathbb{E}\left[\tau_f(\sigma)\right] \sim \sigma^{-2},$$

where we have highlighted the dependence on σ for τ_f.

As we can see from the table, there is a significance decay in the mean time as the intensity grows, and, as expected, the standard deviation became smaller.

Brownian intensity	Mean time ($\times\Delta t$)	Standard Deviation ($\times\Delta t$)
1	636	114.9043
0.9	641.4	119.8025
0.8	691.5	93.29014
0.7	734.9	170.0514
0.6	808	165.7607
0.5	917.6	234.5115
0.4	1086.9	312.3816
0.3	1569.8	260.9294
0.2	2896.5	387.9338;
0.1	4567	434.2

Table 1.1: Brownian diffusion coefficient and the respective mean time of formation

In fact, as σ grows the initial condition of the system became less and less important for the mean formation time, as we can see as the standard deviation decrease as σ increases.

To understand the decay we proceed our analysis with a quadratic and logarithmic regression on the model. In Figure 1.1 we can see plotted, (a), the decay of mean formation time that shows the time decay in dependence with the increase in σ, intensity of the Brownian motions. We can appreciate the stabilization of the randomness in the standard deviation, plotted as black bar in figure.

First, we performed a quadratic regression, for which we show the results in Figure 1.1 (b) as a Lin-Log plot respect τ_f^{-1}. We can already notice how the behavior of the numerical data, interpolated in red, fit the regression line in blue and the most significant error are in the very small regime of $\sigma \sim 0.1$, since the particle are almost still in their motion and the dependence from the randomly generated data is stronger. The regression show a residual plot without any particular structure, with a residual standard error equal to 0.5232, the explained variance, or R-square, equal to 0.992 and a summary that agrees with our conjecture on the quadratic decreasing of time respect to the intensity of the noise with a p-value $< 10^{-8}$.

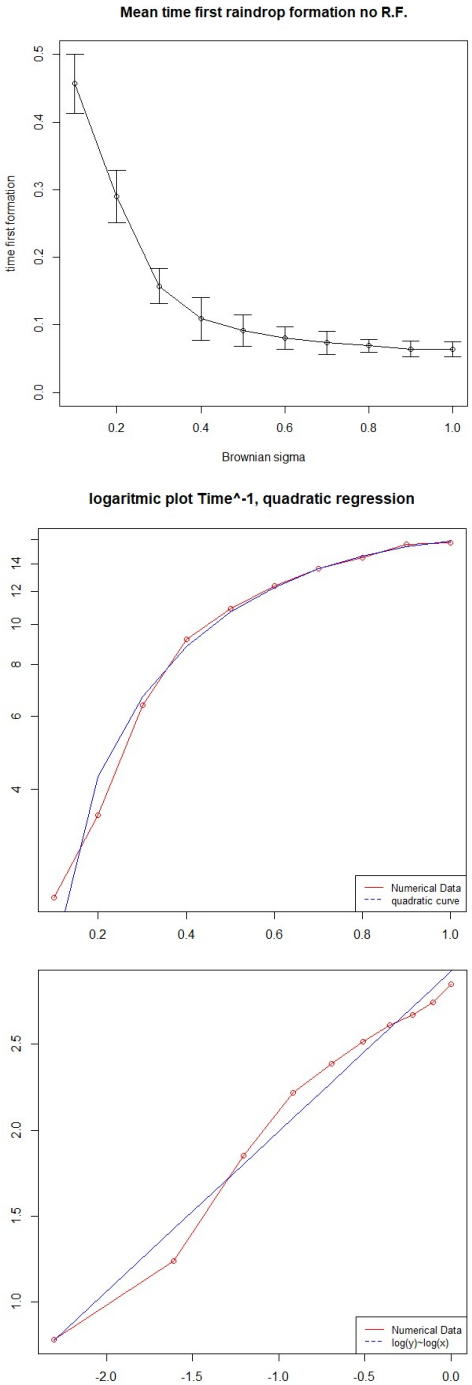

Figure 1.1: On the x-axis the Brownian intensity σ^2, on the $y$axis τ_f^{-1}. From top to bottom: (a) Plot of Brownian Intensity/Formation time that shows the time decay in dependence with increase in σ, intensity; (b) Linear-log plot: quadratic regression, in red the interpolated numerical data and in blue the regression curve;(c) log-log plot: logarithmic regression, in red the interpolated numerical data and in blue the regression curve with slope 1.

To validate our results, we concluded the analysis with a logarithmic regression to capture lower order power and fluctuation in the intensity dependence of the exit time. The results in Figure 1.1 (c) confirm how the behavior of the numerical data, interpolated in red, fit the regression line, in blue, in accordance to the quadratic regression. Small fluctuations around the regression line can be appreciated, showing lower order dependencies on the intensity, but the residual plot showing no structures with a standard error of 0.1, an R-squared equal to 0.979 and a p-value $< 10^{-8}$, agrees with the hypothesis

$$\mathbb{E}[\tau_f^\sigma] \sim \sigma^{-2}.$$

Thus, at the level of tracer particles with an hard collision rule of coagulation, we observe a decrease in the time needed to obtain formation of larger particles quadratically proportional to the parameter of the noise driving the particles.

Even though this first simple example is not in itself fundamental, is a primer example of the phenomenon we are trying to understand in this work: an increase in turbulence or temperature can, in principle, increase the coagulation of particles moving in a field.

1.2.3 Random Field Movement

Motivated by the reasonable result of the previous section, and expecting that the modelling of the velocity field $\mathcal{U}(t,x)$ defined in 1.2.3, as shown in [35, 33], is close to a Brownian motion with a precise variance acting on the particles.

A such, in this section we are going to analyze the particle system under the action of this velocity random field to see if a scaling on the parameters of this noisy fluid velocity can be found. We considered the system 1.2.2, with $\varepsilon_{bm} = 0,\ \varepsilon_{rf} = 1$, for the position of the particles

$$dX_t^i = \sum_{k\in K} \sigma_k(X_t^i)\xi_t^k dt$$

where X_0^i are drawn from a uniform distribution over $\mathbb{T}^2$ and $K \in \mathbb{R}$.

We recall that the velocity random field in which the particles moves, it is defined as the stochastic process $\mathcal{U}\,(t,x)$

$$\mathcal{U}\,(t,x) = \sum_{k\in K} \sigma_k\,(x)\,\xi_t^k$$

$$\sigma_k\,(x) = \frac{1}{2\pi}\frac{(x-x_k)^\perp}{|x-x_k|^2},\ (a,b)^\perp = (b,-a)$$

where points x_k are fixed and selected with a uniform distribution over the considered domain. The real-valued stochastic processes ξ_t^k are Ornstein-Uhlenbeck that satisfy:

$$d\xi_t^k = -\lambda\xi_t^k dt + \lambda dB_t^k,\quad \xi_0^k = 0,\ k = 1,...,K.$$

with $\lambda \in \mathbb{R}$ that represents, with K, the two investigated parameters for the turbulent fluid velocity.

A theoretical conjecture

Before moving to the numerical results, we briefly illustrate a theoretical conjecture on what we expect to find in the next section when we are assuming a hard collision regime on the particles. Following the idea from [35, 34, 33] in which a fluid dynamical equations with a transport noise of the form 1.2.3 converges to deterministic viscous equations such that the viscosity is enhanced by the turbulent random field.

For this reason, since the instantaneous hard collision does not have a direct interpretation as a rate in the Smoluchowski, we approximate the density of our particle system withe the associated Fokker-Planck equation (see Appendix A)

$$\partial_t \rho_t + \sum_{k \in K} \left(\sigma_k(x, v) \cdot \nabla_x \rho_t\right) \xi_t = 0$$

Under suitable assumption we apply the Galeati limit and the solution of such coagulation PDE is close to the solution of the linear Fokker-Plank associated to the Brownian system, i.e.

$$\partial_t \overline{\rho}_t + \frac{\kappa^2}{2} \Delta \overline{\rho}_t = 0$$

where $\kappa := \kappa(K, \lambda)$ depends on the parameters of the system in study.

We expect that, albeit less impactful than independent Brownian motion attach to each particles, the first exit time depends on the random field parameters again as an inverse power

$$\mathbb{E}\left[\tau_f(\kappa)\right] \sim p(\kappa)^{-1}$$

where $p(\kappa)$ is a polynomial at most of degree 2.

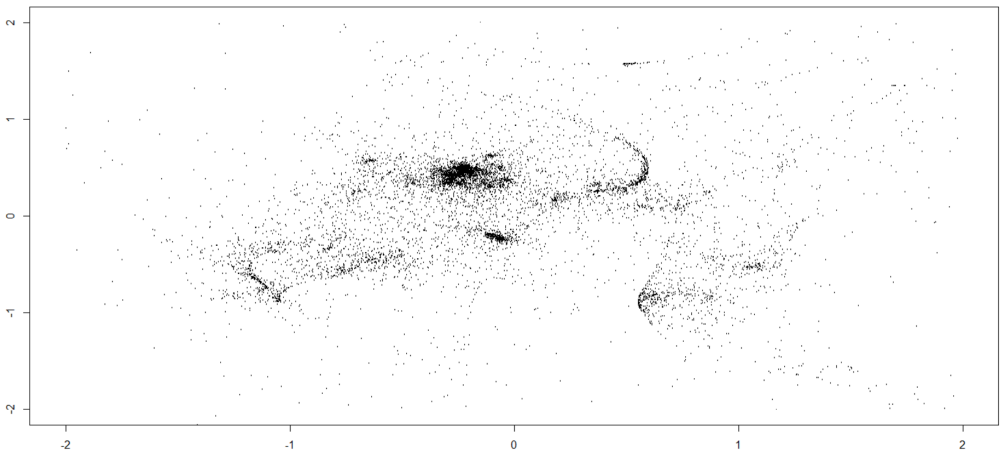

Figure 1.2: Snapshot of particle system dynamics: we can observe the cluster formation obtained from the presence of the vortex. We expect that such cluster, and the randomness of the Ornstein–Uhlenbeck process, are the reason for the decrease in time of rain formation.

1.2.4 Random Field Analysis: Non-Linear Regression

We divide the analysis in two main parts. We start fixing the intensity of the Ornstein-Uhlembeck processes and varying the number of vortex in the cloud; later we fix the vortex number and move the intensity of the environmental stochastic processes.

Following the previous reasoning we expect that our formation time depend with at most a square inverse power with the number of vortex and intensity of the random processes

$$\mathbb{E}\left[\tau_f(|K|,\lambda)\right] \sim p(|K|,\lambda)^{-1},$$

where we have highlighted the dependence on the parameter, where for $|K|$ we intend the cardinality of K.

From the theoretical conjecture in the previous subsection, we expect that as vortex increase, so does linearly the covariance matrix of the noise, resulting in a square decay for the exit time τ_f. While λ model the temporal structure of the phenomena, thus we expect that the effect is smaller on the vector fields σ_k with a inverse decay trend $\sim \sqrt{\lambda}$.

Fixed intensity λ

We analyze here the case in which the intensity of the noise is fixed, to a high value, and the number of vortex in the field changes. We'll see, as claimed at the start of the section that the decay is visible when we increase the number of vortex patches σ_j interacting with the particles. We show here regression that support the conjecture of a polynomial decay of order 2 respect the variable $|K|$.

number of vortex	Mean time	Standard Deviation
190	637.5	180.43
180	659.2	173.4409
170	669	202.1361
160	693.3	190.2665
150	762.8	200.2787
140	796.4	293.6144
130	841	258.6469
120	884.1	252.5955
110	1071.2	448.025
100	1141.2	640.7483
90	1156.4	472.1712

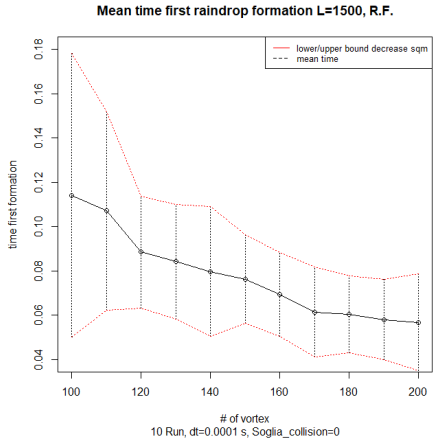

Figure 1.3: **Left:** table of time decay as vortex number increase and as such the number of vortex in the system grows. Mean time and Standard deviation decays accordingly to the growth of $|K|$, number of vortex patches; **Right:** The black line represent the mean time varying the number of vortex, while the red strip are the upper bound and lower bound of the standard deviation.

We note that the initial condition produce a very fluctuating system when the vortex number is small and the particles moves very slowly. This is expected, since the collision

are reduced and the random initial condition became dominant in the system. This is shown in the high variance that decreases as soon as the vortex number increase.

In the simulations we fixed $\lambda = 1500$, the reason is twofold: first, using the formulation of the Ornstein-Uhlembeck process ξ_t^λ, at the increase of the intensity we converge closely to a Wong-Zakai type of result, hence recovering a fluctuating white noise with correlation in space due to the vortex patches $\sigma_k,\ k \in K$. Second, this guaranties us that the particles moves with sufficient high enough speed, making sure that collisions of droplet can be observed outside of the first time iteration in which the initial condition dominates.

In Figure 1.3 we see the decay in the exit time τ_f at the increase of the vortex patches $|K|$, suggesting as expected from theory. We performed a quadratic regression from which the residual plot showed no sign of structure. The analysis show a great adherence of the data to the regression, with an explained variance of ~ 0.98, a residual error of 0.1 and a global p-value $\sim 10^{-7}$ that suggest that our hypothesis on the decay is valid.

To conclude and validate further our conjecture, in Figure 1.4 $(Right)$, we perform a logarithmic regression. The analysis is consistent with the quadratic regression performed and showed a good R-squared value of 0.98. No significant structures were found in the residual plot and the value of the regression supported our hypothesis of a quadratic decay in the time, with small fluctuation due to the randomness of the initial condition that stabilize at higher vortex number.

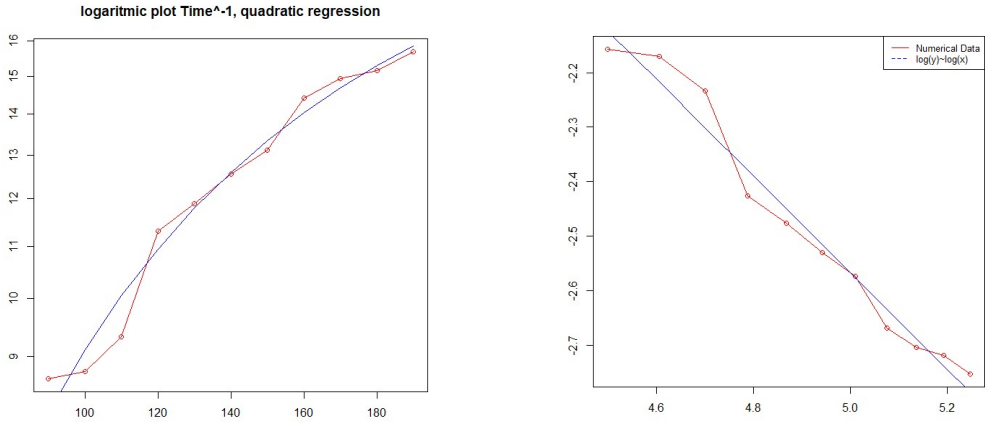

Figure 1.4: On the x-axis the number of vortex at intensity $\lambda = 1500$, on the y-axis τ_f^{-1} and τ_f respectively. **Left:** Lin-Log plot of quadratic regression with fixed intensity and varying vortex number; **Right:** Log-Log plot for Logarithmic regression with fixed intensity and varying vortex number with slope ~ -1.

Fixed Vortex patches $|K|$

We analyze, now, the case in which the number of vortex patches is fixed, while the intensity of the Ornstein-Uhlembeck, defining the temporal structure of the random field, can change freely. Performing statistical analysis, even with few sample, We'll see as expected due to the less effect of the time structure, that tend to delay the coagulation, a decay in the exit time τ_f respect to λ, but with a degree less than 2.

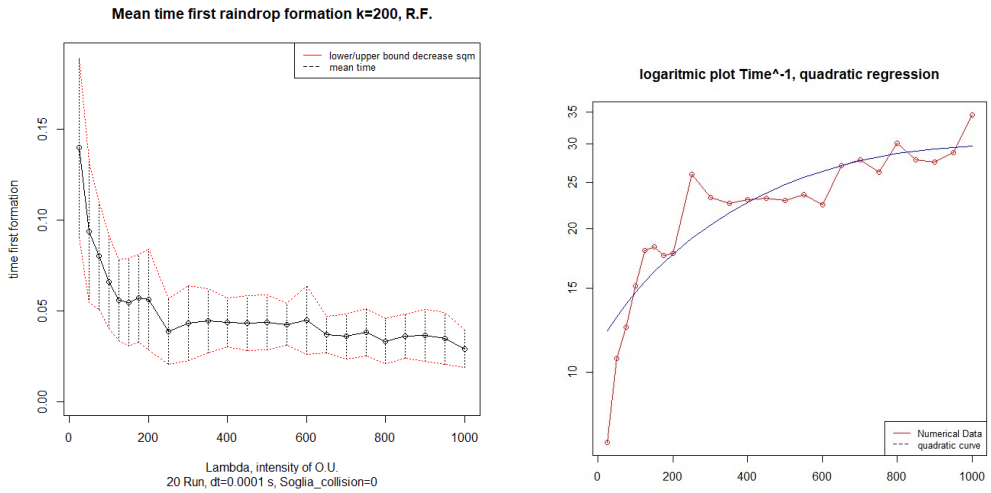

Figure 1.5: On the x-axis λ at fixed vortex number 200, on the y-axis τ_f and τ_f^{-1} respectively. **Left:** numerical plot of mean time with standard deviation. It is shown a decay in time when the intensity increase, with also a decrease in the standard deviation; **Right:** Lin-Log plot quadratic regression of mean time with varying λ, fixed vortex number, showing a different behavior.

We fix the number of vortex patches $|K| = 200$, the choice is made arbitrary after few trial, to obtain a fast coagulating system for the required simulation to be made even with very slow random field intensity. More so, the selected number of vortex patches already showed a nice decay in time, as seen in previous section.

In Figure 1.5 $right$, we performed a quadratic regression, showed in lin-log plot. The residual error was higher, of order 2.7 and the explained variance was overall less than 0.83, even with high intensity parameter that should make coagulation faster. Even though, as showed in Figure 1.5 $left$, that the decay in time is present at the increase of λ, the regression suggested as expected from the intuition, that the influence of the intensity in the time structure is less strong than the number of vortex-like structures in the random field in producing coagulation.

The analysis show a less degree of understanding of the data, and while R-squared is still relatively high, we expect that power of lower order describe the decay curves in a more robust way. To see if a regression with lower power of the parameters can explains better the decay of time formation we performed a logarithmic regression, plotted in Figure 1.6. From the analysis we see that more structure is captured when this type of dependence is conjectured. In fact no bound on the decay exponent is present and as such the analysis is more flexible. In particular the explained variance is around 0.91, while the error is reasonable of order 0.1 and intercept ~ 1, suggesting that a non linear regression of the form $\sim a/(1 + b \cdot \lambda)$ is the right expected decay for the time as a function of the intensity parameter.

Lastly, to pursue this idea and get a more precise estimation on the behaviour of the first formation time $\tau_f(\lambda)$, with fixed number of vortex patches, we performed a non linear regression on a more refined sample of intensity. We iterate the system for intensity $\lambda \in$

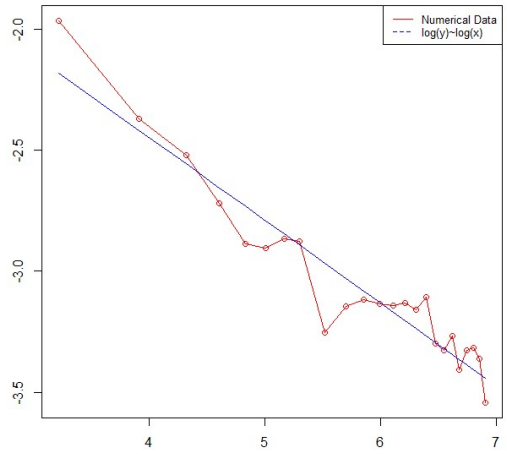

Figure 1.6: On the x-axis λ at fixed vortex number 200, on the y-axis τ_f. Logarithmic Regression: Log-Log plot regression mean time with varying λ, fixed vortex number.

$[100, 1100]$ with a step of order 10.

After the logarithmic regression, we expect a dependence on the parameter of the form $\sim \frac{a}{(1+b\lambda)}$. For this reason we set $a_{in} = 0.08,\ b_{in} = 0.048$ starting parameter, selected from the value at $\lambda_0 = 100$ and the logarithmic regression, and we perform a hyperbolic non linear regression shown in Figure 1.7 $left$.

We arrive at convergence with value $a = 0.06,\ b = 0.001$. with residual error equal to 0.0029 and a correlation with the numerical data equal to 0.79. More so the achieved tolerance of convergence is of order 10^{-6}. As we see in Figure 1.7 $right$, no structure is present in the residual plot and the decay is captured by the regression curve.

In conclusion, all this analysis suggest that when the intensity of the process ξ_t^λ increase we have a decay in the exit time τ_f, but since the noise interact only in the time structure the decay has lower degree, slowing the global behavior of τ_f respect to the classical brownian case.

1.2.5 Conclusion and expected results

In conclusion, our numerical toy experiments, performed on a particle system subjected to two random field approximating a fluid flow, have provided us valuable insights into the relationship between coagulation dynamic and turbulence of the velocity field. Through our investigation, we have discovered that turbulence plays a significant role in influencing the coagulation process, ultimately accelerating the collision time necessary to obtain larger particles.

The downside of this approach, other then not being perfectly comparable with physical data, is that the setting of instantaneous coalescence present a unique challenge in studying the probability density function (PDF) of the particles. Since objective of the thesis is to produce a theoretical framework for the coagulating process of particle in fluid, we had to approximate our process and pass to a probabilistic rate in the coagulating dynamics.

A such, in the next section, given the difficulty associated with analyzing the PDF in

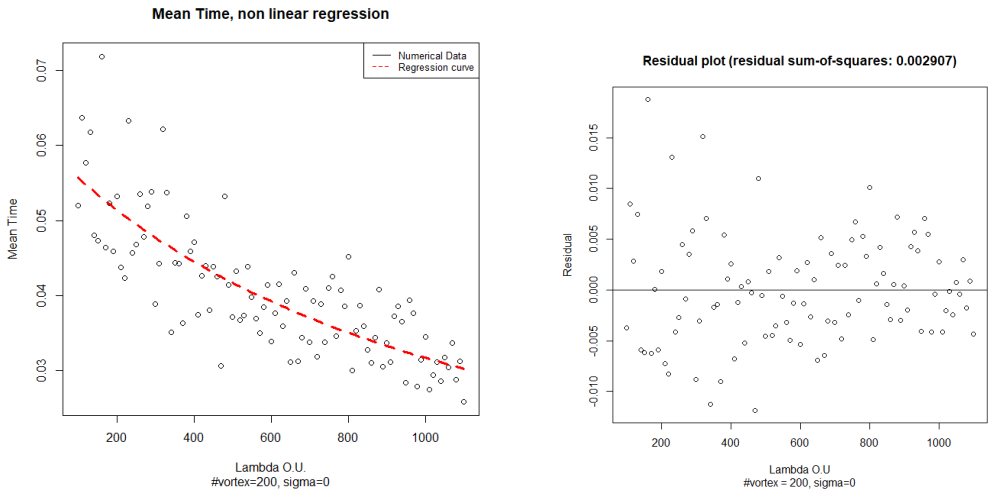

Figure 1.7: Left:Non-linear Regression for moving λ and fixed vortex. Expected decay as $\sim \lambda^{-1}$; Right: Residual plot. There is no presence of structure in the residual.

such cases, we directed our focus towards a scaling limit approach. By recovering the standard Smoluchowski diffusion equation, we could test, numerically, on the solution of our continuous density a more comprehensive understanding of coagulation dynamics. This approach allows us to gain a deeper insight into the behavior of particles and their interactions, shedding light on the underlying mechanisms that govern coagulation processes, more so, finding what does not work in the standard modelling of tracer particles and how to pass to kinetic system.

1.3 A negative result and a new paradigm

In this section, we present a significant finding that challenges the applicability of the PDF framework for tracer particles in turbulent fluid.

Specifically, we demonstrate numerically that the turbulent fluid does not contribute to an improved coagulation process at the level of the spatial-volumetric density, even when the numeric in the hard collision framework show otherwise. The reason must be traced back to the derivation of the coagulation rate in the classical Smoluchowski equation: in fact, without prior modifications based on physical reasoning, it remains unaltered in the limiting Fokker Plank equation, thus going against intuition and experiments that turbulent fluid helps in the realization of an enhanced coagulation.

1.3.1 Smoluchowski equation with diffusion

Starting from the seminal work of Smoluchowski [83] and Aldous [2] a lot of interest has been posed to the description of density function in coagulating processes.

In this direction, one of the main results was provided by Hammond and his collaborator [46, 48, 47], extending rigorously the Smoluchowski equation to a PDE with space

variable, as a scaling limit of a particle system undergoing pairwise coagulation (with an apriori rate, dependent only on the masses).

In particular, they provided a model of time evolution probability distribution $\{f_m(t,x)\}_{m=1}^{\infty}$ of diffusing particles of different sizes $m \in \mathbb{N}$. Particles undergo pairwise coagulation with coagulation rate $\alpha(m,n)$, and their resulting equation could be read as follows

$$\begin{aligned}\partial_t f_m(t,x) =& \kappa \Delta f_m(t,x) + \sum_{n=1}^{m-1} \alpha(n, m-n) f_n(t,x) f_{m-n}(t,x) \\ & -2 \sum_{n=1}^{\infty} \alpha(m,n) f_m(t,x) f_n(t,x), \quad t>0,\ x \in \mathbb{T}^d,\ m \in \mathbb{N}.\end{aligned}$$

In this setting, particle are moved independently subjected to Brownian motions. Indeed, this is not enough to understand the behavior of particle moving into a fluid velocity flow.

In [30], Flandoli and Huang, proposed a new model in which particles advected by fluids may coagulate upon spending time near each other. At particle level, motivated from works of Boussinesq [15] and Majda [63], the influence of a large-scale turbulent flow is modelled as a common transport noise:

$$\dot{\mathcal{W}}(t,x) = \sum_{k \in K} \sigma_k(x) \dot{W}_t^k \tag{1.3.1}$$

a white noise in time with non trivial spatial covariance where $\{\sigma_k(x)\}_{k\in K}$ countable divergence-free smooth vector fields, $\{W_t^k\}_{k\in K}$ independent 1-d Brownian motions. We define the covariance matrix $\mathcal{Q}(x,x) := \sum_{k\in K} \sigma_k(x) \otimes \sigma_k(x)$ derived by easy computation on the transport-type noise.

Under suitable and natural choice $\{\sigma_k\}_{k\in K}$, i.e Kraichanan type covariance [33, 58], we have $\mathcal{Q}(x,x) \equiv \kappa I_d$, for enhanced diffusion coefficient $\kappa > 0$ (see Chapter 2, and [35] with reference therein).

Remark 1.3.1. As a remark, we note that this noise is akin to the one studied in Section 1.2. In fact, consider $k \in K$ and $\xi_t^{k\lambda}$ Ornstein Ulhembeck satisfying the SDE

$$d\xi_t^{k,\lambda} = -\lambda \xi_t^{k,\lambda} dt + \lambda dB_t^k,\ t \geq 0, \lambda > 0,$$

with B_t^k one dimensional Brownian motion defined on a probability space in the usual way. We define a correlated in time and space environmental noise

$$\sum_k \sigma_k(x,m)\, \xi_t^k dt$$

Then in the limit for high λ, the two environmental noise, the one defined in 1.3.1 and in Section 1.2, are close thanks to Wang-Zakai' theorem, implying that

$$\xi_t^{k,\lambda} \to_{\lambda\to\infty} W_t^k,$$

with W_t^k one dimensional Brownian motion.

Using technique from [48], Ito-Stratonovich corrector and the Tanaka trick, from particle system interacting as in Appendix A, a limiting SPDE form of Smoluchowski equation is obtained

$$\begin{aligned} df_m(t,x) =& \Delta f_m(t,x)dt + \sum_{n=1}^{m-1} \alpha(n,m-n) f_n(t,x) f_{m-n}(t,x)dt \\ & -2\sum_{n=1}^{\infty} \alpha(m,n) f_m(t,x) f_n(t,x)dt - \sum_{k\in K} \nabla f_m(t,x)\cdot \sigma_k(x)\, dW_t^k \\ & + \mathrm{div}\left(\mathcal{Q}(x,x)\nabla f_m(t,x)\right), \quad m\in\mathbb{N} \end{aligned} \tag{1.3.2}$$

Considering a suitable formulation of the environmental noise and performing a Galeati limit, a Smoluchowski diffusion equation, akin to the one proposed in [48, 46] is obtained, but the effect of the turbulent fluid has produced a turbulent enhancement represented by the second order elliptic operator preserved in the limit, i.e.

$$\begin{aligned} df_m(t,x) =& \Delta f_m(t,x)dt + \sum_{n=1}^{m-1} \alpha(n,m-n) f_n(t,x) f_{m-n}(t,x)dt \\ & -2\sum_{n=1}^{\infty} \alpha(m,n) f_m(t,x) f_n(t,x)dt + \mathrm{div}\left(\mathcal{Q}(x,x)\nabla f_m(t,x)\right), \quad m\in\mathbb{N} \end{aligned} \tag{1.3.3}$$

This is the main object of study of this section. We use this equation, with a constant rate of coagulation, to see if improvement in the mass displacement is obtained in dependence of the turbulence operator

$$\mathrm{div}\left(\mathcal{Q}(x,x)\nabla f_m(t,x)\right)$$

that we reduce to the form $\kappa\Delta f_m(t,x)$, when Q is of Kraichnan type.

A digression on the theoretical selection of the noise

As a remark, before stating the results, in the same spirit as [31, 32, 39], we explore more in detail some property of the environmental noise that we use to rpoduce the limiting equation.

Following the works on modeling of passive scalars [58], when considering the scaling limit of 1.3.2 to the Smoluchowski equation with diffusion 1.3.3, we consider a model of noise in the fluid which is delta-correlated in time, namely a white noise with a precise space dependence.

$$\mathbf{W}(t,\mathbf{x})\, dt = \sum_{k\in K} \sigma_k(\mathbf{x})\, dB_t^k \tag{1.3.4}$$

where $(\sigma_k(\mathbf{x}))_k$ is a family of smooth divergence free vector fields on the domain of the equation, and B_t^k are independent one-dimensional Brownian motions; K is, usually, a finite index set, but with suitable assumption we could consider also the case of countable family of smooth fields.

In this case, the term $\mathbf{W}(t,\mathbf{x})\cdot\nabla f_m(t,\mathbf{x})$ obtained in the convergence result of the particle system empirical measure, must be interpreted as a Stratonovich integral

$$\sum_{k\in K}\sigma_k(\mathbf{x})\cdot\nabla f_m(t,\mathbf{x})\circ dW_t^k. \tag{1.3.5}$$

Assume that the solution is sufficiently smooth so that the Stratonovich integral makes sense, then this is given by an Itô-Stratonovich corrector plus an Itô integral; precisely, is given by:

$$-\frac{1}{2}\sum_{k\in K}\sigma_k(\mathbf{x})\cdot\nabla\left(\sigma_k(\mathbf{x})\cdot\nabla f_m(t,\mathbf{x})\right)dt+dM(t,\mathbf{x})$$

where $M(t,\mathbf{x})$ is a (local) martingale. Follows that the Itô-Stratonovich corrector takes the form of an elliptic operator:

$$-\frac{1}{2}\operatorname{div}\left(\mathcal{Q}(\mathbf{x},\mathbf{x})\nabla f_m(t,\mathbf{x})\right)dt$$

where $\mathcal{Q}(\mathbf{x},\mathbf{y})$ is the space-covariance function of the noise

$$\mathcal{Q}(\mathbf{x},\mathbf{y})=\sum_{k\in K}\sigma_k(\mathbf{x})\otimes\sigma_k(\mathbf{y}).$$

As an example, we take the noise [58], which is relevant to numerical investigation, e.g. in the choice of the divergence-free field in the point vortex model for fluid [40]. For simplicity, assume the domain to be $\mathbb{R}^2$, but modifications on $\mathbb{T}^2$ are possible, see for example [35, 33].

Its covariance function is space-homogeneous, i.e. $\mathcal{Q}(\mathbf{x},\mathbf{y})=\mathcal{Q}(\mathbf{x}-\mathbf{y})$, with the form

$$\mathcal{Q}(\mathbf{z})=\nu k_0^{\zeta}\int_{k_0\le|\mathbf{k}|<k_1}\frac{1}{|\mathbf{k}|^{d+\zeta}}e^{i\mathbf{k}\cdot\mathbf{z}}\left(I-\frac{\mathbf{k}\otimes\mathbf{k}}{|\mathbf{k}|^2}\right)d\mathbf{k}.$$

The famous Kolmogorov 41 case follows if we take $\zeta=4/3$. Taking $k_1=+\infty$, then $\mathcal{Q}(\mathbf{0})=K\sigma^2$ where the constant K is given by

$$K=\int_{1\le|\mathbf{k}|<\infty}\frac{1}{|\mathbf{k}|^{d+\zeta}}\left(I-\frac{\mathbf{k}\otimes\mathbf{k}}{|\mathbf{k}|^2}\right)dk\quad.$$

We consider small-scale turbulent velocity fields depending on a scaling parameter and taking the scaling limit in 1.3.2, as in [33, 42]. In the case of [58] we have

$$k_0=k_0^N\to\infty$$

The result $\mathcal{Q}(\mathbf{0})=K\nu$ is independent of N, so that the Itô-Stratonovich corrector becomes equal to

$$\nu\Delta f_{m,t}(\mathbf{x}),$$

and simultaneously, we may have that the Itô term goes to zero, hence recovering 1.3.3.

Let us sketch the argument which explains why the Itô term may go to zero, in spite of the convergence to a finite non-zero limit of the Itô-Stratonovich corrector. Let ϕ be a smooth test function. One has

$$\mathbb{E}\left[\left(\sum_{k\in K}\int_0^T \langle \sigma_k \cdot \nabla f_{m,t}, \phi\rangle_{L^2}\, dB_t^k\right)^2\right] = \mathbb{E}\left[\sum_{k\in K}\int_0^T \langle \sigma_k \cdot \nabla f_{m,t}, \phi\rangle_{L^2}^2\, dt\right]$$

by the isometry formula of Itô integrals,

$$= \mathbb{E}\left[\sum_{k\in K}\int_0^T \langle f_{m,t}, \sigma_k \cdot \nabla\phi\rangle_{L^2}^2\, dt\right]$$

since $\operatorname{div}\sigma_k = 0$,

$$\begin{aligned}
&= \mathbb{E}\left[\int_0^T \int\int \sum_{k\in K} \sigma_k(x)\cdot\nabla\phi(x)\,\sigma_k(y)\cdot\nabla\phi(y)\, f_m(t,x)\, f_m(t,y)\, dxdydt\right]\\
&= \mathbb{E}\left[\int_0^T \int\int \nabla\phi(y)^T\cdot\mathcal{Q}(x,y)\cdot\nabla\phi(x)\, f_m(t,x)\, f_m(t,y)\, dxdydt\right]\\
&= \mathbb{E}\int_0^T \langle \mathcal{Q}\theta_t, \theta_t\rangle_{L^2}\, dt
\end{aligned}$$

where is the linear operator on vector fields with kernel $\mathcal{Q}(x,y)$ and $\theta_t(x) = \nabla\phi(x)\, f_m(t,x)$,

$$\leq \|\mathcal{Q}\|_{L^2\to L^2}\,\mathbb{E}\int_0^T \|\theta_t\|_{L^2}^2\, dt.$$

Now, one can prove uniform bounds on $\mathbb{E}\int_0^T \|\theta_t\|_{L^2}^2\, dt$ with respect to the scaling of the noise and one can choose a noise such that $\|\mathcal{Q}\|_{L^2\to L^2}$ goes to zero. Notice that in the Itô-Stratonovich corrector only the diagonal $\mathcal{Q}(x,x)$ counts, while the smallness of $\|\mathbf{C}\|_{L^2\to L^2}$ is related to the smallness of $C(x,y)$ when $x \neq y$.

1.3.2 A one dimensional counterexample

In the previous section we have derived a partial differential equation 1.3.3, akin to both Fokker-Plank and Smoluchowski, representing a coagulating system of tracer particles under the effect of a turbulent flow.

In this section we show, with few numerical counterexamples, how this system results to be too crude to investigate both the coagulation rate and mass displacement of the density trough time, and how to overcome this rigidity.

In the framework of tracer particles, the selection of the kernel $\alpha(m,n)$ in 1.3.3 is crucial and must be made beforehand, taking into account the fluid's characteristics to effectively incorporate its impact on the coagulation dynamics. The eddy diffusion's influence, obtained through Galeati's limit, represented by the operator $\kappa\Delta_x$, manifests as a diffusion of masses, hastening their movement and reducing the time they spend in close proximity. Consequently, the likelihood of coagulation within a given time unit diminishes.

To show this, we first identifies few objects and quantities, that in Chapter 2 will be studied in great details for a system of inertial particles, to understand the behavior of the space-mass system 1.3.3.

We recall that objective of this research is to find a link between turbulence parameters and decay of (random) mixing time, mass displacement and the computation of the coagulation rate between particles.

For the convenience of numerical simulations, we consider from now on only finitely many mass levels. That is, we close the set of equations into a finite system of PDE-s whose solution is $(f_1, f_2, ..., f_M)$, for some integer $M > 0$.

$$\begin{aligned} df_m(t,x) =& \Delta f_m(t,x)dt + \sum_{n=1}^{m-1} f_n(t,x) f_{m-n}(t,x)dt \\ & -2\sum_{n=1}^{M} f_m(t,x) f_n(t,x)dt + \text{div}\left(\mathcal{Q}(x,x)\nabla f_m(t,x)\right), \quad m \in \mathbb{N}, \end{aligned} \tag{1.3.6}$$

This amounts to replacing the $\sum_{n=1}^{\infty}$ in the loss term by $\sum_{n=1}^{M}$, with everything else unchanged. This correspond, in the particle system (Appendix A), to the fact that each particle's mass is restricted to $m_i \in \{1, 2, ..., M\}$.

The interpretation is that when the mass of a rain droplet exceeds the threshold M, it falls down (as rain) and hence exits the system. More so, it is natural to assume $\alpha(n, m) \equiv 1$ and using the Kraichnan covariance $\text{div}\left(\mathcal{Q}(x,x)\nabla f_m(t,x)\right) \equiv \kappa\Delta_x f_m(t,x)$.

Evolution of densities

Let us consider the system of equation in a slightly simple setting, yet amenable. Fix dimension $d = 1$ and the spatial doamin be the one-dimensional torus $\mathbb{T}^1$. We fix $M = 2$ and define the system as follow. Call $f_1 = u,\ f_2 = v$, then:

$$\begin{cases} \partial_t u = \nu\Delta u - u^2 \\ \partial_t v = \nu\Delta v + u^2 \end{cases} \tag{1.3.7}$$
$$u_0 = h(x),\ v_0 = g(x),\ x \in \mathbb{T}^1,\ t \geq 0.$$

where h, g are two positive probability functions. Mass of type 1 and type 2 can coagulate and does not interact in other way and this system represent a prototype in which tracer particles with enhanced spatial diffusion interact, without prior modification to the collision rate and the kernel of the Smoluchowski equation.

We simulate this system of equations with a finite difference method on the time interval $t \in [0, 1]$ with a partition of equally distributed points in time $\{t_j\}_{j=0}^{N}$. The space variable is identified as $x \in [0, 1]$ with the boundary identified and partition of point $\{x_k\}_{k=0}^{K}$.

We do the simulation with κ that satisfied the FCL stability, i.e.

$$\nu\frac{\Delta t}{(\Delta x)^2} < 1/2.$$

First, we consider an initial condition constant in space of the form $u_0 \equiv 1, v_0 \equiv 0$. We

see that in this case the solution is in fact the one of the system od ODE:

$$\begin{cases} \dot{u} = -u^2 \\ \dot{v} = u^2 \end{cases} \tag{1.3.8}$$

with same initial condition and periodic boundary.

In Figure 1.8, we simulate two solutions with constant initial condition and 2 different diffusion rate. This choice of the initial conditions show that there is no real dependence on the turbulence parameter. Without considering a coagulation rate directly dependent on the fluid velocity, which cannot be recovered from 1.3.3 in the tracer setting, no growth in dependence of the parameter ν is visible. The density of type 2 mass $v(t,x)$ increase independently in space.

As a second example, we consider an initial condition in which a space dependence is present, i.e. $u_0 = f(x),\ v_0 \equiv 0$, with $f(x)$ sinusoidal function, with periodic boundary

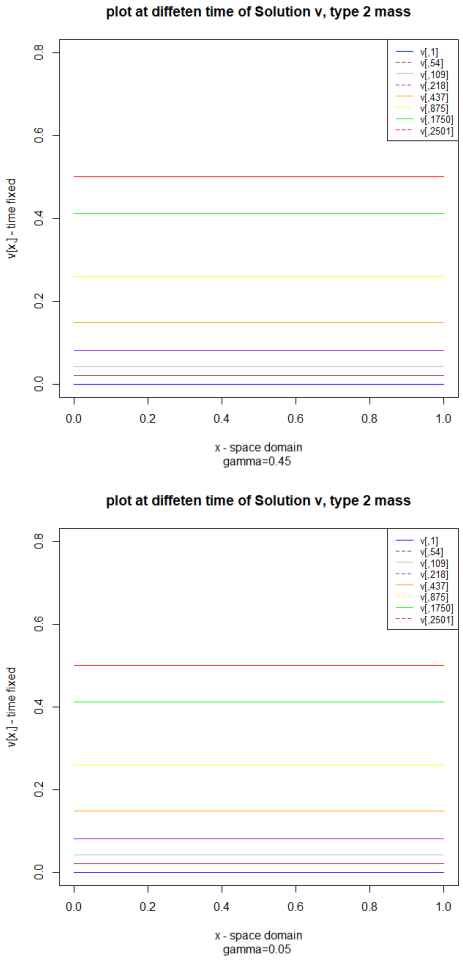

Figure 1.8: Side by side comparison of growth in time of v, mass type 2 solution for the system with different diffusion, respectively from left to right, $\nu = 0.45,\ 0.05$ and same constant initial solution $u_0 \equiv 1,\ v_0 \equiv 0$.

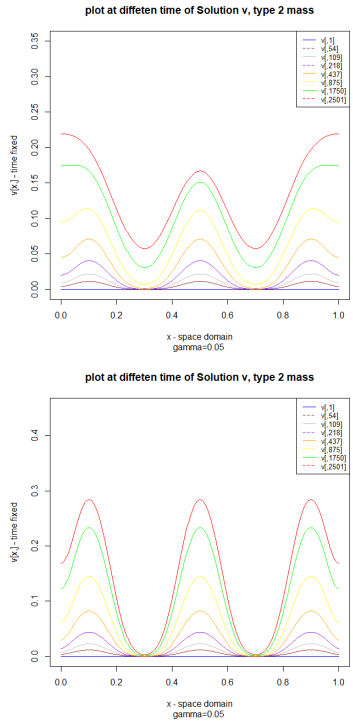

Figure 1.9: Side by side comparison of growth in time of v, mass type 2 solution for the system with different diffusion, respectively from left to right, $\nu = 0.45,\ 0.05$ and non constant initial condition $u_0 \equiv f(x),\ v_0 \equiv 0$.

condition. As before, we simulate the system with 2 different diffusion.

In Figure 1.9, we show two solution at different diffusion rate, with the initial condition u_0 that depends on the space domain. As a difference from system 1.3.8, we see a clear dependence on the diffusion rate, but there is no clear sign of a coagulation enhancement. In particular, considering the average over the space domain, no sign of improved coagulation or mass displacement is shown in the system. Suggesting that the the diffusion parameter κ in the crude space-mass Smoluchowski system works against the coagulation process.

Formation time

For this reason, as an analogous of the discrete formation time τ_f, defined in Section 1.2 equation 1.2.1, we define τ_κ which represent the first time the total density has put enough mass on effective rain drops:

$$\tau_\eta(f.) := \inf\{t \geq 0 \mid \sum_{i=1}^{M} \int f_i(t,x)dx \leq \mathcal{M}_0\}, \tag{1.3.9}$$

with $\mathcal{M}_0$ a positive constant.

We know that $\mathbb{E}\tau_f \to 0$ as κ^{-2}, when $\kappa \to \infty$ in the discrete system with instantaneous collision. So the question we ask is: does $\tau_\kappa(f.)$ has a behavior akin to the one

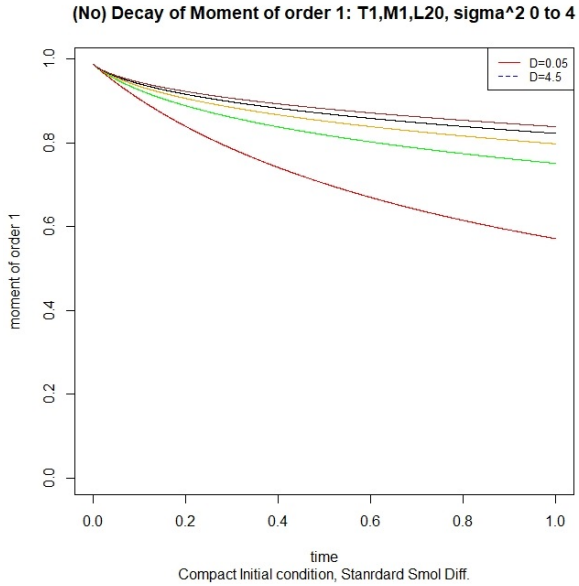

Figure 1.10: Plot of the decay of $\mathcal{M}_1(t)$ showing no enhancement in decay of the total mass with initial condition $f_1(0,x) = \mathbb{1}_{[-\frac{1}{2},\frac{1}{2}]}(x)$.

displayed by the tracer particles system?

To understand the effect of the turbulent velocity field on coagulation and drown conclusion on 1.3.9, we reverse the idea of the formation time and identify and build on a key quantity, $\mathcal{M}_1^\kappa(t)$ below, which is essentially the total mass left in the system at time t. Since $M < \infty$ this quantity measure the efficiency of coagulation by looking at how fast the mass decays in time, with respect to different values of κ.

To this end, we give a name to the Total Mass appearing in 1.3.9:

$$\mathcal{M}_1^\kappa(t) := \sum_{m=1}^{M} m \int f_m(t,x)\,dx. \tag{1.3.10}$$

We simulate the system of equation 1.3.6 on the one dimensional torus, limiting ourself to the study of $\mathcal{M}_1^\kappa$ with $M = 1$.

We set our initial condition as $f_1(0,x) = \mathbb{1}_{[-\frac{1}{2},\frac{1}{2}]}(x)$, producing solution with a finite difference scheme and a trapezoidal rule for the computation of the integral $\mathcal{M}$. We selected a range of parameter for $\kappa \equiv D \in [0,4]$, satisfying the FCL condition. The result is shown in Figure 1.10: as expected from the analysis of the density realization, we don't see an enhanced coagulation, more so a decrease in such phenomena. In red the curve for $\kappa = 0.005$ and blue the curve for $\kappa = 4.5$, showing the decrease in effectiveness of mass movement trough level, hence increasing the time needed to form fully fleshed rain drop.

1.3.3 How to overcome: probabilistic coagulation rate

Drawing conclusion from the previous simulations, we notice how conceptually and mathematically, the most difficult step in the program partaken in this thesis is to verify that diffusion enhancement leads to coagulation enhancement, namely, the fast increase of probability densities f_m for $m >> 1$ (large masses) for large diffusion coefficient. In fact, the model 1.3.6 turns out to be too crude, and numerically we cannot verify a coagulation enhancement.

we notice how to overcome this obstacle we already have all the ingredients, but we need to consider them at the beginning of the conceptualization of the model, even if this make computation more cumbersome. Here we propose this change of point of view that will be analyzed throughout the thesis.

We already know from Section 1.1 that the coagulation kernel, describing the probabilistic interaction of moving particles must depend theoretically from the difference of velocity of particles. This assumption, in the context of tracer particles was bypassed with an already approximated kernel, dependent only on the masses, that does not take into account all the nuances of the kinetic evolution due to turbulence at the level of the particle system, more so on the final density, making impossible to construct a rigours theory.

To be more precise, considering the rate of Coalescence of particles, we can think of two two typical mathematical models:

- Deterministic: two particles meet, they become a new particle with mass given by the sum of the masses and momentum given by conservation of momentum;
- Probability rates: two particles below a certain distance one from the other have a probability per unit of time to merge in one.

The Kernels in the Smoluchowski equations are the macroscopic footprint of such probabilistic rates.

In the realm of deterministic models, it is evident that coalescence invariably occurs at a specific distance, irrespective of the duration spent in close proximity.

However, when considering models based on rates in the space-mass system, there arises a limitation concerning their connection to turbulence. Coalescence transpires due to a probability per unit of time, which diminishes as the time spent by neighboring particles decreases.

This presents a stark contrast: models based on rates in the space-mass framework facilitate coalescence through slow moving particles. Regrettably, this contradicts the practical understanding of turbulence. To resolve this predicament, it is imperative to avoid favoring slow motion in the modeling process.

In the field of atmospheric physics [25, 26], it is commonplace to analyze the coagulation of cloud particles by employing a rate that is directly proportional to their relative velocity $\sim |v_1 - v_2|$ where $v_i,\ i = 1, 2$ are the velocities of two particles.

This factor is usually studied apriori with conceptual reasoning and then applied to a Spatial Smoluchowski equation, hence making impossible to derive the right coagulation dynamics directly from the density. More so, this factor, when multiplied by the time spent in close proximity, remains relatively constant on average, thereby ensuring a con-

sistent probability of coalescence. To solve this problem and incorporate both position and velocity variables, a new system of inertial particles is introduced.

1.4 Fundamental aggregation model: Inertial particles

Motivated by the negative results of Section 1.3.8 and the reasoning on how to overcome such obstacles, we go back to the foundation and propose an approach for particles that take into account their velocity, hence their inertia.

Here we'll describe the ideas both for the particle system and for the definition of coagulation rate, leaving the rigours computation to Section .1 and Chapter 2.

The model is composed of N moving particles, with position-velocity $\left(X_t^i, V_t^i\right), i = 1, ..., N$, embedded into a fluid with velocity $U\left(t, x\right)$. To each particle, we associate a mass $m_i(t)$ and radius $r_i(t)$, and we let these particles the possibility of coalesce. The motion of the particles before coalescence follows the Stokes' law and is given by

$$\begin{aligned} \frac{dX_t^i}{dt} &= V_t^i \\ \frac{dV_t^i}{dt} &= -\frac{1}{\tau_p}\left(V_t^i - U\left(t, X_t^i\right)\right) \end{aligned}$$

Note that this regime is valid when droplets have a density, ϕ_p, which is larger than the density of the fluid ϕ_f. As such, in this thesis we analyze setting in which $\phi_p/\phi_f >> 1$.

The fluid is idealized as the solution of

$$\begin{aligned} dU\left(t, x\right) &= -\frac{1}{\tau_f}\left(U\left(t, x\right)dt - dW\left(t, x\right)\right) \\ W\left(t, x\right) &= \sum_k \sigma_k\left(x\right) W_t^k. \end{aligned}$$

When two particles, with position X_t^i, X_t^j and masses m_t^i, m_t^j, are at distance

$$\left|X_t^i - X_t^j\right| \leq |r_i(t) + r_j(t)|,$$

they may aggregate, forming a new particle with mass $m = m_t^i + m_t^j$, while velocity agrees with the conservation of momentum.

To do so, they have a rate of coalescence, a probability to aggregate by unit of time, given by a function $\lambda\left(V_t^i, V_t^j\right)$ that, following the logic explained in the remarks below, Section 1.1 and atmospheric literature [25, 26, 90],with some idealizations, we take as

$$\lambda\left(V_t^i, V_t^j\right) \sim \left|V_t^i - V_t^j\right| / 2a.$$

Remark 1.4.1. At the beginning of our studies, illustrated in Section 1.3.8, it seemed natural to us, for simplicity, to assume this rate to be constant, that is, independent of V_t^i, V_t^j. Later, we understood that this assumption distorted reality because, during a "collision" between particles (collision = an event where they are in proximity for a short interval of time under the condition $\left|X_t^i - X_t^j\right| \leq 2a$), since the rate λ was constant, the probability

of coalescence was $\lambda\Delta t$, where Δt was the duration of the collision. This was intuitively absurd: we wanted each collision to result in coalescence, or in a more realistic physics, coalescence with a certain fixed probability θ (later, $\theta = 1$ for simplicity).

Hence, Following the literature as in [25] and taking

$$\lambda\left(V_t^i, V_t^j\right) = \left|V_t^i - V_t^j\right| / 2a,$$

since we have

$$\Delta t = 2a / \left|V_t^i - V_t^j\right|$$

from this we get

$$\lambda\Delta t = 1$$

making the probability rate of collision meaningful as the speed of particle changes, regarding the time spent together, losing the erroneous bias toward slow motion.

Then, given λ, the *average aggregation rate* will be

$$\left\langle\left|V_t^i - V_t^j\right|\right\rangle / 2a$$

where the term "average" means the following: we consider all the collisions that occur and take the average of the values $\left|V_t^i - V_t^j\right|$.

So, we need to take two generic particles at a distance $|\Delta X| \leq 2a$ and evaluate $|\Delta V|$. Let's call them $\left(X_t^1, V_t^1\right), \left(X_t^2, V_t^2\right)$ without loss of generality, and consider the two-point motion:

$$\begin{aligned}
\frac{dX_t^i}{dt} &= V_t^i \\
\frac{dV_t^i}{dt} &= -\frac{1}{\tau_p}\left(V_t^i - U\left(t, X_t^i\right)\right) \quad i = 1, 2.
\end{aligned}$$

We consider the steady-state regime because if we impose fixed initial conditions, they would influence the result. In the steady-state regime, whenever $\left|X_t^1 - X_t^2\right| \leq 2a$, we calculate $\left|V_t^1 - V_t^2\right|$ and then take the average. In other words, in an ergodic sense, we compute

$$\lim_{T\to\infty} \frac{\int_0^T \left|V_t^1 - V_t^2\right| 1_{\left\{\left|X_t^1 - X_t^2\right| \leq 2a\right\}} dt}{\int_0^T 1_{\left\{\left|X_t^1 - X_t^2\right| \leq 2a\right\}} dt}.$$

Assuming the validity of an ergodic theorem, by multiplying and dividing by T, we obtain

$$= \frac{\mathbb{E}\left[\left|V^1 - V^2\right| 1_{\{|X^1 - X^2| \leq 2a\}}\right]}{\mathbb{P}\left(|X^1 - X^2| \leq 2a\right)}$$

where the random variables $\left(X^1, X^2, V^1, V^2\right)$ are distributed according to the invariant measure of the system that defines the 2-point motion.

Let us focus on a system consisting of only one mass type that can coagulate, let us

call this $m^i = 1$ for the $i-th$ particle at time t before having a collission. We are interested to define the number of aggregation of particle of this type, i.e. understanding the density of particles $m = 2$, in a unitary time Δt and a unitary volume Q.

Consider the non normalized empirical measure $\tilde{\mu}_t^{N,2}$ associated to particles of mass of type $m = 2$, which are the one generated when two particle of unitary mass collide, i.e.

$$\tilde{\mu}_t^{N,2} := \sum_{i \in \mathcal{N}(t)} \mathbb{1}_{\{m_t^i = 2\}}$$

Applying Dynkin formula with an observable ϕ on the particle empirical measure, we get

$$\begin{aligned}\langle \phi, \mu_T^{N,2} \rangle =& \langle \phi, \mu_0^{N,2} \rangle + \int_0^T (\text{velocity field operator and Brownian semigroup})\, ds \\ &+ \int_0^T \sum_{\substack{i,j \in \mathcal{N}(t), \\ i \neq j}} \lambda \left(X_t^i, X_t^j, V_t^i, V_t^j \right) \\ &\qquad \cdot \phi \left(x_i^N(t), \frac{n v_i^N(t) + (m-n) v_j^N(t)}{m} \right) 1_{\{m_i^N(t)=1,\, m_j^N(t)=1\}} dt \\ &+ M_T^{N,J}\end{aligned}$$

So, the quantity we are looking for is

$$\int_{t_0}^{t_0+\Delta t} \sum_{i \neq j} \lambda \left(X_t^i, X_t^j, V_t^i, V_t^j \right) \mathbb{1}_{\{m_t^i=1\}} \mathbb{1}_{\{m_t^j=1\}} \phi(X_t^i, X_t^j) ds \tag{1.4.1}$$

this is the number of collision of particle of mass $m = 1$, in the volume Q (i.e. take $\phi = \mathbb{1}_Q$) in the unit time Δt.

Remark 1.4.2. Note that in principle there is a martingale term and this is already an approximation. If we take ϕ to be not infinitesimal concentrated, then the martingale term is of order smaller than N, does vanishing in the limit.

So, the quantity we are looking for is (1.4.1), and we can exploit two possible way to compute it. First, if we suppose a mean field convergence, as we'll propose in Section .1 and Chapter 2 for particles with high inertia (i.e. $St >> 1$), we obtain from 1.4.1 the final coagulation rate

$$N^2 \int_{t_0}^{t_0+\Delta t} \iint \iint \lambda(x,y,v,w) f_1(x,v) f_1(y,w) \phi(x,y)\, dxdv\, dydw \tag{1.4.2}$$

This, multiplied by the uniform density of particles, give use a description of the collision rate in the asymptotic of large St.

The second approach, explored in Chapter 3, is to consider a firs approximation of (1.4.1) when Δt is infinitesimal, since we want an instantaneous rate. In this regime, we can approximate the integral as

$$\sum_{i \neq j,\ i,j \in \mathcal{N}(t_0)} \left(\mathbb{1}_{\{m_{t_0}^i=1\}} \mathbb{1}_{\{m_{t_0}^j=1\}} \right) \times \int_{t_0}^{t_0+\Delta t} \lambda \left(X_t^i, X_t^j, V_t^i, V_t^j \right) \phi(X_t^i, X_t^j) ds \tag{1.4.3}$$

Computing this quantity is too complex; since the time step is infinitesimal, we can argue that an approximated computation of (1.4.3) could be done with an averaged reasoning, i.e.

$$(1.4.3) \sim \langle \mathcal{N}_1(t_0)^2 \rangle \underbrace{\left\langle \sum_{i\neq j,\ i,j\in\mathcal{N}(t_0)} \int_{t_0}^{t_0+\Delta t} \lambda\left(X_t^i, X_t^j, V_t^i, V_t^j\right) \phi(X_t^i, X_t^j) ds \right\rangle}_{(A)}$$

To compute (A) we have to use again a mean field reasoning, even though this time we need to consider the two-point motion of moving particles. As such we have

$$(A) \sim \int_{t_0}^{t_0+\Delta t} \iint \iint \lambda(x,y,v,w)\phi(x,y) f_t(x,v,y,w)\, dxdv\, dydw\, dt, \tag{1.4.4}$$

where f_t is the joint density of the two-point motion of particles of mass $M = 1$. Note that, as of now, f_t as no restriction on the position, but this is the role due to $\phi(x,y)$. In fact we'll see that, selecting an infinitesimal volume of length scale ℓ_f, in Chapter 3 we can recover a close form for (A).

Since we don't want a dependence on the initial condition, we again pass to the invariant density of the two-point motion $f_\infty(x,y,v,w)$ and we obtain the following:
In an infinitesimal time interval Δt, in a volume of Kolmogorv lenght scale $Q(\ell_f)$, the average number of collision of particle of mass 1 is approximated by

$$\Delta t \mathcal{N}_1(\infty) \iint \iint \lambda(x,y,v,w)\mathbb{1}_Q(x,y) f_\infty(x,v,y,w)\, dxdv\, dydw,$$

where $\mathcal{N}_1(\infty)$ is the stationary fraction of particles of mass 1 able to collide.

Remark 1.4.3. Note that also in this second proposed computation, in the gas kinetic regime of decoupled particles, i.e. $f_\infty = f(x,v)f(y,w)$, we retrieve the result of Chapter 2 and Abrhamson [1].

We'll show, in following Chapters, how this formulation is the right framework to retrieve a complete description of the relative velocity, main factor contributing to the coagulation rate of particles.

Since we are working with normalizing densities, we have to multiply the averaged velocity with

Concerning now the quantity $\mathcal{N}_1(t_0)$, we consider the Dynkin formula for $\mu_t^{N,1}$. Opposite to $\mu_t^{N,2}$ we obtain the same result but with a menus in the coagulation operator, representing the particle coagulating to form the one of mass $m = 2$.

We can argue, considering $\mathcal{N}_1(t_0) = \langle 1, \mu_t^{N,1} \rangle$ and using 1.4.1, the following estimation:

$$\begin{aligned}
&\mathbb{E}[\mathcal{N}_1(t_0+\Delta t)] = \\
&= \mathbb{E}[\mathcal{N}_1(t_0)] - \int_{t_0}^{t_0+\Delta t} \sum_{\substack{i,j\in\mathcal{N}(t),\\ i\neq j}} \lambda\left(X_t^i, X_t^j, V_t^i, V_t^j\right) \phi\left(x_i^N(t), v_i^N(t) + v_j^N(t)\right) 1_{\{m_i^N(t)=1,\, m_j^N(t)=1\}} dt \\
&\lesssim \mathbb{E}[\mathcal{N}_1(t_0)] + \Delta t \mathbb{E}[\mathcal{N}_1(t_0+\Delta t)] \langle (A) \rangle .
\end{aligned}$$

Hence, we can argue that the behavior of the density of particles is

$$\mathbb{E}[\mathcal{N}_1(t_0+\Delta t)] \sim \mathbb{E}[\mathcal{N}_1(t_0)]e^{-\Delta t\langle A\rangle},$$

where $\langle A\rangle$ is the averaged velocity difference.

So, as we'll see in Chapter 3, under the hypothesis of a steady state distribution, i.e. particle marge but are replaced with new particles since we are looking at infinitesimal volume, we expect a gas-kinetic boltzmann like distribution for the portion of particle colliding, i.e. $\mathcal{N}_1(\infty) \sim \mathcal{N}_1(0)e^{-\langle A\rangle}$.

This framework is the baseline to construct a rigorous theory that, from simple mathematical equation can naturally give rise to all the fundamental quantity of rain coalescence.

1.5 Inertial particles: scaling limit

In this section, summarizing the results of previous sections, we provide our original motivation that gives rise naturally to the PDE system we study in this thesis and for which we'll derive in Chapter 2 and 3 rigorous estimate for the coagulation rate. The Smoluchowski type SPDE system we study is conjectured to be the scaling limit of the empirical measure of a system of diffusion particles (idealized rain droplets in the atmosphere) undergoing locally in space coagulation, while subject to an idealized form of turbulence, cf. [31] for a discussion. More precisely, for any $d \geq 1$ and $N \in \mathbb{N}$, consider a second-order particle system with space variable $x_i^N(t)$ in $\mathbb{T}^d$, velocity variable $v_i^N(t)$ in $\mathbb{R}^d$, mass variable $m_i^N(t)$ in a finite set $\{1,...,M\}$, and initial cardinality $N(0)=N$. Between coagulation events, the motion of an active particle obeys

$$\begin{aligned} dx_i^N(t) &= v_i^N(t)dt, \quad i \in \mathcal{N}(t) \\ m_i^N(t)dv_i^N(t) &= \alpha(m_i^N(t))^{1/d}\left[\sqrt{2\mu}dB_i(t) + \sum_{k\in K}\sigma_k(x_i^N(t)) \circ dW_t^k - v_i^N(t)dt\right], \end{aligned} \tag{1.5.1}$$

(whereas after each coagulation, the velocity will be reset according to the conservation of momentum, to be precised below), where

- $\mathcal{N}(t)$ denotes the set of indices of active particles in the system at time t, whose cardinality $|\mathcal{N}(t)| \leq N$,
- $\{B_i(t)\}_{i=1}^{\infty}$ is a given, countable collection of independent standard Brownian motions in $\mathbb{R}^d$
- molecular diffusivity $\mu > 0$
- $\sigma_k(x) : \mathbb{T}^d \to \mathbb{R}^d$, $k \in K$ is a given, finite (or more generally countable, subject to additional assumptions) collection of divergence free vector fields
- $\{W_t^k\}_{k\in K}$ is a given, finite (or countable) collection of standard Brownian motions in $\mathbb{R}$
- $\circ$ denotes Stratonovich integration.

The velocity component of the dynamics obeys Stokes' law with random force (that depends linearly on the radius $r_i^N = (m_i^N)^{1/d}$) given by an intrinsic noise for each particle, plus a common noise of transport type

$$\dot{\mathcal{W}}(t,x) := \sum_{k\in K} \sigma_k(x)\dot{W}_t^k$$

that acts simultaneously on all particles, and as such is seen as an idealized form of turbulent flow in the atmosphere. We denote the $d\times d$ spatial covariance matrix of $\mathcal{W}(t,x)$ by

$$\mathcal{Q}(x,y) := \sum_{k\in K} \sigma_k(x)\otimes\sigma_k(y).$$

Moreover, for any fixed $x\in\mathbb{T}^d$ we denote the uniformly elliptic second-order divergence form operator, acting on suitable functions on $\mathbb{R}^d$

$$(\mathcal{L}_v^{\mathcal{Q},x} f)(v) := \left(\mu I + \frac{1}{2}\mathcal{Q}(x,x)\right)\Delta_v f(v).$$

Note that $\mathcal{Q}(x,x)$ is nonnegative definite for any x. For simplicity, in the sequel we consider the case that

$$\mathcal{L}_v^{\mathcal{Q},x} \equiv \kappa\Delta_v, \tag{1.5.2}$$

for some constant $\kappa\geq\mu$ and all $x\in\mathbb{T}^d$. In view of diffusion enhancement, we have in mind that $\kappa\gg\mu$.

Each particle $i\in\mathcal{N}(t)$ has a mass $m_i^N(t)\in\{1,2,..,M\}$ which changes over time according a stochastic coagulation rule to be described below. The initial mass $m_i(0)$, $i=1,...,N$, are chosen i.i.d. from $\{1,2,..,M\}$ according to a probability distribution so that $\mathbb{P}(m_1(0)=m)=r(m)$ with $\sum_{m=1}^M r(m)=1$. We are also given deterministic probability density functions $g_m(x,v):\mathbb{T}^d\times\mathbb{R}^d\to\mathbb{R}_+$, $m=1,2,...,M$, satisfying additional assumptions, [1] such that if $m_i(0)=m$ then the initial distribution of $(x_i(0),v_i(0))$ is chosen with probability density $g_m(x,v)$, independently across i. We denote

$$f_m^0(x,v) = r(m)g_m(x,v),\quad (x,v)\in\mathbb{T}^d\times\mathbb{R}^d,\ m=1,..,M,$$

which satisfy the same assumptions as those imposed on $\{g_m(x,v)\}_{m=1}^M$.

The rule of coagulation between pairs of particles is as follows. Let $\theta(x):\mathbb{R}^d\to\mathbb{R}_+$ be a given, C^∞-smooth, symmetric probability density function in $\mathbb{R}^d$ with compact support in $\mathbb{B}(0,1)$ (the unit ball around the origin in $\mathbb{R}^d$) and $\theta(0)=0$. Then, for any $\varepsilon\in(0,1)$, denote $\theta^\varepsilon(x):\mathbb{T}^d\to\mathbb{R}_+$ by

$$\theta^\varepsilon(x) := \varepsilon^{-d}\theta(\varepsilon^{-1}x),\quad x\in\mathbb{T}^d.$$

Suppose the current configuration of the particle system is

$$\eta = (x_1,v_1,m_1,x_2,v_2,m_2,...,x_N,v_N,m_N)\in(\mathbb{T}^d\cup\emptyset)^N\times(\mathbb{R}^d\cup\emptyset)^N\times\{1,...,M,\emptyset\}^N$$

[1] those we impose on the initial condition of the PDE system

where (x_i, v_i, m_i) denotes the position, velocity and mass of particle i, by convention if particle i_0 is no longer active in the system, we set $x_{i_0} = v_{i_0} = m_{i_0} = \emptyset$. Independently for each pair (i, j) of particles, where $i \neq j$ each running over the index set of active particles in η, with a rate

$$s(m_i^N, m_j^N)\frac{|v_i - v_j|}{N}\theta^\varepsilon(x_i - x_j) \tag{1.5.3}$$

we remove $(x_i, v_i, m_i, x_j, v_j, m_j)$ from the configuration η, and then add

$$\left(x_i, \frac{m_i v_i + m_j v_j}{m_i + m_j}, m_i + m_j, \emptyset, \emptyset, \emptyset\right)$$

with probability $\frac{m_i}{m_i+m_j}$, and instead add

$$\left(\emptyset, \emptyset, \emptyset, x_j, \frac{m_i v_i + m_j v_j}{m_i + m_j}, m_i + m_j\right)$$

with probability $\frac{m_j}{m_i+m_j}$. We call the new configuration obtained this way by $S^1_{ij}\eta$ and $S^2_{ij}\eta$ respectively. In words, if (i, j) coagulate, we decide randomly which of x_i and x_j is the new position of the mass-combined particle. If the position chosen is x_i, then we consider j as being eliminated (no longer active) and the new particle has index i, whereas if the position chosen is x_j, then we consider i as being eliminated and the new particle has index j. On the other hand, the velocity of the mass-combined particle is obtained by the conservation of momentum as in perfectly inelastic collisions.

Note that the form of the coagulation rate (1.5.3) is such that (i, j) can coagulate only if $|x_i - x_j| \leq \varepsilon$, that is, their spatial positions have to be ε-close. We are interested in the case when $\varepsilon = \varepsilon(N) \to 0$ as $N \to \infty$, so that the interaction is not of mean-field type, but rather local, see the statement of our conjectured result below. In particular, if $\varepsilon = O(N^{-1/d})$ then each particle typically interacts with a bounded number of others at any given time. The essential feature of our coagulation rate, that of the appearance of $|v_i - v_j|$, is inspired by the coagulation kernels used in the physics literature for describing cloud particles (which in general can depend also on m_i, m_j and other physically relevant quantities), and we believe it is key to demonstrating coagulation enhancement.

For each $N \in \mathbb{N}$, $T \in (0, \infty)$ and $m \in \{1, .., M\}$, we denote the process of empirical measure on position and velocity of mass-m particles in the system by

$$\mu_t^{N,m}(dx, dv) := \frac{1}{N}\sum_{i \in \mathcal{N}(t)} \delta_{x_i^N(t)}(dx)\delta_{v_i^N(t)}(dv)1_{\{m_i^N(t)=m\}} \in \mathcal{M}_{1,+}(\mathbb{T}^d \times \mathbb{R}^d)$$

where $\mathcal{M}_{1,+} := \mathcal{M}_{1,+}(\mathbb{T}^d \times \mathbb{R}^d)$ denotes the space of subprobability measures on $\mathbb{T}^d \times \mathbb{R}^d$ equipped with weak topology. The choice of the initial conditions for our system implies that $\mathbb{P}$-a.s.

$$\mu_0^N(dx, dv) \to f^0(x, v)dxdv, \quad \text{as } N \to \infty$$

where the limit is absolutely continuous. We conjecture that, under the assumption of local interaction, i.e.

$$\lim_{N\to\infty} \varepsilon(N) = 0, \quad \limsup_{N\to\infty} \frac{\varepsilon(N)^{-d}}{N} < \infty.$$

for every finite T, the collection of empirical measures $\{\mu_t^N(dx,dv) : t \in [0,T]\}_{m=1}^M$ converges in probability, as $N \to \infty$, in $\mathcal{D}([0,T],\mathcal{M}_{1,+})^M$ the space of càdlàg paths taking values in $\mathcal{M}_{1,+}$, equipped with the Skorohod topology, towards an absolutely continuous limit, which is the pathwise unique weak solution $\{f_m(t,x,v) : t \in [0,T]\}_{m=1}^M$ of a Smoluchowski-type SPDE system, see (1.5.6). The latter SPDE degenerates to the PDE system we study in this thesis, Chapter 4 equation (4.1.2), when the Itô term is switched off. While we do not provide a rigorous proof here, we sketch below a heuristic argument and postpone the rigorous derivation of the SPDE from the particle system to a future work. We think that this heuristic argument is sufficient to justify our interest in studying our PDE system. In fact, in the literature there exists specific limiting procedures cf. [42, 35] that allow, in principle, to obtain the PDE from the SPDE by carefully choosing the vector fields $\sigma_k(x)$.

Let $\phi(x,v)$ be any function of class $C_c^\infty(\mathbb{T}^d \times \mathbb{R}^d)$, for any m we apply Itô's formula to the process

$$\langle \phi, \mu_t^{N,m} \rangle := \frac{1}{N} \sum_{i \in \mathcal{N}(t)} \phi(x_i^N(t), v_i^N(t)) 1_{\{m_i^N(t)=m\}}$$

and we get

$$\begin{aligned}
\langle \phi, \mu_T^{N,m} \rangle &= \langle \phi, \mu_0^{N,m} \rangle + \int_0^T \frac{1}{N} \sum_{i \in \mathcal{N}(t)} v_i^N(t) \cdot \nabla_x \phi(x_i^N(t), v_i^N(t)) 1_{\{m_i^N(t)=m\}} dt \\
&- c(m) \int_0^T \frac{1}{N} \sum_{i \in \mathcal{N}(t)} v_i^N(t) \cdot \nabla_v \phi(x_i^N(t), v_i^N(t)) 1_{\{m_i^N(t)=m\}} dt \\
&+ c(m) \int_0^T \frac{1}{N} \sum_{i \in \mathcal{N}(t)} \nabla_v \phi(x_i^N(t), v_i^N(t)) 1_{\{m_i^N(t)=m\}} \cdot dB_i(t) \\
&+ \mu c(m)^2 \int_0^T \frac{1}{N} \sum_{i \in \mathcal{N}(t)} \Delta_v \phi(x_i^N(t), v_i^N(t)) 1_{\{m_i^N(t)=m\}} dt \\
&+ \frac{1}{2} c(m)^2 \int_0^T \frac{1}{N} \sum_{i \in \mathcal{N}(t)} \mathcal{Q}(x_i^N(t), x_i^N(t)) \Delta_v \phi(x_i^N(t), v_i^N(t)) 1_{\{m_i^N(t)=m\}} dt \\
&+ c(m) \int_0^T \frac{1}{N} \sum_{i \in \mathcal{N}(t)} \sum_{k \in K} \sigma_k(x_i^N(t)) \cdot \nabla_v \phi(x_i^N(t), v_i^N(t)) 1_{\{m_i^N(t)=m\}} dW_t^k \\
&+ \int_0^T \frac{1}{N^2} \sum_{n=1}^{m-1} \sum_{\substack{i,j \in \mathcal{N}(t), \\ i \neq j}} s(n, m-n) |v_i^N(t) - v_j^N(t)| \theta^\varepsilon(x_i^N(t) - x_j^N(t)) \\
&\qquad \cdot \phi\left(x_i^N(t), \frac{n v_i^N(t) + (m-n) v_j^N(t)}{m} \right) \frac{n}{m} 1_{\{m_i^N(t)=n,\, m_j^N(t)=m-n\}} dt \\
&+ \int_0^T \frac{1}{N^2} \sum_{n=1}^{m-1} \sum_{\substack{i,j \in \mathcal{N}(t), \\ i \neq j}} s(n, m-n) |v_i^N(t) - v_j^N(t)| \theta^\varepsilon(x_i^N(t) - x_j^N(t))
\end{aligned}$$

$$\cdot \phi\left(x_j^N(t), \frac{nv_i^N(t)+(m-n)v_j^N(t)}{m}\right)\frac{m-n}{m}1_{\{m_i^N(t)=n,\, m_j^N(t)=m-n\}}dt$$

$$-\int_0^T \frac{2}{N^2}\sum_{n=1}^{M}\sum_{i,j\in\mathcal{N}(t),\, i\neq j} s(n,m)|v_i^N(t)-v_j^N(t)|\theta^\varepsilon(x_i^N(t)-x_j^N(t))$$
$$\cdot \phi(x_i^N(t),v_i^N(t))1_{\{m_i^N(t)=m,\, m_j^N(t)=n\}}dt$$
$$+M_T^{N,J}$$

where $\{M_t^{N,J}\}_{t\geq 0}$ is a martingale associated with coagulation (or jumps) that we do not write explicitly. We can rewrite, using the simplification (1.5.2), the previous identity more compactly as

$$\langle \phi, \mu_T^{N,m}\rangle = \langle \phi, \mu_0^{N,m}\rangle + \int_0^T \Big\langle v\cdot\nabla_x\phi - c(m)v\cdot\nabla_v + c(m)^2\kappa\Delta_v,\ \mu_t^{N,m}\Big\rangle dt$$
$$+ c(m)\int_0^T \frac{1}{N}\sum_{i\in\mathcal{N}(t)}\nabla_v\phi(x_i^N(t),v_i^N(t))1_{\{m_i^N(t)=m\}}\cdot dB_i(t)$$
$$+ c(m)\int_0^T \sum_{k\in K}\Big\langle \sigma_k(x)\cdot\nabla_v\phi,\ \mu_t^{N,m}\Big\rangle dW_t^k + M_T^{N,J}$$
$$+\int_0^T\sum_{n=1}^{m-1}\frac{n}{m}\Big\langle s(n,m-n)|v-w|\theta^\varepsilon(x-y)\phi\Big(x,\frac{nv+(m-n)w}{m}\Big),\ \mu_t^{N,n}(dx,dv)\mu_t^{N,m-n}(dy,dw)\Big\rangle dt$$
$$+\int_0^T\sum_{n=1}^{m-1}\frac{m-n}{m}\Big\langle s(n,m-n)|v-w|\theta^\varepsilon(x-y)\phi\Big(y,\frac{nv+(m-n)w}{m}\Big),\ \mu_t^{N,n}(dx,dv)\mu_t^{N,m-n}(dy,dw)\Big\rangle dt$$
$$-\int_0^T 2\sum_{n=1}^{M}\Big\langle s(n,m)|v-w|\theta^\varepsilon(x-y)\phi(x,v),\ \mu_t^{N,m}(dx,dv)\mu_t^{N,n}(dy,dw)\Big\rangle dt. \tag{1.5.4}$$

We expect that $M_T^{N,J}$ and the stochastic integrals in $dB_i(t)$ vanish in limit as $N\to\infty$ in $L^2(\mathbb{P})$, whereas the martingale associated with the common noise persists in the limit. Further, suppose that we have proved that the laws of the collection of $\mathcal{D}_T(\mathcal{M}_{1,+})^M$-valued random variables $\{\mu_t^{N,m}: t\in[0,T]\}_{m=1}^M$, $N\in\mathbb{N}$, is tight hence weakly relatively compact. Consider any weak subsequential limit

$$\{\mu_t^{N_\ell,m}: t\in[0,T]\}_{m=1}^M \overset{\ell\to\infty}{\to} \{\overline{\mu}_t^m: t\in[0,T]\}_{m=1}^M. \tag{1.5.5}$$

For the sake of arguments, apply Skorohod's representation theorem and there exists some auxiliary probability space and on which a sequence of random variables having the same laws as the ones in (1.5.5) so that the above convergence holds almost surely. By an abuse of notation, below we use the same letters for the variables on the auxiliary space. Assume that we can prove that $\overline{\mu}_t^m$ has a density $f_m(t,x,v)$ with respect to Lebesgue measure for every m and t. Then, with minor work the linear part of the identity (1.5.4) converges as $\ell\to\infty$, i.e.

$$\langle \phi, \mu_T^{N_\ell,m}\rangle \to \langle \phi, f_m(T,x,v)\rangle,$$

$$\langle \phi, \mu_0^{N_\ell,m}\rangle \to \langle \phi, f_m^0(x,v)\rangle,$$
$$\int_0^T \left\langle v\cdot\nabla_x\phi - c(m)v\cdot\nabla_v + \kappa c(m)^2\Delta_v,\ \mu_t^{N_\ell,m}\right\rangle dt$$
$$\to \int_0^T \left\langle v\cdot\nabla_x\phi - c(m)v\cdot\nabla_v + \kappa c(m)^2\Delta_v,\ f_m(t,x,v)\right\rangle dt,$$
$$\int_0^T \sum_{k\in K}\left\langle \sigma_k(x)\cdot\nabla_v\phi,\ \mu_t^{N_\ell,m}\right\rangle dW_t^k \to \int_0^T \sum_{k\in K}\langle \sigma_k(x)\cdot\nabla_v\phi,\ f_m(t,x,v)\rangle\, dW_t^k.$$

The proof that the nonlinear terms also converge to the corresponding limits is more difficult, hence here we content ourselves with a very heuristic "two-step argument". Consider each summand of the last term of (1.5.4) :

$$\int_0^T \left\langle s(n,m)|v-w|\theta^\varepsilon(x-y)\phi(x,v),\ \mu_t^{N_\ell,m}(dx,dv)\mu_t^{N_\ell,n}(dy,dw)\right\rangle dt,\quad 1\le m,n\le M.$$

Assume we take $\ell\to\infty$ first, keeping ε fixed, we get

$$\int_0^T \left\langle s(n,m)|v-w|\theta^\varepsilon(x-y)\phi(x,v),\ \mu_t^{N_\ell,m}(dx,dv)\mu_t^{N_\ell,n}(dy,dw)\right\rangle dt$$
$$\overset{\ell\to\infty}{\to} \int_0^T\int s(n,m)|v-w|\theta^\varepsilon(x-y)\phi(x,v)f_m(t,x,v)f_n(t,y,v)dxdydvdwdt\ ;$$

then we take $\varepsilon\to 0$, and since $\theta^\varepsilon(\cdot)$ approximates the delta-Dirac δ_0, we get

$$\int_0^T\int s(n,m)|v-w|\theta^\varepsilon(x-y)\phi(x,v)f_m(t,x,v)f_n(t,y,v)dxdydvdwdt$$
$$\overset{\varepsilon\to 0}{\to} \int_0^T\int s(n,m)|v-w|\phi(x,v)f_m(t,x,v)f_n(t,x,w)dxdvdwdt.$$

Similarly, each summand of the second and third terms from the bottom in (1.5.4) also converge under the two-step argument (using also $n/m+(m-n)/m=1$)

$$\int_0^T \frac{n}{m}\left\langle s(n,m-n)|v-w|\theta^\varepsilon(x-y)\phi\left(x,\frac{nv+(m-n)w}{m}\right),\ \mu_t^{N_\ell,n}(dx,dv)\mu_t^{N_\ell,m-n}(dy,dw)\right\rangle dt$$
$$+\int_0^T \frac{m-n}{m}\left\langle s(n,m-n)|v-w|\theta^\varepsilon(x-y)\phi\left(y,\frac{nv+(m-n)w}{m}\right),\ \mu_t^{N_\ell,n}(dx,dv)\mu_t^{N_\ell,m-n}(dy,dw)\right\rangle dt$$
$$\to \int_0^T\int s(n,m-n)|v-w|\phi\left(x,\frac{nv+(m-n)w}{m}\right)f_n(t,x,v)f_m(t,x,w)dvdwdt.$$

Hence, we have (at least under Skorohod's representation) the limit identity satisfied by $\{f_m(t,x,v)\}$:

$$\langle\phi, f_m(T)\rangle = \langle\phi, f_m^0\rangle + \int_0^T \left\langle v\cdot\nabla_x\phi - c(m)v\cdot\nabla_v + \kappa c(m)^2\Delta_v,\ f_m(t,x,v)\right\rangle dt$$
$$+\sum_{n=1}^{m-1}\int_0^T\int s(n,m-n)|v-w|\phi\left(x,\frac{nv+(m-n)w}{m}\right)f_n(t,x,v)f_{m-n}(t,x,w)dxdvdwdt$$

$$
\begin{aligned}
&- 2\sum_{n=1}^{M}\int_0^T \int s(n,m)|v-w|\phi(x,v)f_m(t,x,v)f_n(t,x,w)dxdvdwdt \\
&+ c(m)\int_0^T \sum_{k\in K} \langle \sigma_k(x)\cdot\nabla_v\phi,\ f_m(t,x,v)\rangle\, dW_t^k, \quad m=1,...,M,
\end{aligned}
$$

which is the weak formulation of the SPDE system

$$
\begin{cases}
df_m(t,x,v) = & \left(-v\cdot\nabla_x + c(m)\mathsf{div}_v\,(v\cdot) + \kappa c(m)^2\Delta_v\right) f_m(t,x,v)dt \\
& -c(m)\sum_{k\in K}\sigma_k(x)\cdot\nabla_v f_m(t,x,v)dW_t^k \\
& +\sum_{n=1}^{m-1}\int_{\{nw'+(m-n)w=mv\}} s(n,m-n)|w'-w|f_n(t,x,w')f_{m-n}(t,x,w)dwdw'dt \\
& -2\sum_{n=1}^{M}\int s(n,m)|v-w|f_m(t,x,v)f_n(t,x,w)dwdt \\
f_m(\cdot,x,v)|_{t=0} = & f_m^0, \quad m=1,...,M.
\end{cases}
\tag{1.5.6}
$$

Rewriting the Itô integral as a Stratonovich integral plus a corrector, we equivalently have that

$$
\begin{aligned}
df_m(t,x,v) = &\left(-v\cdot\nabla_x + c(m)\mathsf{div}_v\,(v\cdot) + \mu c(m)^2\Delta_v\right) f_m(t,x,v)dt \\
&- c(m)\sum_{k\in K}\sigma_k(x)\cdot\nabla_v f_m(t,x,v)\circ dW_t^k \\
&+\sum_{n=1}^{m-1}\int_{\{nw'+(m-n)w=mv\}} s(n,m-n)|w'-w|f_n(t,x,w')f_{m-n}(t,x,w)dwdw'dt \\
&-2\sum_{n=1}^{M}\int s(n,m)|v-w|f_m(t,x,v)f_n(t,x,w)dwdt.
\end{aligned}
$$

Thus, we see that the same Stratonovich transport-type noise that acts on the particle system (1.5.1) also acts on the SPDE.

Lastly, at the rigorous level, we need to prove that the solution of this SPDE system (1.5.6) is pathwise unique, which allows to conclude (via nontrivial arguments) that the full sequence of empirical measure converges. More so, Under certain simplifications, it leads to the following kinetic version of Smoluchowski's equation (see [35, 33, 39] for similar studies)

$$
\begin{cases}
\partial_t f_m(t,x,v) = -v\cdot\nabla_x f_m + c(m)\mathsf{div}_v\,(vf_m) + \kappa c(m)^2\Delta_v f_m + Q_m(f,f) \\
f_m|_{t=0} = f_m^0(x,v), \quad m=1,...,M,
\end{cases}
\tag{1.5.7}
$$

where $(t,x,v) \in [0,T] \times \mathbb{T}^d \times \mathbb{R}^d$, and

$$\begin{aligned} &Q_m(f,f)(t,x,v) \\ &:= \sum_{n=1}^{m-1} \iint_{\{nw'+(m-n)w=mv\}} s(n,m-n) f_n(t,x,w') f_{m-n}(t,x,w) |w-w'| dw dw' \\ &\quad - 2 \sum_{n=1}^{M} \int s(n,m) f_m(t,x,v) f_n(t,x,w) |v-w| dw, \end{aligned} \tag{1.5.8}$$

where

$$c(m) := \alpha m^{(1-d)/d}, \quad s(n,m) := (n^{1/d} + m^{1/d})^{d-1}. \tag{1.5.9}$$

We have sketched here the proof of the scaling limit from inertial coagulating microscopic particle system subjected to a common noise, to an SPDE that eventually gives rise to this PDE. Although it is not fully rigorous, it is enough to justify the interest of this equation. Here again, turbulence contributes to large κ versus small κ when no turbulence.

The eddy diffusion occurs now in the velocity variable and this will be the key to understand rigorously the coagulating property of colliding particles directly from the limiting equation for their density. As such, this will be the main system analyzed throughout the thesis.

Chapter 2

Turbulence enhancement of coagulation: inertial particles

2.1 Introduction

Turbulence increases the relative velocity of particles suspended into a fluid, favours their collision and thus increases the collision rate. A key factor of the collision rate is the average relative velocity between particles of mass m_1 and m_2:

$$R_{m_1,m_2} = \langle |\mathbf{v}_1 - \mathbf{v}_2| \rangle . \tag{2.1.1}$$

This quantity is of major importance since it relates the properties of particles and fluid to the intensity of the aggregation and thus it has been extensively investigated in several works, based on various arguments and models of turbulence, see for instance [1, 7, 19, 20, 25, 26, 45, 64, 73, 75, 76, 78, 81, 84, 88, 90, 93]. We shall add more specific comments below on some of these results in connection with our own.

We propose a new modeling approach here. Many ingredients are classical, like the fact that we use an *inertial model* for particle motion (instead of a model when particles are transported) where each particle moves following Stokes' law

$$\frac{d\mathbf{x}}{dt} = \mathbf{v}, \qquad \frac{d\mathbf{v}}{dt} = \gamma \left(\mathbf{U}(t, \mathbf{x}) - \mathbf{v} \right) \tag{2.1.2}$$

(here γ is the the damping coefficient and $\mathbf{U}(t, \mathbf{x})$ is the fluid velocity), and *Smoluchowski equations* with a kernel depending on the relative velocity $|\mathbf{v} - \mathbf{v}'|$ to describe macroscopically the system. The novelty is that we introduce a Boussinesq hypothesis, namely the fact that a small-scale turbulence acts on particles as a dissipation. And the key feature is that it acts as a *dissipation in the velocity component*, namely it spreads the distribution of particles in velocity (not or not only in space). This spread increases the value of R_{m_1,m_2} and thus the collision rate.

In order to describe the equations we use and the results, let us recall a few quantities associated to the particles and to the fluid. The damping coefficient γ appearing in equation (2.1.2) is given by Stokes' law $\frac{6\pi r\mu}{m}$ where r, m are the particle radius and mass and μ is the dynamic viscosity of the fluid. If we denote by τ_P and $\tau_{\mathbf{U}}$ the relaxation times of the particle and of the fluid respectively, we have $\gamma = \tau_P^{-1}$ and we define the Stokes

number as $St = \tau_P/\tau_{\mathbf{U}} = 1/(\gamma\tau_{\mathbf{U}})$. When we want to stress the dependence of the damping coefficient γ from the mass m, we write γ_m; and similarly for St_m. Two relevant quantities of the fluid for our study are the turbulence kinetic energy $k_T = \frac{1}{2}\left|\overline{\mathbf{U}}\right|^2$ and the turbulent viscosity $\nu_T = \tau_{\mathbf{U}} k_T$. Our model is based on the idealization that the turbulent small-scale fluid is white noise in time, space-homogeneous, with intensity σ (precisely, as a vector field, its space-covariance matrix $C(\mathbf{x})$ is assumed to have the auto-covariance $C(\mathbf{0})$ equal to $\sigma^2 I_d$). As explained in the Appendix .2, the link between these fluid quantities is

$$\frac{\sigma^2}{2} = \frac{2}{d}\tau_{\mathbf{U}} k_T = \frac{2}{d}\nu_T. \tag{2.1.3}$$

The first main result of our work is that we derive the following Smoluchowski-type system for the particle densities of masses $m = 1, 2, ...$

$$\begin{aligned} &\frac{\partial f_m(t,\mathbf{x},\mathbf{v})}{\partial t} + \mathbf{v}\cdot\nabla_x f_m(t,\mathbf{x},\mathbf{v}) - \gamma_m \operatorname{div}_v\left(\mathbf{v} f_m(t,\mathbf{x},\mathbf{v})\right) \\ &- \frac{\gamma_m^2\sigma^2}{2}\Delta_v f_m(t,\mathbf{x},\mathbf{v}) = \left(\mathcal{Q}_m^+ - \mathcal{Q}_m^-\right)(\mathbf{f},\mathbf{f})(t,\mathbf{x},\mathbf{v}) \end{aligned} \tag{2.1.4}$$

where $\mathbf{f} := (f_1, f_2, ...)$, $\mathbf{x} \in \mathbb{T}^d$ (the d-dimensional torus), $\mathbf{v} \in \mathbb{R}^d$ and the collision kernels are given by

$$\begin{aligned} \mathcal{Q}_m^+(\mathbf{f},\mathbf{f})(t,\mathbf{x},\mathbf{v}) := \sum_{n=1}^{m-1} \iint_{\{n\mathbf{v}'+(m-n)\mathbf{v}''=m\mathbf{v}\}} s_{n,m-n} \\ \cdot|\mathbf{v}'-\mathbf{v}''| f_n(t,\mathbf{x},\mathbf{v}') f_{m-n}(t,\mathbf{x},\mathbf{v}'') d\mathbf{v}' d\mathbf{v}'', \end{aligned} \tag{2.1.5}$$

$$\begin{aligned} \mathcal{Q}_m^-(\mathbf{f},\mathbf{f})(t,\mathbf{x},\mathbf{v}) := 2 f_m(t,\mathbf{x},\mathbf{v}) \sum_{n=1}^{\infty} \int s_{n,m} \\ \cdot|\mathbf{v}-\mathbf{v}'| f_n(t,\mathbf{x},\mathbf{v}')\, d\mathbf{v}' \end{aligned} \tag{2.1.6}$$

with $s_{n,m}$ defined in (2.2.1) below.

This equation proposes a change of viewpoint. In previous works, the central problem was determining the correct collision kernel which takes into account the fact that the fluid is turbulent. Here we use the original collision kernel depending on the relative velocity $|\mathbf{v}-\mathbf{v}'|$, without modifying its coefficients, but incorporate the presence of a small-scale turbulent background by adding the dissipative operator in the velocity variable. Collision and aggregation is not due to a stronger collision kernel, in this model, but to the spread-in-$\mathbf{v}$ of densities, produced by the additional diffusion term.

We explain the derivation of this Smoluchowski-type system in Sections 2.4 and 2.5 and in the Appendix .1. This derivation is heuristic but reasonable in analogy with rigorous results proved recently for other models [35, 33, 42]. From the viewpoint of the Physical validity of the result, let us stress that the rigorous proof would require very small $\tau_{\mathbf{U}}$, with γ_m having a finite limit. Therefore St must be large.

We analyze this new model both using approximate analytical computations and numerically. In Section 2.6 we prove, up to some approximation, the formula

$$R_{m_1,m_2} = \frac{2}{\sqrt{\pi}}\sqrt{\gamma_{m_1}+\gamma_{m_2}}\,\sigma = \frac{4}{\sqrt{3\pi}}\sqrt{\frac{k_T}{St_{m_1}} + \frac{k_T}{St_{m_2}}}, \tag{2.1.7}$$

in the physical dimension $d = 3$. In the large St regime, which is the regime of validity of our results, this formula confirms known results (see the discussion in [90]) and it is known as the gas-kinetic model, after [1]. Let us notice that it is obtained without any use of dimensional analysis; it is derived from basic equations, except for the stochastic model of the turbulent fluid. It is not immediately clear, however, if we may modify our approach to incorporate the concentration effects related to singularities described in [25, 64, 90].

In Section 2.7, finally, we investigate numerically the Smoluchowski equations, quantifying in various ways the efficiency of aggregation of the turbulence model.

2.2 The microscopic model

The model used below will be of Smoluchowski type with random transport. However, the description of its microscopic origin may help. Call $D \subset \mathbb{R}^d$, $d = 1, 2, 3$, the space domain of the system, occupied by the fluid and by small rain droplets. The number $\mathcal{N}(t)$ of droplets changes in time due to coalescence. Droplet motion is described in a Newtonian way by position and velocity $\left(\mathbf{x}^i(t), \mathbf{v}^i(t)\right)$, $i = 1, ..., \mathcal{N}(t)$. Droplets have masses $m^i(t)$ taking values in the positive integers $\{1, 2, ...\}$. During the intertime between a collision and the next one, the motion is given by

$$\frac{d\mathbf{x}^i}{dt} = \mathbf{v}^i, \qquad \frac{d\mathbf{v}^i}{dt} = \gamma_{m_i}\left(\mathbf{U}\left(t, \mathbf{x}^i\right) - \mathbf{v}^i\right)$$

where $\mathbf{U}(t, \mathbf{x})$ is the fluid velocity; we adopt a Stokes law for the particle-fluid interaction and denote by

$$\gamma_{m_i} = \alpha (m^i)^{(1-d)/d}$$

the damping rate, α a positive constant (including the dynamic viscosity coefficient of the fluid), and the term $\left(m^i\right)^{1/d}$ playing the role of the radius of the particle.

The rule of coalescence is crucial, see [20, 25, 45, 75, 78]. There are two typical mathematical models: one is based on deterministic coalescence, the other on probability rates. The first one is easier to describe: when two particles meet, they become a new single particle with mass given by the sum of the masses and momentum given by conservation of momentum. For mathematical investigation of the macroscopic limit, this scheme is usually more difficult. Easier is thinking in terms or *rate of coalescence*: when two particles are below a certain small distance one from the other, they have a certain probability per unit of time to become a new single particle, with the mass and momentum law as above. The kernels in Smoluchowski equations are the macroscopic footprint of rates.

The model based on rates has a flaw precisely in connection with the turbulence background we want to investigate here. Since coalescence happens due to a probability per unit of time, if the time spent by two particles, at the prescribed distance of potential coalescence, is small, the probability that their encounter leads to coalescence is smaller. This is in sharp contrast with the deterministic model where coalescence always happens, at a certain distance, independently of the time spent nearby. In other words, in the model based on rates, without employing an approximating strategy to compute terminal velocity, coalescence is facilitated by slow motion, which is false in practice and goes in the opposite direction of understanding whether turbulence enhances coalescence.

To avoid this bias towards slow motion, of say particles i and j, and leave velocity as a studied attribute of the system, we maintain in their coalescence rate the factor $|\mathbf{v}^i - \mathbf{v}^j|$. This factor multiplied by the time spent nearby is constant, on average, hence the probability of coalescence is roughly constant.

Finally, since the probability of coalescence should depend on the particle surface, main factor involved in the collision, we multiple the rate by the surface factor

$$s_{m^i,m^j} = \left(\left(m^i\right)^{1/d} + \left(m^j\right)^{1/d}\right)^{d-1}. \tag{2.2.1}$$

Hence, summarising, in our work the adopted point of view is consistent with the case of hydrodynamic motion, as in e.g. [25, 64], where the coagulation kernel is

$$E(i,j)s_{m^i,m^j}|\mathbf{v}^i - \mathbf{v}^j|, \tag{2.2.2}$$

and the scalar $E(i,j)$ can be regarded as collision efficiency between real droplets i and j. For simplicity, we set $E(i,j) = 1$ in our phenomenological study.

2.3 The Smoluchowski-type model

A rigorous study of the link between the microscopic model and the macroscopic one is under investigation, following [37, 36, 48, 73] where similar models have been already treated. However, following the mean field paradigm we may safely choose the following macroscopic model as a good one for the density evolution.

Denote by $f_m(t,\mathbf{x},\mathbf{v})$, $m = 1,2,...$, the density of droplets of mass m at position $\mathbf{x} \in D$ having velocity $\mathbf{v} \in \mathbb{R}^d$. Then (dropping the time variable) the density satisfies

$$\begin{aligned} &\frac{\partial f_m(\mathbf{x},\mathbf{v})}{\partial t} + \operatorname{div}_x\left(\mathbf{v} f_m(\mathbf{x},\mathbf{v})\right) \\ &+ \gamma_m \operatorname{div}_v\left(\left(\mathbf{U}(t,\mathbf{x}) - \mathbf{v}\right) f_m(\mathbf{x},\mathbf{v})\right) = \mathcal{Q}_m^+ - \mathcal{Q}_m^- \end{aligned} \tag{2.3.1}$$

where $\gamma_m = \alpha m^{(1-d)/d}$, and $\mathcal{Q}_m^+$ and $\mathcal{Q}_m^-$ are the two collision terms as given in (2.1.5). Crucial is the kernel $|\mathbf{v}' - \mathbf{v}''|$, as described above. The first collision term describes the amount of new particles of mass m created by collision of smaller ones, with the momentum conservation rule

$$n\mathbf{v}' + (m-n)\mathbf{v}'' = m\mathbf{v}. \tag{2.3.2}$$

The second collision term gives us the percentage of the density $f_m(\mathbf{x},\mathbf{v})$ of particles of mass m which disappears by coalescence into larger particles.

In the next section, we explain how this model can be studied using techniques from passive scalars, thus obtaining in (2.1.4) a simplified coagulation equation in which the velocity of the particles is still a driving component of the coalescence process. We postpone to the Appendix .1 (see also [31]) for a more rigourous heuristic of the scaling limit from a coagulating microscopic particle system subjected to a common noise, to a stochastic partial differential equation (SPDE), that eventually gives rise to the PDE (2.1.4). Although it is not yet fully rigorous, we believe that it justifies the interest of this equation. The eddy diffusion now occurs in the velocity variable.

2.4 Stochastic model of turbulent velocity field

Similarly to a large body of simplified modeling of passive scalars, we consider a model of velocity fluid which is delta-correlated in time, namely a white noise with suitable space dependence. We may write

$$\mathbf{U}(t,\mathbf{x})\,dt=\sum_{k\in K}\sigma_k(\mathbf{x})\,dW_t^k \tag{2.4.1}$$

where $\sigma_k(\mathbf{x})$ are smooth divergence free deterministic vector fields on D and W_t^k are independent one-dimensional Brownian motions; K is a finite index set (or countable, with some care on summability assumptions). In this case the term $\gamma_m\mathbf{U}(t,\mathbf{x})\cdot\nabla_v f_m(\mathbf{x},\mathbf{v})$ must be interpreted as a Stratonovich integral (still written here in differential form for sake of clarity)

$$\gamma_m\sum_{k\in K}\sigma_k(\mathbf{x})\cdot\nabla_v f_m(\mathbf{x},\mathbf{v})\circ dW_t^k.$$

By the rules of stochastic calculus, it is given by an Itô-Stratonovich corrector plus an Itô integral; precisely, the previous term is given by

$$-\frac{\gamma_m^2}{2}\sum_{k\in K}\sigma_k(\mathbf{x})\cdot\nabla_v\left(\sigma_k(\mathbf{x})\cdot\nabla_v f_m(\mathbf{x},\mathbf{v})\right)dt+dL(t,\mathbf{x},\mathbf{v})$$

where $L(t,\mathbf{x},\mathbf{v})$ is a (local) martingale, the Itô term. The Itô-Stratonovich corrector takes also the form

$$-\frac{\gamma_m^2}{2}\operatorname{div}_v\left(C(\mathbf{x},\mathbf{x})\nabla_v f_m(\mathbf{x},\mathbf{v})\right)dt$$

where $C(\mathbf{x},\mathbf{y})$ is the matrix-valued function given by the space-covariance function of the noise

$$C(\mathbf{x},\mathbf{y})=\sum_{k\in K}\sigma_k(\mathbf{x})\otimes\sigma_k(\mathbf{y}). \tag{2.4.2}$$

Summarizing, the stochastic model, in Itô form, is

$$\begin{aligned}&df_m(\mathbf{x},\mathbf{v})+\left(\mathbf{v}\cdot\nabla_x f_m(\mathbf{x},\mathbf{v})-\gamma_m\operatorname{div}_v\left(\mathbf{v}f_m(\mathbf{x},\mathbf{v})\right)\right)dt\\&-\frac{\gamma_m^2}{2}\operatorname{div}_v\left(C(\mathbf{x},\mathbf{x})\nabla_v f_m(\mathbf{x},\mathbf{v})\right)dt\\&=\left(\mathcal{Q}_m^+-\mathcal{Q}_m^-\right)dt-dL(t,\mathbf{x},\mathbf{v}).\end{aligned} \tag{2.4.3}$$

Also for later reference, let us mention an example of noise, introduced by R. Kraichnan [56, 57], relevant to our analysis. For the sake of simplicity of exposition, assume we are in full space $\mathbb{R}^d$, but modifications in other geometries are possible. Its covariance function is space-homogeneous, $C(\mathbf{x},\mathbf{y})=C(\mathbf{x}-\mathbf{y})$, with the form

$$C(\mathbf{z})=\sigma^2k_0^{\zeta}\int_{k_0\le|\mathbf{k}|<k_1}\frac{1}{|\mathbf{k}|^{d+\zeta}}e^{i\mathbf{k}\cdot\mathbf{z}}\left(I-\frac{\mathbf{k}\otimes\mathbf{k}}{|\mathbf{k}|^2}\right)d\mathbf{k}. \tag{2.4.4}$$

The case $\zeta > 0$ includes Kolmogorov 41 case $\zeta = 4/3$. In this case, take $k_1 = +\infty$. Then

$$C(\mathbf{0}) = A\sigma^2$$

where the constant A is given by

$$\int_{1\leq|\mathbf{k}|<\infty} \frac{1}{|\mathbf{k}|^{d+\zeta}} \left(I - \frac{\mathbf{k}\otimes\mathbf{k}}{|\mathbf{k}|^2}\right) d\mathbf{k}.$$

2.5 The deterministic scaling limit

Following [35, 33, 42], we may consider small-scale turbulent velocity fields depending on a scaling parameter and take their scaling limit. In the case of Kraichnan model above, choose

$$k_0 = k_0^N \to \infty$$

The result $C(\mathbf{0}) = A\sigma^2 I_d$ is independent of N, so that the Itô-Stratonovich corrector becomes equal to (without loss of generality we set $A = 1$)

$$\frac{1}{2}\gamma_m^2\sigma^2\Delta_v f_m(\mathbf{x},\mathbf{v});$$

and simultaneously we may have that the Itô term goes to zero. The final equation is deterministic, and precisely given by

$$\frac{\partial f_m(\mathbf{x},\mathbf{v})}{\partial t} + \mathbf{v}\cdot\nabla_x f_m(\mathbf{x},\mathbf{v}) - \gamma_m \operatorname{div}_v(\mathbf{v} f_m(\mathbf{x},\mathbf{v})) - \frac{\gamma_m^2\sigma^2}{2}\Delta_v f_m(\mathbf{x},\mathbf{v}) = \mathcal{Q}_m^+ - \mathcal{Q}_m^-.$$

Now, for sake of numerical simplicity, we assume that all densities are uniform in $\mathbf{x}$. Then we have

$$\boxed{\frac{\partial f_m(\mathbf{v})}{\partial t} - \gamma_m \operatorname{div}_v(\mathbf{v} f_m(\mathbf{v})) - \frac{\gamma_m^2\sigma^2}{2}\Delta_v f_m(\mathbf{v}) = (\mathcal{Q}_m^+ - \mathcal{Q}_m^-)(\mathbf{f},\mathbf{f})(\mathbf{v})} \tag{2.5.1}$$

where now the collision term $\mathcal{Q}_m^+ - \mathcal{Q}_m^-$ includes only functions of $\mathbf{v}$. This is our final equation for the density of droplets. It is parametrized by σ^2, the intensity of noise covariance which, in the approximation of this white noise model, corresponds to the concept of *turbulence kinetic energy*, cf. [22]. Even though (2.5.1) is of variable $\mathbf{v}$ only, it is fundamentally different from a Smoluchowski equation with only $\mathbf{x}$ variable, due to the presence of velocity difference $|\mathbf{v}-\mathbf{v}'|$ in the nonlinearity. This term is the source that turns diffusion enhancement into coagulation enhancement.

2.6 Formula for the average relative velocity

In order to approximate analytically the average value $\langle|\mathbf{v}_1 - \mathbf{v}_2|\rangle$ we adopt the mean field viewpoint of Smoluchowski equations, where particles are independent. Therefore, if $p_m(\mathbf{v})$ is the probability density of velocity of mass m, we have

$$R_{m_1,m_2} = \iint |\mathbf{v}_1 - \mathbf{v}_2| \, p_{m_1}(\mathbf{v}_1) \, p_{m_2}(\mathbf{v}_2) \, d\mathbf{v}_1 d\mathbf{v}_2. \tag{2.6.1}$$

The natural choice of $p_m(\mathbf{v})$ is the normalized density $f_m(\mathbf{v}) / \int f_m(\mathbf{w}) \, d\mathbf{w}$ where $f_m(\mathbf{v})$ is a solution of Smoluchowski equation. However, we have to avoid a dependence on the initial conditions. We make the following heuristic argument. In the Smoluchowski system, the linear terms

$$\gamma_m \operatorname{div}_v(\mathbf{v} f_m(\mathbf{v})) + \frac{\gamma_m^2 \sigma^2}{2} \Delta_v f_m(\mathbf{v})$$

are associated with the transient phase which moves the initial distribution towards a certain limit shape. Simultaneously and afterwards, the nonlinear terms shift mass from lower to higher levels, but their impact on the modification of shape is minor. Therefore we take, as $p_m(\mathbf{v})$ the invariant distribution of the linear part, which is a centered Gaussian with covariance matrix $\frac{1}{2}\gamma_m \sigma^2 I_d$ (I_d is the identity matrix):

$$p_m \sim N\left(0, \frac{1}{2}\gamma_m \sigma^2 I_d\right).$$

The difference of two independent centered Gaussians, with covariances $\frac{1}{2}\gamma_{m_1}\sigma^2 I_d$ and $\frac{1}{2}\gamma_{m_2}\sigma^2 I_d$ is a centered Gaussian with covariance $\frac{1}{2}(\gamma_{m_1} + \gamma_{m_2})\sigma^2 I_d$. Therefore the random quantity $\mathbf{v}_1 - \mathbf{v}_2$ has this law. By properties of Gaussians,

$$\mathbf{v}_1 - \mathbf{v}_2 \overset{(d)}{=} \sqrt{\frac{1}{2}(\gamma_{m_1} + \gamma_{m_2})}\sigma \mathbf{Z}$$

where $\mathbf{Z}$ is distributed as $N(0, I_d)$, and

$$\langle|\mathbf{Z}|\rangle = \sqrt{2}\frac{\Gamma(\frac{d+1}{2})}{\Gamma(\frac{d}{2})}$$

since $|\mathbf{Z}|$ has a Chi distribition with parameter d. Thus we have

$$R_{m_1,m_2} = \langle|\mathbf{v}_1 - \mathbf{v}_2|\rangle = \frac{\Gamma(\frac{d+1}{2})}{\Gamma(\frac{d}{2})}\sqrt{\gamma_{m_1} + \gamma_{m_2}}\sigma.$$

By (2.1.3), $\sigma^2 = \frac{4}{d}\tau_{\mathbf{U}} k_T$ and taking $d = 3, \Gamma(2) = 1, \Gamma(\frac{3}{2}) = \frac{\sqrt{\pi}}{2}$, we arrive at

$$\begin{aligned} R_{m_1,m_2} &= \sqrt{\frac{4}{3}}\frac{2}{\sqrt{\pi}}\sqrt{(\gamma_{m_1}\tau_{\mathbf{U}} + \gamma_{m_2}\tau_{\mathbf{U}})k_T} \\ &= \frac{4}{\sqrt{3\pi}}\sqrt{\frac{k_T}{St_{m_1}} + \frac{k_T}{St_{m_2}}}, \end{aligned}$$

as announced in (2.1.7).

Up to the multiplicative constant, this also agrees with the formula obtained by Abrahamson [1]. Indeed, in [1] the energy dissipation rate $\varepsilon \sim k_T/\tau_{\mathbf{U}}$, clear from the energy balance of Navier-Stokes equation since all three quantities correspond to the turbulent fluid:

$$\frac{\partial}{\partial t}\left(\frac{1}{2}|\mathbf{U}|^2\right) = -\varepsilon + \text{other terms}.$$

2.7 Numerical results

For the convenience of numerical simulations, we consider from now on only finitely many mass levels. That is, we truncate (2.5.1) into a finite system of PDE-s whose solution is $(f_1, f_2, ..., f_M)$, for some integer M. This amounts to replacing the $\sum_{n=1}^{\infty}$ in the loss term $\mathcal{Q}_m^-$ (2.1.5) by $\sum_{n=1}^{M}$, with everything else unchanged. Correspondingly, in the particle system (2.1.2), each particle's mass is restricted to $m_i \in \{1, 2, ..., M\}$. The interpretation is that when the mass of a rain droplet exceeds the threshold M, it falls down and hence exits the system.

To understand the effect of the turbulent velocity field on coagulation, we identify and build on a key quantity, $\mathcal{M}_1^\sigma(t)$ below, which is essentially the first moment of the mass in the system at time t. Since $M < \infty$ in the truncated model, eventually all masses leave the system, hence we measure the efficiency of coagulation by looking at how fast this first moment decays in time, with respect to different values of σ. In the last part of this section, using results on the total mass, we will build a procedure to estimate the mean Collision Rate (see section 2.6), validating our theoretical results in simple settings.

Total mass

To this end, we define

$$\mathcal{M}_1^\sigma(t) := \sum_{m=1}^{M} m \int f_m(t, \mathbf{v})\, d\mathbf{v}\,, \tag{2.7.1}$$

which we also call "total mass" for simplicity. Analyzing the nonlinearity of our PDE, we notice that

$$\sum_{m=1}^{M} \int m(\mathcal{Q}_m^+ - \mathcal{Q}_m^-)\, d\mathbf{v} \le 0, \quad \forall t \tag{2.7.2}$$

implying that $d\mathcal{M}_1^\sigma(t)/dt \le 0$, that is, the function (2.7.1) is non-increasing in time. Moreover, for the infinite system $M = \infty$, equality is achieved in (2.7.2), hence we see that the mass deficiency in the finite system is not lost at all and it is simply sent to higher order ($> M$) of mass-type densities.

Indeed, in view of the form of the negative part of coagulation operator $\mathcal{Q}_m^-$, every coagulation at the level of f_m, f_n, with $m + n > M$, represents a decrease in mass that, ideally, increases the density f_{m+n} that is outside of our system. In particular, fixing $M < \infty$, in the framework of rain formations, is equivalent to saying that such a threshold

represents the largest droplets that are falling outside of the cloud and do not interact any more with the system. As such $M = \infty$ is just the precise abstract setting in which no rainfall is present and serves as a limiting behavior for the single masse $m \in \mathbb{N}$, and as a right derivation of the conserved mass in the system as all: both for the falling particles and the ones remaining in the cloud. Hence, the more and faster the quantity $\mathcal{M}_1^\sigma(t)$ decreases over time, the faster and richer the coagulation to higher mass-type is achieved.

Faster barrier exit time

The second quantity we consider is closely linked to the enhanced coagulation due to turbulence that we will establish with the "total mass" and gives more quantitative information. We will consider the same numerical setting as we will do above, and estimate a decay law that links the first time that the total mass $\mathcal{M}_1^\sigma(t)$ drops below a certain level to the turbulence parameter σ. Specifically, let

$$m_0^T := \inf_{t\in[0,T]} \mathcal{M}_1^0(t)$$

and define a sequence of "barrier exit times" $(\tau_\sigma)_{\sigma\geq 0}$

$$\tau_\sigma := \inf\left\{t \geq 0,\, \mathcal{M}_1^\sigma(t) \leq m_0^T\right\} \wedge T. \tag{2.7.3}$$

Since $t \mapsto \mathcal{M}_1^0(t)$ is decreasing, we have that $\tau_0 = T$. Since $\mathcal{M}_1^\sigma(t)$ is expected to decay faster as σ increases, $\sigma \mapsto \tau_\sigma$ should be decreasing.

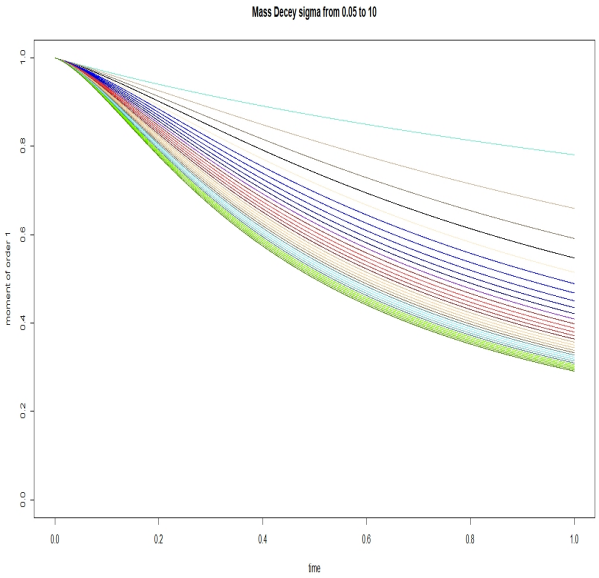

Figure 2.1: $M = 1$; Decay of $\mathcal{M}_1^\sigma(t)$ for $t \in [0, 1]$, with maximal mass level $M = 1$, initial density $f_1(0, \mathbf{v})$ of mass $m = 1$ concentrated on the set $\mathbf{v} \in [-1/2, 1/2]$. The parameter σ^2 ranges from a sample in the set 0.05 to 10 (around 30 points). A visible increase in coagulation is present at the increase of σ^2.

2.7.1 On a limiting behavior: $M = 1$

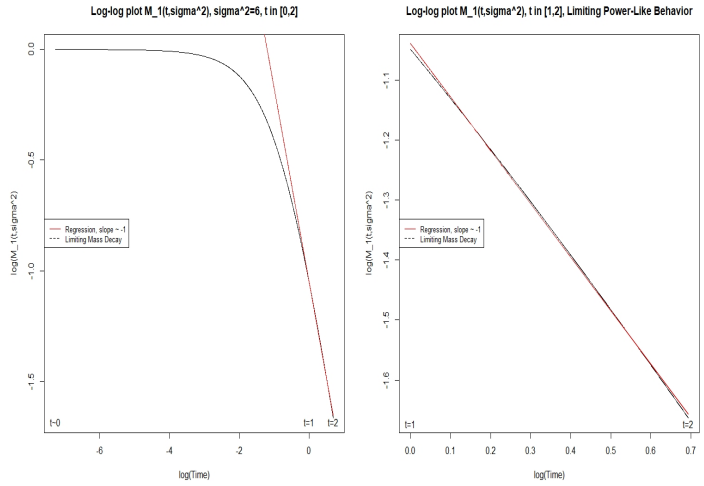

Figure 2.2: $M = 1$; On the left, a plot of $\log\left(\mathcal{M}_1^\sigma(t)\right)$ versus $\log(t)$ in the time window $[0, 2]$ at fixed $\sigma^2 = 6$, and on the right a close-up in the time window $[1, 2]$, suggest that $t \mapsto \mathcal{M}_1^\sigma(t)$ is of inverse power 1. However, for small time, the dependence is different and could represent a transient behavior.

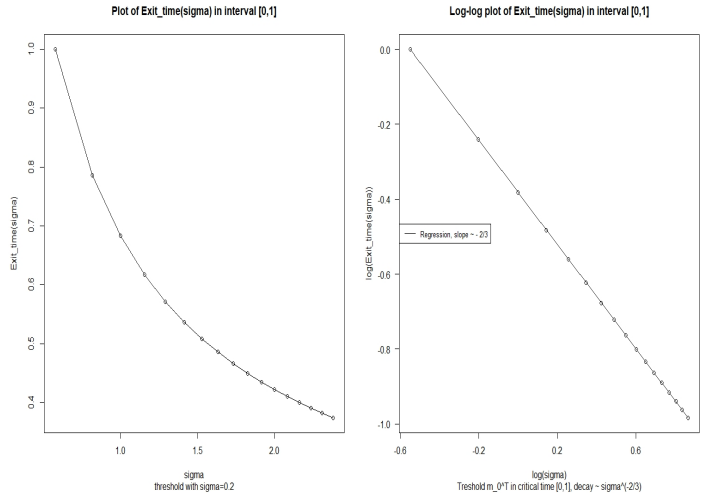

Figure 2.3: $M = 1$; A plot of the barrier exit time τ_σ with respect to the turbulence parameter σ, and the corresponding log-log regression in the time window $[0, 1]$ yields $\tau_\sigma \propto \sigma^{-2/3}$.

We perform a numerical simulation of the system (2.5.1) for dimension $d = 1$, maximal mass level $M = 1$ and time window $[0, 2]$, with a semi-implicit method to compute its solutions, with time step $dt \sim 10^{-4}$ and spatial step $dv \sim 10^{-2}$. Thanks to the fast decay to zero as $|\mathbf{v}| \to \infty$ of the solution [31], we truncate the velocity variable in the range $\mathbf{v} \in [-20, 20]$ both for the numerical integration of the nonlinearity and for the

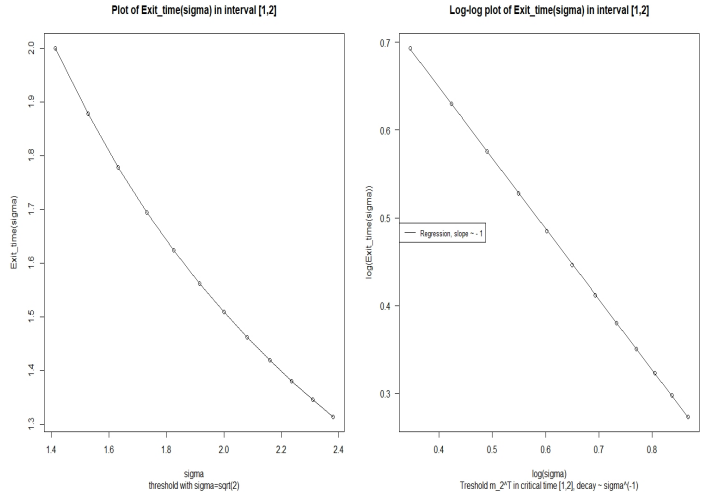

Figure 2.4: $M = 1$; A plot of the barrier exit time τ_σ with respect to the turbulence parameter σ, and the corresponding log-log regression in the time window $[0, 2]$, taking into consideration only those exit times in the interval $[1, 2]$, yields $\tau_\sigma \propto \sigma^{-1}$.

total mass (2.7.1).

In Figure 2.1, we plot the function (2.7.1) for different values of the turbulence parameter σ^2 that range from 0.05, that we refer to as the non-turbulent case, to 10, which represents an intense eddy diffusivity. It shows a faster decay correlated to the increase of turbulence, and a speedup coagulation process.

For fixed $\sigma^2 = 6$ we performed a log-log plot in time window $[0, 2]$ as shown in Figure 2.2 that shows $t \mapsto \mathcal{M}_1^\sigma(t)$ is of inverse power 1, after a transient time period.

We see from Figures 2.3 and 2.4 that the expected behavior on the barrier time is obtained, and the curve exhibits a power like decay, with an asymptotic limit to zero. In Figure 2.3, we performed a log-log plot and regression taking $T = 1$ and it yields $\tau_\sigma \propto \sigma^{-2/3}$ (here and in the sequel $\propto$ denotes proportional to), whereas the same analysis in Figure 2.4 taking $T = 2$ and considering only those exit times that are in the interval $[1, 2]$ yields $\tau_\sigma \propto \sigma^{-1}$.

We conjecture that the function (2.7.1) can be expressed as (for t suitably large, say $t > 1$ in our simulations)

$$\mathcal{M}_1^\sigma(t) \sim \frac{1}{A_d(\sigma)t + \mathcal{M}_1^\sigma(0)^{-1}}, \tag{2.7.4}$$

for some function A_d that depends on dimension d, and that $A_1(\sigma) \propto \sigma$. Here and in the sequel, $\sim$ denotes asymptotically for large t.

A rough explanation of the numerical findings may be the following one, that will be explored more closely in a future work, since - as shown below - our understanding is still incomplete. When $M = 1$, the density $f(t, \mathbf{v})$ of the unique level $m = 1$ satisfies the identity

$$\frac{d}{dt}\int f(t, \mathbf{v})\, d\mathbf{v} = -\iint \left|\mathbf{v} - \mathbf{v}'\right| f(t, \mathbf{v})\, f\left(t, \mathbf{v}'\right) d\mathbf{v} d\mathbf{v}'$$

because the differential terms cancel by integration by parts. Assume that, at least after a transient time (confirmed by Figure 2.2), up to a small approximation,

$$f(t, \mathbf{v}) \sim \alpha(t) f_0(\mathbf{v})$$

namely the decay of $f(t, \mathbf{v})$ is self-similar [23]. Then (up to approximation) $\alpha' = -\sigma_0 \alpha^2$ where

$$\sigma_0 = \iint |\mathbf{w} - \mathbf{w}'| f_0(\mathbf{w}) f_0(\mathbf{w}') d\mathbf{w} d\mathbf{w}'$$

is an average variation of velocity under f_0, namely

$$\alpha(t) \sim \frac{1}{\sigma_0 t + C}$$

after an initial transient period. Moreover, speculating that the standard deviation of f_0 should be of order σ (since the dispersion produced by the linear differential operator is proportional to σ), we expect that σ_0 increases linearly with σ. The numerical results of Figures 2.3 and 2.4 show that this looks the trend for sufficiently large time but for a short time another power, $\sigma^{2/3}$, emerges, that should be understood. As for the behavior in time, since this computation can be carried out for every $d > 1$, when $M = 1$, we believe that the decay in time is dimension-independent.

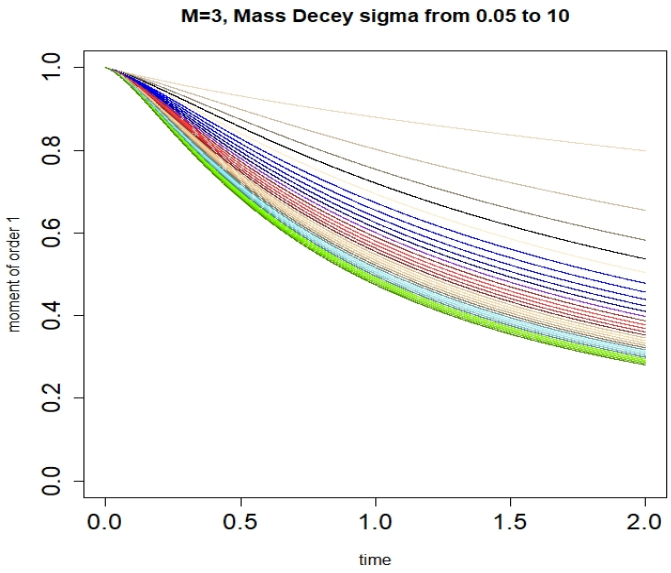

Figure 2.5: $M = 3$; Decay of $\mathcal{M}_1^q(t)$ for $t \in [0, 2]$, with maximal mass level $M = 3$, initial density $f_1(0, \mathbf{v})$ of mass $m = 1$ concentrated on the set $\mathbf{v} \in [-1/2, 1/2]$, $f_j(0, \mathbf{v}) = 0, j \neq 1$. The parameter σ^2 ranges from a sample in the set 0.05 to 10 (around 30 points). A visible increase in coagulation is present at the increase of σ^2.

2.7.2 Localized mass concentration: $M > 1$

When considering $M > 1$, we can expect two natural settings to investigate: the one where initially all the mass is concentrated on the first level, i.e. $m = 1$, and the one

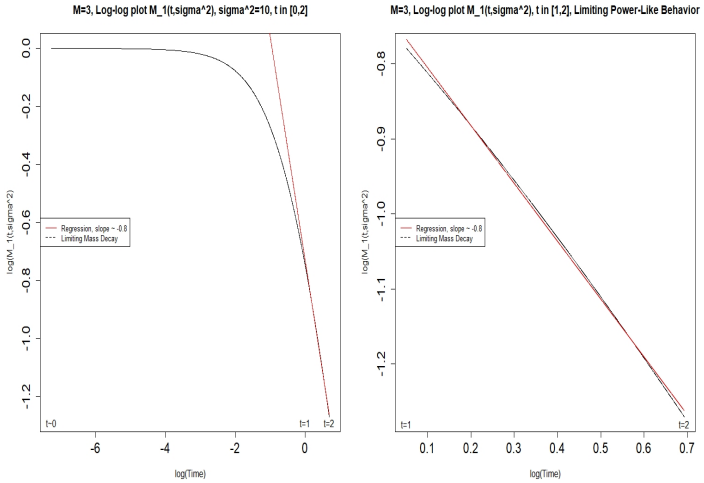

Figure 2.6: $M = 3$; On the left, a plot of $\log\left(\mathcal{M}_1^\sigma(t)\right)$ versus $\log(t)$ in the time window $[0, 2]$ at fixed $\sigma^2 = 10$, and on the right a close-up in the time window $[1, 2]$, suggests that $t \mapsto \mathcal{M}_1^\sigma(t)$ is of inverse power 0.8. However, for small time, the dependence is different and could represent a transient behavior.

that follows the theoretical assumptions of [48, 31, 36]. Concerning the first setting, we perform a numerical simulation of the system (2.5.1) for dimension $d = 1$, maximal mass level $M = 3$ and time window $[0, 2]$.

In Figure 2.5, we plot the function (2.7.1) for different values of the turbulence parameter σ^2 that ranges from 0.05, that we refer to as the non-turbulent case, to 10, which represents an intense eddy diffusivity. As in the case of $M = 1$, it shows a faster decay correlated to the increase of turbulence, and a speedup coagulation process.

For fixed $\sigma^2 = 10$, we perform a log-log plot in time window $[0, 2]$ as shown in Figure 2.6 that shows $t \mapsto \mathcal{M}_1^\sigma(t)$ is of inverse power approximately of 0.8, after a transient time period. Thus, we see a difference in the behavior of the "total mass" when M increases: this is not unexpected when all the initial mass is concentrated in the first layer $m = 1$. In fact, analyzing the coagulation operator (2.1.5), we see that $\mathcal{Q}_m^+$ is responsable for the generation of bigger particles in higher mass-levels and it is dominant when all the mass of the system is selected as a single type. Therefore, for a transient period, we see an increase in mass for $m \neq 1$ and as such a slower decay of $\mathcal{M}_1^\sigma(t)$, the total mass.

For this reason, as shown in Figure 2.7, we study the decay of the single mass $m \in \{1, 2, 3\}$, where analogous to (2.7.1), the single mass at level $m = k$ is defined as

$$\mathcal{M}_1^\sigma(t)|_{m=k} := k \int f_k(t, \mathbf{v})\, d\mathbf{v}. \tag{2.7.5}$$

The figure shows the regression curves plotted with dashed lines. As in Figure 2.2, for $m = 1$ we maintain a relation of inverse power in time, approximately of 1, after a transient time period. As a further exploration, we see from Figure 2.8 that the same behavior is present, and the curve exhibits a power like decay, with an asymptotic limit to zero.

Concerning the behavior of the barrier time, we see from Figures 2.9 and 2.10 that the curve exhibits a power like decay, with an asymptotic limit to zero.

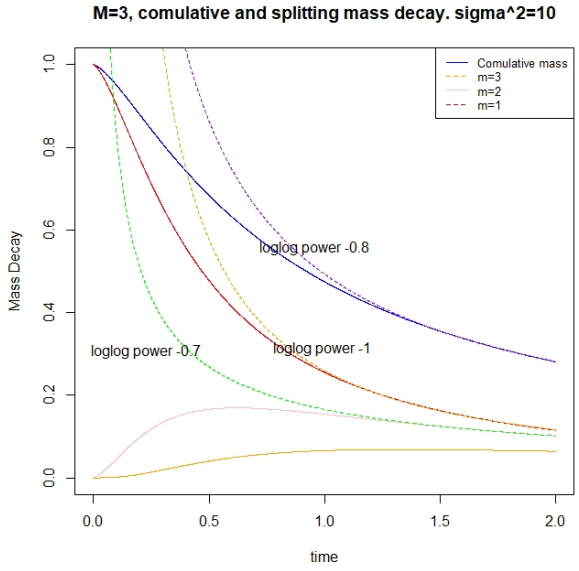

Figure 2.7: $M = 3$; Decay of $\mathcal{M}_1^\sigma(t)$ for the total mass, and the single behavior $\mathcal{M}_1^\sigma(t)|_{m=k}$ of each lever $k \in \{1, 2, 3\}$ in the case $\sigma^2 = 10$. With the dashed lines, one can see the expected limiting behaviors of each curve and their relative power. This suggest a log-logistic behavior of the full system with $M < \infty$.

In Figure 2.9, we perform a log-log plot and regression taking $T = 1$ and it yields $\tau_\sigma \propto \sigma^{-2/3}$, whereas the same analysis in Figure 2.10 taking $T = 2$ and considering only those exit times that are in the interval $[1, 2]$ yields $\tau_\sigma \propto \sigma^{-1}$.

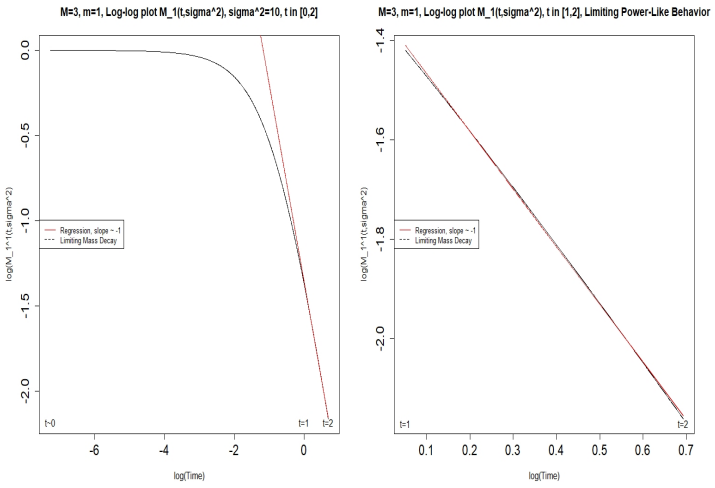

Figure 2.8: $M = 3$, $m = 1$; On the left, a plot of $\log\left(\mathcal{M}_1^\sigma(t)|_{m=1}\right)$ versus $\log(t)$ in the time window $[0, 2]$ at fixed $\sigma^2 = 10$, and on the right a close-up in the time window $[1, 2]$, suggest that $t \mapsto \mathcal{M}_1^\sigma(t)|_{m=1}$ is of inverse power 1. This is consistent with the case $M = 1$.

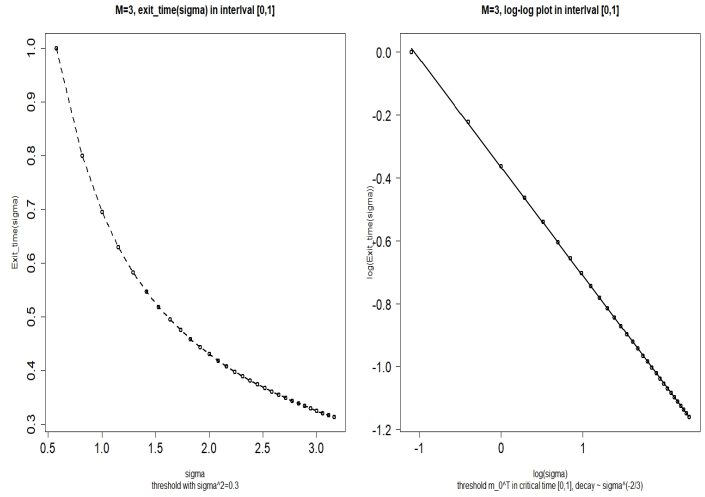

Figure 2.9: $M = 3$; A plot of the barrier exit time τ_σ with respect to the turbulence parameter σ, and the corresponding log-log regression in the time window $[0, 1]$ yields $\tau_\sigma \propto \sigma^{-2/3}$.

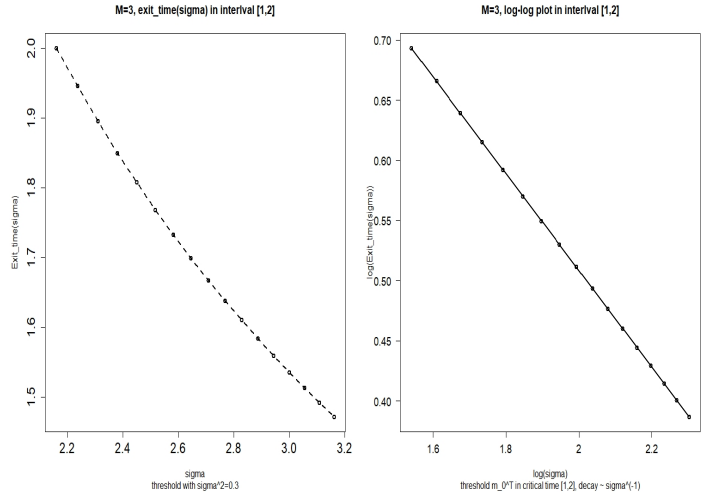

Figure 2.10: $M = 3$; A plot of the barrier exit time τ_σ with respect to the turbulence parameter σ, and the corresponding log-log regression in the time window $[0, 2]$, taking into consideration only those exit times in the interval $[1, 2]$, yields $\tau_\sigma \propto \sigma^{-1}$.

Thus, when $M > 1$, and the initial mass is located on a single level, we lose the conjectured behavior of Subsection 2.7.1, and we can only expect that the function (2.7.1) has the same asymptotic limit as

$$\mathcal{M}_1^\sigma(t) \gtrsim \frac{1}{A_d(\sigma)t + \mathcal{M}_1^\sigma(0)^{-1}},$$

for some function A_d that depends on dimension d, and that $A_1(\sigma) \propto \sigma$. A rough explanation of this numerical finding may be the following one: when $M > 1$ and the density

$f(0, \mathbf{v})$ is in the unique level $m = 1$, from (2.1.5) we see that the poisitive part $\mathcal{Q}_m^+$ is greater than the negative part $\mathcal{Q}_m^-$ for a transient period of time in which, for $m > 1$ mass should increase before decay, suggesting a delay, and as such a reported slower decay, of the "total mass". Also supporting this idea are the numerical simulations performed on the rapidity of decay for level $m = 1$. Here $\mathcal{Q}_1^+ = 0$, and we see the same behavior as the limiting case in which only one type of mass is considered.

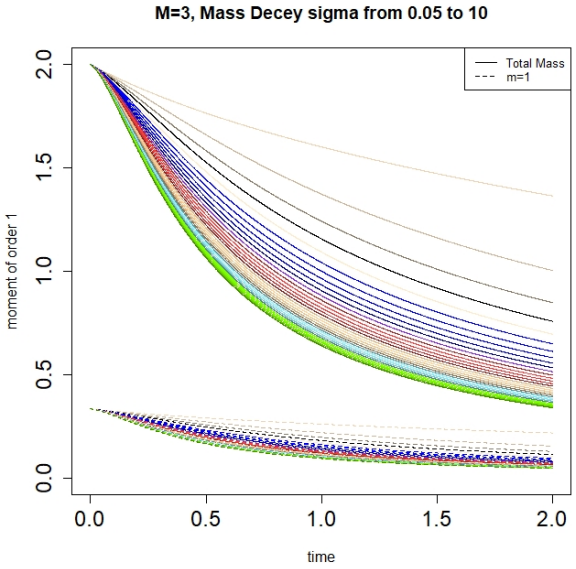

Figure 2.11: $M = 3$; Decay of $\mathcal{M}_1^\sigma(t)$, $t \in [0, 2]$. Initial density $f_j(0, \mathbf{v})$, $j = 1, 2, 3$ concentrated on $\mathbf{v} \in [-1/2, 1/2]$, following [48]. The parameter σ^2 ranges in the set 0.05 to 10. A visible increase in coagulation is present. Dashed lines are the single mass for $m = 1$, $\mathcal{M}_1^\sigma(t)|_{m=1}$.

2.7.3 Diffused mass concentration: $M > 1$

Here we propose a first analysis of the aformentioned second setting: the one that follows the theoretical assumptions as in [48, 31, 36]. In detail, the initial mass is not concentrated only in one layer, but is generated according to two probability distributions so that $\mathbb{P}(m_1(0) = m) = r(m)$ with $\sum_{m=1}^M r(m) = 1$, and deterministic probability densities functions $g_m(\mathbf{v})$, $m = 1, 2, ..., M$, satisfying suitable regularity and decay assumptions, such that

$$f_m^0(\mathbf{v}) = r(m) g_m(\mathbf{v}), \quad \forall m. \tag{2.7.6}$$

As such, we select initial conditions compactly supported in a small range of velocity, i.e. $[-1/2, 1/2]$, to better look at the behavior of the mass decay through time. We note here that this is the natural setting that generalizes the case of $M = 1$. We perform a numerical simulation of the system (2.5.1) for dimension $d = 1$, maximal mass level $M = 3$ and time window $[0, 2]$.

In Figure 2.11, we plot the function (2.7.1) for different values of the turbulence parameter σ^2 that ranges from 0.05, that we refer to as the non-turbulent case, to 10, which represents an intense eddy diffusivity. As in the case of $M = 1$, it shows a faster decay correlated with the increase of turbulence, and a speedup coagulation process. Plotted with dotted lines we show the decay of mass $m = 1$. This behavior is analogous for $m = 1, 2, 3$.

For fixed $\sigma^2 = 10$ we perform a log-log plot in time window $[0, 2]$ as presented in Figure 2.13. It shows that $t \mapsto \mathcal{M}_1^\sigma(t)$ is of inverse power approximatly 1, after a transient time period dependent on the finiteness of the initial condition. As conjectured in the case $M = 1$, we see a consistency in the behavior of the "total mass" when M increase: the initial condition is active everywhere, maintaining the structure of a probability density, thus making the results not unexpected. In fact, analyzing the coagulation operator (2.1.5), we see that $\mathcal{Q}^+$ is not dominant when all the masses of the system are spread over all the analyzed layers. Therefore, we see an immediate decrease in mass for $m \neq 1$ and as such a maintained global decay of $\mathcal{M}_1^\sigma(t)$, the total mass.

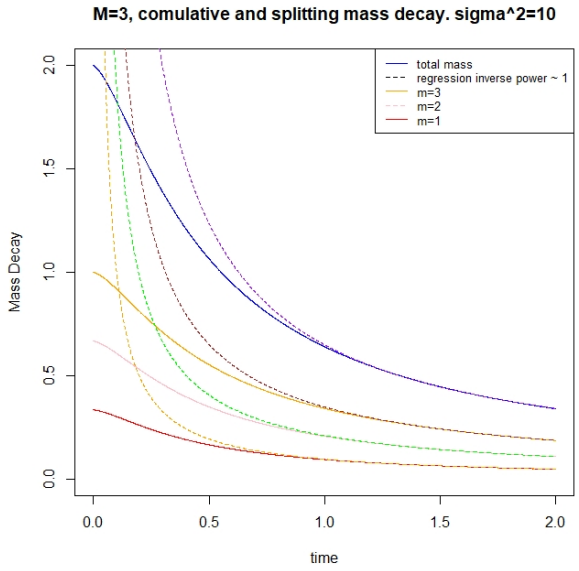

Figure 2.12: $M = 3$; $\mathcal{M}_1^\sigma(t)$ for the total mass and the single levels $\mathcal{M}_1^\sigma(t)|_{m=k}$, $k \in \{1, 2, 3\}$ for $\sigma^2 = 10$. In dashed lines we see the expected limiting behaviors and the relative power of order ≈ 1, suggesting consistent log-logistic behaviors as conjectured for system with $M < \infty$.

For this reason, as shown in Figure 2.12, we study the decay of the single mass $m \in \{1, 2, 3\}$. The figure shows the regression curves plotted with dashed lines. As in Figure 2.2, we maintain a relation of inverse power in time, approximately of 1, after a transient time period. As a further exploration, we see that the same behavior is present, and the curve exhibits a power like decay, with an asymptotic limit to zero.

Concerning the behavior of the barrier exit time, we see from Figures 2.14 and 2.15 that the curve exhibits a power like decay, with an asymptotic limit to zero. In Figure 2.14, we perform a log-log plot and regression taking $T = 1$ and it yields $\tau_\sigma \propto \sigma^{-2/3}$, whereas the

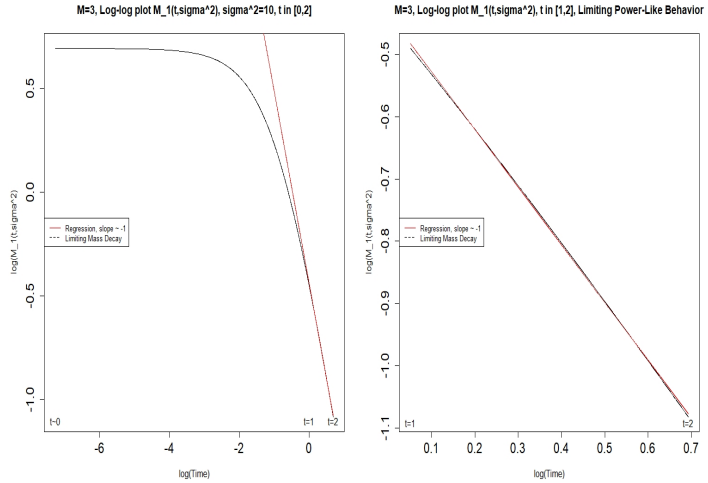

Figure 2.13: $M = 3$; On the left, a plot of $\log\left(\mathcal{M}_1^\sigma(t)\right)$ versus $\log(t)$ in the time window $[0, 2]$ at fixed $\sigma^2 = 10$, and on the right a close-up in the time window $[1, 2]$, suggest that $t \mapsto \mathcal{M}_1^\sigma(t)$ is of inverse power ≈ 1. A transient behavior is present due to the finite initial condition.

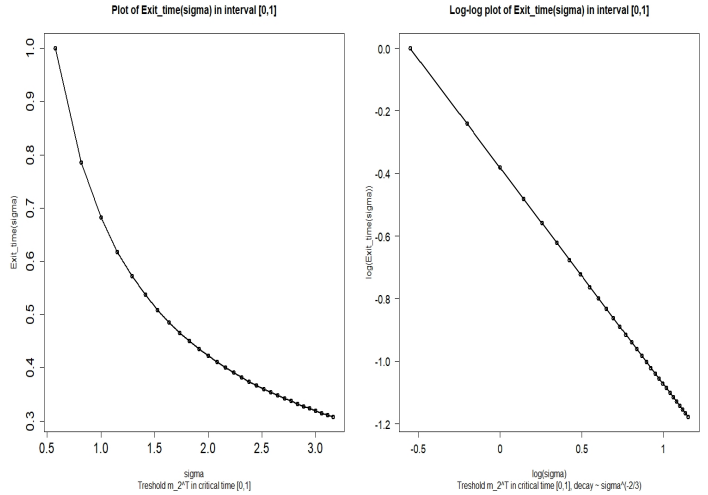

Figure 2.14: $M = 3$; A plot of the barrier exit time τ_σ with respect to the turbulence parameter σ, and the corresponding log-log regression in the time window $[0, 1]$ yields $\tau_\sigma \propto \sigma^{-2/3}$.

same analysis in Figure 2.15 taking $T = 2$ and considering only those exit times that are in the interval $[1, 2]$ yields $\tau_\sigma \propto \sigma^{-1}$. Thus, when $M > 1$, and the initial mass is spread over all the mass levels, we are close to the conjectured behavior of previous section, and we can expect that the function (2.7.1) has the same asymptotic limit as

$$\mathcal{M}_1^\sigma(t) \sim \frac{1}{A_d(\sigma)t + \mathcal{M}_1^\sigma(0)^{-1}}, \tag{2.7.7}$$

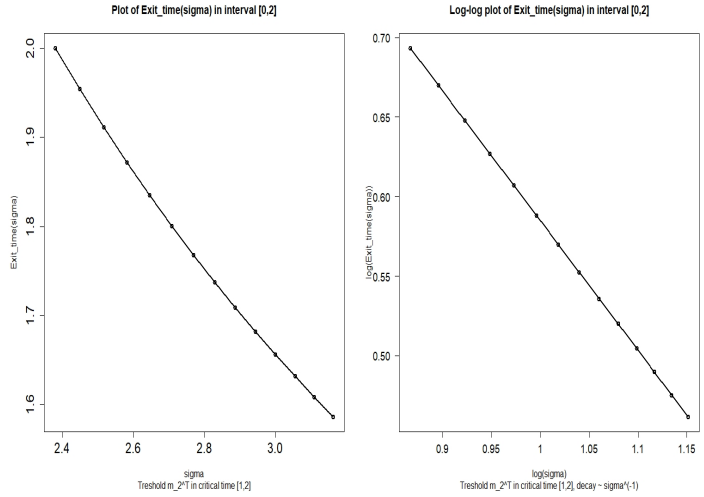

Figure 2.15: $M = 3$; A plot of the barrier exit time τ_σ with respect to the turbulence parameter σ, and the corresponding log-log regression in the time window $[0, 2]$, taking into consideration only those exit times in the interval $[1, 2]$, yields $\tau_\sigma \propto \sigma^{-1}$.

$$\mathcal{M}_1^\sigma(t)|_{m=1} \sim \frac{1}{A_d^1(\sigma)t + \mathcal{M}_1^\sigma(0)|_{m=1}^{-1}}, \tag{2.7.8}$$

for some function A_d that depends on dimension d, and that $A_1(\sigma) \propto \sigma$. A rough explanation of this numerical finding may be the following one: when $M > 1$ and the density $f(t, \mathbf{v})$ is spread over all levels $m = 1, ..., M$, from (2.1.5) we see that the positive part $\mathcal{Q}_m^+$ is already negligible with respect to that of $\mathcal{Q}_m^-$, for all m. In particular, the masses are drawn immediately to masses $> M$, that we interpret as falling rain outside of our system. Supporting this we see in Figure 2.12 no transient period of time in which, for $m > 1$, mass increases before decaying, suggesting no delay, and as such the decay of the "total mass" is maintained. Note that $\mathcal{Q}_1^+ = 0$ and, as expected, we see the same behavior as the limiting case in which only one type of mass is condidered.

We summarize in Table 2.1 the precise fitting obtained through non-linear regression for all the analyzed quantities. The table shows accordance with our proposed decay behavior and suggests a future analysis for different initial conditions and higher dimensions.

	$M = 1$	$M = 3$ **localized**	$M = 3$ **diffused**
$\boldsymbol{\tau_\sigma[0,1]}$	-0.66	-0.69	-0.68
$\boldsymbol{\tau_\sigma[1,2]}$	-0.94	-0.92	-0.91
$\boldsymbol{\mathcal{M}_1^\sigma(\sigma^2 = 10)}$	-0.96	-0.81	-0.94

Table 2.1: Table showing precise fitting parameters, on a log-log scale, for the decay in time of $\boldsymbol{\mathcal{M}_1^\sigma(t)}$ and for the exit barrier $\boldsymbol{\tau_\sigma}$.

2.7.4 Mean Collision Rate

Finally, in this segment we propose numerical simulations that validate the theoretical behavior proposed in Section 2.6.

In particular, we have analyzed the same setting as in 2.7.1, which either $M = 1$ or $M = 3$. Computed with the procedure that we will explain below, all the case agree with equation 2.6.1 and the theory proposed in 2.6. As such, for visual clarity, here we illustrate results in the simpler case $M = 1$, with $m = 1$, and compute the behavior of $R_{1,1}$ and its law respect to the fluctuation parameter of the velocity, σ.

The same simulations, with $M = 3$, focusing on different mass level $m \in \{1, 2, 3\}$ and different initial conditions are briefly discussed in Appendix .3, Figure 19. There, computed limiting value R_{m_1,m_2} show accordance with the simulations with $M = 1$.

From here on, we fix $\gamma = 1$ since objective of the paper is the understanding of the dependence on the turbulent kinetic energy of collision rate $R_{m,m}$. However, we note that this parameter is important to the complete understanding of the behavior of this kind of systems, thanks to is relation with Stokes Number, and as such would be subject of future studies.

We know from 2.6.1 that a candidate estimation for R_{m_1,m_2} is obtain throughout the steady state density of the system. For this reason, concerning the simulation, independently on M, we selected a concentrated initial condition with moderate velocity and we let the system evolve in the time frame $t \in [0, 4]$, producing solution $(f_m^\sigma(t, v))_m$.

Since no mass conservation is present for the finite system $M < \infty$, and density is moved to higher levels not preserving the starting probability, we normalize at each time step the density $f^\sigma(t, \mathbf{v})$, solution of our Smoluchowski equation, i.e. we consider

$$\xi_1^\sigma(t, \mathbf{v}) := f_1^\sigma(t, \mathbf{v}) \left(\int f_1^\sigma(t, \mathbf{v}) dv \right)^{-1}$$

and, with this, the product probability $\xi_1(v)dv \otimes \xi_1(w)dw$. We are able to compute a time dependent, mean in velocity, collision rate:

$$\mathbf{R_g}(\mathbf{t}, \sigma) := \iint |\mathbf{v} - \mathbf{w}| \xi_1^\sigma(t, \mathbf{v}) \xi_1^\sigma(t, \mathbf{w}) dv dw$$

In Figure 2.16, is shown the result for $M = 1,\ m = 1$ and this re-normalize collision rate. Each of the curves $R_g^\xi(\sigma)$ as an inverse behavior of a log-logistic function with exponent 1 in σ, suggesting a plateau in time. A such, this time dependent probability distribution on the product space of the velocity domains as a limiting density and we can argue that

$$\mathbf{R_g}(\mathbf{t}, \sigma) = \mathbb{E}_{m,m}[|\mathbf{v} - \mathbf{w}|] \to_{t\to\infty} R_{1,1}^M.$$

In fact, as shown in Appendix .3, Figure 20, the computed quantity $\xi(T, \mathbf{v})$ approximate the theoretical limiting density $p_1(\mathbf{v}) \sim \mathcal{N}(0, \sigma^2)$, for this reason we initialize the evolving system with the proposed steady state condition $f_0^1(t, \mathbf{v}) := \xi(T, \mathbf{v})$, for different σ.

This means that we expect $\xi(T, v, \sigma)$ to be closer to the steady state distribution after a small time and the computed $\mathbf{R_g}(\mathbf{t}, \sigma)$ will be $\propto R_{m_i,m_j}$. As such, we restart the system with this new initial condition. To take into account that the velocity is spread,

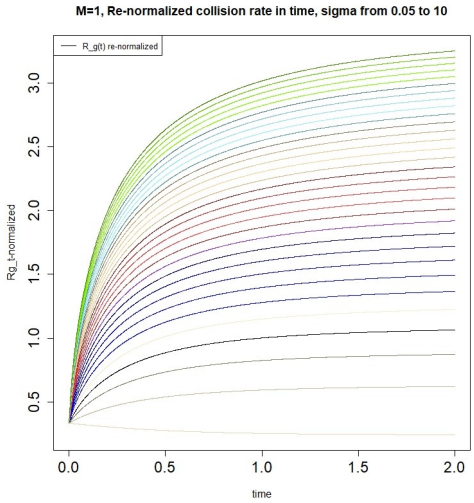

Figure 2.16: M=1; concentrated initial ccondition $f_0(v)$. The **re-normalized time dependent collision rate** $\mathbf{R_g}(\mathbf{t},\sigma)|_{[\mathbf{0},\mathbf{2}]}$ obtained with the new probability density $\xi_1^\sigma \otimes \xi_1^\sigma$.

with value greater than one, and the total density near this high value is not negligible in comparison with the concentrated initial condition that we used throughout our experiment, we enlarged the velocity domain and the time domain to produce stable results on the decay of the masses and also on the mean rate $R_g(t,\sigma)$.

In Figure 2.17 we show result on the re-started system, conferming the asymptotic limit of the collision rate and an increase in σ, the turbulent parameter of the system. We see a small flactuating period in which the rate is not increasing and than a fast stabilization that is linked to the velocity displacement of the steady state solution. In fact the new initial density condition produce, as expected, the same decay in the mass (since this depends only on σ and integral of the initial condition), but for a transient period the interaction kernel $Q_m(f)$ is much stronger that the speed in which diffusion of the Laplacian act, since the new initial condition is not negligible for high value of velocity. As such the plateau, which agrees with Figure 2.16, is reached after a small period of activation of the diffusion parameter.

Concluding, in Figure 2.18 we see that a linear relation with σ is present with angular coefficinet near 1, validating the expected behavior of $R_{1,1}$ with theoretical equation 2.6.1. This is expected and in line with the previuos reasoning and also with the small transient initialization.

2.8 Conclusion

In this article, we presented a new kinetic model of a modified Smoluchowski PDE system with discrete and finite mass levels, that takes advantage of small scale turbulence and eddy diffusion in the velocity variable to enhance coagulation. We presented the derivation of the PDE system from a particle-fluid model subjected to a transport-type noise, and we analyzed numerically the behavior of its solutions. We showed that coagulation efficiency

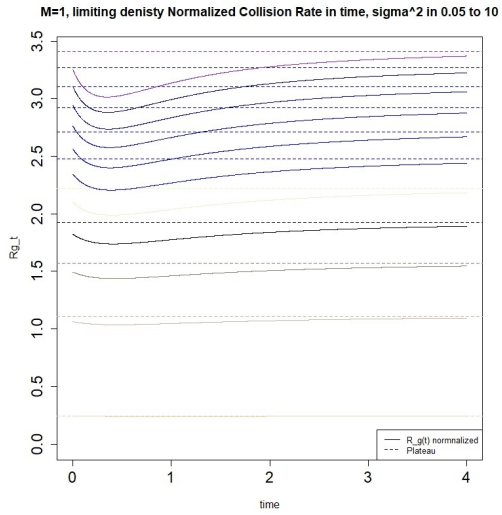

Figure 2.17: M=1; Initial condition $f_0(v) = \xi(T, v)$ approximation of stationary density. The **re-normalized time dependent collision rate** $\mathbf{R_g}(\mathbf{t}, \sigma)$ show stationary behavior. Darker line corresponds to higher sigma in the set $[0.05, 10]$.

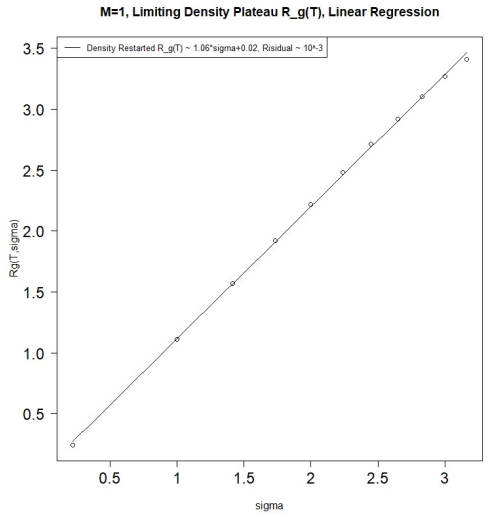

Figure 2.18: M=1; Initial condition $f_0(v) = \xi(T, v)$ re-normalized ending point of the simulation. Plotted limit in time $R_g(t, \sigma)$ show increase with σ. A linear regression in σ is performed with mean error 0.001.

increases steadily with the increase of turbulence and, moreover, a power-law decay in time and in the turbulence parameter is present.

Conluding, we have presented analytic and numerical presentation to understand the key factor of the collision rate as the average relative velocity between particles.

.1 Derivation of (2.1.4) from particle-fluid interaction

We present the sketch of the scaling limit to an SPDE from particle-fluid interaction for the truncated model (at threshold M).

For any $d \geq 1$ and $N, M \in \mathbb{N}$, consider an interacting particle system with space variable $\mathbf{x}_i^N(t)$ in $\mathbb{T}^d$, velocity variable $\mathbf{v}_i^N(t)$ in $\mathbb{R}^d$, mass variable $m_i^N(t)$ in a finite set $\{1, ..., M\}$, and initial cardinality $N(0) = N$. Between coagulation events, the motion of an individual active particle obeys (recall (2.1.2))

$$\begin{cases} d\mathbf{x}_i^N(t) = \mathbf{v}_i^N(t)dt, \\ d\mathbf{v}_i^N(t) \\ = \dfrac{\alpha}{(m_i^N(t))^{1-1/d}} \left[\displaystyle\sum_{k \in K} \sigma_k(\mathbf{x}_i^N(t)) \circ dW_t^k - \mathbf{v}_i^N(t)dt \right] \\ \quad , i \in \mathcal{N}(t), \end{cases} \tag{.1.1}$$

where

- $\sigma_k(\mathbf{x}) : \mathbb{T}^d \to \mathbb{R}^d$, $k \in K$ is a given (at most countably infinite) collection of smooth, deterministic, divergence-free vector fields.
- $\{W_t^k\}_{k \in K}$ is a given collection of standard Brownian motions in $\mathbb{R}$.
- $\circ$ denotes Stratonovich integration, according to Wong-Zakai principle [91].
- α is a positive constant that appears in Stokes' law, that includes the dynamic viscosity coefficient of the fluid.
- $\mathcal{N}(t) \subset \{1, 2, ..., N\}$ is the set of indices of particles that are still active at time t, with $\mathcal{N}(0) = \{1, 2, .., N\}$.

After each coagulation, the index set $\mathcal{N}(t)$ will change (decrease), and the velocity of a still-active particle i will be reset according to the conservation of momentum, to be described a few paragraphs below.

We note again that the velocity component of the dynamics (.1.1) obeys Stokes' law for the frictional force exerted on a spherical particle immersed in a fluid, cf. [64, 90], with the fluid velocity idealized by the white noise velocity field $\mathbf{U}(t, \mathbf{x})$ (2.4.1) (that acts simultaneously on all particles). This goes in the spririt of Kraichnan's model [58, 53].

We denote the $d \times d$ spatial covariance matrix of $\mathbf{U}(t, \mathbf{x})$ by

$$C(\mathbf{x}, \mathbf{y}) := \sum_{k \in K} \sigma_k(\mathbf{x}) \otimes \sigma_k(\mathbf{y}).$$

Moreover, for any fixed $\mathbf{x} \in \mathbb{T}^d$ we denote the second-order divergence form elliptic operator, acting on suitable functions on $\mathbb{R}^d$

$$(\mathcal{L}_v^{C,\mathbf{x}} f)(\mathbf{v}) := \frac{1}{2} \mathrm{div}_v \left(C(\mathbf{x}, \mathbf{x}) \nabla_v f(\mathbf{v}) \right).$$

With suitable choice of $\{\sigma_k\}_{k\in K}$, see [42, 35, 32], we can have that

$$\mathcal{L}_v^{C,\mathbf{x}} \equiv \frac{\sigma^2}{2}\Delta_v, \quad \forall \mathbf{x}. \tag{.1.2}$$

Each particle $i \in \mathcal{N}(t)$ has a mass $m_i^N(t) \in \{1, 2, .., M\}$ which changes over time according a stochastic coagulation rule to be described below. The initial mass $m_i(0)$, $i = 1, ..., N$, are chosen i.i.d. (independent and identically distributed) from $\{1, 2, .., M\}$ according to a probability distribution so that $\mathbb{P}(m_1(0) = m) = r(m)$ with $\sum_{m=1}^M r(m) = 1$. We are also given deterministic probability density functions $g_m(\mathbf{x}, \mathbf{v}) : \mathbb{T}^d \times \mathbb{R}^d \to \mathbb{R}_+$, $m = 1, 2, ..., M$, satisfying suitable regularity and decay assumptions, such that if $m_i(0) = m$ then the initial distribution of $(\mathbf{x}_i(0), \mathbf{v}_i(0))$ is chosen with probability density $g_m(\mathbf{x}, \mathbf{v})$, independently across i. We denote

$$f_m^0(\mathbf{x}, \mathbf{v}) := r(m)g_m(\mathbf{x}, \mathbf{v}), \quad \forall m. \tag{.1.3}$$

The rule of coagulation between pairs of particles is as follows. Let $\theta(\mathbf{x}) : \mathbb{R}^d \to \mathbb{R}_+$ be a given smooth symmetric probability density function in $\mathbb{R}^d$, that is, $\int \theta d\mathbf{x} = 1$, with compact support in $\mathbb{B}(0, 1)$ (the unit ball around the origin in $\mathbb{R}^d$) and $\theta(0) = 0$. Then, for any $\varepsilon \in (0, 1)$, denote $\theta^\varepsilon(\mathbf{x}) : \mathbb{T}^d \to \mathbb{R}_+$ by

$$\theta^\varepsilon(\mathbf{x}) := \varepsilon^{-d}\theta(\varepsilon^{-1}\mathbf{x}), \quad \mathbf{x} \in \mathbb{T}^d.$$

Suppose the current configuration of the particle system is

$$\begin{aligned}\eta &= (\mathbf{x}_1, \mathbf{v}_1, m_1, \mathbf{x}_2, \mathbf{v}_2, m_2, ..., \mathbf{x}_N, \mathbf{v}_N, m_N)\\ &\in (\mathbb{T}^d \cup \emptyset)^N \times (\mathbb{R}^d \cup \emptyset)^N \times \{1, ..., M, \emptyset\}^N\end{aligned}$$

where $(\mathbf{x}_i, \mathbf{v}_i, m_i)$ denotes the position, velocity and mass of particle i, by convention if particle i_0 is no longer active in the system, we set $\mathbf{x}_{i_0} = \mathbf{v}_{i_0} = m_{i_0} = \emptyset$ (a cemetery state). Independently for each pair (i, j) of particles, where $i \neq j$ run over the index set of active particles in η, with a rate (derived from the collision kernel as in [25], compare with (2.2.2))

$$s_{m_i^N, m_j^N} \frac{|\mathbf{v}_i - \mathbf{v}_j|}{N} \theta^\varepsilon(\mathbf{x}_i - \mathbf{x}_j) \tag{.1.4}$$

we remove $(\mathbf{x}_i, \mathbf{v}_i, m_i, \mathbf{x}_j, \mathbf{v}_j, m_j)$ from the configuration η, and then in case $m_i + m_j \leq M$, we add

$$\left(\mathbf{x}_i, \frac{m_i\mathbf{v}_i + m_j\mathbf{v}_j}{m_i + m_j}, m_i + m_j, \emptyset, \emptyset, \emptyset\right)$$

with probability $\frac{m_i}{m_i+m_j}$, and instead add

$$\left(\emptyset, \emptyset, \emptyset, \mathbf{x}_j, \frac{m_i\mathbf{v}_i + m_j\mathbf{v}_j}{m_i + m_j}, m_i + m_j\right)$$

with probability $\frac{m_j}{m_i+m_j}$. We call the new configuration obtained this way by $S_{ij}^1\eta$ and $S_{ij}^2\eta$ respectively. On the other hand, in case $m_i + m_j > M$, then after removing $(\mathbf{x}_i, \mathbf{v}_i, m_i, \mathbf{x}_j, \mathbf{v}_j, m_j)$ from η we do not add a new element.

In words, if (i,j) coagulate, we decide randomly which of $\mathbf{x}_i$ and $\mathbf{x}_j$ is the new position of the mass-combined particle, provided that the combined mass does not exceed the threshold M. If the position chosen is $\mathbf{x}_i$, then we consider j as being eliminated (no longer active) and the new particle has index i; whereas if the position chosen is $\mathbf{x}_j$, then we consider i as being eliminated and the new particle has index j. On the other hand, the velocity of the mass-combined particle is obtained by the conservation of momentum as in *perfectly inelastic collisions*.

Note that the form of the coagulation rate (.1.4) is such that a pair (i,j) can coagulate only if $|\mathbf{x}_i-\mathbf{x}_j|\leq\varepsilon$, that is, their spatial positions have to be ε-close. We are interested in the case when $\varepsilon=\varepsilon(N)\to 0$ as $N\to\infty$, so that the interaction is not of mean-field type, but local. Correspondingly, the final equation we get (see (.1.7)) is local in the $\mathbf{x}$ variable. In particular, choosing $\varepsilon=O(N^{-1/d})$ ensures that each particle typically interacts with a bounded number of others at any given time, which is the analogue in our continuum context, of nearest-neighbor or bounded-range interactions common in interacting particle systems defined on lattices, see [54] and references therein.

The essential feature of our coagulation rate is the presence of $|\mathbf{v}_i-\mathbf{v}_j|$, which results in the same velocity difference appearing in the limit PDE (2.1.4). Although such rates are widely accepted in the physics literature on rain formations, our approach views $\mathbf{v}$ as an active variable; we do not approximate it by a constant that depends on other physical parameters. Diffusion enhancement feeds back on coagulation enhancement through the presence of this velocity difference. As such, our Smoluchowski equation is new with respect to existing literature.

For each $N\in\mathbb{N}$, $T\in(0,\infty)$ and $m\in\{1,..,M\}$, we denote the process of empirical measure on position and velocity of mass-m particles in the system by

$$\begin{aligned}\mu_t^{N,m}(d\mathbf{x},d\mathbf{v}) :&= \frac{1}{N}\sum_{i\in\mathcal{N}(t)}\delta_{\left(\mathbf{x}_i^N(t),\mathbf{v}_i^N(t)\right)}(d\mathbf{x},d\mathbf{v})1_{\{m_i^N(t)=m\}}\\ &\in\mathcal{M}_{1,+}(\mathbb{T}^d\times\mathbb{R}^d)\end{aligned}\tag{.1.5}$$

where $\mathcal{M}_{1,+}:=\mathcal{M}_{1,+}(\mathbb{T}^d\times\mathbb{R}^d)$ denotes the space of subprobability measures on $\mathbb{T}^d\times\mathbb{R}^d$ equipped with weak topology. The choice of the initial conditions for our system implies that $\mathbb{P}$-a.s.

$$\mu_0^{N,m}(d\mathbf{x},d\mathbf{v})\Rightarrow f_m^0(\mathbf{x},\mathbf{v})dxdv,\quad \text{as } N\to\infty$$

for $m=1,...,M$, where $\Rightarrow$ indicates weak convergence of probability measures, and the limit f_m^0 (.1.3) is absolutely continuous. We conjecture that, under the assumption of local interaction, i.e.

$$\lim_{N\to\infty}\varepsilon(N)=0,\quad \limsup_{N\to\infty}\frac{\varepsilon(N)^{-d}}{N}<\infty,\tag{.1.6}$$

for every finite T, the collection of empirical measures $\left\{\mu_t^N(d\mathbf{x},d\mathbf{v}):t\in[0,T]\right\}_{m=1}^M$ converges in probability, as $N\to\infty$, in $\mathcal{D}\left([0,T],\mathcal{M}_{1,+}\right)^{\otimes M}$, where $\mathcal{D}\left([0,T],\mathcal{M}_{1,+}\right)$ is the space of càdlàg functions taking values in $\mathcal{M}_{1,+}$ equipped with the Skorohod topology, towards an absolutely continuous limit $\{f_m(t,\mathbf{x},\mathbf{v}):t\in[0,T]\}_{m=1}^M$. which is the pathwise unique weak solution to a Smoluchowski-type SPDE system (.1.7). The latter SPDE

degenerates to the PDE system we study in this paper (2.1.4) when the Itô term is switched off. Through recent progresses in stochastic fluid mechanics, cf. [42, 35, 32, 33, 44], there exist specific limiting procedures that allow, in principle, to obtain the PDE from the SPDE by carefully choosing the vector fields $\{\sigma_k(\mathbf{x})\}_{k\in K}$. While we do not provide a rigorous proof here, we think that this heuristic argument is sufficient to justify our interest in studying our PDE system.

$$\begin{cases} df_m(t,\mathbf{x},\mathbf{v}) &= \left(-\mathbf{v}\cdot\nabla_x + \gamma_m \mathsf{div}_v\left(\mathbf{v}\cdot\right) + \dfrac{\gamma_m^2\sigma^2}{2}\Delta_v\right) f_m(t,\mathbf{x},\mathbf{v})dt \\ & \quad -\gamma_m \sum_{k\in K}\sigma_k(\mathbf{x})\cdot\nabla_v f_m(t,\mathbf{x},\mathbf{v})\, dW_t^k + \left(\mathcal{Q}_m^+ - \mathcal{Q}_m^-\right)(\mathbf{f},\mathbf{f})(t,\mathbf{x},\mathbf{v}). \\ f_m(\cdot,\mathbf{x},\mathbf{v})|_{t=0} &= f_m^0(\mathbf{x},\mathbf{v}), \quad m=1,...,M. \end{cases} \tag{.1.7}$$

.2 Explanation of the link (2.1.3)

Recall the stochastic equation 2.3.1. In real turbulent fluids, the fluid vector field $\mathbf{U}(t)$ is not exactly white in time, but has a correlation length approximately $\tau_{\mathbf{U}}$. Alleviating notations, let us only analyze the transport term involving $\mathbf{U}(t)$ and introduce a time delay of duration $\tau_{\mathbf{U}}$:

$$\begin{aligned} &\gamma_m \operatorname{div}_v\left(\left(\mathbf{U}(t)\right) f_m(t)\right) = \gamma_m \mathbf{U}(t)\nabla_v f_m(t) \\ &= \gamma_m \mathbf{U}(t)\nabla_v f_m(t-\tau_{\mathbf{U}}) + \gamma_m \mathbf{U}(t)\nabla_v\left(f_m(t) - f_m(t-\tau_{\mathbf{U}})\right) \\ &= \gamma_m \mathbf{U}(t)\nabla_v f_m(t-\tau_{\mathbf{U}}) \\ &\quad - \gamma_m \mathbf{U}(t)\nabla_v\left(\int_{t-\tau_{\mathbf{U}}}^t \gamma_m \mathbf{U}(s)\nabla_v f_m(s)ds\right) + \text{other terms}, \end{aligned} \tag{.2.1}$$

where the first equality is due to $\mathbf{U}(t)$ independent of v, and in the last line we applied the equation 2.3.1 a second time (assuming the other terms are minor).

In the limit $\tau_{\mathbf{U}} \to 0$, $\mathbf{U}(t)$ approaches white noise in time, the first term of (.2.1) yields a local-martingale, the Itô term. From the second term of (.2.1) emerges a second-order elliptic operator

$$-\gamma_m^2 \nabla_v\left(\int_{t-\tau_{\mathbf{U}}}^t \mathbf{U}(t)\otimes\mathbf{U}(s)\nabla_v f_m(s)ds\right)$$

that in the limit $\tau_{\mathbf{U}} \to 0$ is expected to converge to

$$-\frac{1}{2}\gamma_m^2 \mathsf{div}_v\left(C(\mathbf{0})\nabla_v f_m(t)\right) = -\frac{1}{2}\gamma_m^2\sigma^2\Delta_v f_m(t).$$

Since the turbulence kinetic energy k_T is the half-trace of the velocity covariance tensor [22], idealizing the tensor structure of $\mathbf{U}(t)\otimes\mathbf{U}(s)$ with $|t-s|\le\tau_{\mathbf{U}}$, we may have that

$$\frac{1}{2}\mathbf{U}(t)\otimes\mathbf{U}(s) \sim \frac{k_T}{d} I_d, \quad |t-s|\le\tau_{\mathbf{U}}$$

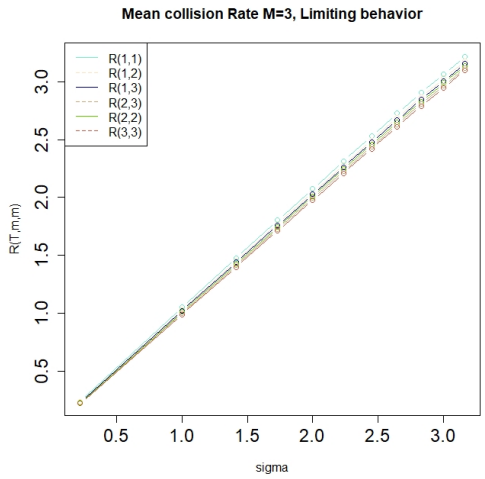

Figure 19: $M = 3$; Plotted estimated $R_{m_1,m_2}(\sigma)$ with $m_j \in \{1, 2, 3\}$. A linear dependence in σ is performed with mean error between 10^{-2} and 10^{-3}.

and consequently,

$$\frac{1}{2}\int_{t-\tau_{\mathbf{U}}}^{t} \mathbf{U}(t) \otimes \mathbf{U}(s)ds \sim \tau_{\mathbf{U}} \frac{k_T}{d} I_d.$$

This yields $\frac{\sigma^2}{2} = \frac{2\tau_{\mathbf{U}} k_T}{d}$ as claimed in (2.1.3).

In the above argument, it is crucial that we can take $\tau_{\mathbf{U}}$ very small while having γ of order 1. With $St = 1/(\gamma\tau_{\mathbf{U}})$, the argument thus works only when St is very large, and the regime where St is of order 1 requires a different analysis, consistent with the findings of [1, 25, 64, 90].

.3 Mean Collision Rate $M > 1$ and Guassianity assumption

Using the same method proposed in Section 2.7, we obtain analogous result for $M = 3$. We analyzed two initial condition: a localized one in the mass $m = 1$, and a theoretical one following [48]. In both of this case we used the restarting limiting density ξ_T either averaged $\{\frac{1}{M}\xi_T^1, \frac{1}{M}\xi_T^2, \frac{1}{M}\xi_T^3\}$ or localized $\{\xi_T^1, 0, 0\}$ obtaining analogous results. In Figure 19, the case of localized density is shown with all combination of Collision Rate, showing agreement with the theory.

Finally, in Figure 20, we show the comparison between expected steady state probability and computed starting stationary solution $\xi_T(v)$, in the case $M = 1$ and $T = 4$. The difference in L^2 norm of the two function is less then 10^{-1}, as per the difference between theoretical R_{m_i,m_j} and computed $R_{m_i,m_j}(T)$ estimated in less than 10^{-2}, showing the same linear behavior.

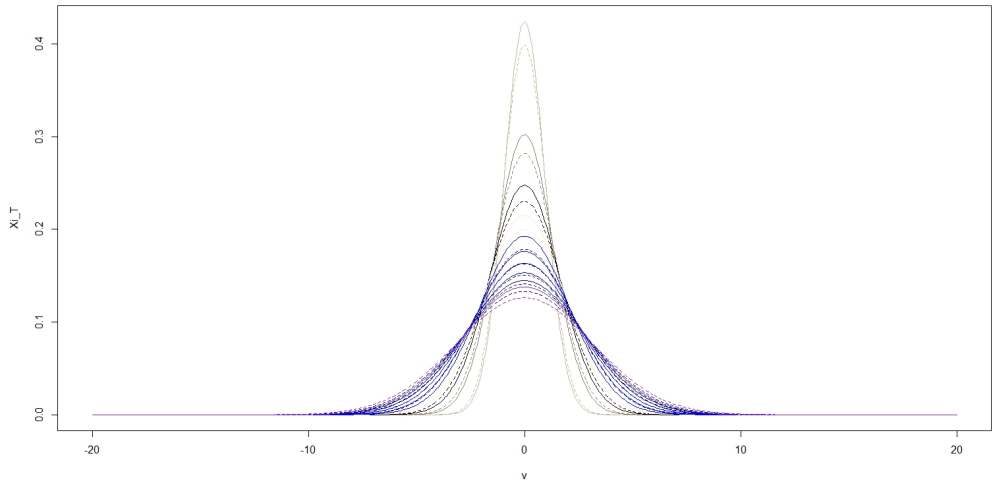

Figure 20: Solid line $\xi(T, \sigma)$ where darker colors means higher σ. Dashed lines are the Gaussian densities $\mathcal{N}(0, \sigma^2)$. The supremum norm and the L^2 norm of the difference differ from zero around 5% to 10% respectively.

Chapter 3

Future directions: two-point motion and a unified theory

In Chapter 2 a Smoluchowski type equation is derived to study the collision rate of inertial particles in high stokes number regime under the effect of a turbulent fluid.

While this regime is of interest for astrophysical context, it has less impact for atmospheric physics, in which particles have, usually, low to moderate $\mathbf{St}$ numbers. In particular the regime we have recovered is the same of Abrhamson [1], which is a limiting behavior of coagulating particle akin to gas-kinetic theory.

Motivated from this, we are trying to study heavy (respect to fluid density) inertial particles in a turbulent environment with a two point statistic approach. This way, dependence on radius and relative distance of particle is still present in the computation of the PDF and, hopefully, all range of $\mathbf{St}$ could be investigated.

This problem will be formalized in the following chapter, leaving different comment, heuristics and proofs, more so open questions to be answered.

Main achievement of the chapter is the complete formulation for the average relative velocity of two particle advected by a turbulent fluid, i.e.

$$\langle \mathbf{v} \rangle \sim \sqrt{\langle \mathbf{v}^2 \rangle} \sim \sqrt{\frac{k_T}{St}} \sqrt{1 - q\left(\frac{v_p St}{\sqrt{2k_T}}\right)}.$$

where $\mathbf{St}$ is the Stokes number, $\mathbf{k_T}$ the turbulent kinetic energy and q is a function that help modelling the fluctuating structure of the fluid. As we'll se in the following section, different regime can be recovered and differences on the average velocity are obtained.

We discuss the consequences of this formula depending on the choice of the modelling of $\mathbf{U}(\mathbf{x}, t)$ fluid velocity and its link with others given in the literature.

3.1 Introduction

In the same spirit of Chapter 2, we start with the assumption that particle satisfy the approximation of the Stokes law, and we consider the kinetic equation for two same-masses particles:

$$\frac{d}{dt}\mathbf{X}_i = \mathbf{V}_i$$

$$\frac{d}{dt}\mathbf{V}_i = -\frac{1}{\tau_p}\left(\mathbf{V}_i - U\left(\mathbf{X}_i\right)\right), \quad \mathbf{X}, \mathbf{V} \in \mathbb{R}^2, \quad i = 1, 2.$$

where $\tau_{\mathbf{p}} = \frac{\mathbf{m}}{\mathbf{6\pi r}\mu}$ is the relaxing time of a particle, μ is the dynamic viscosity of the fluid and $\mathbf{r}$, $\mathbf{m}$ the radius and mass of the particle respectively.

In a similar fashion to passive scalars, and stochastic modelling via transport noise, we are still considering the assumption on the noise to be turbulent and fluctuating, i.e.

$$U\left(\mathbf{x}\right) = \sigma \sum_k e_k\left(\mathbf{x}\right) W_k'\left(t\right).$$

As before, Section .2, we can still give meaning to the quantity σ as the product of the turbulent kinetic energy, k_T, and relaxation time of the fluid, τ_f. Here $e_k(x)$ are smooth vector field with almost compact support.

With the same reasoning we obtain at the level of the stochastic system, neglecting for now the coagulation, a SPDE for the joint density of the two point motion: $f_t(\mathbf{x_1}, \mathbf{x_2}, \mathbf{v_1}, \mathbf{v_2})$, i.e.

$$\begin{aligned}\partial_t f + \operatorname{div}_{x_1}\left(v_1 f\right) + \operatorname{div}_{x_2}\left(v_2 f\right) - \frac{1}{\tau_p}\operatorname{div}_{v_1}\left(v_1 f\right) - \frac{1}{\tau_p}\operatorname{div}_{v_2}\left(v_2 f\right) = \\ = \frac{\sigma}{\tau_p}\sum_k e_k\left(\mathbf{x_1}\right)\cdot\nabla_{v_1} f \circ dW_k\left(t\right) + \frac{\sigma}{\tau_p}\sum_k e_k\left(\mathbf{x_2}\right)\cdot\nabla_{v_2} f \circ dW_k\left(t\right)\end{aligned} \tag{3.1.1}$$

It is interesting to note that investigate well posedness (existence, uniqueness and regularity) of (3.1.1) is still an open problem. Anyway, thanks to work like (J. Bedrossian 2022) in which well posedness of Vlasov and Vlasov-Fokker-Planck system was studied, see [13] and reference therein, we can safely expect that solution to such equation exist in the usual space.

Writing the Ito-Stratonovich corrector in (3.1.1) we obtain a second order elliptic operator that depends on the covariance matrix of the noise. Call Q such matrix we have:

$$Q(x_i, x_l) = \sigma^2 \sum_k e_k\left(x_i\right) \otimes e_k\left(x_l\right).$$

and computing the Ito formula and the corrector, we get mixed derivatives in the $\mathbf{v} = (\mathbf{v_1}, \mathbf{v_2})$ variables, giving the following second order operator (we assume for simplicity $Q(\mathbf{x_1}, \mathbf{x_2}) = Q(\mathbf{x_2}, \mathbf{x_1})$):

$$\begin{aligned}\mathcal{D}f = &\frac{\sigma^2}{2\tau_p^2} div_{v_1}(Q(\mathbf{x_1}, \mathbf{x_1})\nabla_{v_1} f) + \frac{\sigma^2}{2\tau_p^2} div_{v_2}(Q(\mathbf{x_2}, \mathbf{x_2})\nabla_{v_2} f) \\ &+ \frac{\sigma^2}{\tau_p^2} div_{v_1}\left(Q(\mathbf{x_1}, \mathbf{x_2})\nabla_{v_2} f\right).\end{aligned}$$

Which reads, at the level of the SPDE, as:

$$\begin{aligned}\partial_t f + \operatorname{div}_{x_1}\left(v_1 f\right) + \operatorname{div}_{x_2}\left(v_2 f\right) - \frac{1}{\tau_p}\operatorname{div}_{v_1}\left(v_1 f\right) - \frac{1}{\tau_p}\operatorname{div}_{v_2}\left(v_2 f\right) - \mathcal{D}f = \\ = \frac{\sigma}{\tau_p}\sum_k e_k\left(\mathbf{x_1}\right)\cdot\nabla_{v_1} f dW_k\left(t\right) + \frac{\sigma}{\tau_p}\sum_k e_k\left(\mathbf{x_2}\right)\cdot\nabla_{v_2} f dW_k\left(t\right)\end{aligned} \tag{3.1.2}$$

Under suitable condition on a scaling parameter $\varepsilon_N \to 0$ as $N \to \infty$, we expect that taking a Galeati limit, we can approximate this stochastic equation with the associated PDE for the density of the two-point statistics.

$$\partial_t f + \mathrm{div}_{x_1}(v_1 f) + \mathrm{div}_{x_2}(v_2 f) - \frac{1}{\tau_p}\mathrm{div}_{v_1}(v_1 f) - \frac{1}{\tau_p}\mathrm{div}_{v_2}(v_2 f) = \mathcal{D}f \quad (3.1.3)$$

Remark 3.1.1. Note that under the same assumption of Chapter 2 on the covariance matrix

$$Q(\mathbf{x_1}, \mathbf{x_1}) = Q(\mathbf{x_2}, \mathbf{x_2}) = c\mathbf{I}, \quad Q(\mathbf{x_1}, \mathbf{x_2}) = Q(\mathbf{x_1} - \mathbf{x_2}),\ c \in \mathbb{R}$$

We recover the same equation for the one point statistic of a single particle. This can be done integrating in the desired variable and using divergence theorem and the symmetry of the covariance matrix. There Q is basically independent on the position, the only contribution is given by $\sigma^2 \sim k_T$.
Here the position is essential and change the behavior of the relative velocity.

Therefore, to simplify, we can consider the differential operator with $Q(\mathbf{x_1} - \mathbf{x_2})$ not trivial, maintaining a footprint of the space modification due to the fluid in the relative density of the two particles:

$$\mathcal{D}f = \frac{\sigma^2}{2\tau_p^2}(\Delta_{v_1} f + \Delta_{v_2} f) + \frac{\sigma^2}{\tau_p^2} div_{v_1}(Q(\mathbf{x_1} - \mathbf{x_2})\nabla_{v_2} f). \quad (3.1.4)$$

Remark 3.1.2. Note that well posedness (existence/uniqueness and regularity) of (3.1.3) can be proven in the same fashion as seminal work of (V. Dean 1990), and following on that, where well posedness of linear and non linear Vlasov-Fokker-Planck equation is studied, [85], proving regularity of the associated semigroup.

3.2 Setting the computation for Collision Rate

To compute the mean velocity we need to investigate the density function of the two point motion. Since we are interested to obtain an average value that is independent from the initial condition, we focus on the steady state solution of the PDE 3.1.3. The stationary equation associated to (3.1.3), where $\mathcal{D}f$ as in (3.1.4), is the following

$$\mathrm{div}_{x_1}(v_1 f) + \mathrm{div}_{x_2}(v_2 f) - \frac{1}{\tau_p}\mathrm{div}_{v_1}(v_1 f) - \frac{1}{\tau_p}\mathrm{div}_{v_2}(v_2 f) = \mathcal{D}f \quad (3.2.1)$$

Note that, opposite to the 1-particle case, there is no way to eliminate the $\mathbf{x}$-dependence and, moreover, this dependence is essential to obtain meaningful result for general $\mathbf{St}$ numbers.

Remark 3.2.1. Note that this equation is not precisely suitable for the objective we seek. If exist a solution $f = f(\cdot, \mathbf{v_1}, \mathbf{v_2})$ to (3.2.1), it should satisfy

$$-\frac{1}{\tau_p}\mathrm{div}_{v_1}(v_1 f) - \frac{1}{\tau_p}\mathrm{div}_{v_2}(v_2 f) = \frac{\sigma^2}{2\tau_p^2}(\Delta_{v_1} f + \Delta_{v_2} f) + \frac{\sigma^2}{\tau_p^2} div_{v_1}(Q(\mathbf{x_1} - \mathbf{x_2})\nabla_{v_2} f)$$

for every value of $\mathbf{x_1} - \mathbf{x_2}$, which is impossible.

However, following similar ideas from [10, 75, 90, 89] and others, we note that is the distance of the two particles the meaningful quantity. We search solution of the form:

$$f\left(\mathbf{x_1}, \mathbf{x_2}, \mathbf{v_1}, \mathbf{v_2}\right) = \widetilde{f}\left(\mathbf{x_1} - \mathbf{x_2}, \mathbf{v_1}, \mathbf{v_2}\right)$$

Call $\mathbf{r} := \mathbf{x_1} - \mathbf{x_2}$, the function $\widetilde{f} = \widetilde{f}\left(\mathbf{r}, \mathbf{v_1}, \mathbf{v_2}\right)$ satisfy the equivalent PDE:

$$\begin{aligned} -\frac{1}{\tau_p}\operatorname{div}_{v_1}\left(v_1\widetilde{f}\right) - \frac{1}{\tau_p}\operatorname{div}_{v_2}\left(v_2\widetilde{f}\right) &= \mathcal{D}\widetilde{f} \\ \mathcal{D}\widetilde{f} = \frac{\sigma^2}{2\tau_p^2}\left(\Delta_{v_1}\widetilde{f} + \Delta_{v_2}\widetilde{f}\right) + \frac{\sigma^2}{\tau_p^2} div_{v_1}\left(Q(\mathbf{r})\nabla_{v_2}\widetilde{f}\right) \end{aligned} \tag{3.2.2}$$

this equation is the adiabatic formulation, i.e. constant in space, of Equation 3.2.1 where we impose:

$$\operatorname{div}_{x_1}\left(v_1\widetilde{f}\left(x_1 - x_2, v_1, v_2\right)\right) + \operatorname{div}_{x_2}\left(v_2\widetilde{f}\left(x_1 - x_2, v_1, v_2\right)\right) = 0. \tag{3.2.3}$$

This make the task of finding a solution for 3.2.2 feasible, and we show in Section 3.7 that solution of such equation are close respect to the problem of finding the relative velocity of particles to solutions of Equation 3.2.1. Therefore, finding a solution of the form $\widetilde{f} = \widetilde{f}\left(\mathbf{r}, \mathbf{v_1}, \mathbf{v_2}\right)$ for equation (3.2.2), we have an approximate solution of the general one, which are homogeneous in space, namely invariant by space-translation.

Remark 3.2.2. We can prove that existence and uniqueness for such an equation is possible using standard technique for elliptic equations (see reference on bounded domain [74]). Thus becomes our main equation and, without misunderstanding, we call it its solution f.

Note that, assuming a covariance matrix similar to a Kraichan ensemble, e.g. [10], we maintain the dependence on the relative distance of the particles. In the next sections we are going to compute such average and then show different model for the fluid turbulence, represented by different covariance matrix.

3.2.1 Space as a parameter

Given any $\mathbf{r}$, we can find solution pdf $\theta_{\mathbf{r}}\left(\mathbf{v_1}, \mathbf{v_2}\right)$ which satisfies equation (3.2.2). We have, for each fixed $\mathbf{r}$,

$$\int\int \theta_x\left(v_1, v_2\right) dv_1 dv_2 = 1 \tag{3.2.4}$$

Remark 3.2.3. Using last remark, we can obtain f from (3.2.2) and from $\theta_{\mathbf{r}}$:

$$f\left(\mathbf{r}, \mathbf{v_1}, \mathbf{v_2}\right) := \theta_{\mathbf{r}}\left(\mathbf{v_1}, \mathbf{v_2}\right) \tag{3.2.5}$$

up to constant depending on the space we are working, e.g. constant being 1 if we work on a torus of Lebesgue measure 1, otherwise it is sufficient to change it computing the integral. Defined like this, f is non negative, the integral in all variables is equal to the integral of 1 on the space domain using (3.2.4) up to constant, and it satisfies equation (3.2.2).

The important consequence is that, following from classical theory of both stochastic processes and elliptic equation, we have

$$\theta_{\mathbf{r}}(\cdot) \sim N(0, C_{\mathbf{r}})$$

with a known $C_{\mathbf{r}}$ which will depend on our choice of $Q(\mathbf{r})$ covariance of our noisy fluid modelling. In fact, this follow from equation 3.2.2 being the invariant distribution of an Ornstein-Ulhembeck process.

3.2.2 Conditioning on same position

The structure function that we want to compute is the average relative velocity between two particle considering all the inertial range of the particles in the fluid, i.e.

$$\mathbb{E}[|\mathbf{V_1} - \mathbf{V_2}|]$$

this is the average difference of velocities between particles at the "same" position. In this context "same position" is not clearly defined. In particular we could interpret the same position condition as to take particle that are at a collision length scale, i.e. we look at a portion of space where there is a myriad of transported particles, pointwise from the macroscopic viewpoint, enormous from the microscopic viewpoint. A portion of space in which collision happens with high probability.

Remark 3.2.4. Following [75, 25] and reference therein, the structure function associated to the relative velocity is tied to the collision rate $\mathcal{R}$ of coagulating particle in a domain $\mathbb{D} \subset \mathbb{R}^d$. In particular, recalling the splitting $\mathcal{R} = \mathcal{R}_{adv} + \mathcal{R}_{tur}$, we know that $\mathbb{E}[|\mathbf{V_1} - \mathbf{V_2}|]$ is fundamental for the computation of $\mathcal{R}_{tur}$, but also rise the following question: is the uniform density still valid in such regime of turbulent fluid? does the folding of the flow changes the average distribution of the particle with the computed relative velocity? Should we consider some radial distribution $g(\mathbf{r})$ that multiply the collision rate to obtain a more reasonable kernel, or change the particle distribution accordingly to the motion and the inertial regime?

From here on we start assuming the following:

$$\|\mathbf{r}\| \sim \ell_{\mathbf{p}} \tag{3.2.6}$$

namely we consider positions which differ by the typical length scale of colliding particles.

In the computation of $\mathbb{E}[|\mathbf{V_1} - \mathbf{V_2}|]$ we use the equilibrium probability density of pairs of particles, conditioned to have the "same position", which is our f in (3.2.5), where under our assumption conditioning to the same position, under the approximation (3.2.6), mean we use the new density

$$\widetilde{f}(\mathbf{v_1}, \mathbf{v_2}) := \frac{f(\ell_{\mathbf{p}}, \mathbf{v_1}, \mathbf{v_2})}{\int\int f(\ell_{\mathbf{p}}, \mathbf{v_1}, \mathbf{v_2})\, d\mathbf{v_1} d\mathbf{v_2}} \underbrace{\sim}_{\text{on the unitary torus for 3.2.4}} \theta_{\ell_{\mathbf{p}}}(\mathbf{v_1}, \mathbf{v_2}).$$

In 1D notation this is already enough replacing $\mathbf{r}$ by $\|\mathbf{r}\| \sim \ell_p$. In more dimensions it is similar since we can suppose invariance by rotation, and that indeed the the collision of

particles really depends on the magnitude of their distance. This will become clear when we'll write down the covariance matrix $Q(\mathbf{r})$.

Thus, assuming to work on the unitary torus, we have:

$$\begin{aligned}\mathbb{E}\left[|\mathbf{V_1}-\mathbf{V_2}|\right] &= \frac{\int\int |\mathbf{v_1}-\mathbf{v_2}|\, f\left(\ell_{\mathbf{p}},\mathbf{v_1},\mathbf{v_2}\right) d\mathbf{v_1}d\mathbf{v_2}}{\int\int f\left(\ell_{\mathbf{p}},\mathbf{v_1},\mathbf{v_2}\right) d\mathbf{v_1}d\mathbf{v_2}} \\ &= \int\int |\mathbf{v_1}-\mathbf{v_2}|\, \theta_{\ell_{\mathbf{p}}}\left(\mathbf{v_1},\mathbf{v_2}\right) d\mathbf{v_1}d\mathbf{v_2} \\ &\sim \sqrt{C^{11}_{\ell_{\mathbf{p}}}+C^{22}_{\ell_{\mathbf{p}}}-2C^{12}_{\ell_{\mathbf{p}}}}.\end{aligned}$$

Hence, main objective of the following section is to give fair assumption on $Q(\mathbf{r})$ to compute $C_{\mathbf{r}}$ from which we'll derive: $C^{11}_{\ell_{\mathbf{p}}}$, $C^{22}_{\ell_{\mathbf{p}}}$, $C^{12}_{\ell_{\mathbf{p}}}$ and as such the relative velocity.

Remark 3.2.5 (Relaxation time of the fluid). In the previous chapter, under the one-point motion, we collapsed the relaxation time τ_f of the fluid to zero. The reason was that such parameter is the one involved in the white noise limit for our model. Now we are going to compute the covariance matrix of the noise, making it dimensionless, and introducing again this time in the limiting computation. in fact we have:

$$\tau_{\mathbf{f}} = \ell_{\mathbf{f}}/\sqrt{2\mathbf{k_T}}$$

where $\sqrt{2\mathbf{k_T}}$ is the typical velocity of the turbulent fluid, $\ell_{\mathbf{f}}$ is the typical length scale of the fluid. As such, we assume

$$\begin{aligned}Q(\mathbf{r}) &:= \tilde{Q}(\|\mathbf{r}\|/\ell_{\mathbf{f}}) \\ \ell_{\mathbf{f}} &= \tau_{\mathbf{f}}\sqrt{2\mathbf{k_T}}.\end{aligned}$$

This way we have reintroduced the time scale of the fluid.
At last, we introduce again the foundamental quantities:

$$\mathbf{St} = \frac{\tau_{\mathbf{p}}}{\tau_{\mathbf{f}}}, \quad \sigma = \sqrt{2\tau_{\mathbf{f}}\mathbf{k_T}}.$$

In the following sections we are going to show two reasonable model to interpret (in different Stokes number regime) the covariance of our considered noise.

To do this, we'll start recalling:

$$\ell_{\mathbf{f}} = \tau_{\mathbf{f}}\sqrt{2\mathbf{k_T}} = \frac{\tau_{\mathbf{p}}\sqrt{2\mathbf{k_T}}}{\mathbf{St}}.$$

Moreover, we want to solve the equation when the *parameter* $\mathbf{r}$ satisfies (3.2.6). Hence

$$\ell_{\mathbf{p}} = \tau_{\mathbf{p}}\mathbf{v_p}$$

where $\mathbf{v_p}$ is a typical velocity of the particles in the steady state regime of the particle density.

3.3 Mean velocity with "scalar" covariance function $q\left(r/\ell_f\right)$

Here, we propose to compute the structure function (3.2.2) in a general setting without an explicit formulation for the covariance matrix $Q\left(\mathbf{x}-\mathbf{y}\right)$.

The only apriori hypothesis we employ in the selection of Q is the space homogeneity (already expressed by the formula $Q\left(\mathbf{x}-\mathbf{y}\right)$) and is direct relation with the identity matrix.

For this reason, consider a scalar function $q(r)$ dependent on the magnitude of the relative distance.

$$\begin{cases} Q\left(\mathbf{x},\mathbf{y}\right) & = Q\left(\mathbf{x}-\mathbf{y}\right) = \sigma q\left(\frac{\mathbf{x}-\mathbf{y}}{\ell_\mathbf{f}}\right) Id \\ q\left(0\right) & = 1 \end{cases}$$

(Note that we can always assume $q\left(0\right)=1$ since we can always modify σ with a dimensionless constant dependent only on the domain).

Thus the matrix C_r is linked to $q\left(\frac{r}{\ell_f}\right)$. From the elliptic equation we obtain

$$-\frac{1}{\tau_p}\operatorname{div}_{v_1}\left(v_1\overline{f}\right)-\frac{1}{\tau_p}\operatorname{div}_{v_2}\left(v_2\overline{f}\right)=\frac{\sigma^2}{2\tau_p^2}\left(\Delta_{v_1}\overline{f}+\Delta_{v_2}\overline{f}\right)+\frac{\sigma^2 q\left(\frac{r}{\ell_f}\right)}{\tau_p^2}div_{v_1}\nabla_{v_2}\overline{f}$$

which reads out

$$-\operatorname{div}_{v_1}\left(v_1\overline{f}\right)-\operatorname{div}_{v_2}\left(v_2\overline{f}\right)=\frac{\sigma^2}{2\tau_p}\left(\Delta_{v_1}\overline{f}+\Delta_{v_2}\overline{f}+2q\left(\frac{r}{\ell_f}\right)div_{v_1}\nabla_{v_2}\overline{f}\right).$$

From the usual computation we obtain the covariance matrix

$$C_r=\frac{\sigma^2}{\tau_p}\begin{pmatrix} Id & q\left(\frac{r}{\ell_f}\right)Id \\ q\left(\frac{r}{\ell_f}\right)Id & Id \end{pmatrix}$$

Using the results of previous section and the computation on C_r, we can obtain for the structure function the following closed form:

$$\mathbb{E}\left[|\mathbf{V_1}-\mathbf{V_2}|\right]\sim\frac{\sigma}{\sqrt{\tau_p}}\sqrt{1-q\left(\frac{\ell_p}{\ell_f}\right)}.$$

Before delving into the fluid modelling, we can expand the constant in the covariance matrix to ease the computation. In particular, we recall from [31]:

$$\sigma=\sqrt{2\tau_f k_T}$$

Hence

$$\mathbb{E}\left[|\mathbf{V_1}-\mathbf{V_2}|\right]\sim\sqrt{2\frac{\tau_f}{\tau_p}k_T}\sqrt{1-q\left(\frac{\ell_p}{\ell_f}\right)}.$$

Recall now that the Stokes number for particle in fluid can be expressed as

$$St=\frac{\tau_p}{\tau_f}$$

this give us:

$$\mathbb{E}\left[|\mathbf{V_1}-\mathbf{V_2}|\right] \sim \sqrt{\frac{k_T}{St}}\sqrt{1-q\left(\frac{\ell_p}{\ell_f}\right)}.$$

Trying to expand $\frac{\ell_p}{\ell_f}$ in relation to St we have

$$\frac{\ell_p}{\ell_f} = \frac{\tau_p v_p}{\tau_f\sqrt{2k_T}} = \frac{v_p St}{\sqrt{2k_T}}.$$

In conclusion:

$$\mathbb{E}\left[|\mathbf{V_1}-\mathbf{V_2}|\right] \sim \sqrt{\frac{k_T}{St}}\sqrt{1-q\left(\frac{v_p St}{\sqrt{2k_T}}\right)}.$$

This is the final expression for the structure function of the relative velocity under different modelling of the fluid fluctuations and in the steady state regime of the particles' density.

3.4 Covariance with Gaussian decay

We assume that the covariance structure of the noisy fluid $U_t(\mathbf{r}) - U_t(\mathbf{0})$ is

$$Q(\mathbf{r}) := \exp(-\|\mathbf{r}\|^2/{\ell_\mathbf{f}}^2)\mathbf{Id}$$
$$\ell_\mathbf{f} = \tau_\mathbf{f}\sqrt{2\mathbf{k_T}} = \frac{\tau_\mathbf{p}\sqrt{2\mathbf{k_T}}}{\mathbf{St}}.$$

Under this assumption, we may rewrite the differential operator (3.1.4) in the form

$$\mathcal{D}f = \frac{\sigma^2}{2{\tau_\mathbf{p}}^2}\left(\Delta_{v_1}f + \Delta_{v_2}f + 2\exp(-\|\mathbf{r}\|^2/\ell_f^2)\,\mathrm{div}_{v_1}\nabla_{v_2}f\right).$$

Multiply the stationary Fokker Plank equation (3.2.2) by $\tau_\mathbf{p}$ we write it in the form

$$-\mathrm{div}_{v_1}(v_1 f) - \mathrm{div}_{v_2}(v_2 f) = \tau_\mathbf{p}\mathcal{D}f$$

where

$$\begin{aligned}\tau_\mathbf{p}\mathcal{D}f &= \frac{\sigma^2}{2\tau_\mathbf{p}}\left(\Delta_{v_1}f + \Delta_{v_2}f + 2\exp(-\|\mathbf{r}\|^2/{\ell_\mathbf{f}}^2)\,\mathrm{div}_{v_1}\nabla_{v_2}f\right)\\ &= \frac{\mathbf{k_T}}{\mathbf{St}}\left(\Delta_{v_1}f + \Delta_{v_2}f + 2\exp\left(-\left(\frac{\|\mathbf{r}\|}{\ell_\mathbf{f}}\right)^2\right)\mathrm{div}_{v_1}\nabla_{v_2}f\right).\end{aligned}$$

We want to solve this equation when the *parameter* $\|\mathbf{r}\| \sim \ell_\mathbf{f}$ satisfies (3.2.6). Hence, we couple $\ell_\mathbf{p} = \tau_\mathbf{p}\mathbf{v_p}$ with the equation

$$-\mathrm{div}_{v_1}(v_1 f) - \mathrm{div}_{v_2}(v_2 f) = \frac{\mathbf{k_T}}{\mathbf{St}}\left(\Delta_{v_1}f + \Delta_{v_2}f + 2\exp\left(-\left(\frac{\ell_\mathbf{p}}{\ell_\mathbf{f}}\right)^2\right)\mathrm{div}_{v_1}\nabla_{v_2}f\right).$$

Which gives the final equation:

$$-\operatorname{div}_{v_1}(v_1 f) - \operatorname{div}_{v_2}(v_2 f) = \frac{\mathbf{k_T}}{\mathbf{St}}\left(\Delta_{v_1} f + \Delta_{v_2} f + 2\exp\left(-\left(\frac{\mathbf{v_p}}{\sqrt{2\mathbf{k_T}}}\mathbf{St}\right)^2\right)\operatorname{div}_{v_1}\nabla_{v_2} f\right)$$

Recall that $C_{\ell_\mathbf{p}}$ is the covariance of the Gaussian solving this equation, i.e.

$$C_{\ell_\mathbf{p}} = \frac{\mathbf{k_T}}{\mathbf{St}}\left(\begin{array}{c|c} Id_d & \exp\left(-\left(\frac{\mathbf{v_p}}{\sqrt{2\mathbf{k_T}}}\mathbf{St}\right)^2\right) Id_d \\ \hline \exp\left(-\left(\frac{\mathbf{v_p}}{\sqrt{2\mathbf{k_T}}}\mathbf{St}\right)^2\right) Id_d & Id_d \end{array}\right).$$

Therefore, under the model, our final formula is:

$$\begin{aligned}\mathbb{E}\left[|\mathbf{V_1} - \mathbf{V_2}|\right] &\sim \sqrt{C^{11}_{\ell_\mathbf{p}} + C^{22}_{\ell_\mathbf{p}} - 2C^{12}_{\ell_\mathbf{p}}} \\ &\sim \sqrt{\frac{\mathbf{k_T}}{\mathbf{St}}}\sqrt{1 - \exp\left(-\left(\frac{\mathbf{v_p}}{\sqrt{\mathbf{2k_T}}}\mathbf{St}\right)^2\right)}. \end{aligned} \tag{3.4.1}$$

Remark 3.4.1 (**Recovered limiting behavior**). The choice of the Gaussian covariance is inspired by work like [1, 58, 64, 75]. As such, we show here that formula (3.4.1) agrees, at least in the two extremely limit of $St \to 0$ or ∞, i.e. tracer particles or complete inertial particles moving in a bullet-like motion.

When St is large, $\exp\left(-\left(\frac{v_p}{\sqrt{2k_T}}St\right)^2\right)$ is small, we get

$$\mathbb{E}\left[|V_1 - V_2|\right] \sim \sqrt{\frac{k_T}{St}},$$

which agrees, as shown in Chapter 2, with the Abrahamson limit [1].

Conversely, when St is small we get

$$1 - \exp\left(-\left(\frac{v_p}{\sqrt{2k_T}}St\right)^2\right) \sim \left(\frac{v_p}{\sqrt{2k_T}}St\right)^2$$

which means at the level of the structure function

$$\begin{aligned}\mathbb{E}\left[|V_1 - V_2|\right] &\sim \sqrt{\frac{k_T}{St}}\left(\frac{v_p}{\sqrt{2k_T}}St\right) \\ &\sim \frac{k_T}{v_p}\sqrt{St} \sim \sqrt{k_T St}\end{aligned}$$

where we have used the fact that $v_p \sim \sqrt{k_T}$ for small Stokes where particles are almost in solidarity with the flow. This formula agrees with classical computation as [14, 72] for both atmospheric particle and gas in proto-planetary disks.

3.4.1 Covariance as Kolmogorov scaling

Suppose that our fluid has a covariance modelled to cover a Kolmogorov scaling in the energy dissipation [10, 11], i.e. for small relative distance $\|\mathbf{r}\|$ the covariance has the form

$$Q(\mathbf{r}) = \mathbf{Id}\left(1 - \left(\frac{\|\mathbf{r}\|}{\ell_f}\right)^{4/3} \varepsilon^{2/3}\right) e^{(} - St).$$

where ε is the average rate of energy injection. This give us, for small $\|\mathbf{r}\|$,

$$\mathbb{E}\left[|V_1 - V_2|\right] \sim \sqrt{\frac{k_T}{St}} g\left(\frac{v_p}{\sqrt{2k_T}} St\right) \sim \sqrt{\frac{k_T}{St}} \left(\frac{\|x\|}{\ell_f}\right)^{2/3} \varepsilon^{1/3}$$

Combining the estimate on $\|\mathbf{r}\| \sim v_p \tau_p$ and $\ell_f \sim \tau_f \sqrt{k_T}$, that are still true, we get exactly:

$$\left(\frac{\|\mathbf{r}\|}{\ell_f}\right)^{2/3} \sim \left(\frac{v_p}{\sqrt{2k_T}} St\right)^{2/3}.$$

This implies that, for small $St << 1$ we get:

$$\begin{aligned}\mathbb{E}\left[|V_1 - V_2|\right] &\sim \sqrt{\frac{k_T}{St}} \left(\frac{\|x\|}{\ell_f}\right)^{2/3} \varepsilon^{1/3} \\ &\sim \sqrt{\frac{k_T}{St}} \left(\frac{v_p}{\sqrt{2k_T}} St\right)^{2/3} \varepsilon^{1/3} \\ &\sim (St)^{1/6} (k_T)^{1/6} v_p^{2/3} \varepsilon^{1/3}.\end{aligned}$$

which in principle means that, for small distance the rate of velocity, while still going to zero, is stronger than the expected Gaussian assumption.it is not clear if it is the expected limit for small St in [90, 89, 75, 26, 25, 11, 10]. It is worth mentioning that, for inertial regime where $St >> 1$, we can still recover the Abrahamson limit, even if the distance $\|\mathbf{r}\|$ is small.

3.4.2 Kraichnan Noise

As a last example of modelling of our fluid, let's consider an approximation of $U(t, \mathbf{x}_t)$ in the sense of Kraichnan, i.e. the fluid velocity difference is a Gaussian vector field with correlation

$$Q_{i,j}(\mathbf{x} - \mathbf{y}) = 2K^{i,j}(\mathbf{x} - \mathbf{y})$$

This is similar to what it is considered in [10, 11]. In order to model turbulent flows, the tensorial structure of the spatial correlation $\mathbf{K} := \left(K^{i,j}(\mathbf{x} - \mathbf{y})\right)_{i,j}$ is chosen to ensure incompressibility, isotropy and scale invariance. This helds when $\tau_p >> \tau_f$. Call $(\mathbf{x} - \mathbf{y}) := \mathbf{r}$, then:

$$K^{i,j}(\mathbf{r}) = C_0 \delta_{i,j} - C_1 \|\mathbf{r}\|^{2h} \left[(1 + 2h)\, \delta_{i,j} - 2h \frac{\mathbf{r_i r_j}}{\|\mathbf{r}\|^2}\right],\ i, j = 1, 2.$$

We have that $C_0/\tau_p \sim \frac{k_T}{St}$ is our usual constant. More so we have, from Falcovich, Cencini and Bec [26, 10, 11], that $C_1/\tau_p \sim \frac{1}{\tau_p}\frac{St\ell_f^{2(1-h)}}{\tau_p}$, where the first $\frac{1}{\tau_p}$ comes from the Stokes' law. The covariance of the Gaussian process then is

$$C_{\ell_p} = \frac{k_T}{St}\left(\begin{array}{c|c} Id_d & \mathbf{K} \\ \hline \mathbf{K} & Id_d \end{array}\right).$$

Therefore

$$\begin{aligned}\mathbb{E}\left[|V_1 - V_2|\right] &\sim \sqrt{C^{11}_{\ell_p} + C^{22}_{\ell_p} - 2C^{12}_{\ell_p}} \\ &\sim \sqrt{2C_1\|\mathbf{r}\|^{2h}} \\ &\sim \sqrt{\frac{1}{\tau_p}\frac{St\,\ell_f^{2(1-h)}}{\tau_p}}\sqrt{2\|\mathbf{r}\|^{2h}} \\ &\sim \sqrt{\frac{k_T}{St}}\sqrt{2\frac{\|\mathbf{r}\|^{2h}}{\ell_f^{2h}}}.\end{aligned}$$

This is more or less our final formula. Let us check it.

When $\|\mathbf{r}\| << \ell_p$, then $\|\mathbf{r}\| \sim v_p\tau_p$ while $\ell_f \sim \sqrt{k_T}\tau_f$. Hence

$$\begin{aligned}\sqrt{\frac{k_T}{St}}\sqrt{2\frac{\|\mathbf{r}\|^{2h}}{\ell_f^{2h}}} &\sim \sqrt{\frac{k_T}{St}}\sqrt{2\frac{\left(v_p\tau_p\right)^{2h}}{\left(\sqrt{k_T}\tau_f\right)^{2h}}} \\ &\sim \sqrt{2}\sqrt{k_T}St^{\left(h-\frac{1}{2}\right)}\frac{\left(v_p\right)^h}{\left(\sqrt{k_T}\right)^h}.\end{aligned}$$

If $v_p \sim \sqrt{k_T}$ then: $\sqrt{2}\sqrt{k_T}St^{\left(h-\frac{1}{2}\right)}, \quad h \in (0,1]$.
Note that, for $h = 2/3$ we recover the Kolmogorov scaling (3.4.1)

3.5 On Collision rate

In the physics community there is now a general consensus [90, 89, 75, 10, 11, 26, 25], thanks to works of Mehlig, Pumir, Falcovich, Cencini, Bec and Wilkinson, that the coagulation rate, introduced in Chapter 1, has a natural splitting in two main components

$$\mathcal{R} = \mathcal{R}_{adv} + \mathcal{R}_{tur}.$$

This tow uncorrelated main components are: R_a, the coagulation due to advection, and R_T, due to the turbulent flow.

This last term R_T is obtained independently from two differnt computation both from Falkovich [26, 25] and Mehlig [90, 89], while it is being considerd in works of Bec [11, 10] and Pumir [75]. This is called *sling effect* or *caustic effect*.

Both of this effect are obtained considering the usual collision kernel when turbulent flow is involved,

$$\mathcal{R}_{kin} \sim \langle \mathbf{v} \rangle,$$

is mostly dependent on the relative velocity of the particles. They propose a correction due to the fluid turbulence that create singularity on the gradient of the particles velocity and the modified their density.

To be more precise, the contribution is due to the radial distribution of the particle and, more so, the stress tensor given by

$$\mathbb{A} := \left(\frac{\partial}{\partial \mathbf{x}_j} U_i(\mathbf{x}) \right), \quad \forall i, j.$$

Discussing the advecting part $\mathcal{R}_{adv}$, there is the famous Suffmann-Turner formula, estimate for low Stokes regime with a uniform density of almostr tracer particles [78], that read as

$$R_a := \sqrt{\frac{8\pi}{15}} n_0 \left(2\mathbf{r}\right)^2 {\tau_{\mathbf{f}}}^{-1},$$

where n_0 is the density and $\mathbf{r}$ the radius of the particles.

During our computations, and under our hypothesis, we arrive at a close form for the expression of the relative velocity $\langle |\mathbf{v}| \rangle$ between particles. Assigned a covariance matrix for the noisy modellization of the fluid' velocity, $Q(\mathbf{r}) = q(\mathbf{r}/\ell_{\mathbf{f}})\mathbf{Id}$, with suitable condition on q. We obtain the following:

$$\langle |\mathbf{v}| \rangle \sim \sqrt{\langle \mathbf{v}^2 \rangle} \sim \sqrt{\frac{\mathbf{k_T}}{\mathbf{St}}} \sqrt{1 - q(\ell_{\mathbf{p}}/\ell_{\mathbf{f}})}.$$

If we still maintain the idea that we have a statistically uniform spatial distribution of particles, call such density n_0, then we have the relation between the tubrulent collision rate, $\mathbf{R_T}$, and the relative velocity, i.e.

$$\mathcal{R}_{tur} \sim n_0 \langle \mathbf{v} \rangle .$$

Under this hypothesis, we fail to describe in fullness the turbulent part described by different author such as [90, 75, 26] with complex formulas. In particular, while the maxima and the limit for high stokes regime is capture, see Figure (3.1), there is an anomaly for small Stokes number that is not captured with just the relative velocity computed directly by the density function. The same limit point is shown, but the abrupt increase in the rate for low St is not captured.

The non uniform behavior, and the overestimation is not an unexpected occurrence. It can be argued, considering the derivation of the relative velocity, that the assumption of statistically uniform spatial distribution, in the limit of small Stokes number, is not what we are really obtaining. In particular, all of our assumption in the computation of the structure function needs to work in the steady state regime, after the tubrulent behavior of the fluid is being observed. As such, also the density of particles must be taken at is steady limit, after the one-point statistic as evolved the system under the turbulent regime. More so, since in our equation velocity is an active variable, this must be carried on, as a Maxwellian-like average for the particles and to be computed in a domain as big as two colliding particles. The first reasonable guess, e.g. [59],is to consider the collision rate in the following form:

$$\mathcal{R} \sim n_0 g(\mathbf{r}) \langle \mathbf{v}(\mathbf{r}) \rangle$$

where $g(\mathbf{r})$ is somewhat analogous to a radial density function of the particles at such distance and such radius/mass, which in principle is a different fraction of n_0. More so, we need to find a way to incorporate $\dot{\mathbf{r}}$ in this fraction of colliding particles: this would be possible considering the one point statistic and the Maxwell distribution, analogous to the Boltzmann's one in the kinetic gas theory. In this way, the energy of the particles, modified by the turbulent behavior of the fluid, can be taken into account when we consider the spatial distribution of the colliding particle at the mean velocity $\langle|\mathbf{v}_1 - \mathbf{v}_2|\rangle$.

3.5.1 A comparison of St number

We recall that in Mehlig, et all. [90, 89] they derive the following analytic formula from DNS simulation:

$$\mathcal{R} = \mathcal{R}_{adv} + \underbrace{\mathcal{R}_{kin} e^{-\mathcal{S}/\mathcal{I}}}_{=\mathcal{R}_{tur}}$$

where they estimate $\mathcal{S}/\mathcal{I} \sim 1/\mathbf{St}$, with $\mathcal{S}$ being the action of the trajectories of particles and $\mathcal{I}$ the strain-rate correlation function. They explain this factor as the caustic formation/sling effect noted by Falkovich [26, 25]. In particular they derive the following computation regarding the term $\mathcal{R}_{kin}$ (see page 4 of [90]):

$$\begin{cases} St << 1, & \mathcal{R}_{kin} \sim \sqrt{\mathbf{St}}\sqrt{\mathbf{k_T}} \\ St >> 1, & \mathcal{R}_{kin} \sim \sqrt{\mathbf{k_T}}/\sqrt{\mathbf{St}} \end{cases}$$

Without the factor $e^{-\mathcal{S}/\mathcal{I}}$, representing this rare events, this would be in line with our initial assumption of a Gaussian modelled fluid velocity for our difference of velocity of colliding particles. Unfortunately, with the caustic effect taken in considerations, the decay is faster and we can see the difference in the following figure. From Figure (3.1), we note that for high stokes number (roughly $St \gtrsim 5$) we complete capture the same behavior as the literature with decay $1/\sqrt{\mathbf{St}}$. Regarding the limit for $St \to 0$, we see from figure 1 in [90] that the advection rate $\mathcal{R}_{adv}$ is dominant and the decay of $\mathcal{R}_{tur}$ have a little influence. All of the modelling of $\mathcal{R}_{tur}$ goes to zero, but with different velocity, this different must be searched in the caustic effect due to the fluid. In the next section we are going to propose our correction factor that, even though is derived from a different point of view, can be linked back to such rare events due to the fluid behavior.

3.6 Conclusion: new factor and energy state density

As proposed in the last section of this chapter and following reasoning from Chapter 1, Section 1.4, seems reasonable to correct the collision kernel to obtain a collision rate that is weighted with the fraction of particle that are indeed colliding with each other with a rate dependent on the mean relative velocity. This reasoning is motivated by the work on fractal dispersion of passive particles into turbulent filed [12, 41], indeed particles deviates from a uniform initial distribution when the St number is small and they tend to cluster, changing the overall density number of colliding particles. Again, for simplicity we consider particle with the same mass m_p and velocity $\mathbf{v}_p$ as previously stated.

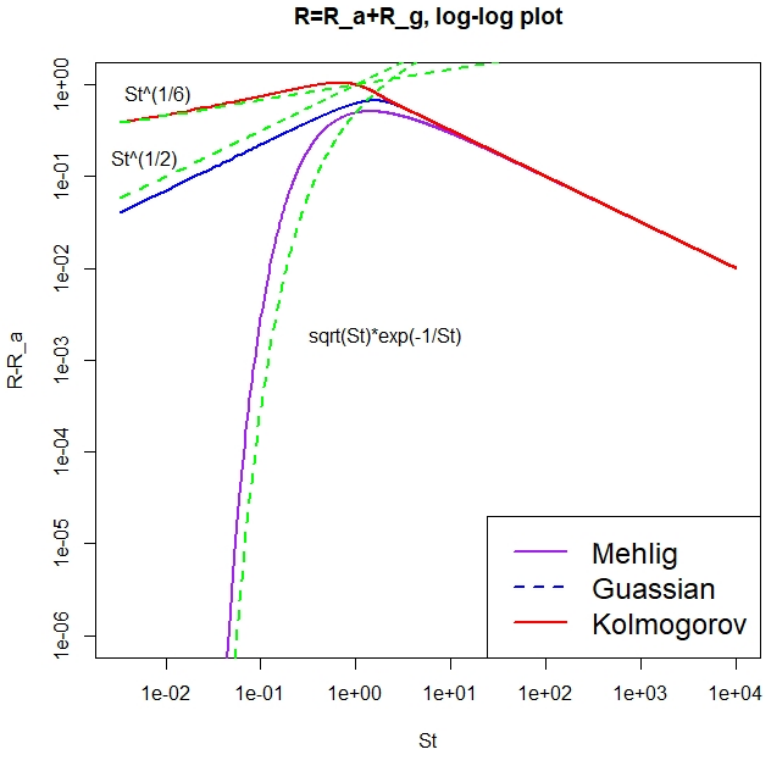

Figure 3.1: Comparison, log-log plot, of $\mathbf{R_T}$ in 3 setting: (red): kolmogorov scaling $q(x) = (1 - x^{4/3})e^{-x^2}$, (blue): Guassian scaling $q(x) = e^{-x^2}$, (purple): Mehlig [90] formula without constants. In (green) dotted the limit for $St \to 0$.

In analogy with Maxwell-Boltzmann-Arrhenius density, we expect to multiply the relative velocity $\langle |\mathbf{v}_1 - \mathbf{v}_2| \rangle$ with the number density of particle at a certain length distance with their related "mean velocity", in the Maxwellian sense, derived from the single point statistic density equation in Section 2.5. Call h this new factor, then we expect:

$$h := \exp\left(-\frac{1}{2} m_p \frac{\langle |\mathbf{v}|^2 \rangle}{\mathbf{k_T}}\right) \sim \exp\left(-\frac{1}{2} m_p \frac{\mathbf{v}_p^2 \tau_\mathbf{p}}{\sigma^2}\right)$$

Note that the length scale ℓ_p is contained in $\langle |\mathbf{v}| \rangle$, hence in $\mathbf{v}_p$.

This is analogous to Maxwell distribution in which we have

$$h \sim \exp\left(-\frac{E}{T}\right)$$

where E is the energy and T is the temperature and in our case it the turbulent intensity of the fluid, given by $\sigma^2/\tau_\mathbf{p}$. In particular, we van argue that this h is not an artificial factor, but nothing more than the steady state solution of the modified Smoluchowski, which is a type of Vlasov-Fokker-Plank equation. In particular h being the Maxwellian represent the number density of particle in the infinitesimal volume around the averaged velocity.

Under this assumption, then, the turbulent rate $\mathcal{R}_{tur}$ is, calling n_0 the initial density of particles

$$\mathcal{R}_{tur} \sim n_0 \exp\left(-\frac{1}{2} m_p \frac{\mathbf{v}_p^2 \tau_{\mathbf{p}}}{\sigma^2}\right) \langle |\mathbf{v}_1 - \mathbf{v}_2| \rangle$$

Under our Gaussian covariance hypothesis we get:

$$n_0 \exp\left(-\frac{m_p}{2} \frac{\mathbf{v}_p^2 \tau_{\mathbf{p}}}{\sigma^2}\right) \sqrt{\frac{\mathbf{k_T}}{\mathbf{St}}} \sqrt{1 - \exp\left(-\left(\frac{\mathbf{v_p}}{\sqrt{\mathbf{2k_T}}} \mathbf{St}\right)^2\right)}$$

In the exponential:

$$\begin{aligned}
\exp\left(-\frac{m_p}{2} \frac{\mathbf{v}_p^2 \tau_{\mathbf{p}}}{\sigma^2}\right) &= \exp\left(-\frac{m_p}{2} \frac{\ell_p^2 \tau_{\mathbf{p}}}{{\tau_{\mathbf{p}}}^2 \mathbf{k_T} \tau_{\mathbf{f}}}\right) \\
&= \exp\left(-\frac{m_p}{2} \frac{\ell_p^2 \tau_{\mathbf{p}} {\tau_{\mathbf{f}}}^2}{{\tau_{\mathbf{p}}}^2 {\ell_{\mathbf{f}}}^2 \tau_{\mathbf{f}}}\right) \\
&= \exp\left(-\frac{m_p}{2} \frac{\ell_p^2}{{\ell_{\mathbf{f}}}^2} \frac{1}{\mathbf{St}}\right).
\end{aligned}$$

will leave us with

$$\boxed{\mathcal{R}_{tur}(\mathbf{m}_p) \sim n_0 \exp\left(-\frac{m_p}{2} \frac{\ell_p^2}{{\ell_{\mathbf{f}}}^2} \frac{1}{\mathbf{St}}\right) \sqrt{\frac{\mathbf{k_T}}{\mathbf{St}}} \sqrt{1 - \exp\left(-\left(\frac{\mathbf{v_p}}{\sqrt{\mathbf{2k_T}}} \mathbf{St}\right)^2\right)}} \tag{3.6.1}$$

Analytically speaking, formula 3.6.1 agrees with Pumir and Flakovich [26, 25] ideas and Mehlig [64] formulations. This factor, albeit essential, is formulated with a reasoning due to kinetic theory, and well represent the activation aspect and the fast decay at $\mathbf{St}$ near 0. Anyhow, it is still fundamental to understand how we can capture this from the particle system at play, as shown in Chapter 1, Section 1.4 and, in a rigorous way, from the limiting equation 3.2.2. This would be primary work for future development of this theory.

In a similar vein, a natural progression of the theory involves conducting DNS simulations with adjusted parameters that align with our hypothesis. By comparing these results with established classical outcomes, we can provide a comprehensive and robust explanation of our unified theory concerning the turbulent collision rate and our analytic formulation.

3.7 Adiabatic hypothesis and Gaussian approximation

In Equation (3.2.3), we put forward the conjecture that the model describing the combined distribution of space and velocity, denoted as $f(\mathbf{x}, \mathbf{v})$, can be effectively approximated by an adiabatic distribution in terms of space. This approximation treats the spatial variable as a parameter within the distribution. In the following section, we delve into this simplification, demonstrating its validity in effectively representing the model through the simplified equations. Furthermore, we tackle the constraint arising from the non-vanishing

nature of $\nabla_r \cdot (f(v_1 - v_2))$. We address this constraint by contrasting it with various length-scale regimes relative to the ratio between the particles' relative distance, denoted as **r**, and the Kolmogorov length-scale, symbolized as η. This analysis introduces novel avenues for potential model enhancements in future research works.

3.7.1 Lagrangian description with fluid velocity modelling

We start, as in Chapter 3, with the Lagrangian description of the relative motion of two point into a fluid:

$$\begin{cases} x_i' &= v_i \\ v_i' &= -\frac{1}{\tau_p}\left(v_i - u_L\left(x_i\right) - u_S\left(x_i\right)\right) \end{cases}, \; i = 1, 2$$

While they don't interact directly, they are allowed to collide and coalesce. More so, they are subject to the same fluid velocity flow making their motion correlated.

The fluid velocity component can be expressed as a sum of two component:u_L and u_S. Both of them are turbulent flow, but u_L act on large scale respect to the particles dimension, while u_S act on small scale.

We are interested in the relative motion, hence we name: $x = x_1 - x_2,\; v = v_1 - v_2$ for which we get a unique system of equations:

$$\begin{aligned} x' &= v \\ v' &= -\frac{1}{\tau_p} v + \frac{1}{\tau_p}\left(u_L\left(x_1\right) - u_L\left(x_2\right)\right) + \frac{1}{\tau_p}\left(u_S\left(x_1\right) - u_S\left(x_2\right)\right). \end{aligned}$$

Due to the large scale effect, we neglect u_L, which will be incorporated only in later discussion. The reason to maintain u_S is due to the transport noise type of construction we used during the thesis and the limiting property of such a system.

In particular, taking the diffusive limit of u_S we can recover a kinetic system made up of an ODE and an SDE:

$$\begin{aligned} x' &= v \\ dv &= -\frac{1}{\tau_p} v dt + \frac{\sigma_S}{\tau_p}\sqrt{1 - q\left(|x|\right)} dW \end{aligned} \tag{3.7.1}$$

a close equation for position and velocity difference of the particles. Here q represent the spatial correlation of the fluid and depends on the separation of the particles $\mathbf{r} := |x|$, $\sigma_S = u_\eta \sqrt{\tau_\eta}$ obtained as in Chapter 2. Such a system has, naturally, two temporal scale. The velocity component v varies quickly, due to the factor $\frac{1}{\tau_p}$While the component x varies more slowly. This system in the Eulerian framework has a corresponding Fokker Plank that reads out as:

$$\partial_t f + \operatorname{div}_x\left(vf\right) - \frac{1}{\tau_p}\operatorname{div}_v\left(vf\right) = \frac{\sigma_S^2}{2\tau_p^2}\operatorname{div}_v\left(\left(1 - q\left(|x|\right)\right)\nabla_v f\right).$$

This equation is analogous to the one in (3.2.2). More so, we had no problem obtaining such a system without the use of the Stratonovich interpretation since x here is smooth.

Then the invariant distribution is, as in (3.2.2),

$$\operatorname{div}_x(vf) - \frac{1}{\tau_p}\operatorname{div}_v(vf) = \frac{\sigma_S^2}{2\tau_p^2}\operatorname{div}_v\left(\left(1-q\left(|x|\right)\right)\nabla_v f\right)$$

and as such f is still a function of both (x,v), with partial derivative in all the variables. Thus, the solution is not a precisely a Gaussian due to the non linearity in the variables, thanks to $\nabla_x \cdot$ and $q\left(|x|\right)$.

Remark 3.7.1. Is it worth mentioning that this kind of steady state is very similar to the Boltzmann equation' steady state solution, with an elliptic kernel. It could be interesting in future works to explore the possibility of finding explicit solutions of such system: from works of Villani and Gamba [43] it one possible guess is to consider a Maxwellian solution, a Gaussian with a multiplicative correction due to $|x|^2$.

Adiabatic approximation

In Section 3.2, we used the approximation of fixing x constant, adiabaticly, while v varies, in the Lagrangian framework this is equivalent to study the one-equation system:

$$dv = -\frac{1}{\tau_p}vdt + \frac{\sigma_S}{\tau_p}\sqrt{1-q\left(r\right)}dW \tag{3.7.2}$$

for different value of $\mathbf{r} = |x|$. This system is exaclty the one associated to the FP equation studied in the first half of this chapter, and have a stationary solution of the form

$$f_r\left(v\right) \sim N\left(0, \frac{\sigma_S^2}{2\tau_p}\left(1-q\left(r\right)\right)\right).$$

Thus, we'll show numerically, computing the steady state solution of both equations 3.7.1 and 3.7.2, that the adyabatic one well represents the model for all the scale of ratio $\mathbf{r}/\eta$.

Numerical simulations

As a first analysis of the two model with Brownian diffusion, we consider numerically Equations 3.7.1 and 3.7.2, for a fixed $|x| =: \mathbf{r}$ in the range of the separation distance between two particles in the range of $r/\eta \sim [1,10]$ and $r/\eta \sim [20,60]$.

We compute the invariant distribution of both the non-linear conditional on $|x| = \mathbf{r}$ and the one of the linear system with fixed r, in the adiabatic regime, approximated through the Gaussian function $f_r\left(v\right)$.

For simplicity we fix dimension $d = 1$, and select initial condition as follows:

$$X_0 = 0.1 \text{ in computational unit, } V_0 = 0,\ dt = 10^{-4}$$

while for the constant of the system we select

$$\sigma_S = 0.1,\ \tau_p = 0.001,\ \eta = 0.001m,\ q(r) = \min\{r^{1/6}, 1\}$$

Where q is selected with Kolmogorov Scaling criterion. We simulate with Euler-Maruyama scheme for 10^6 iterations and then restart it for another 10^6 iterations to take the invariant distribution.

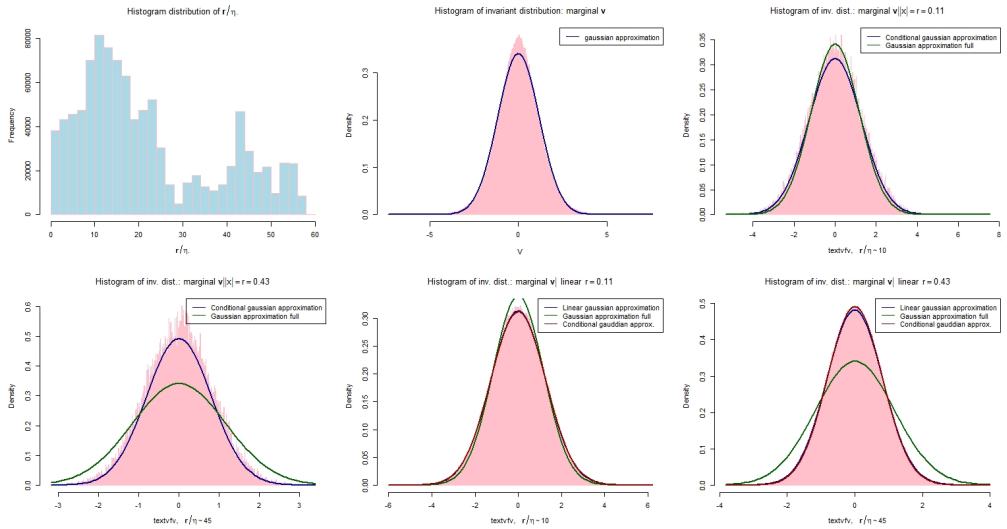

Figure 3.2: Results on marginal distribution respect to velocity variable in different regime of $\mathbf{r}/\eta$, showing good approximation with Gaussian hypothesis.

In Figure 3.2, we present the comprehensive outcomes of the one-dimensional simulation. These results exhibit a favorable alignment with the Gaussianity assumption applied in the preceding chapter. More so, it's worth noting that the value of $\eta = 0.001m$ resides within the Kolmogorov length scale range pertinent to atmospheric fluid dynamics. This provides a reasonable foundation for selecting two distinct values: $\mathbf{r} \approx 0.11$, corresponding to $\mathbf{r}/\eta \approx 10$, and $\mathbf{r} \approx 0.43$, corresponding to $r/\eta \approx 45$. Such choices enable us to encompass both small and large $\mathbf{r}$ scenarios.

The upper row of images reveals the following:

The leftmost image portrays a frequency histogram showcasing the normalized steady-state distribution of particle relative positions, centered around the particles' initial distances. In the center image, a comparison is drawn between the non-linear case's marginal probability distribution $\int f(\mathbf{x}, \mathbf{v})d\mathbf{x}$ and its corresponding Gaussian approximation, depicted in blue. The rightmost image illustrates the conditional probability distribution $f(\mathbf{r}, \mathbf{v})$ for $\mathbf{r}/\eta \approx 10$ in the non-linear case, contrasted with the Gaussian approximation shown in blue. The green line represents the Gaussian approximation of the marginal probability distribution $\int f(\mathbf{x}, \mathbf{v})d\mathbf{x}$.

The lower row of images displays the subsequent analyses:

The leftmost image showcases the probability distribution $f(\mathbf{r}, \mathbf{v})$ for $\mathbf{r}/\eta \approx 45$ in the non-linear case, alongside its Gaussian approximation in blue. The green line signifies the Gaussian approximation of the marginal probability distribution $\int f(\mathbf{x}, \mathbf{v})d\mathbf{x}$.

In the middle image, the probability distribution $f_{\mathbf{r}}(\mathbf{v})$ is presented for $\mathbf{r}/\eta \approx 10$ in the adiabatic case. The blue line represents its Gaussian approximation, while the green line denotes the Gaussian approximation of the marginal probability distribution $\int f(\mathbf{x}, \mathbf{v})d\mathbf{x}$, and the red line signifies the Gaussian approximation of the conditioned probability distribution $f(\mathbf{r}, \mathbf{v})$.

The rightmost image concludes with the probability distribution $f_{\mathbf{r}}(\mathbf{v})$ for $\mathbf{r}/\eta \approx 45$ in the adiabatic case. Similar to the previous cases, its Gaussian approximation is illustrated

in blue, with the green line symbolizing the Gaussian approximation of the marginal probability distribution $\int f(\mathbf{x}, \mathbf{v})d\mathbf{x}$, and the red line representing the Gaussian approximation of the conditioned probability distribution $f(\mathbf{r}, \mathbf{v})$.

Remark 3.7.2. In the case of $\mathbf{r}/\eta \sim 10$ error in the approximated Gaussian respect to predicted $f_{\mathbf{r}}$ (via the computation $\frac{\sigma_S}{2\tau_p}\sqrt{1-q(\mathbf{r})}$ for the variance) is 10^{-1}, while for $\mathbf{r}/\eta \sim 45$ error in the approximated Gaussian respect to predicted is 10^{-3}. More so, in $\sup$-norm the difference between the approximated Gaussian and the real distribution is less than 10^{-2} for $\mathbf{r}/\eta \sim 45$ and 5×10^{-2} for $r/\eta \sim 10$, and a Kolmogorov-Smirnov test confirms the goodness of the Gaussian hypothesis.

Conclusions

These basic numerical experiments yield results in agreement with the approximation method, showing a small error in the estimation. While assuming Gaussianity with an error magnitude of 10^{-2} may slightly underestimate the value, its effectiveness remains reasonable.

More so, this leads us to contemplate the implications for diverse regimes of relative distance $\mathbf{r}/\eta$ at different Stokes numbers: while under this Gaussianity assumption we derive a complete formula respect to **St** for the collision rate, as in 3.6.1, does this model's validity extend solely to cases where $\mathbf{r}/\eta$ exceeds 1?

This crucial question drives our exploration towards a more inclusive model that can encapsulate a broader spectrum of scenarios, showing gap in the noisy modelling of the fluid velocity that we address in future works.

3.7.2 A more general approximation result

In this section we are going to consider a more general modeling of the velocity of the fluid in which particles moves and collide. In suitable limit, this system reduces to the one studied in previous part of the chapter, making it a reasonable generalization to study.

The modelling of $u(\mathbf{x})$ is obtained through the use of an Ornstein–Uhlenbeck process Z with a suitable space covariance and a time correlation that depends on the Kolmogorov scale of the fluid.

This define the following second order random system for particles advected by a turbulent fluid:

$$\begin{aligned} x' &= v \\ v' &= -\frac{1}{\tau_p}v + \frac{1}{\tau_p}\sqrt{1-q\left(|x|\right)}u_\eta Z \\ dZ &= -\frac{1}{\tau_\eta}Zdt + \frac{1}{\sqrt{\tau_\eta}}dW. \end{aligned} \tag{3.7.3}$$

In analogy to what we did in Section 3.7.1 we define **x** as the relative position between two particles and **v** the difference in velocity. Here we use u_η to indicate the fluid velocity

at the Kolmogorov scale, with the relative length and relaxation time, η, τ_η respectively. Regarding $q(\mathbf{r}/)$, this is non other than the spatial correlation of the fluid at the Kolmogorov scale. As in Chapter 2, $q(\mathbf{r}) \in [0,1]$, decreasing, $\lim_{\mathbf{r}\to 0} q(\mathbf{r}) = 1$, $\lim_{\mathbf{r}\to\infty} q(\mathbf{r}) = 0$.

The difference respect to the previous model is in that involves the explicit introduction of temporal correlation into the Kolmogorov scale, τ_η. More so, this model recovers the well-known results for high St and, naturally, makes more precise results for small to medium St, concerning the relative velocity and the corrective factor of previous sections.

Then, in the same fashion, we define the adiabatic approximated system, where the position is fixed a t a given distance **r**

$$\begin{aligned} v' &= -\frac{1}{\tau_p} v + \frac{1}{\tau_p}\sqrt{1-q(r)}\, u_\eta Z \\ dZ &= -\frac{1}{\tau_\eta} Z dt + \frac{1}{\sqrt{\tau_\eta}} dW \end{aligned} \tag{3.7.4}$$

We'll show that this system is close in its solutions to the full system 3.7.3, for every range of $\mathbf{r}/\eta$, recovering the complete description of the relative velocity for all range of Stokes number. The reason of the following analysis lies in the highlight of a key quantity that, as of now, was not considered in the model, i.e. the relative distance of the particles and how big or small it is respect to the Kolmogorov length-scale. In fact all of our conclusion are true whenever $\mathbf{r}/\eta \gtrsim 1$, while whene **r** is close to the Kolmogorov scale, i.e.

$$\frac{r}{\eta} \in [1, 10]$$

Then the complete description of the relative velocity through the simplified stochastic model fail. In the next paragraph we'll derive again the relative velocity when **r** is big compared to η and highlight the numerical results showing how the Gaussian approximation is suitable to work with such systems. We conclude the section proposing a problem concerning particles that are closer than the Kolmogorov scale and how to enhance the model in future works.

Relative velocity for $\mathbf{r}/\eta \gtrsim 1$

We consider system 3.7.3 and normalize it respect to the fluid velocity u_η

$$\begin{aligned} \left(\frac{v}{u_\eta}\right)' &= -\frac{1}{\tau_p}\left(\frac{v}{u_\eta}\right) + \frac{1}{\tau_p}\sqrt{1-q(|x|)}\, Z \\ dZ &= -\frac{1}{\tau_\eta} Z dt + \frac{1}{\sqrt{\tau_\eta}} dW \end{aligned}$$

Starting from this normalized equations, we pass to the adiabatic modelling and thus we have

$$dV = -\frac{1}{\tau_p} V dt + \frac{1}{\tau_p}\sqrt{1-q(r)}\, Z dt$$

$$dZ = -\frac{1}{\tau_\eta} Z dt + \frac{1}{\sqrt{\tau_\eta}} dW$$

Naming $X = (V, Z)$ the velocity variable and Ornstein-Uhlembeck process, and fixing $R = (B, W)$ two independent Brownian motion, we can rewrite the system as

$$dX = \begin{pmatrix} -\frac{1}{\tau_p} & \frac{1}{\tau_p}\sqrt{1-q(r)} \\ 0 & -\frac{1}{\tau_\eta} Z \end{pmatrix} X dt + \begin{pmatrix} 0 & 0 \\ 0 & \frac{1}{\sqrt{\tau_\eta}} \end{pmatrix} \begin{pmatrix} dB \\ dW \end{pmatrix}$$

Which read as

$$dX = AX dt + \sqrt{Q} \begin{pmatrix} dB \\ dW \end{pmatrix}$$

This system as a stationary solution given by the closed formula

$$X(0) = \int_{-\infty}^{0} e^{(-t)A} \sqrt{Q} dR_t$$

For which the variance can be computed easily:

$$\mathbb{E}\left[X(0) \otimes X(0)\right] =: Q_\infty = \int_0^\infty e^{tA} Q e^{tA^*} dt.$$

For simplicity in the exposition, we fix dimension $d = 1$, but everything said from here on is valid for $d \geq 1$ with a little bit of effort in the notations. We are interested in the variance of the component V:

$$Q_\infty^{11} = \int_0^\infty \sum_{ij} e_{1i}^{tA} Q_{ij} e_{1j}^{tA} dt = \frac{1}{\tau_\eta} \int_0^\infty \left(e_{12}^{tA}\right)^2 dt.$$

While for the variable Z we have

$$Q_\infty^{22} = \int_0^\infty \sum_{ij} e_{2i}^{tA} Q_{ij} e_{2j}^{tA} dt = \frac{1}{\tau_\eta} \int_0^\infty \left(e_{22}^{tA}\right)^2 dt$$

which must be unitary since is the variance of Z, a OU process with right scaling on the drift and diffusion.

To obtain the quantities

$$e_{12}^{tA} = \left(e^{tA} \begin{pmatrix} 0 \\ 1 \end{pmatrix}\right)_1, \quad e_{22}^{tA} = \left(e^{tA} \begin{pmatrix} 0 \\ 1 \end{pmatrix}\right)_2 = Z.$$

we need to solve the following ODE system

$$\begin{aligned} V' &= -\frac{1}{\tau_p} V + \frac{1}{\tau_p}\sqrt{1-q(r)} Z \\ Z' &= -\frac{1}{\tau_\eta} Z \\ V(0) &= 0, \qquad Z(0) = 1 \end{aligned}$$

and take V and Z. We have:

$$\begin{aligned} V' &= -\frac{1}{\tau_p}V + \frac{1}{\tau_p}\sqrt{1-q(r)}e^{-\frac{1}{\tau_\eta}t} \\ V(0) &= 0 \end{aligned}$$

Using the formula $\frac{1}{\tau_p} - \frac{1}{\tau_\eta} = \frac{\tau_\eta - \tau_p}{\tau_p \tau_\eta}$, we can reduce the computation and obtain:
If $\tau_p \neq \tau_\eta$:

$$\begin{aligned} e_{12}^{tA} &= \int_0^t e^{-\frac{1}{\tau_p}(t-s)} \frac{1}{\tau_p}\sqrt{1-q(r)}e^{-\frac{1}{\tau_\eta}s} ds \\ &= \frac{1}{\tau_p}\sqrt{1-q(r)}e^{-\frac{1}{\tau_p}t} \int_0^t e^{\left(\frac{1}{\tau_p}-\frac{1}{\tau_\eta}\right)s} ds \\ &= \frac{1}{\tau_p}\sqrt{1-q(r)}e^{-\frac{1}{\tau_p}t} \frac{e^{\left(\frac{1}{\tau_p}-\frac{1}{\tau_\eta}\right)t} - 1}{\frac{1}{\tau_p}-\frac{1}{\tau_\eta}} \\ &= \sqrt{1-q(r)}\frac{\tau_\eta}{\tau_\eta - \tau_p}\left(e^{-\frac{1}{\tau_\eta}t} - e^{-\frac{1}{\tau_p}t}\right) \end{aligned}$$

While, If $\tau_p = \tau_\eta$:

$$e_{12}^{tA} = \sqrt{1-q(r)}\frac{1}{\tau_p}e^{-\frac{1}{\tau_p}t}t$$

Putting all together we have a formula for Q_∞^{11} given by:

$$\begin{aligned} Q_\infty^{11} &= \frac{1}{\tau_\eta}\int_0^\infty \left(e_{12}^{tA}\right)^2 dt \\ &= (1-q(r)) \begin{cases} \frac{1}{\tau_\eta}\left(\frac{\tau_\eta}{\tau_\eta - \tau_p}\right)^2 \int_0^\infty \left(e^{-\frac{1}{\tau_\eta}t} - e^{-\frac{1}{\tau_p}t}\right)^2 dt & \text{se } \tau_p \neq \tau_\eta \\ \frac{1}{\tau_\eta \tau_p^2}\int_0^\infty e^{-\frac{2}{\tau_p}t}t^2 dt & \text{se } \tau_p = \tau_\eta \end{cases} \end{aligned}$$

We focus now on the case $\tau_p \neq \tau_\eta$, we'll show that the final formula agrees also in the case when $\tau_p = \tau_\eta$, being general. We have

$$\begin{aligned} \int_0^\infty \left(e^{-\frac{1}{\tau_\eta}t} - e^{-\frac{1}{\tau_p}t}\right)^2 dt &= \int_0^\infty \left(e^{-\frac{2}{\tau_\eta}t} + e^{-\frac{2}{\tau_p}t} - 2e^{-\left(\frac{1}{\tau_\eta}+\frac{1}{\tau_p}\right)t}\right) dt \\ &= \frac{\tau_\eta}{2} + \frac{\tau_p}{2} - 2\frac{1}{\frac{1}{\tau_\eta}+\frac{1}{\tau_p}} = \frac{\tau_\eta}{2} + \frac{\tau_p}{2} - 2\frac{\tau_\eta \tau_p}{\tau_p + \tau_\eta} \end{aligned}$$

This gives

$$\begin{aligned} Q_\infty^{11} &= \frac{1}{\tau_\eta}\int_0^\infty \left(e_{12}^{tA}\right)^2 dt \\ &= (1-q(r))\frac{1}{\tau_\eta}\left(\frac{\tau_\eta}{\tau_\eta - \tau_p}\right)^2 \left(\frac{\tau_\eta}{2} + \frac{\tau_p}{2} - 2\frac{\tau_\eta \tau_p}{\tau_p + \tau_\eta}\right) \end{aligned}$$

Remembering now the definition of Stokes number $St := \tau_p/\tau_\eta$, we get

$$Q_\infty^{11} = \frac{\left(\frac{1}{2} + \frac{St}{2} - 2\frac{St}{1+St}\right)}{(1-St)^2}\left(1 - q\left(r\right)\right)$$

Reducing to the final formulation

$$\boxed{Q_\infty^{11} = \frac{1}{2\left(1+St\right)}\left(1 - q\left(r\right)\right).}$$

This formula is perfect if **r** is large and **St** is arbitrary, being adherent in the limit to the one obtained in the previous computation. More so, comparing it with the experimental result in [21], figure 12, for cases where $\frac{r}{\eta} \gtrsim 1$, we found similar behavior, and the quantity $\frac{\langle w(r)\rangle}{u_\eta}$ in that figure is $\sim \sqrt{Q_\infty^{11}}$.

Conjecture 3.7.3 (What about $r/\eta \lesssim 1$?)**.** *According to [21], figure 12, for cases where $\frac{r}{\eta} \in [1, 10]$, the function $\sqrt{Q_\infty^{11}} \sim \frac{\langle w(r)\rangle}{u_\eta}$ should start close to zero for small St, remaining almost constant for a while, and then increase. This is in contrast to what was found above using the adiabatic approximation and the simplified OU model. How to enhance the model to have a complete formulation for particles closer than Kolmogorov length scale is a complex and interesting modelling problem that should be investigated using results from [75, 25, 26].*

Numerical results: justified adiabatic approximation

In this section we are going to propose a numerical analysis of the steady state solutions for the non linear system (3.7.3) and the linearized one (3.7.4), showing that, in all regime of **St** and relative distance **r**, the Gaussian approximation is a suitable and simplified approximation to the full solution of 3.7.3. In both cases we are going to consider $x, v, Z \in \mathbb{R}$ for different selection of Stokes number **St** and distance ratio $\mathbf{r}/\eta$, with values $\mathbf{r}/\eta \sim 1$ and $\mathbf{r}/\eta \sim 10$.

We check invariant distribution of $(3.7.3)$, then invariant distribution of $(3.7.3)$ conditioned on $|x| = \mathbf{r}$, the invariant distribution of $(3.7.4)$ with fixed **r** and comparison with theoretical $f_{\mathbf{r}}\left(\mathbf{v}\right)$ from previous sections.

The parameters of the system are selected from [64] and are:

$$\eta = 3\times 10^{-4}m,\ \tau_\eta = 10^{-2}s,\ \mathbf{u}_\eta = \frac{\eta}{\tau_\eta} = 3\times 10^{-2}\frac{m}{s},\ \sqrt{1-q(r)} = \min\{r^{1/6}, 1\}$$

The inital conditions for x, v, Z and the numerical setting are selected as

$$x_0 = 10\times\eta,\ v_0 = 0,\ Z_0 = 0,\ dt = 10^{-4}$$

while we selected **St** $\in \{0.01, 0.1, 1\}$, i.e $\tau_p \in \{10^{-4}, 10^{-3}, 10^{-2}\}s$.

The theoretical variance used is obtained from previous computations:

$$\frac{(1-q(\mathbf{r}))}{2(1+\mathbf{St})}\mathbf{u}_\eta \sim \frac{\mathbf{r}^{1/3}}{2(1+\mathbf{St})}\mathbf{u}_\eta.$$

We simulate the system with Euler-Maruyama scheme for 10^6 iterations and then restart it for another 2×10^6 iterations and take the value as the invariant distribution.

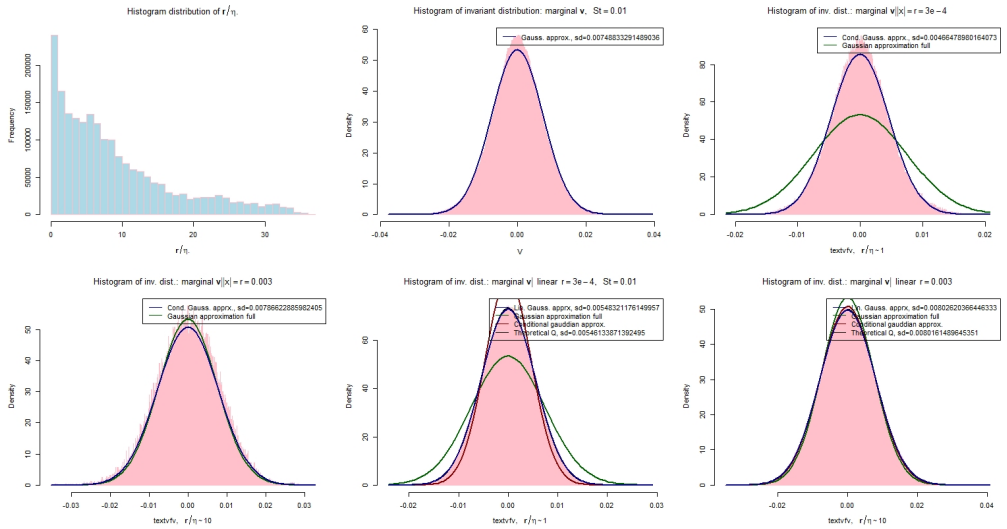

Figure 3.3: Comparison of the steady state distribution for different **r** for linear and non linear system. Comparison with approximated and theoretical Gaussian.

St $= 0.01,$ **r**$/\eta = 1, 10$

In Figure 3.3, we present the comprehensive findings from the one-dimensional simulation under fixed parameters. Despite the particle inertia being small, the model demonstrates a reasonable fit with the Gaussianity simplification discussed in the preceding chapter.

From the Upper Section (left to right):

The first image depicts a frequency histogram of particle relative positions within the steady-state distribution, normalized with respect to η. It reveals a concentration around the initial relative distance and a power-law decay at larger distances.

The second image illustrates the marginal probability distribution $\int f(\mathbf{x}, \mathbf{v}), d\mathbf{x}$ in the nonlinear case, superimposed with the Gaussian approximation shown as a blue curve. This visualization effectively demonstrates the interplay between $\nabla_r \cdot (fv)$ within the system and its coupling with $q(\mathbf{r})$.

The third image presents the conditional probability distribution $f(\mathbf{r}, \mathbf{v})$ for $\mathbf{r}/\eta \sim 1$ in the nonlinear case. The blue line represents the Gaussian approximation, and the green line corresponds to the Gaussian approximation of the marginal probability distribution $\int f(\mathbf{x}, \mathbf{v}), d\mathbf{x}$.

From the Lower Section (left to right):

The first image illustrates the probability distribution $f(\mathbf{r}, \mathbf{v})$ for $\mathbf{r}/\eta \sim 10$ in the nonlinear scenario. The blue line signifies the Gaussian approximation, and the green line represents the Gaussian approximation of the marginal probability distribution $\int f(\mathbf{x}, \mathbf{v}), d\mathbf{x}$.

The second image displays the probability distribution $f_{\mathbf{r}}(\mathbf{v})$ for $\mathbf{r}/\eta \sim 1$ in the adiabatic case. The blue line denotes the Gaussian approximation, the green line represents the Gaussian approximation of the marginal probability distribution $\int f(\mathbf{x}, \mathbf{v}), d\mathbf{x}$, and the red line corresponds to the Gaussian approximation of the conditioned probability distribution $f(\mathbf{r}, \mathbf{v})$.

The third image portrays the probability distribution $f_{\mathbf{r}}(\mathbf{v})$ for $\mathbf{r}/\eta \sim 10$ in the adia-

batic case. As in previous cases, the blue line represents the Gaussian approximation, the green line signifies the Gaussian approximation of the marginal probability distribution $\int f(\mathbf{x}, \mathbf{v}), d\mathbf{x}$, and the red line denotes the Gaussian approximation of the conditioned probability distribution $f(\mathbf{r}, \mathbf{v})$.

In this examined case, we observe a percentage relative error in the theoretical and linearized Gaussian cases compared to the conditional nonlinear system. This error is less than 15% for small **r** and less than 2% for large **r**, which provides motivation for the simplification due to the Gaussian assumption.

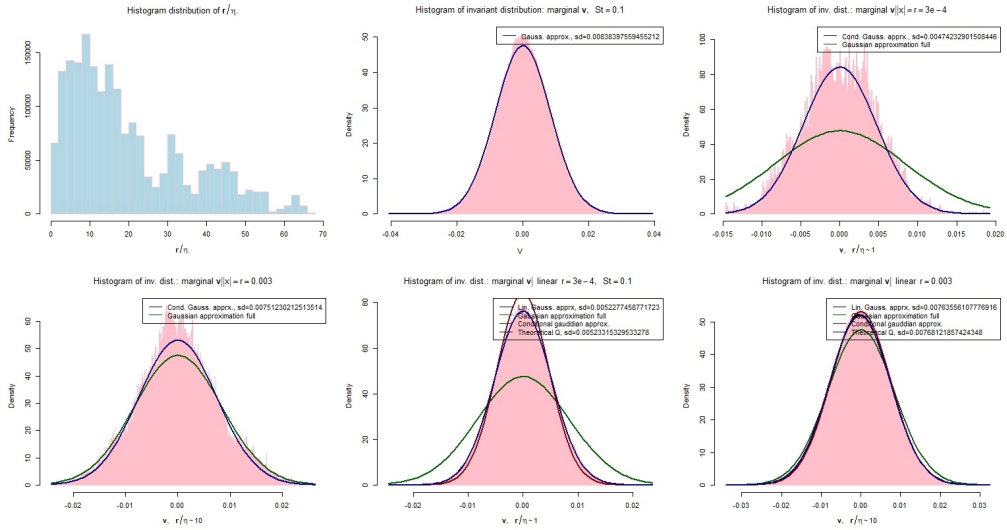

Figure 3.4: Comparison of the steady state distribution for different **r** for linear and non linear system. Comparison with approximated and theoretical Gaussian.

$\mathbf{St} = 0.1,\ \mathbf{r}/\eta = 1, 10$

In Figure 3.4, we present the comprehensive findings from the one-dimensional simulation with higher **St**. at the increase of particles inertia, the model demonstrates an even more reasonable fit with the Gaussianity simplification discussed in the preceding chapter. Concerning the figure, in analogy with Figure 3.3, we have the same object with few difference: the first image on the top left depicts again the frequency histogram of particle relative positions within the steady-state distribution, normalized with respect to η. It reveals a concentration around the initial relative distance and a slower power-law decay at larger distances, with a decay dependent on the **St**-parameter. The other image show similar behavior as the previous picture, suggesting the goodness of the approximation for the model.

In this examined case, we observe a percentage relative error in the theoretical and linearized Gaussian cases compared to the conditional nonlinear system. This error is less than 10% for small **r** and less than 1% for large **r**, which provides motivation for the simplification due to the Gaussian assumption, More so, it shows that for higher **St** regime the approximation is even tighter.

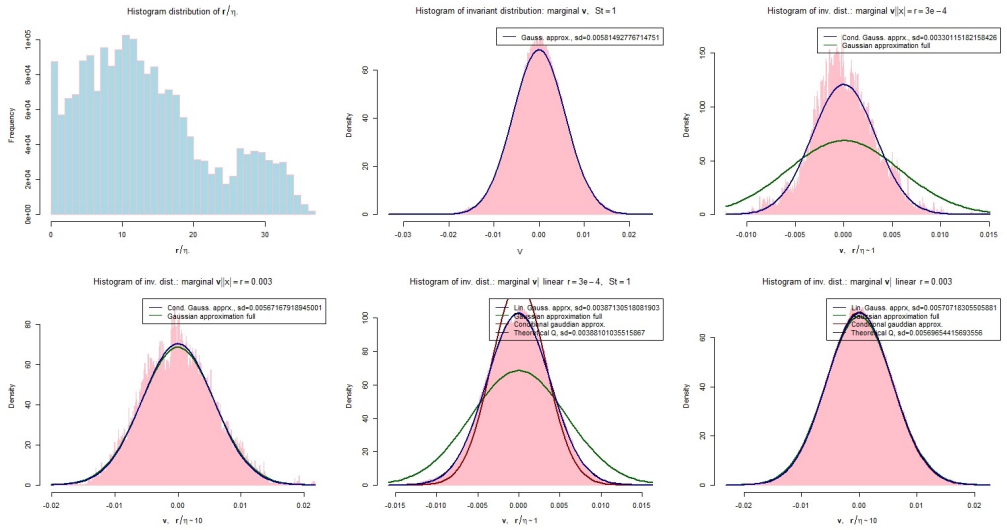

Figure 3.5: Comparison of the steady state distribution for different **r** for linear and non linear system. Comparison with approximated and theoretical Gaussian.

St $= 1,$ **r**$/\eta = 1, 10$

In Figure 3.5, we present the comprehensive findings from the one-dimensional simulation with unitary **St**, high-end regime for cloud droplets. At this higher particles inertia, the model maintain an continue to show an even more reasonable fit with the Gaussianity simplification discussed in the preceding chapter. Concerning the figure, in analogy with Figure 3.3 and 3.4, we have the same object with few difference: the first image on the top left depicts again the frequency histogram of particle relative positions and show an even slower power-law decay at larger distances, with a decay dependent on the **St**-parameter. The other image show similar behavior as the previous picture, with different standard deviation, but similar quantity results. More so the picture suggest that the overall marginal distribution of the non linear system tends to match the high **r**-value when $f(\mathbf{x}, \mathbf{v})$ is conditioned at $|x| =$ **r**. This, all in all, suggest the goodness of the Gaussian approximation for the model.

In this examined case, we observe a percentage relative error in the theoretical and linearized Gaussian cases compared to the conditional nonlinear system. This error is less than 11% for small **r** and less than 0.5% for large **r**, which provides motivation for the simplification due to the Gaussian assumption. Confirming that in the higher **St** regime the Gaussian approximation is even strongly supported.

Cumulative results: $\langle \mathbf{v} \rangle \mathbf{u}_\eta \times$ St-plot

In Figure 3.6, we depict the standard deviation for the studied distributions that exhibit distinct characteristics, each represented by a different color. The **red** curve showcases the standard deviation (*s.d.*) of the conditional density, denoted as $f(\mathbf{r}, v)$, where **r**$/\eta = 1$ and 10. In a complementary manner, the **blue** curve illustrates the *s.d.* of the linear density. Here, the function $q(|x|)$ is computed at $q(\mathbf{r})$ for **r**$/\eta = 1$ and 10.

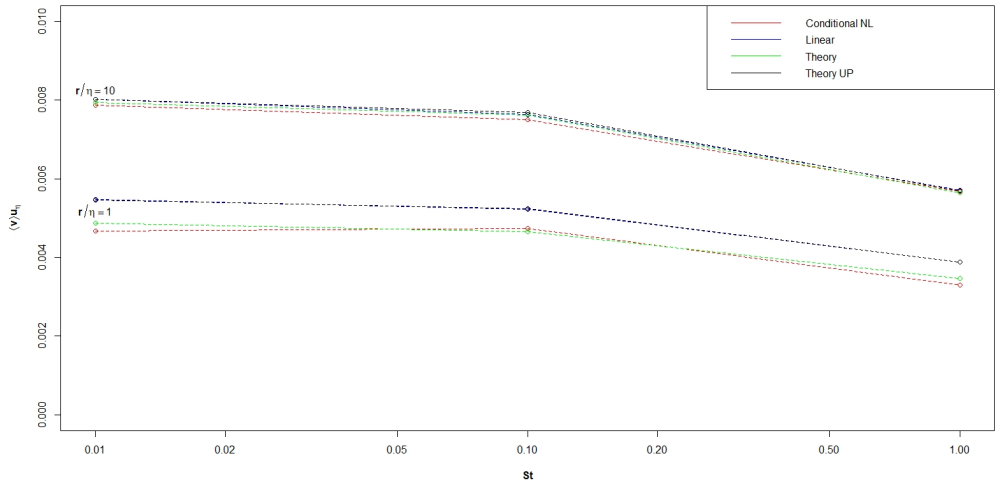

Figure 3.6: Plot of the mean velocity times fluid velocity at Kolmogorov scale, at various **St**, computed through the standard deviation of steady state density both theoretical and from the complete model for different value of $\mathbf{r}/\eta$.

Theoretical value come into play with the **green** curve, which represents the computed *s.d.*, denoted as $\sqrt{Q_{11}^{\infty}}\mathbf{u}_{\eta}$, for mean values of **r** as they align with the small histogram bars in the position plot. Meanwhile, the **black** curve corresponds to the theoretical *s.d.* $\sqrt{Q_{11}^{\infty}}\mathbf{u}_{\eta}$ for the upper values of **r** in the histogram bars, satisfying $\mathbf{r}/\eta = 1$ and 10 exactly.

Remarkably, these results collectively demonstrate an exceptionally high degree of approximation accuracy. Notably, the approximation accuracy is particularly pronounced for values where $\mathbf{r}/\eta$ exceeds 10. This is further affirmed by a percentage-relative error that remains below 1%. Additionally, the approximations remain suitable across a range of scenarios, even as the error margin gradually increases for smaller **r**, when transitioning from low to high **St** parameter, it gets from 10% to just under 10%. In conclusion, this analysis underscores the robustness of the proposed approximations across a spectrum of conditions and establishes their utility in practical computations.

Remark 3.7.4. As a closing remark of the section, we notice that, comparing it with results of Zhou et all. [21], Figure 12, we have a discrepancy with the behavior of our model for small value of **r**. When $\mathbf{r}/\eta$ is large, the behavior of relative velocity seems reasonable and the approximation very consistent for all **St**, either low or high. Regarding the small value of $\mathbf{r}/\eta$ the behavior seems a bit off respect to laboratory experiments: the Gaussian approximation and the non-linear system itself are a bit less precise for small **St** in the small **r** regime. This leave open the question on how to modify the non linear model 3.7.3 in such a way that for relative distance smaller than the Kolmogorov length-scale, the correlation of the fluid and the velocity of the particles are properly considered. This will be addressed in future studies.

3.8 Galeati limit on two-points motion

In this final section we propose a study to show how to derive our limiting PDE and justify our approximation in the coagulation rate computation. This section is to be intended as a sketch and a justification, postponing to future work a rigorous study of the Galeati limit.

In this direction, let us consider the two point motion stochastic Vlasov-Fokker-Planck equation in the space $(x_i, v_i)_{i=1,2} \in (\mathbb{T}^2 \times \mathbb{R}^2)^2$, with a "degenerate" transport noise acting on each of the velocity variable, i.e.

$$\partial_t f + \mathrm{div}_{x_1}(v_1 f) + \mathrm{div}_{x_2}(v_2 f) - \frac{1}{\tau_p}\mathrm{div}_{v_1}(v_1 f) - \frac{1}{\tau_p}\mathrm{div}_{v_2}(v_2 f) = \nabla_{v_1,v_2} f \circ \dot{W}$$

where $\nabla_{v_1,v_2} \circ \dot{W}$ is

$$\nabla_{v_1,v_2} \circ \dot{W} = \sum_{k\in\Lambda} \sigma_k(x_1)\cdot\nabla_{v_1} f \circ dW_t^k + \sum_{k\in\Lambda} \sigma_k(x_2)\cdot\nabla_{v_2} f \circ dW_t^k$$

We would like to find a renormalizing term ε_N, and a selection of, regular enough, fields $\sigma_k^N : \mathbb{T}^2 \to \mathbb{R}^2,\ k \in \Lambda_N$ such that in the limit of $N \to \infty$ we have the limiting equation:

$$\begin{cases} \partial_t f + \mathrm{div}_{x_1}(v_1 f) + \mathrm{div}_{x_2}(v_2 f) - \frac{1}{\tau_p}\mathrm{div}_{v_1}(v_1 f) - \frac{1}{\tau_p}\mathrm{div}_{v_2}(v_2 f) = \mathcal{D} f \\ \mathcal{D} f = \frac{\sigma^2}{2\tau_p^2} div_{v_1}(Q(x_1,x_1)\nabla_{v_1} f) + \frac{\sigma^2}{2\tau_p^2} div_{v_2}(Q(x_2,x_2)\nabla_{v_2} f) + \frac{\sigma^2}{\tau_p^2} div_{v_1}(Q(x_1,x_2)\nabla_{v_2} f) \end{cases}$$

We use the domain of the x-variable, $\mathbb{T}^2$, with the same construction to obtain the Brownian motions as in [35, 38].

3.8.1 The Transient PDE

Regarding the Galeati limit, strictly speaking, it cannot work in the usual way as in [35, 38].

In such a framework, it is required that $Q_N(x-y) \to 0$ when $x \neq y$. Therefore, strictly speaking, the SPDE (3.8) in your file would tend to the PDE (3.8) with $\mathcal{D}$ as a diagonal operator, meaning without the mixed term that we need in the theory.

So we are in one of those situations, e.g. [33], where we cannot take the true and proper limit, but we have to settle for proximity. This is not the first case: it also happens when, for example, $Q_N(0)$ diverges. In this case too, the limiting PDE is not the right object, but rather a kind of transient PDE. Let us explain this in more details.

We have the SPDE

$$df + \left(\mathrm{div}_{x_1}(v_1 f) + \mathrm{div}_{x_2}(v_2 f) - \frac{1}{\tau_p}\mathrm{div}_{v_1}(v_1 f) - \frac{1}{\tau_p}\mathrm{div}_{v_2}(v_2 f)\right) dt \tag{3.8.1}$$

$$= \frac{\sigma}{\tau_p}\sum_k e_k(\mathbf{x_1})\cdot\nabla_{v_1} f \circ dW_k(t) + \frac{\sigma}{\tau_p}\sum_k e_k(\mathbf{x_2})\cdot\nabla_{v_2} f \circ dW_k(t) \tag{3.8.2}$$

and the PDE

$$\partial_t \overline{f} + \mathrm{div}_{x_1}(v_1\overline{f}) + \mathrm{div}_{x_2}(v_2\overline{f}) - \frac{1}{\tau_p}\mathrm{div}_{v_1}(v_1\overline{f}) - \frac{1}{\tau_p}\mathrm{div}_{v_2}(v_2\overline{f}) = \mathcal{D}\overline{f} \tag{3.8.3}$$

where

$$\mathcal{D}\overline{f} = \frac{\sigma^2}{2\tau_p^2} div_{v_1}(Q(\mathbf{x_1},\mathbf{x_1})\nabla_{v_1}\overline{f}) + \frac{\sigma^2}{2\tau_p^2} div_{v_2}(Q(\mathbf{x_2},\mathbf{x_2})\nabla_{v_2}\overline{f}) + \frac{\sigma^2}{\tau_p^2} div_{v_1}\left(Q(\mathbf{x_1},\mathbf{x_2})\nabla_{v_2}\overline{f}\right).$$

We are not trying to prove that the first one tends to the second one when a certain parameter N in the coefficients tends to the limit; otherwise, the term

$$\frac{\sigma^2}{\tau_p^2} div_{v_1}\left(Q(\mathbf{x_1},\mathbf{x_2})\nabla_{v_2}\overline{f}\right)$$

would be zero. We are only trying to estimate the difference between the two:

$$\mathbb{E}\left[\left\langle f-\overline{f},\phi\right\rangle^2\right] \leq C\left\|\mathbb{Q}\right\|_{L^2\to L^2}\left\|f_0\right\|_{L^2}.$$

We work in this direction, refining this estimate as much as possible, and as such supporting the fact that we transition from the SPDE to the PDE.

To ease the computation and show the proximity of solution, for simplicity, we consider the same setting as in [33, 39], working on a bounded domain $\mathcal{D} \subset \mathbb{R}^2 \times \mathbb{R}^2$ for both the space and velocity variables. In the same spirit the noise construction is made borrowing ideas of small scale vortex patches in 2 dimension.

Vortex noise in 2D

Consider an usual a filtered probability space $(\Omega, \mathcal{F}, (\mathcal{F}_t)_{t\geq 0}, \mathbb{P})$, with expectation $\mathbb{E}$ and let $(W_t^k)_{k\in K}$ be a family of independent one-dimensional Brownian motion. The noisy velocity field added in (3.8.1) can be seen as a generalize process of the form

$$u(t,x_1,x_2) = \sum_{k\in K}\sigma_k(x_1)\frac{dW_t^j}{dt} + \sum_{k\in K}\sigma_k(x_2)\frac{dW_t^j}{dt},$$

white noise in time, divergence free and with a space covariance Q as before.

Regarding the small-scale field generating the correlation in space, restricting for simplicity first to $\mathcal{D}$ open, bounded and connected, we select

$$\sigma_k(x) = \sigma_\varepsilon(x-x_k),\ \sigma_\varepsilon(x) = \varepsilon^{-1}\sigma(\frac{x}{\varepsilon})$$

for a suitable choose of σ and ε.

The reason why we call this a vortex patch come from the point vortex expansion of Euler equation. As such, we call x_k the centers of the vortex patch and σ is selected to mimic the Biot-Savart kernel of a vorticy formulation for the fluid velocity, i.e.

- σ is smooth and divergence free;
- σ is compactly supported on the unit ball;
- σ has the Biot-Savart law singularity at the origin $\sim \frac{1}{|x|}$ and is constructed as a mollified Green function on $\mathbb{R}^2$.

Concerning the center x_k we selected in the same fashion as in [39], dividing the domain $\mathcal{D}$ in region such that each σ_k has disjoint support from each other. With this construction we obtain the derided bound on $\|\mathbb{Q}\|$, see [33] page 8 section $(b.ii)$ and $(b.iii)$ for complete details on such construction.

Semigroup and estimate

Denote by $\mathcal{L}$ the following operator on $(\mathbb{R}^2 \times \mathbb{R}^2)^2$

$$\mathcal{L}\overline{f} := \mathcal{D}\overline{f} - \mathrm{div}_{x_1}\left(v_1\overline{f}\right) - \mathrm{div}_{x_2}\left(v_2\overline{f}\right) + \frac{1}{\tau_p}\mathrm{div}_{v_1}\left(v_1\overline{f}\right) + \frac{1}{\tau_p}\mathrm{div}_{v_2}\left(v_2\overline{f}\right) \quad (3.8.4)$$

where $\mathcal{D}$ is defined as in 3.8.1,3.8.3, with, for simplicity the Gaussian covariance Q as in 3.4. This make our PDE, for proper function on $\mathcal{D}$, of the compact form

$$\partial_t\overline{f} - \mathcal{L}\overline{f} = 0 \quad (3.8.5)$$

$$\partial_t f - \mathcal{L}f = \nabla_{v_1,v_2} f \circ \dot{W} \quad (3.8.6)$$

It is well-known that $\mathcal{L}$ is an hypoelliptic operator in the sense of Hörmander [50] and generalizing the classical works from [85], proposition $II.1$, theorem $II.2, II.3$ and [4, 27, 28, 51, 55, 62, 69, 71, 77, 79], we can construct a semigroup P_t associated to such system. $P_t \geq 0$ and we have a maximum principle for such operator. As such we define for both the deterministic and stochastic equation the classical mild solution with the usual definition for the stochastic convolution

$$\overline{f}(t,x,v,y,w) = \iint_{\mathcal{D}}\iint_{\mathcal{D}} P_t(x-x',y-y',v-v',w-w')f_0(x',y',v',w')dx'dy'dv'dw'$$

$$f(t,x,v,y,w) = P_t * f_0 + \int_0^t P_{t-s} * \nabla_{v,w} \circ \dot{W} ds$$

and we interpret the solution in the weak sense against a test function.

Here we postpone to future work the existence and uniqueness result for such system, since with minor modification from [6, 68, 85] and reference therein, can be obtained with regularity in $C_b^2 \cap L^1$ as soon as $f_0 \in L^2 \cap L^\infty$.

Recall that the covariance matrix of our noise is given by

$$Q(x,y) = \sum_{j\in J} \sigma_j(x) \otimes \sigma_j(y), \qquad x, y \in \overline{\mathcal{D}}.$$

Associated we can identify the bounded linear operator

$$\mathbb{Q} : L^2(\mathcal{D},\mathbb{R}^2) \to L^2(\mathcal{D},\mathbb{R}^2), \mathbb{Q}g(x) = \int_{\mathcal{D}} Q(x,y)g(y)dy$$

and with that the fundamental quantity

$$\|\mathbb{Q}\|_{L^2} = \sup_{g\neq 0} \frac{\int_{\mathcal{D}}\int_{\mathcal{D}} g(x)^T Q(x,y)g(y)dxdy}{\int_{\mathcal{D}} g(x)^T g(x)dx}$$

Theorem 3.8.1. *Assume $f_0 \in L_{\mathcal{F}_0}(\Omega; L^2(\mathcal{D}^2) \cap L^\infty(\mathcal{D}^2))$. Then, for all $\phi \in L^\infty(\mathcal{D})$ we have, for f and $\overline{f}$ solutions respectively of 3.8.1 and 3.8.3,*

$$\mathbb{E}\left[\left\langle f - \overline{f}, \phi\right\rangle^2\right] \leq C \|\mathbb{Q}\|_{L^2\to L^2} \|f_0\|_{L^2}.$$

where C depend on the turbulent kinetic energy σ/τ_p.

Proof. First we reformulate the stochastic equation in the Stratonovich sense with its Ito corrector

$$d_t f = \mathcal{L} f + \sum_{k\in K} \sigma_k(x_1)\cdot\nabla_v f dW_t^j + \sum_{k\in K} \sigma_k(x_2)\cdot\nabla_w f dW_t^j,$$

with the same $\mathcal{L}$ for both 3.8.1 and 3.8.3. Using the weak formulation of the mild form for both the equation we can write

$$d_t\left(f-\overline{f}\right) = \mathcal{L}\left(f-\overline{f}\right) + \sum_{k\in K} \sigma_k(x_1)\cdot\nabla_v f dW_t^j + \sum_{k\in K} \sigma_k(x_2)\cdot\nabla_w f dW_t^j$$

and, considering a smooth test function ϕ with compact support in $\mathcal{D}$, we have

$$\langle \phi, f_Q - f\rangle = \sum_{k\in K}\int_0^t \left\langle P'_{t-s}\phi, \sigma_k(x_1)\cdot\nabla_v f\right\rangle dW_t^j + \sum_{k\in K}\int_0^t \left\langle P'_{t-s}\phi, \sigma_k(x_2)\cdot\nabla_w f\right\rangle dW_t^j$$

Using the symmetry of exchanging $v\to w$, we can consider only one of the two sum and the other produce the same result. By Ito isometry formula for Ito integrals we have

$$\mathbb{E}\left[\langle \phi, f_Q - f\rangle^2\right] \le \varepsilon_N \sum_{k\in\Lambda_N}\int_0^t \mathbb{E}[\left\langle P'_{t-s}\phi, \sigma_k(x)\cdot\nabla_v f\right\rangle^2]ds$$

For the sake of notation we are going to indicate only the important variable in the computation for every function as $\xi = (x, y, v, w)$ and $\eta = (x', y', v', w')$.

$$\sum_{k\in K}\left\langle P'_{t-s}\phi, \sigma_k\cdot\nabla_v f\right\rangle^2 = \sum_{i,j=1}^{2}\iint_{\mathcal{D}^2}\iint_{\mathcal{D}^2} P'_{t-s}\phi(\xi)P'_{t-s}\phi(\eta)Q_{i,j}(x,x')\partial_{v_i}f(\xi)\partial_{v'_j}f(\eta)d\xi\, d\eta.$$

Recall know the definition of $\|\mathbb{Q}\|$, and the maximum principle for P'_t, i.e $\|P'_t\phi\|_\infty \le \|\phi\|_\infty$, we get

$$\begin{aligned}\sum_{k\in K}\left\langle P'_{t-s}\phi, \sigma_k\cdot\nabla_v f\right\rangle^2 &\le C\|\mathbb{Q}\|_{L^2\to L^2}\iint_{\mathcal{D}^2}\left|P'_{t-s}\phi(\xi)\nabla_v f(\xi)\right|^2 d\xi \\ &\le C\|\mathbb{Q}\|_{L^2\to L^2}\|\phi\|_\infty^2\iint_{\mathcal{D}^2}|\nabla f(\xi)|^2 d\xi.\end{aligned}$$

Using the energy estimate (thanks to the Stratonovich integration) and similar computation as in [6], theorem 2, we have

$$\int_0^\infty\iint_{\mathcal{D}^2}|\nabla f(\xi)|^2 d\xi dt \le C\iint_{\mathcal{D}^2}|f_0(\xi)|^2 d\xi.$$

If we put all together we get

$$\mathbb{E}\left[\left\langle f-\overline{f},\phi\right\rangle^2\right] \le C\,\|\mathbb{Q}\|_{L^2\to L^2}\,\|f_0\|_{L^2}.$$

which concludes the proof. □

Chapter 4

Homogeneous Smoluchowski equation with velocity

4.1 Introduction

Coagulation processes are ubiquitous in nature, from the movement of cells to the atmosphere, and in general complicated to understand experimentally and mathematically. In this work, we are motivated by the question whether a turbulent velocity field in the atmosphere enhances the coagulation of small rain droplets, and therefore favors rain fall. Physics literature on this topic has been vast, at least as early as Saffman-Turner [78] in the fifties, see also [25, 75, 80], arguing in favor of such coagulation enhancement. Here and in subsequent works, we give a novel approach to this problem that is fully mathematical. In particular, we take a kinetic viewpoint and study rigorously a variant of Smoluchowski's coagulation equation with velocity dependence that is akin to Boltzmann equation. It arises as the scaling limit of a system of second-order (microscopic) coagulating particles, modelling the interactions of rain droplets in the clouds, which are subjected to a common noise of transport type. Such a noise, constructed in recent mathematical works [42, 35], possesses several characteristics of real turbulence, such as it enhances diffusion of passive scalars. In the present work, we focus on the existence, uniqueness and regularity of this new PDE, after briefly introducing its origin.

Smoluchowski's classical equation [83] provides a first model for the time evolution of the probability distribution $\{f_m(t,x)\}_{m=1}^{\infty}$ of diffusing particles of different sizes (or masses) $m \in \mathbb{N}$, say in $\mathbb{T}^d := (\mathbb{R}/\mathbb{Z})^d$, when they undergo pairwise coagulation with certain coagulation rate $\alpha(m,n)$:

$$\begin{aligned}\partial_t f_m(t,x) = \Delta f_m(t,x) &+ \sum_{n=1}^{m-1} \alpha(n,m-n) f_n(t,x) f_{m-n}(t,x) \\ &-2\sum_{n=1}^{\infty} \alpha(m,n) f_m(t,x) f_n(t,x), \quad t>0,\, x\in\mathbb{T}^d,\, m\in\mathbb{N}.\end{aligned}$$

The nonlinearity has two parts, a gain term and a loss term. Such a system of equations has been derived from scaling limits of Brownian particle systems by Hammond-Rezakhanlou [48, 46]. To model the influence of a large-scale turbulent flow, it is natural

to introduce a common noise. If we adopt a transport noise of the type in [35]

$$\dot{\mathcal{W}}(t,x) = \sum_{k\in K} \sigma_k(x)\dot{W}_t^k$$

where $\{\sigma_k(x)\}_{k\in K}$ is a countable collection of divergence-free smooth vector fields and $\{W_t^k\}_{k\in K}$ independent one-dimensional Brownian motions, then we get a stochastic version of Smoluchowski's equation (an SPDE)

$$\begin{aligned} df_m(t,x) =& \Delta f_m(t,x)dt + \sum_{n=1}^{m-1} \alpha(n,m-n) f_n(t,x) f_{m-n}(t,x)dt \\ & -2\sum_{n=1}^{\infty} \alpha(m,n) f_m(t,x) f_n(t,x)dt - \sum_{k\in K} \nabla f_m(t,x)\cdot \sigma_k(x)\, dW_t^k \\ & + \mathsf{div}\left(\mathcal{Q}(x,x)\nabla f_m(t,x)\right), \quad m\in\mathbb{N} \end{aligned} \tag{4.1.1}$$

where $\mathcal{Q}(x,x) := \sum_{k\in K} \sigma_k(x)\otimes\sigma_k(x)$ coming from the transport-type noise. Under specific choice of $\{\sigma_k\}_{k\in K}$, we can have that $\mathcal{Q}(x,x)\equiv \kappa I_d$, for an enhanced diffusion coefficient $\kappa > 0$, the so-called "eddy diffusion" [15]. This picture, in its special case of finitely many mass levels $m = 1,2,...,M$ and unit coagulation rate $\alpha(m,n)\equiv 1$, has been derived from particle systems in [30]. Another version of the SPDE with continuous mass variables $m\in\mathbb{R}$ has also been derived from particle systems with mean-field interactions in [73].

However, conceptually and mathematically, the most difficult step in this program is to verify that diffusion enhancement leads to coagulation enhancement, namely, the fast increase of probability densities f_m for $m \gg 1$ (large masses) for large diffusion coefficient case. In fact, the model (4.1.1) turns out to be too crude, and even numerically we cannot verify a coagulation enhancement.

The problem lies in the fact that quick diffusion of masses may not lead to enhanced collision unless the coagulation rate depends on the velocity variable. Otherwise, the masses merely move around. We introduce a new system with both position and velocity variables. In the atmospheric physics literature, e.g. [25, 75, 80, 45], it is also common to consider cloud particles coagulate with a rate that is proportional to (when $d = 3$)

$$\alpha(m_1,m_2) := |v_1 - v_2|(r_1+r_2)^2$$

where v_i, $i = 1,2$ are the velocities of two colliding rain droplets and $r_i := m_i^{1/3}$, $i = 1,2$ their respective radius. Under certain simplifications, it leads to the following kinetic version of Smoluchowski's equation (cf. Appendix .1)

$$\begin{cases} \partial_t f_m(t,x,v) = -v\cdot\nabla_x f_m + c(m)\mathsf{div}_v\left(v f_m\right) + \kappa c(m)^2 \Delta_v f_m + Q_m(f,f) \\ f_m|_{t=0} = f_m^0(x,v), \quad m = 1,...,M, \end{cases} \tag{4.1.2}$$

where $(t,x,v)\in[0,T]\times\mathbb{T}^d\times\mathbb{R}^d$, and

$$\begin{aligned}&Q_m(f,f)(t,x,v)\\&:=\sum_{n=1}^{m-1}\iint_{\{nw'+(m-n)w=mv\}}s(n,m-n)f_n(t,x,w')f_{m-n}(t,x,w)|w-w'|dwdw'\\&\quad-2\sum_{n=1}^{M}\int s(n,m)f_m(t,x,v)f_n(t,x,w)|v-w|dw,\end{aligned}\tag{4.1.3}$$

where

$$c(m):=\alpha m^{(1-d)/d},\quad s(n,m):=(n^{1/d}+m^{1/d})^{d-1}.\tag{4.1.4}$$

In Appendix .1, we sketch the proof of the scaling limit from a coagulating microscopic particle system subjected to a common noise, to an SPDE that eventually gives rise to this PDE. Although it is not fully rigorous, it should justify the interest of this equation. Here again, turbulence contributes to large κ versus small κ when no turbulence. The eddy diffusion occurs now in the velocity variable.

The aim of our research is two-fold. Theoretically, we are interested in proving the well-posedness of the PDE and associated SPDE cf. (1.5.6), as well as the passage from the one to the other. Then, both theoretically and numerically we aim to demonstrate that the larger the κ, i.e. the more intense is the turbulence, the faster masses coagulate. See [31] for a first numerical study in this direction. In the present article, we focus on the PDE system (4.1.2) in the spatially-homogeneous case, i.e. by considering the initial conditions f_0^m constant in x for every m, we can reduce (4.1.2) to

$$\begin{cases}\partial_t f_m(t,v)=c(m)\mathsf{div}_v\left(vf_m(t,v)\right)+\kappa c(m)^2\Delta_v f_m(t,v)+Q_m(f,f)(t,v)\\ f_m|_{t=0}=f_m^0(v),\quad m=1,...,M,\end{cases}\tag{4.1.5}$$

where $(t,v)\in[0,T]\times\mathbb{R}^d$ and $Q_m(f,f)$ is as in (4.1.3) but without the x-dependence, and we prove existence, uniqueness and regularity of the solutions of (4.1.5), for every fixed $\kappa>0$.

Denote a weighted L^p space

$$L^p_k(\mathbb{R}^d):=\left\{f:\mathbb{R}^d\to\mathbb{R}\ \text{ s.t. }\ f\langle v\rangle^k\in L^p(\mathbb{R}^d)\right\},\quad p\in[1,\infty],\,k\in\mathbb{N},\tag{4.1.6}$$

where

$$\langle v\rangle:=\sqrt{1+|v|^2}$$

and a weighted Sobolev space

$$H^n_k(\mathbb{R}^d):=\left\{f\in L^2_k\ \text{ s.t. }\nabla^\ell f\in L^2_k(\mathbb{R}^d),\ \forall 1\le\ell\le n\right\}.\tag{4.1.7}$$

The main result of this article is as follows.

Theorem 4.1.1. *Fix any finite T and $\kappa > 0$. Suppose that initial conditions $f_m^0(v) \in (L^2 \cap L_2^1)(\mathbb{R}^d)$ and nonnegative, for every $m = 1, ..., M$, then there exists at least one nonnegative solution in the class $L^\infty \left([0,T]; L_2^1(\mathbb{R}^d)\right)^{\otimes M}$.*

If the initial conditions $f_m^0(v) \in (H_1^1 \cap L_2^1)(\mathbb{R}^d)$ and nonnegative, then there exists a unique nonnegative solution, and in this case $f_m(t) \in C_b^\infty(\mathbb{R}^d)$ for any $t > 0$.

The most difficult part in our opinion is uniqueness, due mainly to the presence of $|w - w'|$ in the nonlinear term, and the fact that the velocity variable $v \in \mathbb{R}^d$ is unbounded, hence in the presence of Laplacian, $f_m(t, v)$ is never compactly supported even if starting with so. These together with the fact that we have a system rather than just one equation, cause a severe difficulty in closing a Gronwall inequality for uniqueness. As far as we are able, the weighted L^1 space is the only one in which a Gronwall argument can work, even if one is willing to assume that solutions are Schwartz functions. (The problem is related to integrability rather than smoothness.) Indeed, with weighted L^1 we can find certain cancellations that remove those terms with higher weights brought by the kernel, and this seems not achievable with other spaces such as weighted L^2. Equally essential to this cancellation is considering the sum over the norms of all the densities f_m, $m = 1, .., M$, rather than treating them individually. Indeed, this is already essential to derive various apriori estimates.

On the other hand, existence is proved by constructing a family of approximating equations each corresponding to a truncation of the kernel $|w - w'|$ in the nonlinearity. These approximating problems are more amenable to study since the difficulty related to the kernel is no longer severe, for each fixed truncation parameter.

There is an unexpected connection to the vast area of Boltzmann equations [86]. Our (4.1.2) may be viewed as a Boltzmann-type equation with perfectly inelastic collision, rather than the classical elastic collision. Indeed, it is derived from particles undergoing pairwise coagulation, hence two particles merge into one based on the principle of conservation of momentum (and not energy). It is also local in nature in that the nonlinearity acts on the velocity variable, per (t, x). The closest works in the Boltzmann literature seem to be the ones on excited granular media, see [43] and references therein, and on multispecies Boltzmann equations, see [17] and references therein. In a sense our equation combines the features of both of them. From a technical point of view, the aforementioned difficulty with uniqueness are also present in [67, 43] and some references therein, and we have learned from these sources. On the other hand, there are various differences that set our model apart from these references. Since $M < \infty$, we do not have the conservation of mass and momentum, and we do not expect nontrivial stationary solutions – indeed all $f_m(t)$ should decay to zero as $t \to \infty$ (i.e. eventually all masses are transferred out of the system). In general, our nonliearity $Q_m(f, f)$ does not enjoy any particular kind of symmetry. Our derivation of the apriori estimates is also quite different, in particular we need not invoke entropy estimates and Povzner-type inequalities, as are standard in the Boltzmann literature.

Without loss of generality and simplifying notations, in the main part of the paper, we set $\kappa = 1$, $c(m) = 1$, $s(n, m) = 1$.

4.2 Deterministic Smoluchowski system with Velocity

4.2.1 Non-local Smoluchowski Equations

Recall our system of nonlinear integral-differential equations for $\{f_m(t,x,v)\}_{m=1}^M$ defined as:

$$\begin{cases} \partial_t f_m = -v\cdot\nabla_x f_m + \mathrm{div}_v\left(vf_m\right) + \Delta_v f_m + Q_m(f,f) \\ f_m|_{t=0} = f_m^0 \end{cases}, \quad m=1,...,M \tag{4.2.1}$$

where $(t,x,v)\in[0,T]\times\mathbb{T}^d\times\mathbb{R}^d$. The nonlinear term $Q_m(f,f)$, representing the masses interactions is given by (4.1.3). Since we expect the system to represent density of particles with different masses we take $f_m^0\geq 0, \forall\, m=1,...,M$.

We focus on the case when the initial condition is constant in the space variable x, and so this property pass to the solution of (4.2.1). We get a new set of equations solved by $f_m(t,v), m=1,...,M$, where we omit the subscript v in the derivatives in the sequel (since there is no ambiguity)

$$\begin{cases} \partial_t f_m = \mathrm{div}\left(vf_m\right) + \Delta f_m + Q_m(f,f) \\ f_m|_{t=0} = f_m^0 \end{cases}, \quad m=1,...,M \tag{4.2.2}$$

where $(t,v)\in[0,T]\times\mathbb{R}^d$ and $f_m^0\geq 0,\ \forall\, m$. By a change of variables

$$w' = \varphi(v,w) := \frac{mv-(m-n)w}{n},$$

the nonlinear term can be written as:

$$\begin{aligned} Q_m(f,f)(t,v) :=& \sum_{n=1}^{m-1}\iint_{\{nw'+(m-n)w=mv\}} f_n(t,w')f_{m-n}(t,w)|w-w'|dwdw' \\ &- 2\sum_{n=1}^{M}\int f_m(t,v)f_n(t,w)|v-w|dw \\ =& \sum_{n=1}^{m-1}\int f_n\left(t,\varphi(v,w)\right)f_{m-n}(t,w)\left(\frac{m}{n}\right)^2|v-w|dw \\ &- 2\sum_{n=1}^{M}\int f_m(t,v)f_n(t,w)|v-w|dw. \end{aligned}$$

We will consider the following notion of weak solutions to (4.2.2).

Definition 4.2.1 ($L_t^\infty L_v^1$-weak solution). *Fix $T>0$, and $f_m^0\in L_2^1\cap L^2$. A solution for equation (4.2.2) is a set of functions $f_m\in L^\infty(0,T;L_2^1(\mathbb{R}^d))$ indexed by the masses $m=1,...,M$ such that $\forall m,\ Q_m(f,f)\in L^\infty(0,T;L^1(\mathbb{R}^d))$ and the following holds:*

$$\sum_{m=1}^{M}\langle f_m(t),\phi\rangle - \sum_{m=1}^{M}\langle f_m^0,\phi\rangle = \int_0^t\sum_{m=1}^{M}\langle f_m(s),\Delta\phi\rangle\,ds$$

$$-\int_0^t \sum_{m=1}^{M} \langle f_m(s), v\cdot\nabla\phi\rangle\, ds + \int_0^t \sum_{m=1}^{M} \langle Q_m(f(s),f(s)),\phi\rangle\, ds,$$

for a.e. $t\in[0,T]$*, and* $\forall\phi\in C_c^\infty(\mathbb{R}^d)$.

4.2.2 A priori estimate and conserved quantities for system (4.2.2)

We prove for the system with finite number of masses a decay in time of the total mass and the conservation of such quantity in the infinite system.

Our first result is valid even in the system with space variable, hence we state it more generally.

Lemma 4.2.2. *Suppose that* $f_m^0(x,v)\in L^1(\mathbb{T}^d\times\mathbb{R}^d)$ *and* $\{f_m(t)\}_{m=1}^M$ *is a nonnegative solution of the equation* (4.2.1)*, such that* $f_m(t)$ *and its gradient* $\nabla f_m(t)$ *have a fast decay at infinity. Then if* $M<\infty$*, then the quantity*

$$\mathcal{T}(t) := \iint \sum_{m=1}^{M} m\, f_m(t,x,v)dxdv \tag{4.2.3}$$

is non-increasing in t*; if* $M=\infty$*, then it is constant in* t.

Remark 4.2.3. It is not clear how to relate the finite- and infinite-level systems. We only work with $M<\infty$. Since $t\mapsto\mathcal{T}(t)$ is decreasing in this case, we interpret $\mathcal{T}(0)-\mathcal{T}(t)$ as the amount of mass falling out of the system. It can be viewed as an indicator of how efficient the coagulation is (by transferring densities from small masses to large masses, see [31]).

Proof. Consider first the nonlinear part. For every fixed t,x we have that

$$\begin{aligned}
&\int \sum_{m=1}^{M} m\, Q_m(f,f)dv\\
&= \sum_{m=1}^{M}\sum_{n=1}^{m-1} m\int dv \iint_{\{nw+(m-n)w'=mv\}} f_n(t,x,w)f_{m-n}(t,x,w')|w-w'|dwdw'\\
&\quad - 2\sum_{m=1}^{M}\sum_{n=1}^{M} m\iint f_m(t,x,v)f_n(t,x,w)|v-w|dwdv\\
&= \sum_{m=1}^{M}\sum_{n=1}^{m-1} m\iint f_n(t,x,w)f_{m-n}(t,x,w')|w-w'|dwdw'\\
&\quad - 2\sum_{m=1}^{M}\sum_{n=1}^{M} m\iint f_m(t,x,v)f_n(t,x,w)|v-w|dwdv
\end{aligned}$$

Exchanging the order of summations in the first term, and setting $k=m-n$, the above equals

$$\sum_{n=1}^{M}\sum_{k=1}^{M-n}(k+n)\iint f_n(t,x,w)f_k(t,x,w')|w-w'|dwdw'$$

$$
\begin{aligned}
&- 2\sum_{m=1}^{M}\sum_{n=1}^{M} m \iint f_m(t,x,v) f_n(t,x,w)|v-w|dwdv \\
&\leq \sum_{n=1}^{M}\sum_{k=1}^{M}(k+n) \iint f_n(t,x,w) f_k(t,x,w')|w-w'|dwdw' \\
&- 2\sum_{m=1}^{M}\sum_{n=1}^{M} m \iint f_m(t,x,v) f_n(t,x,w)|v-w|dwdv = 0
\end{aligned}
$$

where equality is achieved if and only if $M = \infty$. For the linear part, we note that for every m, t, x we have that

$$
\int_{\mathbb{R}^d} \mathrm{div}_v \left(v f_m + \nabla_v f_m\right) dv = 0
$$

due to integration by parts and $|v f_m| + |\nabla_v f_m| \to 0$ as $|v| \to \infty$ for every fixed t, x. Also, for every m, t, v we have that

$$
\int_{\mathbb{R}^d} v \cdot \nabla_x f_m dx = 0
$$

due to integration by parts and $|f_m| \to 0$ as $|x| \to \infty$ for every fixed t, v. Thus we can conclude since $\mathcal{T}(t)$ (4.2.3) can be written as

$$
\begin{aligned}
\partial_t \mathcal{T} = \int_{\mathbb{R}^d}\int_{\mathbb{R}^d} \sum_{m=1}^{M} m\, \partial_t f_m(t,x,v) dxdv = -\sum_{m=1}^{M} m \iint v \cdot \nabla_x f_m dxdv \\
+ \sum_{m=1}^{M} m \iint \mathrm{div}_v \left(v f_m + \nabla_v f_m\right) dvdx + \iint \sum_{m=1}^{M} m\, Q_m(f,f) dvdx \leq 0
\end{aligned}
$$

with equality if and only if $M = \infty$. □

We specialize now to consider the spatially-homogeneous case, i.e. $f_m(t,x,v) = f_m(t,v)$ independent of $x \in \mathbb{T}^d$.

Recall the weighted L^p spaces $L^p_k(\mathbb{R}^d)$ (4.1.6) and we will indicate by $L^p_{k,M}$ the space in which the sequence $\{f_m(t)\}_{m=1}^M$ lives, with norm given by

$$
\|f\|_{p,M,k} := \sum_{m=1}^{M} \|f_m\|_{p,k} = \sum_{m=1}^{M} \left(\int |f_m(v)|^p \langle v \rangle^{pk} dv \right)^{1/p}.
$$

The reason we are going to introduce such spaces is motivated not only to understand the regularity of the solution of the system in study, but also to deal with the terms $|v-w|$ in the coagulation kernel since, as we have already noted in the explicit formulation of the nonlinearity $Q_m(f,f)$.

There are a few ways to control the norm of such a quantity, and we prove here the main estimates that we apply in all the a priori estimates for the equation.

Proposition 4.2.4. *For every $p \in [1, \infty]$ and $k \geq 0$, there exists a constant C depending only on p, k, M and the dimension d, such that we have the following bound on the nonlinearity*

$$\|Q_m(g,f)\|_{p,k} \leq C\left(\|g\|_{p,M,k+1}\|f\|_{1,M,k+1}\right)$$

and more general

$$\|Q(g,f)\|_{p,M,k} \leq MC\left(\|g\|_{p,M,k+1}\|f\|_{1,M,k+1}\right).$$

Proof. We prove this with a simple computation, using the duality of the norm for L^p spaces. For simplicity of notation during the proof we omit whenever is possible the appendix M on the norm. Fix $m \in \{1, ..., M\}$ and consider $Q_m(g,f)$ for $(g_n)_{n=1,...,M}$ and $(f_n)_{n=1,...,M}$:

$$\|Q_m(g,f)\|_{p,k} = \sup_{\phi \in L^{p'},\, \|\phi\|_{p'}=1} \int Q_m(g,f)\left\langle v\right\rangle^k \phi(v)dv,$$

where $1/p + 1/p' = 1$. We now work directly on each term of the summation in the nonlinearity both in the positive and negative part. For the negative part we have:

$$\begin{aligned}\iint g_m(v)f_n(w)|v-w|\left\langle v\right\rangle^k \phi(v)dwdv &\leq \iint g_m(v)f_n(w)\left\langle v\right\rangle^{k+1}\left\langle w\right\rangle \phi(v)dwdv \\ &= \|f_n\|_{1,1}\int g_m(v)\left\langle v\right\rangle^{k+1}\phi(v)dv \\ &\underbrace{\leq}_{\|\phi\|_{p'}=1} \|g_m\|_{p,k+1}\|f_n\|_{1,1} \leq \|g\|_{p,k+1}\|f\|_{1,k+1}.\end{aligned}$$

And now for the positive:

$$\begin{aligned}&\iint c_m^n g_n(h(v,w))f_{m-n}(w)|v-w|\left\langle v\right\rangle^k \phi(v)dwdv \\ &\lesssim \iint g_n(h)f_{m-n}(w)\left\langle v\right\rangle^{k+1}\left\langle w\right\rangle \phi(v)dwdv \\ &\underbrace{=}_{h(v,w)=z} \iint g_n(z)f_{m-n}(w)\left\langle \tilde{h}(z,w)\right\rangle^{k+1}\left\langle w\right\rangle \phi(\tilde{h})dwdv \\ &\leq \iint g_n(z)f_{m-n}(w)(\left\langle z\right\rangle^{k+1}\left\langle w\right\rangle + \left\langle w\right\rangle^{k+1})\phi(\tilde{h})dwdv \\ &= \iint g_n(z)f_{m-n}(w)\left\langle z\right\rangle^{k+1}\left\langle w\right\rangle \phi(\tilde{h})dwdv + \iint g_n(z)f_{m-n}(w)\left\langle w\right\rangle^{k+1}\phi(\tilde{h})dwdv \\ &= \int f_{m-n}(w)\int g_n(z)\left\langle z\right\rangle^{k+1}\phi(\tilde{h})dv\left\langle w\right\rangle dv + \int f_{m-n}(w)\left\langle w\right\rangle^{k+1}\int g_n(z)\phi(\tilde{h})dvdw \\ &\underbrace{\leq}_{\text{Hölder inequality}} \int f_{m-n}(w)\|\left\langle w\right\rangle \|g_n\|_{p,k+1}dv + \int f_{m-n}(w)\left\langle w\right\rangle^{k+1}\|g_n\|_p dw \\ &\underbrace{\leq}_{\text{Translation invariance}} 2\|g_n\|_{p,k+1}\|f_{m-n}\|_{1,k+1} \leq 2\|g\|_{p,k+1}\|f\|_{1,k+1}.\end{aligned}$$

Putting everything together we conclude the proof. □

We begin now proving the a priori estimates for the standard moments of regular enough solution to the system of coagulation equations.

Lemma 4.2.5. *For any $\ell \in \mathbb{N}$, suppose that $f_m^0 \in L^1_\ell$ and $\{f_m(t)\}_{m=1}^M$ is a nonnegative solution of the equation (4.2.2), such that $f_m(t)$ and its gradient $\nabla f_m(t)$ have a fast decay at infinity. Then, there exists some finite constant C_ℓ depending only on ℓ, d, and the initial data $\{f_m(0)\}_{m=1}^M$ such that for any $t \geq 0$,*

$$\sum_{m=1}^{M} \int |v|^\ell f_m(t,v)dv \leq C_\ell. \tag{4.2.4}$$

Proof. We first consider $\ell = 2k$ even, and prove by induction on $k \in \mathbb{N}$. The case $k = 0$ follows from Lemma 4.2.2. Now assume $k \geq 1$ and assume (4.2.4) is proved for the case $\ell = 2(k-1)$. Note that for each $m = 1, ..., M$, by (4.2.2)

$$\begin{aligned}
&\partial_t \int |v|^{2k} f_m(t,v)dv = \int |v|^{2k} \partial_t f_m(t,v)dv \\
=& \int |v|^{2k} \mathrm{div}_v \left(v f_m\right) dv + \int |v|^{2k} \Delta_v f_m dv \\
&+ \int dv \sum_{n=1}^{m-1} \iint_{\{nw+(m-n)w'=mv\}} |v|^{2k} f_n(t,w) f_{m-n}(t,w')|w-w'|dwdw' \\
&- 2\int dv \sum_{n=1}^{M} \int |v|^{2k} f_m(t,v) f_n(t,w)|v-w|dw \\
=& -2k \int |v|^{2k} f_m dv + 2k(2k+d-2) \int |v|^{2k-2} f_m dv \\
&+ \sum_{n=1}^{m-1} \iint \left|\frac{nw+(m-n)w'}{m}\right|^{2k} f_n(t,w) f_{m-n}(t,w')|w-w'|dwdw' \\
&- 2\sum_{n=1}^{M} \iint |v|^{2k} f_m(t,v) f_n(t,w)|v-w|dwdv.
\end{aligned}$$

Above, we assumed that for every $t > 0$,

$$|v|^{2k+1}|f_m| \to 0, \quad |v|^{2k}|\nabla_v f_m| \to 0, \quad \text{as } |v| \to \infty$$

such that the boundary terms vanish in the integration by parts. Summing the above in $m = 1, ..., M$ and noticing by Jensen's inequality

$$\begin{aligned}
\left|\frac{nw+(m-n)w'}{m}\right|^{2k} &\leq \left(\frac{n|w|+(m-n)|w'|}{m}\right)^{2k} \\
&\leq \frac{n}{m}|w|^{2k} + \frac{m-n}{m}|w'|^{2k} \leq |w|^{2k} + |w'|^{2k},
\end{aligned}$$

whenever $1 \leq n \leq m-1$, we obtain that

$$\partial_t \sum_{m=1}^{M} \int |v|^{2k} f_m(t,v)dv$$

$$
\begin{aligned}
&\leq -2k\sum_{m=1}^{M}\int |v|^{2k} f_m(t,v)dv + 2k(2k+d-2)\sum_{m=1}^{M}\int |v|^{2k-2} f_m(t,v)dv\\
&+\sum_{m=1}^{M}\sum_{n=1}^{m-1}\iint \left(|w|^{2k}+|w'|^{2k}\right) f_n(t,w) f_{m-n}(t,w')|w-w'|dwdw'\\
&-2\sum_{m=1}^{M}\sum_{n=1}^{M}\iint |v|^{2k} f_m(t,v) f_n(t,w)|v-w|dwdv\\
&\leq -2k\sum_{m=1}^{M}\int |v|^{2k} f_m(t,v)dv + 2k(2k+d-2)C_{2(k-1)}\\
&+\sum_{n=1}^{M}\sum_{m=n+1}^{M}\iint \left(|w|^{2k}+|w'|^{2k}\right) f_n(t,w) f_{m-n}(t,w')|w-w'|dwdw'\\
&-2\sum_{m=1}^{M}\sum_{n=1}^{M}\iint |v|^{2k} f_m(t,v) f_n(t,w)|v-w|dwdv,
\end{aligned}
$$

where we used the induction hypothesis that for some finite constant $C_{2(k-1)}$ independent of t,

$$
\sum_{m=1}^{M}\int |v|^{2k-2} f_m(t,v)dv \leq C_{2(k-1)}.
$$

Further, setting $\ell = m-n$ we see that

$$
\begin{aligned}
&\sum_{n=1}^{M}\sum_{m=n+1}^{M}\iint \left(|w|^{2k}+|w'|^{2k}\right) f_n(t,w) f_{m-n}(t,w')|w-w'|dwdw'\\
&-2\sum_{m=1}^{M}\sum_{n=1}^{M}\iint |v|^{2k} f_m(t,v) f_n(t,w)|v-w|dwdv\\
&\leq \sum_{n=1}^{M}\sum_{\ell=1}^{M-n}\iint \left(|w|^{2k}+|w'|^{2k}\right) f_n(t,w) f_{\ell}(t,w')|w-w'|dwdw'\\
&-2\sum_{m=1}^{M}\sum_{n=1}^{M}\iint |v|^{2k} f_m(t,v) f_n(t,w)|v-w|dwdv \ \leq 0.
\end{aligned}
$$

Thus we conclude that

$$
\partial_t \sum_{m=1}^{M}\int |v|^{2k} f_m(t,v)dv \leq -2k\sum_{m=1}^{M}\int |v|^{2k} f_m(t,v)dv + 2k(2k+d-2)C_{2(k-1)}.
$$

Assuming the initial data is such that

$$
A_0(k) := \sum_{m=1}^{M}\int |v|^{2k} f_m(0,v)dv
$$

is finite, it follows that for any $t \geq 0$ we have that

$$\sum_{m=1}^{M} \int |v|^{2k} f_m(t,v)dv \leq A_0(k)e^{-2kt} + (2k+d-2)C_{k-1}(1-e^{-2kt})$$
$$\leq A_0(k) + (2k+d-2)C_{2(k-1)} =: C_{2k}.$$

This completes the induction for $n = 2k$ even. Finally, we turn to the case $n = 2k-1$ for $k \geq 1$. Note that

$$\sum_{m=1}^{M} \int |v|^{2k-1} f_m(v)dv \leq \sum_{m=1}^{M} \int_{|v|\leq 1} |v|^{2k-1} f_m(v)dv + \sum_{m=1}^{M} \int_{|v|>1} |v|^{2k-1} f_m(v)dv$$
$$\leq \sum_{m=1}^{M} \int f_m(v)dv + \sum_{m=1}^{M} \int |v|^{2k} f_m(v)dv \leq C_0 + C_{2k}.$$

□

Remark 4.2.6. Call $A_k := \sum_{m=1}^{M} A_k^m := \sum_{m=1}^{M} \int f_m \langle v \rangle^k dv$ and consider $\int Q(f,f) \langle v \rangle^k dv$. Although we have used other properties, this quantity can be also expanded in the following way:

$$\int Q(f,f) \langle v \rangle^k dv \lesssim -2 \sum_{m=1}^{M} \sum_{n=M-n+1}^{M} \iint f_m(v) f_n(w) |v-w| \langle v \rangle^k dwdv$$

Using Proposition 4.2.4 and the modified triangular inequality: $-2|v-w| \langle v \rangle^k \leq -2 \langle v \rangle^{k+1} + 2|w| \langle v \rangle^k$, we get

$$\lesssim -2 \sum_{m=1}^{M} \sum_{n=M-n+1}^{M} \iint f_m(v) f_n(w) |v-w| \langle v \rangle^k dwdv \leq 2A_1 A_k - 2A_{k+1} C_k^M$$

where $C_k^M := \inf_t \int f_M(w)dw \geq 0$. This give us an equation for A_k of the form:

$$\frac{d}{dt} A_k \leq -2C_k^M A_{k+1} + C_k A_k (A_0 + A_1) + C_{k,k-1} A_{k-1})$$

Using the already proved bound on A_k and the aforementioned equation, integrating in time, is enough to show that moments of order $k \geq 2$ are controlled for $t_0 > 0$, however small, even if f_0 has not bounded moments of higher order.

We can prove also an a priori bound in $L_t^2 H_v^1 \cap L_t^\infty L_v^2$ of solutions of (4.2.2), under regularity assumption.

Lemma 4.2.7. *Suppose that $f_m^0 \in L_2^1 \cap L^2$ and $\{f_m(t)\}_{m=1}^M$ is a nonnegative solution of the equation (4.2.2), such that $f_m(t)$ and its gradient $\nabla f_m(t)$ have a fast decay at infinity. There exists some constant $C > 0$ depending on the initial data $\{f_m(0), \nabla f_m(0)\}_{m=1}^M$, $T < \infty$, $M < \infty$ such that*

$$\sup_{t\in[0,T]} \left(\sum_{m=1}^{M} \int f_m^2(t,v)dv + \int_0^t \int |\nabla f_m(s,v)|^2 dv\, ds \right) \leq C.$$

Proof. Note that for each $m = 1, ..., M$, by (4.2.1)

$$\begin{aligned}
&\frac{1}{2}\partial_t \int f_m^2(t,v)dv = \int f_m(t,v)\partial_t f_m(t,v)dv \\
&= \int f_m \mathsf{div}_v\left(vf_m\right)dv + \int f_m \Delta_v f_m dv \\
&+ \int dv \sum_{n=1}^{m-1} \iint_{\{nw+(m-n)w'=mv\}} f_m(t,v) f_n(t,w) f_{m-n}(t,w')|w-w'|dwdw' \\
&- 2\int dv \sum_{n=1}^{M} \int f_m(t,v) f_m(t,v) f_n(t,w)|v-w|dw \\
&= \frac{d}{2}\int f_m^2 dv - \int |\nabla f_m|^2 dv \\
&+ \sum_{n=1}^{m-1} \iint f_m\left(t, \frac{nw+(m-n)w'}{m}\right) f_n(t,w) f_{m-n}(t,w')|w-w'|dwdw' \\
&- 2\sum_{n=1}^{M} \iint f_m^2(t,v) f_n(t,w)|v-w|dwdv.
\end{aligned}$$

Here, we assumed that $|v\nabla_v f_m| \to 0$, as $|v| \to \infty$ for every t such that the boundary terms vanish in the integration by parts.

Further, we see that each term on the positive nonlinearity can be written using the Young's inequality has (same for v or w variable):

$$\begin{aligned}
&\iint f_m\left(t, \frac{nv+(m-n)w}{m}\right) f_n(t,v) f_{m-n}(t,w)|v|dvdw = \\
&\leq \int \left[\frac{1}{2}\left(\int f_m\Big(t, \frac{nv+(m-n)w}{m}\Big) f_n(t,v)|v|dv\right)^2 + \frac{1}{2} f_{m-n}(t,w)^2\right] dw \\
&= \int \frac{1}{2}\left(\int f_m\left(t, \frac{nv+(m-n)w}{m}\right) f_n(t,v)|v|dv\right)^2 dw + \frac{1}{2}\|f_{m-n}(t,w)\|_{L^2}^2
\end{aligned}$$

Thus we need to take care of the squared factor and we can do this using Jensen and normalizing respect the measure $(\int f_n(t,v)dv)^{-1} f_n(t,v)dv$, so that we obtain:

$$\begin{aligned}
&\int \frac{1}{2}\left(\int f_m\left(t, \frac{nv+(m-n)w}{m}\right) f_n(t,v)|v|dv\right)^2 dw \\
&\leq \frac{1}{2}C_0 \int\int f_m^2\left(t, \frac{nv+(m-n)w}{m}\right)|v|^2 f_n(t,v)dvdw \\
&= (A)
\end{aligned}$$

We have then, using translation invariance of Lebesgue measure:

$$\begin{aligned}
(A) &= \frac{1}{2}C_0 \int \left(\int f_m^2\left(t, \frac{nv+(m-n)w}{m}\right)dw\right) f_n(t,v)|v|^2 dv \\
&\lesssim \|f_m\|_{L^2}^2 \int |v|^2 f_n(t,v)dv \leq C_1\|f_m\|_{L^2}^2
\end{aligned}$$

where the constant $C_1 := C_1(M)$ depend also on M, using the moment bound Lemma 4.2.5 with $\ell = 2$, since we assumed that $f_m^0 \in L^1_2$.

We can repeat the same argument for the $|w|$ part. Thus we conclude that, erasing the negative term of the nonlinearity,

$$\partial_t \sum_{m=1}^{M} \int f_m^2(t,v)dv + \sum_{m=1}^{M} \int |\nabla f_m(t,v)|^2 dv \leq C(M,0,1,A) \sum_{m=1}^{M} \int f_m^2(t,v)dv$$

where $C(M,0,1,A) > 0$, and assuming the initial data is such that

$$C_1 := \sum_{m=1}^{M} \int |v|^2 f_m(0,v)dv,\ C_0 := \sum_{m=1}^{M} \int f_m(0,v)dv,\ C_l := \sum_{m=1}^{M} \int f_m^2(0,v)dv < \infty.$$

It follows that for any $t \in [0,T]$ we pass to integral form

$$\begin{aligned}
&\sum_{m=1}^{M} \int f_m^2(t,v)dv + \kappa c(m)^2 \int_0^t \sum_{m=1}^{M} \int |\nabla f_m(s,v)|^2 dv\, ds \\
&\leq C_l + C(M,0,1,A) \int_0^t \sum_{m=1}^{M} \int f_m^2(s,v)dvds \\
&\leq C_l + C(M,0,1,A) \int_0^t \left(\sum_{m=1}^{M} \int f_m^2(s,v)dv + \int_0^s \sum_{m=1}^{M} \int |\nabla f_m(r,v)|^2 dv\, dr \right) ds
\end{aligned}$$

From Gronwall's lemma, it follows:

$$\sup_{t\in[0,T]} \left(\sum_{m=1}^{M} \int f_m^2(t,v)dv + \int_0^t \sum_{m=1}^{M} \int |\nabla f_m(s,v)|^2 dv\, ds \right) \leq C_l\, e^{TC_{M,0,A,1}} \leq C(T) < \infty.$$

□

Remark 4.2.8. Consider the constant in the previous lemma on the right hand side of the Gronwall inequality and consider $C_T := \sup_{t\leq T} C_t < \infty$. Then from the lemma we can recover the following:

$$\partial_t \left(e^{-C_T t} \|f_t\|^2_{2,M} \right) + \int_0^t e^{-C_T t} \|f_s\|^2_{H^1,M} ds \leq 0$$

using Gronwall' lemma and using the property of sup and exponential, we have that exists $C := C_T e^{C_T T} < \infty$ depending only on the initial condition f_0 and not his gradient, such that:

$$\sup_{t\leq T} \|f_t\|^2_{2,M} + \int_0^t \|f_s\|^2_{H^1,M} ds \leq C.$$

□

Using the already proven a priori estimate and the bound on the nonlinearity we can also show an a priori bound on the solution in the weighted space $L^\infty_t(L^2_k)_v \cap L^2_t(H^1_k)_v$, noting also that $|v|^k \leq \langle v \rangle^k \leq 2^{k-1}(1 + |v|^k)$.

Lemma 4.2.9. *For every $k \in \mathbb{N}$, suppose that $f_m^0 \in L^1_{4k+2} \cap L^2_k$ and $\{f_m(t)\}_{m=1}^M$ is a nonnegative solution of the equation (4.2.2), such that $f_m(t)$ and its gradient $\nabla f_m(t)$ have a fast decay at infinity. Then there exists some constant $C > 0$ depending on the initial data $\{f_m(0), \nabla f_m(0)\}_{m=1}^M$, $T < \infty$, $M < \infty$ such that*

$$\sup_{t\in[0,T]} \left(\sum_{m=1}^{M} \int f_m^2(t,v)|v|^{2k} dv + \int_0^t \int |\nabla f_m(s,v)|^2 |v|^{2k} dv\, ds \right) \leq C.$$

Proof. We perform induction on $k \in \mathbb{N}$. The case $k = 0$ is proved in Lemma 4.2.7. Suppose that the thesis has been proved for the case $k-1$. Then, for each $m = 1, ..., M$, by (4.2.1)

$$\begin{aligned}
&\frac{1}{2}\partial_t \int |v|^{2k} f_m^2(t,v) dv = \int |v|^{2k} f_m(t,v) \partial_t f_m(t,v) dv \\
&= \int |v|^{2k} f_m \mathsf{div}_v \left(v f_m\right) dv + \int |v|^{2k} f_m \Delta_v f_m dv \\
&+ \int dv \sum_{n=1}^{m-1} \iint_{\{nw+(m-n)w'=mv\}} |v|^{2k} f_m(t,v) f_n(t,w) f_{m-n}(t,w') |w-w'| dw dw' \\
&- 2\int dv \sum_{n=1}^{M} \int |v|^{2k} f_m(t,v) f_m(t,v) f_n(t,w) |v-w| dw \\
&\leq (\frac{d}{2} - k) \int |v|^{2k} f_m^2 dv - \frac{1}{2} \int |v|^{2k} |\nabla f_m|^2 dv + 2k^2 \int |v|^{2k-2} f_m^2 dv \\
&+ \sum_{n=1}^{m-1} \iint \left| \frac{nw + (m-n)w'}{m} \right|^{2k} f_m \left(t, \frac{nw + (m-n)w'}{m} \right) f_n(t,w) f_{m-n}(t,w') |w-w'| dw dw' \\
&- 2\sum_{n=1}^{M} \iint |v|^{2k} f_m^2(t,v) f_n(t,w) |v-w| dw dv,
\end{aligned}$$

where we used Young's inequality

$$\begin{aligned}
-2k \int |v|^{2k-2} v \cdot \nabla f_m f_m dv &\leq 2k \int |v|^{2k-1} |\nabla f_m| f_m dv \\
&\leq \frac{1}{2} \int |v|^{2k} |\nabla f_m|^2 dv + 2k^2 \int |v|^{2k-2} f_m^2 dv
\end{aligned}$$

where we assumed that $|v|^{2k} |f_m \nabla f_m| \to 0$, $|v|^{2k+1} |f_m|^2 \to 0$, as $|v| \to \infty$ for every t such that the boundary terms vanish in the integration by parts.

Further, since

$$\left| \frac{nw + (m-n)w'}{m} \right|^{2k} (|w| + |w'|) \leq |w|^{2k+1} + |w'|^{2k+1} + |w|^{2k} |w'| + |w'|^{2k} |w|,$$

we see that each term on the positive nonlinearity can be written using the Young's inequality has (same for v or w variable):

$$\iint f_m \left(t, \frac{nv + (m-n)w}{m} \right) f_n(t,v) f_{m-n}(t,w) |v|^{2k+1} dv dw$$

$$\leq \int \left[\frac{1}{2}\Big(\int f_m\left(t, \frac{nv+(m-n)w}{m}\right) f_n(t,v)|v|^{2k+1}dv\Big)^2 + \frac{1}{2}\left(f_{m-n}(t,w)\right)^2\right] dw$$
$$= \int \frac{1}{2}\left(\int f_m\left(t, \frac{nv+(m-n)w}{m}\right) f_n(t,v)|v|^{2k+1}dv\right)^2 dw + \frac{1}{2}\|f_{m-n}(t,w)\|_{L^2}^2$$

Thus we need to take care of the squared factor and we can do this using Jensen and normalizing respect the measure $(\int f_n(t,v)dv)^{-1}f_n(t,v)dv$, so that we obtain:

$$\frac{1}{2}\left(\int f_m\left(t, \frac{nv+(m-n)w}{m}\right) f_n(t,v)|v|^{2k+1}dv\right)^2 dw$$
$$\leq \frac{1}{2}C_0 \int\int f_m^2\left(t, \frac{nv+(m-n)w}{m}\right)|v|^{4k+2} f_n(t,v)dvdw$$
$$= (A)$$

We have then, using translation invariance of Lebesgue measure:

$$(A) = \frac{1}{2}C_0 \int \left(\int f_m^2\left(t, \frac{nv+(m-n)w}{m}\right) dw\right) f_n(t,v)|v|^{4k+2}dv$$
$$\leq C_0\|f_m\|_{L^2}^2 \int |v|^{4k+2} f_n(t,v)dv \leq C_1\|f_m\|_{L^2}^2$$

where the constant $C_1 := C_1(M)$ depend also on M and comes from the momentum bound of f_m, Lemma 4.2.5 since we assumed that $f_m^0 \in L^1_{4k+2}$.

Similarly, we have another term

$$\iint f_m\left(t, \frac{nv+(m-n)w}{m}\right) f_n(t,v) f_{m-n}(t,w)|v|^{2k}|w|dw$$
$$\leq \int \frac{1}{2}\left(\int f_m\left(t, \frac{nv+(m-n)w}{m}\right) f_n(t,v)|v|^{2k}dv\right)^2 dw + \int \frac{1}{2}f_{m-n}^2(t,w)|w|^2dw$$
$$\leq C_0 \int \frac{1}{2}\int f_m^2\left(t, \frac{nv+(m-n)w}{m}\right) f_n(t,v)|v|^{4k}dvdw + \int \frac{1}{2}f_{m-n}^2(t,w)|w|^2dw$$
$$\leq C_0||f_m||_{L^2}^2 \int f_n(t,v)|v|^{4k}dv + \int \frac{1}{2}f_{m-n}^2(t,w)|w|^2dw$$
$$\leq C_1||f_m||_{L^2}^2 + \int \frac{1}{2}f_{m-n}^2(t,w)|w|^2dw.$$

Thus we conclude that, erasing the negative term of the nonlinearity and summing over $n = 1, ..., m-1$, using the induction hypothesis,

$$\partial_t \sum_{m=1}^M \int |v|^{2k} f_m^2(t,v)dv + \frac{1}{2}\sum_{m=1}^M \int |v|^{2k}|\nabla f_m(t,v)|^2dv$$
$$\leq C(M,0,1,A)\sum_{m=1}^M \int f_m^2(t,v)|v|^{2k}dv + C_B,$$

where $C(M,0,1,A), C_B > 0$, and assuming the initial data is such that

$$C_1 := \sum_{m=1}^M \int |v|^{4k+2} f_m(0,v)dv,\ C_0 := \sum_{m=1}^M \int f_m(0,v)dv \leq \infty$$

$$C_l := \sum_{m=1}^{M} \int |v|^{2k} f_m^2(0,v)dv < \infty$$

It follows that for any $t \in [0,T]$ we pass to integral form

$$\begin{aligned}
&\sum_{m=1}^{M} \int |v|^{2k} f_m^2(t,v)dv + \frac{1}{2}\int_0^t \sum_{m=1}^{M} \int |v|^{2k} |\nabla f_m(s,v)|^2 dv\, ds \\
&\leq C_{l,B} + C(M,0,1,A) \int_0^t \sum_{m=1}^{M} \int |v|^{2k} f_m^2(s,v) dv ds \\
&\leq C_{l,B} + C(M,0,1,A) \int_0^t \left(\sum_{m=1}^{M} \int |v|^{2k} f_m^2(s,v)dv + \int_0^s \sum_{m=1}^{M} \int |v|^{2k} |\nabla f_m(r,v)|^2 dv\, dr \right) ds
\end{aligned}$$

From Gronwall's lemma, it follows:

$$\begin{aligned}
&\sup_{t\in[0,T]} \left(\sum_{m=1}^{M} \int |v|^{2k} f_m^2(t,v)dv + \int_0^t \sum_{m=1}^{M} \int |v|^{2k} |\nabla f_m(s,v)|^2 dv\, ds \right) \\
&\qquad \leq C_{l,B}\, e^{TC_{M,0,A,1}} \leq C(T) < \infty.
\end{aligned}$$

□

We want to extend the inequality to higher derivatives and higher moments, to this end we consider the following proposition regarding the nonlinearity Q:

Proposition 4.2.10. *Let f, g smooth and rapidly decaying function in v at infinity, then*

$$\nabla Q_m(f,g) = Q_m(c_m^n \nabla f, g) + Q_m(f, c_m^n \nabla g),$$

for each $m = 1, .., M$.

Proof. First of all we split the nonlinearity into the positive and negative part and we change variables to get

$$\begin{aligned}
Q_m^+(f,g) &:= \sum_{n=1}^{m-1} \int \left(\frac{m}{n}\right)^2 f_n(\varphi(v,w)) g_{m-n}(w)|v-w|dw \\
&= \sum_{n=1}^{m-1} \int \left(\frac{m}{n}\right)^2 f_n(\tilde{\varphi}(v,w)) g_{m-n}(\theta(v,w))|w|dw \\
Q_m^-(f,g) &:= \sum_{n=1}^{M} f_m(v) \int g_n(w)|v-w|dw = \sum_{n=1}^{M} f_m(v) \int g_n(\theta(v,w))|w|dw,
\end{aligned}$$

where we have set

$$\varphi(v,w) := \frac{mv-(m-n)w}{n}, \quad \theta(v,w) := v+w, \quad \tilde{\varphi}(v,w) := v - \frac{m-n}{n}w.$$

Whit this we can use the differentiation under integral sign and since the dependence on v is only on f and g we have

$$\nabla_v \left(\int f_n(\tilde{\varphi}(v,w)) g_{m-n}(\theta(v,w))|w|dw \right)$$
$$= \int \left(\nabla_v f_n(\tilde{\varphi}(v,w))\right) g_{m-n}(\theta(v,w))|w|dw + \int f_n(\tilde{\varphi}(v,w)) \nabla_v g_{m-n}(\theta(v,w))|w|dw.$$
$$\nabla_v \left(f_m(v) \int g_n(w)|v-w|dw \right) = \nabla_v \left(f_m(v) \int g_n(\theta(v,w))|w|dw \right) =$$
$$= \nabla_v f_m(v) \int g_n(\theta(v,w))|w|dw + f_m(v) \int \nabla_v g_n(\theta(v,w))|w|dw.$$

Taking out the constant in the differentiation, depending only on m and n, and summing all together we conclude the proof. □

Remark 4.2.11. As a corollary, iterating Proposition 4.2.10, higher-order derivatives of Q can be calculated using the following formula:

$$\partial^j Q(f,g) = \sum_{0 \le l \le j} \binom{j}{l} Q_m \left(c_{m,n} \partial^{j-l} f, c_{m,n} \partial^l g \right)$$

where j is a multi-index $|j| = n$ such that $j = j_1 ... j_d$ (with indices possibly being zeroes) and

$$\partial^j := \partial_{v_1}^{j_1} ... \partial_{v_d}^{j_d}.$$

The factor $\binom{j}{l}$ is a multinomial coefficients and the sum is intended in the sense of ordering of multi-indices.

With this in mind we are able to state the following a priori estimate on the space H_k^n for all $k, n \in \mathbb{N}$, defined in (4.1.7) equipped with the norm $\|f\|_{H_k^n} := \left(\sum_{0 \le |j| \le n} \|\partial^j f\|_{2,k}^2 \right)^{1/2}$.

Lemma 4.2.12. *Suppose that $\{f_m\}_{m=1}^M$ is a nonnegative solution of the equation (4.3.1), such that f_m is regular enough. For all $n \in \mathbb{N},\ k \in \mathbb{N}$, there exists some constant $C > 0$ depending on the initial data $\{f_m(0)\}_{m=1}^M$, $T < \infty$, $M < \infty$, n, k such that*

$$\sup_{t \in [0,T]} \left(\sum_{m=1}^M \|f_m\|_{H_k^n}^2 \right) \le C.$$

Proof. We work by induction. We know form previous lemma that $n = 0, 1$ we have already proven the a priori bound. Now we suppose that for every $p < n$ it's true that $f \in H_k^p$ for all k, and we prove that $f \in H_k^n$ for all k. To this end, we consider a multi index $j, |j| = n$ and the quantity $\partial^j f_m$. Using the equation for f_m we get

$$\partial_t \left(\partial^j f_m \right) = \Delta \left(\partial^j f_m \right) + \operatorname{div} \left(v \partial^j f_m \right) + C_j \left(\partial^j f_m \right) + \sum_{0 \le l \le j} \binom{j}{l} Q_m \left(\partial^{j-l} f, \partial^l f \right)$$

where C_j is either 0 or 1 depending if the multi index has the i-th component of the derivative of $\sum_{i=1}^{d} \partial^j (\partial_i f_m v_i)$. We now consider the quantity

$$\sum_{m=1}^{M} \int |\partial^j f_m|^2 \langle v \rangle^{2k} \, dv$$

and derivate in time we have for each m:

$$\begin{aligned}
\frac{1}{2}\partial_t \int \langle v \rangle^{2k} |\partial^j f_m|^2(t,v) dv &= \int \langle v \rangle^{2k} \partial^j f_m(t,v) \partial_t \partial^j f_m(t,v) dv \\
&= \int \langle v \rangle^{2k} \partial^j f_m \mathsf{div} \left(v \partial^j f_m \right) dv + \int \langle v \rangle^{2k} \partial^j f_m \Delta(\partial^j f_m) dv + \\
&+ \int C_j \langle v \rangle^{2k} |\partial^j f_m|^2 dv + \sum_{0 \le l \le j} \int Q_m(\partial^{j-l} f, \partial^l f) \partial^j f_m \langle v \rangle^{2k} dv \\
&\le \frac{d}{2} \int \langle v \rangle^{2k} |\partial^j f_m|^2 dv - k \int \langle v \rangle^{2k-2} |\partial^j f_m|^2 dv + \\
&+ k \int \langle v \rangle^{2k} |\partial^j f_m|^2 dv - k \int \langle v \rangle^{k-2} |v| |\partial^j f_m|^2 dv + \\
&- \int |\nabla(\partial^j f_m)|^2 \langle v \rangle^{2k} dv + \sum_{0 \le l \le j} \int Q_m(\partial^{j-l} f, \partial^l f) \partial^j f_m \langle v \rangle^{2k} dv \\
&\le C'_{d,k} \int \langle v \rangle^{2k} |\partial^j f_m|^2 dv - \int |\nabla(\partial^j f_m)|^2 \langle v \rangle^{2k} dv + \\
&+ \underbrace{\sum_{0 \le l \le j} \int Q_m(\partial^{j-l} f, \partial^l f) \partial^j f_m \langle v \rangle^{2k} dv}_{A} .
\end{aligned}$$

We miss to understand now the nonlinearity. To this end we consider:

$$\|Q_m(f,g)\|_2 \le C \left(\sum_{n=1}^{m-1} \|f_{m-n}\|_{2,k+1} \|g_n\|_{1,k+1} + \|f_m\|_{1,k+1} \sum_{n=1}^{M} \|g_n\|_{2,k+1} \right).$$

In particular we have:

$$\begin{aligned}
&\sup_{\|\phi\|_2=1} \iint C_{m,n} f_n(h(v,w)) f_{m-n}(w) |v-w| \phi(v) dv dw \\
&\le \sup_{\|\phi\|_2=1} \iint C'_{m,n} f_n(z)) f_{m-n}(w) |z-w| \phi(h'(z,w)) dz dw \\
&\lesssim \begin{cases} \sup_{\|\phi\|_2=1} \int \int f_{m-n}(w) \phi(h'(z,w)) \langle w \rangle \, dw f_n(z)) \langle z \rangle \, dz \le C_{n,m} \|f_n\|_{2,1} \|f_{m-n}\|_{1,1} \\ \sup_{\|\phi\|_2=1} \int \int f_n(z)) \phi(h'(z,w)) \langle z \rangle \, dz f_{m-n}(w) \langle w \rangle \, dw \le C_{n,m} \|f_{m-n}\|_{2,1} \|f_n\|_{1,1}. \end{cases}
\end{aligned}$$

With this, in particular, we can select where to put the norm and the weight depending on the index of the derivative and we get summation of quantity that depends on lower order in H^p_k with $p < n$ and a quantity depending on ∂^j.

$$\sum_{0 \le l \le j} \int Q_m(\partial^{j-l} f, \partial^l f) \partial^j f_m \langle v \rangle^{2k} dv \le \int Q_m(\partial^j f, f) \partial^j f_m \langle v \rangle^{2k} dv$$

$$+\int Q_m(f,\partial^j f)\partial^j f_m \langle v\rangle^{2k} dv + \sum_{1\le l\le j-1}\int Q_m(\partial^{j-l}f,\partial^l f)\partial^j f_m \langle v\rangle^{2k} dv$$
$$\le C_{m,n}(k,M)\sum_{m=1}^{M}\|\partial^j f_m\|^2_{2,k+\mu}.$$

Now we note that:

$$\begin{aligned}\|\partial^j f_m\|^2_{2,k+\mu} &\le \delta\|\nabla\partial^j f_m\|_2^2 + c_\delta\|\partial^{j-1}f_m\|^2_{2,2(k+\mu)}\\ &\le \delta\|\nabla\partial^j f_m\|^2_{2,2k} + c_\delta\|\partial^{j-1}f_m\|^2_{2,2(k+\mu)}\\ &\le \delta\|\nabla\partial^j f_m\|^2_{2,2k} + C_{\delta,M,n-1}.\end{aligned}$$

We put together all the estimate and we get:

$$\frac{1}{2}\partial_t\sum_{m=1}^{M}\int\langle v\rangle^{2k}|\partial^j f_m|^2(t,v)dv - C'_{M,d,k}\sum_{m=1}^{M}\int\langle v\rangle^{2k}|\partial^j f_m|^2 dv \le$$
$$-\sum_{m=1}^{M}\int|\nabla(\partial^j f_m)|^2\langle v\rangle^{2k}dv + \delta C(k,M)\sum_{m=1}^{M}\int|\nabla(\partial^j f_m)|^2\langle v\rangle^{2k}dv + C_M(n-1,k)$$

Taking δ small enough, up to constant $C_\delta(M,k,n-1)$ we obtain

$$\frac{1}{2}\partial_t\sum_{m=1}^{M}\int\langle v\rangle^{2k}|\partial^j f_m|^2(t,v)dv - C'_{M,d,k}\sum_{m=1}^{M}\int\langle v\rangle^{2k}|\partial^j f_m|^2 dv \le C_\delta(M,k,n-1).$$

Thanks to Gronwall's lemma we conclude the proof. □

With all this a priori estimates follow also estimates on the L^2_k norm of the solution. At the level of the a priori estimate, Lemmas 4.2.12 and 4.2.7 guarantee us that we have a bound for every $T>0$ on the derivatives in $L^2([0,T]\times\mathbb{R}^d)$ implying that after a arbitrary short time the derivatives $\partial^n f_m(t)\in L^2(\mathbb{R}^d)$ for any n and thus they propagate in time. On the level of a priori estimates the solution results to be immediately infinitely smooth in v and decay faster than any negative power of $|v|$ at infinity.
Using the a priori regularity in H^n_k and the aforementioned propagation, we note that for every $t>0$ and $m=1,...,M$, $f_m(t)$ is in fact a Schwartz function for $\forall t$ and this decay is enough to get that $\partial_t f\in L^2([0,T]\times\mathbb{R}^d)$.

4.3 Approximating Problems and preliminary

We define a sequence of approximating problems, indexed by $R>0$, in the following way:

$$\begin{cases}\partial_t f^R_m = \text{div}\left(v f^R_m\right) + \Delta f^R_m + Q^R_m(f^R,f^R)\\ f^R_m|_{t=0} = f^0_m\end{cases}, \quad m=1,...,M \tag{4.3.1}$$

where $(t,v) \in [0,T] \times \mathbb{R}^d$ and $f_m^0, \forall m = 1,...,M$ are the same as (4.2.2). The approximated nonlinear term is expressed as follows:

$$\begin{aligned} Q_m^R(f,f)(t,v) &:= \sum_{n=1}^{m-1} \chi_R(v) \iint_{\{nw+(m-n)w'=mv\}} f_n(t,w) f_{m-n}(t,w')|w-w'|\chi_R(w)dwdw' \\ &\quad - 2\sum_{n=1}^{M} \chi_R(v) \int f_m(t,v) f_n(t,w)|v-w|\chi_R(w)dw \\ &= \sum_{n=1}^{m-1} \chi_R(v) \int f_n\Big(t,\varphi(v,w)\Big) f_{m-n}(t,w)|v-w|\big(\frac{m}{n}\big)^2\chi_R(w)dw \\ &\quad - 2\sum_{n=1}^{M} \chi_R(v) \int f_m(t,v) f_n(t,w)|v-w|\chi_R(w)dw \end{aligned}$$

where $\chi_R(z) := \chi_{\mathbb{B}(0,R)}(z)$ is the indicator function on the ball of radius $R > 0$ centered at the origin in $\mathbb{R}^d$.

4.3.1 A priori estimate for the approximating equations

We start with the same a priori estimate for the moments and energy, under the same regularity assumption of (4.2.2), that we'll verify once existence and uniqueness is shown. We suppose that $f_m^0 \geq 0, \ \forall \ m = 1,..,M$, the solution of (4.3.1) is nonnegative and regular enough and has a fast decay at infinity, then we have for the nonlinear term:

$$\begin{aligned} &\chi_R(v) \int f_n\Big(t,\varphi(v,w)\Big) f_{m-n}(t,w)|v-w|\chi_R(w)dw \\ &\leq \int f_n\Big(t,\varphi(v,w)\Big) f_{m-n}(t,w)|v-w|dw \end{aligned}$$

And thus we can recover the same a priori estimates, as in Lemmas 4.2.5, 4.2.7, 4.2.9, 4.2.12, on the total mass, moments and energy in both H^1 and H_k^n for the approximated problems with the same constant independent of R.

Lemma 4.3.1. *For any $\ell \in \mathbb{N} \cup \{0\}$, there exists some finite constant C_ℓ depending only on n, d and the initial data $\{f_m(0)\}_{m=1}^M$ such that*

$$\sum_{m=1}^{M} \int |v|^\ell f_m^R(t,v)dv \leq C_\ell, \quad \forall R,$$

as soon as $\{f_m^R\}_m \in L^2$.

Lemma 4.3.2. *As soon as $\{f_m^R\}_m$ is regular enough, there exists some constant $C > 0$ depending on the initial data $\{f_m(0), \nabla f_m(0)\}_{m=1}^M$, $T < \infty$, $M < \infty$ such that*

$$\sup_{t\in[0,T]} \left(\sum_{m=1}^{M} \int |f_m^R(t,v)|^2 dv + \int_0^t \int |\nabla f_m^R(s,v)|^2 dv\, ds \right) \leq C.$$

The constant C does not depend on R and is the same as the one in the full problem.

Lemma 4.3.3. *As soon as $\{f_m^R\}_m$ is regular enough, $\forall k \geq 0$, there exists some constant $C > 0$ depending on the initial data $\{f_m(0), \nabla f_m(0)\}_{m=1}^M$, $T < \infty$, $M < \infty$ such that*

$$\sup_{t\in[0,T]} \left(\sum_{m=1}^{M} \int |f_m^R(t,v)|^2 |v|^{2k} dv + \int_0^t \int |\nabla f_m^R(s,v)|^2 |v|^{2k} dv\, ds \right) \leq C.$$

The constant C does not depend on R and is the same as the one in the full problem.

Lemma 4.3.4. *Suppose that $\{f_m^R\}_{m=1}^M$ is a nonnegative solution of the equation (4.3.1), such that f_m^R is regular enough. For all $n \in \mathbb{N}$, $k \in \mathbb{N}$, there exists some constant $C > 0$ depending on the initial data $\{f_m(0)\}_{m=1}^M$, $T < \infty$, $M < \infty$, n, k such that*

$$\sup_{t\in[0,T]} \left(\sum_{m=1}^{M} \|f_m^R\|_{H_k^n}^2 \right) \leq C.$$

The constant C does not depend on R and is the same as the one in the full problem.

4.3.2 Preliminary on semigroups

We want to construct mild solution for our approximated problems. With this in mind, we define the following operator on function defined on $\mathbb{R}^d$:

$$\mathcal{L}f := \Delta f + v \cdot \nabla f,$$

and rewrite our system of equations as:

$$\begin{cases} \partial_t f_m^R - \mathcal{L} f_m^R = d f_m^R + Q_m^R(f^R, f^R) \\ f_m^R|_{t=0} = f_m^0 \end{cases} \quad , \quad m = 1, ..., M$$

with the usual definition of space, time and initial condition.

We know, [66], that endowed with its maximal domain

$$D_{p,max}(\mathcal{L}) := \left\{ u \in L^p(\mathbb{R}^d) \cap W^{2,p}_{loc}(\mathbb{R}^d) : \ \mathcal{L}u \in L^p(\mathbb{R}^d) \right\}$$

the operator $\mathcal{L}$ is the generator of a strongly continuous semigroup $(P_t)_{t\geq 0}$ in $L^p(\mathbb{R}^d)$. In particular we can characterize the domain of the operator as follow:

Lemma 4.3.5 ([66, Theorem 1])**.** *The domain $D_{p,max}(\mathcal{L})$ of the generator of the semigroup $(P_t)_{t\geq 0}$ coincides with:*

$$D_p(\mathcal{L}) := \left\{ u \in W^{2,p}(\mathbb{R}^d) : \ v \cdot \nabla u \in L^p(\mathbb{R}^d) \right\}.$$

Fur such a semigroup $(P_t)_{t\geq 0}$, one can derive the following properties [66, Theorem 3.3].

Proposition 4.3.6. *The operator $(\mathcal{L}, D_{p,max}(\mathcal{L}))$ generates a semigroup $(P_t)_{t\geq 0}$ in $L^p(\mathbb{R}^d)$ which satisfies the estimate*

$$\|P_t f\|_p \leq \|f\|_p$$

for every $f \in L^p(\mathbb{R}^d)$.

Proposition 4.3.7. *For every $f \in L^p(\mathbb{R}^d)$ and $T > 0$, the function $P(\cdot)f$ belongs to $C((0,T], W^{2,p}(\mathbb{R}^d)) \cap C^1((0,T], L^p_{loc}(\mathbb{R}^d))$, and satisfies the estimates for $t \in (0,T]$,*

$$\|D^2 P_t f\|_p \leq \frac{C_T}{t}\|f\|_p,\ \|\nabla P_t f\|_p \leq \frac{C_T}{\sqrt{t}}\|f\|_p.$$

Proposition 4.3.8. *Let $T > 0$ and $g \in C([0,T], L^p(\mathbb{R}^d))$ be given, and consider the mild solution u of the Cauchy problem*

$$\begin{cases} \partial_t u - \mathcal{L}u = g & in\ [0,T] \times \mathbb{R}^d \\ u(0) = f & in\ \mathbb{R}^d, \end{cases}$$

with $f = 0$. Then, u belongs to $C([0,T], W^{2,p}(\mathbb{R}^d)) \cap W^{1,p}_{loc}([0,T] \times \mathbb{R}^d)$.

Thus, we can define the notion of mild solution for our system. For simplicity of notation we omit the dependence on m.

Definition 4.3.9 (L^2_v-mild solution for approximated problems)**.** *We rewrite first our approximated problems as an evolution equation in L^p space*

$$\dot{f} + \mathcal{L}f = df + Q(f,f),\ t > 0\ f(0) = f^0.$$

Fix $T > 0$, a function $f \in C([0,T], L^2)$ is said to be a L^2-mild solution to (4.3.1) on $[0,T]$ if f solves the integral equation

$$f(t) = P_t f^0 + \int_0^t P_{t-s}\left(df(s) + Q(f(s), f(s))\right) ds,\ t \in [0,T].$$

4.3.3 Aubin-Lions' Theorem in full Space

Lemma 4.3.10 (Aubin-Lions weighted)**.** *Consider $H^1(\mathbb{R}^d)$, the usual Sobolev space, and $L^2(\mathbb{R}^d, |v|^2 dx)$, the weighted Lebesgue space containing functions f for which $\int |f|^2|v|^2 dv < \infty$. Then*

$$H^1(\mathbb{R}^d) \cap L^2(\mathbb{R}^d, |v|^2 dv) \subset\subset L^2(\mathbb{R}^d)$$

and the embedding is compact. As a consequence for every $q, k \geq 1$ we have that

$$L^p\left(0,T; H^1(\mathbb{R}^d) \cap L^2(\mathbb{R}^d, |v|^2 dv)\right) \cap W^{1,q}(0,T; H^{-k}(\mathbb{R}^d)) \subset\subset L^p(0,T; L^2(\mathbb{R}^d))$$

for $p \in [1,\infty]$ and the embedding is compact.

Proof. Call $X := H^1(\mathbb{R}^d) \cap L^2(\mathbb{R}^d, |v|^2 dv)$ and consider $Y \subset X$ a bounded set.
We claim that $\forall \varepsilon > 0, \exists N > 0$ such that for all $f \in Y$:

$$\int_{B_N^c} f^2 < \varepsilon/2,$$

Where B_N^c is the complement in $\mathbb{R}^d$ of the ball of radius N and centered at the origin. Otherwise, assume this is not the case, then for some $\varepsilon > 0$, for every $N > 0$ there is some $f \in Y$ such that $\|f\|_{L^2(B_N^c)} \geq \varepsilon$.

This implies that $\|f\|_X \geq \|f^2|v|^2\|_{L^1(B_N^c)} \geq N^2\varepsilon$ so that the set Y is not bounded, and this contradicts the hypotheses. So we consider the ball B_N and we can apply Rellich-Kondrachov theorem to ensure the compact embedding to $L^2(B_N)$.
Now we recall that compactness of a set $A \subset X$ means that $\forall \varepsilon > 0$ we find $f_1, ..., f_k \in X$, where $k = k(\varepsilon)$, such that $A \subset \cup_{i=1}^k B(f_i, \varepsilon)$.
This means that $\forall \varepsilon > 0$ we find functions $f_1, ..., f_k \in L^2(B_N),\ k = k(\varepsilon)$, such that $\forall f \in Y$ we have some f_j such that

$$\|f - f_j\|_{L^2(B_N)} < \varepsilon/2$$

We recall then that $\|f\|_{L^2(B_N^c)} < \varepsilon/2$, so we even have $\|f - f_j\|_{L^2(\mathbb{R}^d)} < \varepsilon$, which implies the compact embedding $Y \subset\subset L^2(\mathbb{R}^d)$.
The second part of the theorem now follows from the usual Aubin-Lions Theorem cf. [82, Corollary 5], thus concluding the proof. □

4.4 Existence and Uniqueness for the approximating problems

Theorem 4.4.1 (Existence and Uniqueness). *Consider $d \geq 1$. Given any initial value $f_m^0 \in L^2, \forall m = 1, ..., M$, problem (4.3.1) possesses a unique maximal L^2-mild solution $f := f(\cdot; f^0)$ on $[0, T(f^0))$. The maximal interval is such that $[0, T(f^0))$ is an open interval in $\mathbb{R}_+$. In addition,*

$$f \in L^\infty([0, T(f^0)), L^2(\mathbb{R}^d)^{\otimes M}) \cap W^{1,2}_{loc}((0, T(f^0)), H^2(\mathbb{R}^d)^{\otimes M}).$$

In addition: if $T(f^0) < \infty$, then

$$\sup_{T(f^0)/2 < t < T(f^0)} \|f_t\|_2 = \infty.$$

Proof. Let $T_0 > 0$ be arbitrary and define $X_T := L^\infty([0, T], L^2_M)$ for $T \in (0, T_0]$, where we endowed the space with the usual sup norm in time and L^2_M norm in velocity as $\|f\|_{L^2_M} := \sum_{m=1}^M \|f_m\|_{L^2}$.
Consider $f^0 \in L^2_M$ then from Proposition 4.3.7 we know that $P_t f^0 \in X_T$. From the same theorem it is implied that exist a constant $\kappa := \kappa(T_0) > 0$ such that $\|P_t f^=\| \leq e^\kappa(T_0)t$; we show that this is enough to define a map Γ from $X_T \to X_T$, given by

$$\Gamma(f) := P_\cdot f^0 + \int_0^\cdot P_{\cdot - s}(df - Q^R(f, f))ds,\ f \in X_T.$$

First, thanks to the estimate on the semigroup and the property of the truncated nonlinearity, we have that, as soon as $f \in X_T$

$$\begin{cases} \|Q_m^R(f, f)\|_2^2 \leq C_R(\sum_{m=1}^M \|f_m\|_2)^2 < \infty. \\ \int_0^\cdot P_{\cdot - s}(df - Q^R(f, f))ds \in X_T. \end{cases}$$

In particular we obtain the first estimate from the following computation on each of the terms of the nonlinearity

$$\int \left| \int |v - w|_R f_n(h(v, w)) f_{m-n}(w) dw \right|^2 dv$$

$$\leq 2R \int_{B_R} \|f_n\|_2^2 \|f_{m-n}\|_2^2 dv = 2R|B_R| \|f_n\|_2^2 \|f_{m-n}\|_2^2.$$

Now we notice that the function Γ also satisfies

$$\begin{aligned}\|\Gamma(f) - P_\cdot f^0\|_{X_T} &= \left\| \int_0^\cdot P_{\cdot - s}(df - Q^R(f,f))ds \right\|_{X_T} \\ &\leq \kappa T \left(d + C_R(\sum_{m=1}^M \|f_m\|_2) \right) (\sum_{m=1}^M \|f_m\|_2),\end{aligned}$$

for all $f \in X_T$. And we can prove the continuity of the map

$$\begin{aligned}\|\Gamma(f) - \Gamma(g)\|_{X_T} &= \left\| \int_0^\cdot P_{\cdot - s}(d(f-g) + \left(Q^R(g,g) - Q^R(f,f)\right) ds \right\|_{X_T} \\ &\leq T \left(d + C_R\|f\|_{X_T} + C_R\|g\|_{X_T}\right) \|f - g\|_{X_T},\end{aligned}$$

for all $f, g \in X_T$.
If we find a way to restrict the mapping Γ to some closed subset, and prove that it is a contraction then, with a standard fix point argument, we conclude local existence and uniqueness for each approximating problems.
Consider to this extent the norm of the initial condition $\|P_\cdot f^0\|_{X_T} = \gamma$, we choose the ball in X_T, call it B_T, centered in $P_\cdot f^0$ with radius γ. So that every function $f \in B_T$ as norm $\|f\|_{X_T} \leq 2\gamma$. Then selecting

$$T < \min\left\{ \frac{1}{d + 4C_R\gamma}, \frac{1}{\kappa(d + C_R 2\gamma)} \right\}$$

The two inequality implies that the map Γ send function in B_T to itself and it is a contraction. Therefore there exist a unique $\tilde{f} \in B_T$ such that $\Gamma(\tilde{f}) = \tilde{f}$, that is,

$$\tilde{f} \in L^\infty([0,T], L^2_M) \text{ and } \tilde{f} = P_\cdot f^0 + \int_0^\cdot P_{\cdot - s}\left(d\tilde{f} + Q^R(\tilde{f}, \tilde{f})\right) ds.$$

and $\tilde{f}$ is a mild-L^2 solution to the approximated problems.

Clearly we can extend the solution $\tilde{f}$ to a unique maximal solution $\tilde{f} := \tilde{f}(f^0)$ with maximal interval $[0, T(f^0))$ that must be open in $\mathbb{R}^+$.
Consider $T^0 := T(f^0) < \infty$ and suppose there exist an increasing sequence $t_i \to T^0$ such that $\|f_{t_i}\|_p \leq r < \infty$, $\forall i \in \mathbb{N}$. Fix now $\overline{T} > T^0$ and fix $\gamma(\overline{T})$ the constant defined in the existence part of the theorem for the ball in which we perform the contraction. We have from the semigroup P_t in the interval $[0, \overline{T}]$ that

$$\|P_t(f_{t_i})\|_{X_{\overline{T}}} \lesssim r e^{-\overline{T}}.$$

We choose then $\overline{T} > 0$ such that it holds $\|P_t(f_{t_i})\|_{X_{\overline{T}}} \leq \gamma(T^0)$, for $i \in \mathbb{N}$.
We can now repeat the same existence scheme and we obtain that f exists at least on $[t_i, t_i + \overline{T}]$, $\forall i \in \mathbb{N}$ contradicting the maximal extension of the interval. Thus, for $f^0 \in L^2$ we must have

$$\sup_{T(f^0) - \varepsilon < t < T(f^0)} \|f_t\|_{L^2_M} = \infty.$$

This concludes the proof. □

Theorem 4.4.2. *Given the solution $f \in X_T$ of the truncated equation from Theorem 4.4.1, we have that $f(t; f^0) \in L^2_+$ for $t \in [0, T(f^0))$ provided that $f^0 \in L^2_+$.*

Proof. Consider $f^0 \in L^2_+$, and let $T \in [0, T^0)$ be arbitrary. Then there is a constant $\omega := \omega(T) > 0$ such that, for $t \in [0, T]$,

$$\left| \sum_{n=1}^{M} \int |v - w| \chi_R(w) \chi_R(v) f_n(w) dw \right| \leq \sum_{n=1}^{M} C_R \|f_n\|_{X_T} := \omega(T), \ a.e. \ v \in \mathbb{R}^d.$$

Now, for $g \in L^2$ and $0 \leq t \leq T$ set for $m = 1, .., M$

$$\overline{Q}^m_t(g) := dg_m + Q^R_m(g, g) + \omega(T)_R g_m,$$

so, for $t \in [0, T], \ a.e. v \in \mathbb{R}^d$ and $g \in L^p_+$, we have $\overline{Q}(g, g) \geq 0$.
We consider now the evolution equation

$$\dot{g} + (\omega(T) + \mathcal{L})\, g = \overline{Q}(g, g), \ t \in [0, T], \ g(0) = f^0. \tag{4.4.1}$$

We note that f is a solution of such equation and that equation (4.4.1) can be solved by the method of successive approximations exactly as in the existence theorem. So we consider

$$\Theta(g) := P_\omega f^0 + \int_0^{\cdot} P^\omega_{\cdot - s}(\overline{Q}(g, g) ds, \text{ for } g \in X_T$$

where $P_\omega(t) := e^{-\omega t} P_t, \ t \geq 0$.
In the same fashion as Theorem 4.4.1, Θ is a contraction in a suitable ball $B_T \subset X_T$, centered in $P.f^0$, into itself. Taking T small enough we can assume that also $f \in B_T$. Therefore, since there must be existence and uniqueness of a solution we can find a sequence g_i, determined by

$$g_0 = f^0, \ g_{i+1} = \Theta(g_i), \ i \in \mathbb{N},$$

such that converges to f in X_T. This implies that $g_i \to f$ in L^2_M for $t \in (0, T]$.
Since the semigroup P_t preserves positivity, by induction we get that $g_i \in L^2_+$ for $t \in [0, T]$ and $i \in \mathbb{N}$. This means that also $f_t \in L^2_+$ for all $t \leq T$ since the space is closed.
Consider now a $\overline{T} \leq T^0$, the maximal time for which f is positive on $[0, \overline{T}]$, then we claim that $\overline{T} = T^0$. Otherwise, we consider now the same equation (4.4.1) re-scaled in time

$$\dot{g} + (\omega + \mathcal{L})\, g = \overline{Q}(g, g)(t + \overline{T}), \ t \in [0, T^0 - \overline{T}], \ g(0) = f_{\overline{T}},$$

and this would lead to a contradiction on the maximality of T. Since T^0 was arbitrary in the maximal interval of definition we deduce that $f \in L^2_+, \ \forall t \in [0, T^0)$. □

We wish now to understand better the regularity of the truncated solution and the estimate on such computation. To this end we want to use the a priori estimate, but in doing so we first need to establish regularity deriving directly from the semigroup and the nonlinearity.
Following from Proposition 4.3.8 we can derive some regularity on f and its derivatives in L^2 space. In particular, with $f_0 \in L^2_M$, we have

$$f \in L^\infty([0, T], H^2(\mathbb{R}^d)) \cap W^{1,2}_{\text{loc}}([0, T] \times \mathbb{R}^d).$$

This is still not enough and we want to control also the moments of the solution and to this end it is not enough to have $f_0 \in L^2_m$, so we first consider an initial condition such that $f_0 \in L^1_{p,M} := L^1_M(\langle v\rangle^p\, dv)$ for every $p \geq 0$ and also in $L^2_{+,M}$, we show that this is enough to get that the solution

$$f^R \in L^\infty([0,T], L^1_{p,M} \cap L^2_{+,M}(\mathbb{R}^d)),$$

And this holds for every $p \geq 0$.

We want to establish a Gronwall relationship, so we integrate the function f_m (we drop the R for readability) for all $t > 0$. We note first that following the step of Theorem 4.4.1 it is easy to construct the same function adding the condition that $\int |f| dv$ must be bounded. With this in mind, using the consistency[49] of the operator P_t, we can write:

$$\begin{aligned}\|f_m(t)\|_1 \underbrace{=}_{\text{positivity}} \int f_m(t)dv &= \int P_t f_m^0 dv + \int\int_0^t P_{t-s}\left(df_s + Q_m^R(f,f)_s\right) dsdv \\ &\underbrace{\leq}_{\text{property of } P_t} \int f_m^0 dv + d\int_0^t \|f_m(s)\|_1 ds + T\sup_t\left(\int Q_m^R(f,f)dv\right)\end{aligned}$$

analogous to the proof of Lemma 4.2.2 we have $\sup_t \sum_{m=1}^M \int Q_m^R(f,f)dv \leq 0$ and thus summing on m and taking the sup in $t \leq T$ we get the bound of the L^1_M norm, independent on R.

Establish the L^1 bound, we use this results to prove that, depending on R this time, we have bound on the p-th moment for every p. To this end consider:

$$\begin{aligned}&\int f_m(t)\,\langle v\rangle^p\, dv \\ &\leq \iint K(t,w) f_m^0(e^t v - w)\,\langle v\rangle^p\, dwdv + \int_0^t \iint K(s,w) Q_m^R(f,f)(e^s v - w)\,\langle v\rangle^p\, dvdwds \\ &\underbrace{\leq}_{e^t v - w = z} \int K(t,w)\,\langle w\rangle^p\, dw \int C_t f_m^0(z)\,\langle z\rangle^p\, dz \\ &\quad + \int_0^t \int K(s,w)\,\langle w\rangle^p\, dw \int C_s Q_m^R(f,f)(z)\,\langle z\rangle^p\, dzds\end{aligned}$$

Recall that

$$K(t,w) := \frac{1}{(2\pi(e^{2t}-1))^{\frac{d}{2}}} e^{-\frac{|w|^2}{2\pi(e^{2t}-1)}},$$

and that the truncated nonlinearity has a term of the form $\chi_R(z)\chi_R(w)|z-w|$ and as such we get

$$\int f_m(t)\,\langle v\rangle^p\, dv \leq$$

$$\underbrace{\leq}_{\int K(t,w)\langle w\rangle^p dw<\infty\ \forall p} C_T\|f^0\|^1_{p,M} + C(R)\int_0^t C_s \sum_{n=1}^{m-1}\iint f_n(\varphi(v,w))f_m(w)dwdvds$$
$$\leq C_T\|f^0\|^1_{p,M} + C(R)C_T\sum_{n=1}^{m-1}\sup_t\|f_n\|_1\|f_m\|_1$$
$$\leq C_T\|f^0\|^1_{p,M} + C_T(R,\sup_t\|f\|^1_M, M)\sup_t\|f\|^1_{p,M}.$$

Summing on $m = 1, ..., M$, taking the sup over $t \leq T$, we obtain the bound depending on the initial condition, the L^1 norm of the solution and the truncation R.

We show now that a mild solution is indeed a weak solution for our equation and use this to enhance the regularity of the time derivative of the solution.

Lemma 4.4.3 (L^p mild solutions are weak solutions)**.** *Consider $f \in X_T$ a mild solution for equation (4.3.1) corresponding to the initial value f_0, then f is a weak solution in the sense of Definition 4.2.1.*

Proof. Fix $T > 0$ an a time $t \in [0,T]$, fix ϕ a test function. Consider now the weak formulation for equation (4.3.1):

$$\langle f_t,\phi\rangle = \langle f_0,\phi\rangle + \int_0^t \langle f_s, \mathcal{L}^*\phi\rangle\, ds + \int_0^t \langle Q_s(f,f),\phi\rangle\, ds,$$

where $\mathcal{L}^*\phi = -v\cdot\nabla\phi + \Delta\phi$. Notice that

$$\langle f_t, \mathcal{L}^*\phi\rangle = \langle \mathcal{L}(f_t) + df_t, \phi\rangle\,.$$

Under this definition and observation we consider now f mild solution as before

$$f_t = P_t f_0 + \int_0^t P_{t-s}f_s ds + \int_0^t P_{t-s}Q_s(f,f)ds$$

ans analyze the well defined quanity

$$\int_0^t \langle f_s,\mathcal{L}^*\phi\rangle\, ds = \int_0^t \left\langle P_s f_0 + \int_0^s P_{s-r}f_r dr + \int_0^s P_{s-r}Q_r(f,f)dr, \mathcal{L}^*\phi\right\rangle ds$$
$$= \underbrace{\int_0^t \langle P_s f_0,\mathcal{L}^*\phi\rangle\, ds}_{A} + \underbrace{\int_0^t \left\langle \int_0^s P_{s-r}f_r dr, \mathcal{L}^*\phi\right\rangle ds}_{B} + \underbrace{\int_0^t \left\langle \int_0^s P_{s-r}Q_r(f,f)dr, \mathcal{L}^*\phi\right\rangle ds}_{C}.$$

Now we analyze, using the regularity result on f derived in the previous sections and using [66], each of the component on the right hand side.

A:

$$\int_0^t \langle P_s f_0,\mathcal{L}^*\phi\rangle\, ds = \int_0^t \langle \mathcal{L}P_s f_0,\phi\rangle\, ds + \int_0^t \langle P_s f_0,\phi\rangle\, ds$$
$$= \left\langle \int_0^t \frac{d}{ds}P_s f_0 ds, \phi\right\rangle + \int_0^t \langle P_s f_0,\phi\rangle\, ds$$

$$= \langle P_t f_0, \phi \rangle - \langle f_0, \phi \rangle + \int_0^t \langle P_s f_0, \phi \rangle \, ds$$

B:

$$\begin{aligned}
&\int_0^t \left\langle \int_0^s P_{s-r} f_r dr, \mathcal{L}^* \phi \right\rangle ds \\
&= \int_0^t \left\langle \int_0^s \mathcal{L} P_{s-r} f_r dr, \phi \right\rangle ds + \int_0^t \left\langle \int_0^s P_{s-r} f_r dr, \phi \right\rangle ds. \\
&= \int_0^t \left\langle \int_r^t \mathcal{L} P_{s-r} f_r ds, \phi \right\rangle dr + \int_0^t \left\langle \int_0^s P_{s-r} f_r dr, \phi \right\rangle ds \\
&= \int_0^t \left\langle \int_r^t \frac{d}{ds} P_{s-r} f_r ds, \phi \right\rangle dr + \int_0^t \left\langle \int_0^s P_{s-r} f_r dr, \phi \right\rangle ds \\
&= \int_0^t \langle P_{t-r} f_r, \phi \rangle \, dr - \int_0^t \langle f_r, \phi \rangle \, dr + \int_0^t \left\langle \int_0^s P_{s-r} f_r dr, \phi \right\rangle ds
\end{aligned}$$

C:

$$\begin{aligned}
&\int_0^t \left\langle \int_0^s P_{s-r} Q_r(f,f) dr, \mathcal{L}^* \phi \right\rangle ds \\
&= \int_0^t \left\langle \int_0^s \mathcal{L} P_{s-r} Q_r(f,f) dr, \phi \right\rangle ds + \int_0^t \left\langle \int_0^s P_{s-r} Q_r(f,f) dr, \phi \right\rangle ds \\
&= \int_0^t \left\langle \int_0^s \mathcal{L} P_{s-r} Q_r(f,f) dr, \phi \right\rangle ds + \int_0^t \left\langle \int_0^s P_{s-r} Q_r(f,f) dr, \phi \right\rangle ds \\
&= \int_0^t \left\langle \int_r^t \mathcal{L} P_{s-r} Q_r(f,f) ds, \phi \right\rangle dr + \int_0^t \left\langle \int_0^s P_{s-r} Q_r(f,f) dr, \phi \right\rangle ds \\
&= \int_0^t \langle P_{t-r} Q_r(f,f) - Q_r(f,f), \phi \rangle \, dr + \int_0^t \left\langle \int_0^s P_{s-r} Q_r(f,f) dr, \phi \right\rangle ds.
\end{aligned}$$

To prove all the following equality we have used the fact that, if $f \in D(\mathcal{L})$, then $P_t f \in D(\mathcal{L})$ and in that case

$$\frac{d}{dt} P_t f = \mathcal{L} P_t f = P_t \mathcal{L} f.$$

Thanks to the reguliraty on f we can apply this result, thus putting all together we get:

$$\begin{aligned}
&\int_0^t \langle f_s, \mathcal{L}^* \phi \rangle \, ds = \langle P_t f_0, \phi \rangle - \langle f_0, \phi \rangle + \int_0^t \langle P_s f_0, \phi \rangle \, ds \\
&+ \int_0^t \langle P_{t-r} f_r, \phi \rangle \, dr - \int_0^t \langle f_r, \phi \rangle \, dr + \int_0^t \left\langle \int_0^s P_{s-r} f_r dr, \phi \right\rangle ds \\
&+ \int_0^t \langle P_{t-r} Q_r(f,f), \phi \rangle \, dr - \int_0^t \langle Q_r(f,f), \phi \rangle \, dr + \int_0^t \left\langle \int_0^s P_{s-r} Q_r(f,f) dr, \phi \right\rangle ds.
\end{aligned}$$

For which we derive, using the equality of the mild solution:

$$\langle f_0, \phi \rangle + \int_0^t \langle f_s, \mathcal{L}^* \phi \rangle \, ds + \int_0^t \langle Q_r(f,f), \phi \rangle \, dr$$

$$= \underbrace{\langle P_t f_0, \phi\rangle + \int_0^t \langle P_{t-r} f_r, \phi\rangle\, dr + \int_0^t \langle P_{t-r} Q_r(f,f), \phi\rangle\, dr}_{:=\left\langle P_t f_o + \int_0^t P_{t-r} f_r dr + \int_0^t P_{t-r} Q_r(f,f) dr, \phi\right\rangle = \langle f_t, \phi\rangle}$$
$$+ \underbrace{\int_0^t \langle P_s f_0, \phi\rangle\, ds + \int_0^t \left\langle \int_0^s P_{s-r} f_r dr, \phi \right\rangle ds + \int_0^t \left\langle \int_0^s P_{s-r} Q_r(f,f) dr, \phi \right\rangle ds}_{:=\int_0^t \langle f_s, \phi\rangle ds} - \int_0^t \langle f_s, \phi\rangle\, ds.$$

Thus $\langle f_0, \phi\rangle + \int_0^t \langle f_s, \mathcal{L}^*\phi\rangle\, ds + \int_0^t \langle Q_r(f,f), \phi\rangle\, dr = \langle f_t, \phi\rangle$, concluding the proof. □

To conclude we need to extend the regularity on the time derivative and prove that

$$\partial_t f_m \in L^2([0,T]\times\mathbb{R}^d).$$

Analyzing the equation solved by f^R, proving that $\partial_t f_m^R$ is in $L^2([0,T]\times\mathbb{R}^d)$ boils down to prove that the quantity

$$v\cdot\nabla f_m \in L^2([0,T]\times\mathbb{R}^d) \text{ i.e. } \int_0^T \int |v\cdot\nabla f_m(s)|^2 ds < \infty.$$

In order to to this we use the mild formulation of f, the explicit formulation of the nonlinearity Q_m^R and the bound we have previously derived. We reduce again the problem, using Cauchy-Schwartz and the inequality on the weight to prove that

$$\int_0^t \int |\nabla f_m|^2 \langle v\rangle^2\, dvds < \infty.$$

We consider:

$$\int_0^t \int |\nabla f_m|^2 \langle v\rangle^2\, dvds \le \underbrace{\int_0^t \int |\nabla P_t f_0|^2 \langle v\rangle^2\, dsdv}_{A}$$
$$+ \underbrace{\int_0^t \int |\nabla \int_0^s P_{s-r} Q_m^R(f,f) dr|^2 \langle v\rangle^2\, dvds}_{B}$$

we work separately on the two term:

$$\begin{aligned}
A &:= \int_0^t \int |\nabla \int K(t,w) f_0(e^t v - w) dw|^2 \langle v\rangle^2\, dvds \\
&\le e^T c_d \int_0^t \int \int K(t,w) |\nabla f_0(e^t v - w)|^2 \langle v\rangle^2\, dwdvds \\
&\le e^T c_d \int_0^t \int K(t,w) \int |\nabla f_0(e^t v - w)|^2 \langle v\rangle^2\, dvdwds \\
&\lesssim \int_0^t \int K(t,w) \int |\nabla f_0(e^t v - w)|^2 (\langle e^t v\rangle^2 + \langle w\rangle^2) dvdwds \\
&\lesssim \|\nabla f_0\|_{2,2} + \|\nabla f_0\|_2.
\end{aligned}$$

while for the other terms, we use intensively the form of the nonlinearity Q^R. In particular we use the bound obtained with $\chi_R(v)$ and $\chi_R(w)$ to control the weight and conclude.

$$B \lesssim \int_0^t \int_0^s \underbrace{\left(\int |\nabla P_{s-r} Q_m^R(f,f)|^2 \langle v \rangle^2 \, dv \right)}_{C} dr ds$$

and we compute directly on the term C.

$$\begin{aligned}
\left(\int |\nabla P_{s-r} Q_m^R(f,f)|^2 \langle v \rangle^2 \, dv \right) &\leq e^T \int |P_{s-r} \nabla Q_m^R(f,f)|^2 \langle v \rangle^2 \, dv \\
&= e^T \int |P_{s-r}(\left(Q_m^R(\nabla f, f) + Q_m^R(f, \nabla f)\right)|^2 \langle v \rangle^2 \, dv \\
&\lesssim \int P_{s-r} |(\left(Q_m^R(\nabla f, f) + Q_m^R(f, \nabla f)\right)|^2 \langle v \rangle^2 \, dv
\end{aligned}$$

Since the two addenda of the sum are quite similar we focus only on one of them. In particular we focus on each single term one for the "positive" part, the negative part being easier.

$$\begin{aligned}
&\int \int K(s-r,w) \left| \int \nabla f_n(h(v,w,z) f_{m-n}(z) |z| \chi_R(e^t v - w) \chi_R(z) dz \right|^2 dw \langle v \rangle^2 \, dv \\
&\leq \int \int K(s-r,w) \left| \int \nabla f_n(h(v,w,z) f_{m-n}(z) |z| \chi_R(e^t v - w) \chi_R(z) dz \right|^2 dw \langle v \rangle^2 \, dv \\
&\leq C_R^2 \|f\|_1 \int \int K(s-r,w) \int |\nabla f_n(h(v,w,z)|^2 f_{m-n}(z) dz dw \langle v \rangle^2 \, dv \\
&\underbrace{\lesssim}_{\text{change variables}} C_R^2 \|f\|_1 \int \int K(s-r,w) \int |\nabla f_n(\gamma)|^2 f_{m-n}(z) \langle \gamma \rangle^2 \langle w \rangle^2 \langle z \rangle^2 \, d\gamma dz dw \\
&\lesssim e^T \|\nabla f_n(s)\|_{2,2}^2 \| \|f_n\|_{1,2}^2 \|_{\infty,T}.
\end{aligned}$$

Putting this in (B) we get

$$\int_0^t \int_0^s \left(\int |\nabla P_{s-r} Q_m^R(f,f)|^2 \langle v \rangle^2 \, dv \right) dr ds \leq C(R, M, T, \|f\|_1, \|f\|_{1,2}) \int_0^t \int_0^s \|\nabla f(s)\|_{2,2}^2 ds \, dt.$$

Summing on M we get:

$$\sum_m \int_0^t \int |\nabla f_m|^2 \langle v \rangle^2 \, dv ds \leq C(f_0) + C(R, M, T, \|f\|_1, \|f\|_{1,2}) \int_0^t \int_0^s \|\nabla f(s)\|_{2,2}^2 ds \, dt$$

Assuming that f_0 is in $H_1^1 \cap L_2^1$ we have proven:

$$f_m \in H^1([0,T] \times \mathbb{R}^d), \forall m = 1, ..., M.$$

This extended regularity for the truncated solution f^R make it possible to prove rigorously the a priori estimate for the solutions of the approximated problems, obtaining bound that are independent of R.

Corollary 4.4.4. *In the same hypothesis of the last few theorems, the a priori estimate are true for the solution of the approximating problems, with constants independent from R, as soon as f^0 is regular enough.*

Proof. Under the hypothesis, and thanks to the previous lemmas we satisfy the requirement of the a priori estimate and thus conclude the proof. In fact using the established L^1_k bounds and the fact that $f \in H^1([0,T]\times\mathbb{R}^d)$ we can make rigorous the arguments of the a priori estimates lemmas and then proceed to obtain the regularity

$$f^R \in L^\infty([0,T], H^p_k(\mathbb{R}^d)),\ \forall n \in \mathbb{N}, \forall k \geq 0,$$

with bound independent of R. □

We conclude this section with the following:

Theorem 4.4.5 (global existence)**.** *Assume that the initial condition is positive and in L^2_M such that Lemma 4.3.2 and Theorem 4.4.1 holds, then the solution $\tilde{f}$ of the approximated problem is global in time, i.e. $T(f^0) = \infty$.*

Proof. Thanks to Theorem 4.4.1 we know that the maximal interval of the solution $\tilde{f}$ is open in R^+ and of the form $[0, T^0)$.
Under the hypothesis of regularity of the initial condition, and thanks to Lemma 4.3.2, we have that

$$\|\tilde{f}_t\|_{L^2_M} \leq C(T),\ a.e.\ t \in [0,T^0)\cap[0,T].$$

Thus, since being T^0 finite means that $\sup_{t\in[T^0-\varepsilon,T^0)} \|\tilde{f}_t\|_{L^2_M} = \infty$, this cannot be happening and this implies that $T^0 = \infty$ and the solution is global.
This implies that, for each $T > 0$, independently of R, under the regularity of initial condition, we have a weak solution of equation (4.3.1) on X_T. □

4.5 Existence and uniqueness for the full System

Right now we have proven that, fixing T finite, there exists a sequence of function $(f^R)_R$, solutions of (4.3.1).
Under suitable initial condition $(f^0_m)_{m=1}^M$, we prove now the weak convergence of f^R to a map f in $L^2 \cap L^1$ such that solves in the weak sense (4.2.2).
To prove existence for the full problem we begin by recalling the definition of weak solution we are going to use:

Definition 4.5.1. *Fix $T > 0$, and $f^0_m \in L^1_2 \cap L^2$. A solution for equation (4.2.2) is a set of functions $f_m \in L^\infty(0,T; L^1_2(\mathbb{R}^d))$ indexed by the masses $m = 1, ..., M$ such that $\forall m,\ Q_m(f,f) \in L^\infty(0,T; L^1(\mathbb{R}^d))$ and the following holds:*

$$\sum_{m=1}^M \langle f_m(t), \phi\rangle - \sum_{m=1}^M \langle f^0_m, \phi\rangle = \int_0^t \sum_{m=1}^M \langle f_m(s), \Delta\phi\rangle\, ds - \int_0^t \sum_{m=1}^M \langle f_m(s), v\cdot\nabla\phi\rangle\, ds$$
$$+ \int_0^t \sum_{m=1}^M \langle Q_m(f(s), f(s)), \phi\rangle\, ds,$$

for a.e. $t \in [0,T]$, and $\forall \phi \in C^\infty_c(\mathbb{R}^d)$.

We note that if a weak solution is sufficiently smooth and satisfy suitable decay for large $|v|$, then it is also a classical solution. With everything recalled we state the following.

Theorem 4.5.2. *For every $T > 0, M > 0,\ f_0 \geq 0$ such that $f_0 \in L^1_{2,M} \cap L^2_M$ there exists at least one nonnegative weak solution $f \in L^\infty([0,T], L^1_2(\mathbb{R}^d))$ with initial condition $f(0) = f_0$.*
If instead $f_0 \in L^1_{2,M} \cap H^1_{1,M}$, then for every $t_0 > 0$ we have $f \in C^1_b([t_0, T], C^\infty(\mathbb{R}^d))$ with rapid decay for large $|v|$.

We prove here the existence, postponing the uniqueness to the next section.

Proof. (Existence) We start with an initial condition $f_0 \in C^\infty_c(\mathbb{R}^d)$. Using the results obtained in the previous section we have establish the L^1_k bounds and the fact that the sequence $f_R \in H^1([0,T] \times \mathbb{R}^d)$. With this we can make rigorous the a priori estimates and get $f_R \in L^\infty([0,T], H^n_k(\mathbb{R}^d)),\ \forall n \in \mathbb{N}, k \geq 0$, with bounds independent from R.
$f^R \in L^\infty([0,T], L^2)$, and thanks to the a priori estimate we have that, independently of R, $f^R_t \in H^1(\mathbb{R}^d) \cap L^2(\mathbb{R}^d, |v|^2 dv)$ and the sequence is equibounded. Analogously we have that, thanks to the regularity of the semi group P_t, the solution f^R lies in the space $H^1(0,T; H^{-1})$.
Using now the Weighted Aubin-Lions Lemma 4.3.10 we have that, up to subsequence:

1. $f^R \rightharpoonup f$ in H^1;
2. $f^R \to f$ in L^2;
3. up to subsequence $f^R \to f$ pointwise a.e.,

and the a priori estimate pass to the limit function f.
This is enough to allow us to pass to the limit as $R \to \infty$ in the weak formulation of the system and show that the limit solutions satisfy the equation with the full kernel.
Finally we consider $f_0 \in L^1_2 \cap L^2$ and we take a sequence $f^n_0 \in C^\infty_0$ converging to f_0 in $L^1_2 \cap L^2$, obtaining the bound in L^1_2 by Fatou's lemma. Then, since the constants in the moments and energy are independent on n we can pass to the weak L^1-limit in the equations obtaining a solution f as expected.
To study the regularity of the solution with data in H^1_1 we consider that this is enough to get the parabolic regularity $f \in H^1([0,T] \times \mathbb{R}^d)$ for any $T > 0$ and using the fact that we have the bound $f \in L^\infty([0,T], L^1_k(\mathbb{R}^d))$ we can make rigorous the argument of the a priori estimates and proceed to obtain the desired regularity. □

4.5.1 Weak Uniqueness

Consider now two weak solutions f, g of equation (4.2.2) in the sense of Definition 4.2.1, with initial conditions $f^0_m = g^0_m \in H^1_1 \cap L^1_2$ and nonnegative for every m. We know they are actually classical solutions. We want to show that, as soon as they start with the same initial, regular condition, then the two solutions must be equal a.e. in $v \in \mathbb{R}^d$ for every fixed time $T \geq 0$.

Consider for this the set of equation solved by $h_m(t,v) := f_m(t,v) - g_m(t,v),\ \forall m = 1,...,M$ and call $H_m(t,v) := f_m(t,v) + g_m(t,v)$.

$$\begin{cases} \partial_t h_m(t,v) = \Delta h_m + \text{div}(v h_m) + \frac{1}{2}\left(Q_m(h,H) + Q_m(H,h)\right) \\ h_m|_{t=0} = 0 \end{cases} \tag{4.5.1}$$

where we denote

$$\begin{aligned} Q_m(h,H) := &\sum_{n=1}^{m-1} \int \left(\frac{m}{n}\right)^2 h_n(\varphi(v,w)) H_{m-n}(w)|v-w|dw - 2\sum_{m=1}^{M} h_m(v) \int H_n(w)|v \\ &- w|dw, \\ Q_m(H,h) := &\sum_{n=1}^{m-1} \int \left(\frac{m}{n}\right)^2 H_n(\varphi(v,w)) h_{m-n}(w)|v-w|dw \\ &- 2\sum_{m=1}^{M} H_m(v) \int h_n(w)|v-w|dw. \end{aligned}$$

We consider now the function $\psi_\varepsilon(x)$ an approximation of the function $\text{sgn}(x)$ such that

$$\psi_\varepsilon(x) := \begin{cases} -1, & x \le -\varepsilon \\ x/\varepsilon, & -\varepsilon < x < \varepsilon \\ 1, & x \ge \varepsilon \end{cases}$$

We consider the weight $\langle v\rangle^2 := 1+|v|^2$ and thus the function $\Psi_\varepsilon(h_m, v) := \psi_\varepsilon(h_m)\langle v\rangle^2$, multiplying it to the equations (4.2.2) solved by $h_m, \forall m$ and integrating by part. Defining also

$$\chi_\varepsilon(x) := \begin{cases} 1, \text{ if } |x| < \varepsilon \\ 0, \text{ otherwise,} \end{cases}$$

we obtain:

$$\begin{aligned} \partial_t \int h_m \psi_\varepsilon(h_m)\langle v\rangle^2 dv &= \int (\partial_t h_m)\psi_\varepsilon(h_m)\langle v\rangle^2 dv + \frac{1}{\varepsilon}\int (\partial_t h_m)\chi_\varepsilon(h_m) h_m \langle v\rangle^2 dv \\ &=: A_1 + B_1. \end{aligned} \tag{4.5.2}$$

Now we can work on the quantity A_1, using the equation (4.2.2),

$$\begin{aligned} A_1 := &\int \Delta h_m \psi_\varepsilon(h_m)\langle v\rangle^2 + \text{div}(v h_m)\psi_\varepsilon(h_m)\langle v\rangle^2 \\ &+ \frac{1}{2}\left(Q_m(h,H) + Q_m(H,h)\right)\psi_\varepsilon(h_m)\langle v\rangle^2 dv \\ = &-\frac{1}{\varepsilon}\int_{\{|h|<\varepsilon\}} |\nabla h_m|^2 \langle v\rangle^2 dv + d\int h_m \psi_\varepsilon(h_m)\langle v\rangle^2 dv \end{aligned}$$

$$+\underbrace{\int (\nabla h_m \cdot v)\,\psi_\varepsilon(h_m)\left(|v|^2-1\right)dv}_{A_2}$$
$$+\underbrace{\frac{1}{2}\int \left(Q_m(h,H)+Q_m(H,h)\right)\psi_\varepsilon(h_m)\,\langle v\rangle^2\,dv}_{A_3},$$

and we can then drop the first negative term. For A_2 we define first the following function:

$$\zeta_\varepsilon(x) := \begin{cases} -x+\varepsilon/2, & x\le -\varepsilon \\ x^2/(2\varepsilon), & -\varepsilon < x < \varepsilon \\ x-\varepsilon/2, & x\ge \varepsilon \end{cases}$$

with $\nabla\zeta_\varepsilon = \overline{\psi}_\varepsilon$ a.e. and $\zeta_\varepsilon \to |x|$ as $\varepsilon\to 0$, and we can write

$$\begin{aligned} A_2 = \int \left(\nabla\zeta_\varepsilon(h_m)\cdot v\left(|v|^2-1\right)\right)dv &= -\int \zeta_\varepsilon(h_m)\,\mathrm{div}(v\left(|v|^2-1\right))dv \\ &= -\int \zeta_\varepsilon(h_m)\left(d\left(|v|^2-1\right)+2|v|^2\right)dv. \end{aligned}$$

Now we get for A_3:

$$\begin{aligned} A_3 :=& \frac{1}{2}\sum_{n=1}^{m-1}\iint \left[h_n(\varphi(v,w))H_{m-n}(w)+h_{m-n}(w)H_n(\varphi(v,w))\right]|v-w|\psi_\varepsilon(h_m(v))\,\langle v\rangle^2\,dwdv \\ &-\sum_{n=1}^{M}\iint \left[h_m(v)H_n(w)+h_n(w)H_m(v)\right]|v-w|\psi_\varepsilon(h_m(v))\,\langle v\rangle^2\,dwdv. \end{aligned}$$

Next, we turn to the term B_1 of (4.5.2). Since h_m appears in the integrand, the set of v such that $h_m(v)=0$ does not contribute to the integral, hence

$$\begin{aligned} \left|\frac{1}{\varepsilon}\int (\partial_t h_m)\chi_\varepsilon(h_m)h_m\,\langle v\rangle^2\,dv\right| &= \left|\frac{1}{\varepsilon}\int_{\{v:\,0<|h_m(v)|<\varepsilon\}} (\partial_t h_m)h_m\,\langle v\rangle^2\,dv\right| \\ &\le \int_{\{v:\,0<|h_m(v)|<\varepsilon\}} |\partial_t h_m|\,\langle v\rangle^2\,dv. \end{aligned}$$

Since h_m is continuous, $|h_m|$ is also continuous sending open sets to open sets, hence $\{0<|h_m(v)|<\varepsilon\}\downarrow\emptyset$ as $\varepsilon\to 0$. We now claim that $\partial_t h_m(t)\,\langle v\rangle^2 \in L^1$ for every $t\in[0,T]$. It will imply that the last integral goes to 0 as $\varepsilon\to 0$. By linearity $\partial_t h_m = \partial_t f_m - \partial_t g_m$, hence it is enough to verify this claim separately for f_m and g_m. Let us take f_m and prove $\partial_t f_m(t)\,\langle v\rangle^2\in L^1$ for a.e. t. Note that

$$\begin{aligned} \int |\partial_t f_m|\,\langle v\rangle^2\,dv &= \int |\Delta f_m + \mathsf{div}(v f_m) + Q(f_m,f_m)|\,\langle v\rangle^2\,dv \\ &= \int |\Delta f_m + d f_m + v\cdot\nabla f_m + Q(f_m,f_m)|\,\langle v\rangle^2\,dv. \end{aligned}$$

By Sobolev embedding (which extends to the weighted case), if $f_m \in H^n_k$ for n, k suitably large (in particular, since f_m is a Schwartz function), then the above integral is finite.

Now we sum (4.5.2) over $m = 1, .., M$ and we get

$$\begin{aligned}
&\partial_t \sum_{m=1}^{M} \int h_m \psi_\varepsilon(h_m) \langle v\rangle^2 \, dv = \\
&= \sum_{m=1}^{M} \int (\partial_t h_m) \psi_\varepsilon(h_m) \langle v\rangle^2 \, dv + \sum_{m=1}^{M} \frac{1}{\varepsilon} \int (\partial_t h_m) \chi_\varepsilon(h_m) h_m \langle v\rangle^2 \, dv \\
&=: A_1^M + B_1^M.
\end{aligned}$$

We already know that B_1^M is negligible. Further, we have that

$$\begin{aligned}
A_1^M &= \sum_{m=1}^{M} \int \Delta h_m \psi_\varepsilon(h_m) \langle v\rangle^2 + \operatorname{div}(v h_m) \psi_\varepsilon(h_m) \langle v\rangle^2 \, dv \\
&\quad + \frac{1}{2} \int \left(Q_m(h, H) + Q_m(H, h)\right) \psi_\varepsilon(h_m) \langle v\rangle^2 \, dv \\
&\leq d \int \sum_{m=1}^{M} \left(h_m \psi_\varepsilon(h_m)\right) \langle v\rangle^2 \, dv + \underbrace{\sum_{m=1}^{M} \int \left(\nabla h_m \cdot v\right) \psi_\varepsilon(h_m) \left(d\left(|v|^2 - 1\right) + 2|v|^2\right) dv}_{A_2^M} \\
&\quad + \underbrace{\frac{1}{2} \sum_{m=1}^{M} \int \left(Q_m(h, H) + Q_m(H, h)\right) \psi_\varepsilon(h_m) \langle v\rangle^2 \, dv}_{A_3^M}
\end{aligned}$$

before estimating the nonlinear part we note that, using the estimate for each m, as $\varepsilon \to 0$, under our regularity assumption, we get

$$\begin{aligned}
&\partial_t \sum_{m=1}^{M} \int h_m \psi_\varepsilon(h_m) \langle v\rangle^2 \, dv \to \partial_t \sum_{m=1}^{M} \int |h_m| \langle v\rangle^2 \, dv; \\
&A_2^M \to - \sum_{m=1}^{M} \int |h_m| \left(d\left(|v|^2 - 1\right) + 2|v|^2\right) dv \leq \sum_{m=1}^{M} C_d \int |h_m| \langle v\rangle^2 .
\end{aligned}$$

So we miss to estimate the nonlinear term A_3^M and pass to the limit:

$$\begin{aligned}
A_3^M := \frac{1}{2} \sum_{m=1}^{M} \sum_{n=1}^{m-1} \iint \left(\frac{m}{n}\right)^2 &\left(h_n(\varphi(v, w)) H_{m-n}(w) + h_{m-n}(w) H_n(\varphi(v, w))\right) \\
&|v - w| \psi_\varepsilon(h_m(v)) \langle v\rangle^2 \, dw dv \\
- \sum_{m=1}^{M} \sum_{n=1}^{M} \iint &\left(h_m(v) H_n(w) + h_n(w) H_m(v)\right) |v - w| \psi_\varepsilon(h_m(v)) \langle v\rangle^2 \, dw dv
\end{aligned}$$

By the change of variable

$$\begin{cases} v' = \varphi(v, w) \\ w = w \end{cases}, \; |J(v, w)| = \frac{n}{m}.$$

and naming the variable v' again by v, we have that

$$
\begin{aligned}
A_3^M = \frac{1}{2}\sum_{m=1}^{M}\sum_{n=1}^{m-1}\iint &(h_n(v)H_{m-n}(w) + h_{m-n}(w)H_n(v)) \\
&|v-w|\psi_\varepsilon(h_m(v))\left\langle \frac{nv+(m-n)w}{m}\right\rangle^2 dwdv \\
-\sum_{m=1}^{M}\sum_{n=1}^{M}\iint &(h_m(v)H_n(w) + h_n(w)H_m(v))\,|v-w|\psi_\varepsilon(h_m(v))\,\langle v\rangle^2\,dwdv \\
\underbrace{\leq}_{\text{Jensen's ineq. \& } |\psi_\varepsilon(h_m)|\leq 1} &\frac{1}{2}\sum_{n=1}^{M}\sum_{\ell=1}^{m-1}\iint (|h_n(v)|H_\ell(w) + |h_\ell|(w)H_n(v)) \\
&\qquad |v-w|(\langle v\rangle^2 + \langle w\rangle^2)dwdv \\
-\sum_{m=1}^{M}\sum_{n=1}^{M}\iint &|v-w|\left[h_m(v)H_n(w)\psi_\varepsilon(h_m(v))\,\langle v\rangle^2 + h_n(v)H_m(w)\psi_\varepsilon(h_m(w))\,\langle w\rangle^2\right]dwdv \\
\underbrace{\leq}_{\text{symmetry}} &\sum_{n=1}^{M}\sum_{\ell=1}^{M}\iint |h_n(v)|H_\ell(w)|v-w|(\langle v\rangle^2 + \langle w\rangle^2)dwdv \\
-\sum_{m=1}^{M}\sum_{n=1}^{M}\iint &|v-w|\left[h_m(v)H_n(w)\psi_\varepsilon(h_m(v))\,\langle v\rangle^2 + h_n(v)H_m(w)\psi_\varepsilon(h_m(w))\,\langle w\rangle^2\right]dwdv \\
= \iint &\sum_{\ell=1}^{M} H_\ell(w)\sum_{n=1}^{M}|h_n(v)|\left(\langle v\rangle^2 + \langle w\rangle^2\right)|v-w|dwdv \\
-\iint &\sum_{m=1}^{M} H_m(w)\sum_{n=1}^{M}\left\{h_n(v)\psi_\varepsilon(h_n(v))\,\langle v\rangle^2 + h_n(v)\psi_\varepsilon(h_m(w))\,\langle w\rangle^2\right\}|v-w|dwdv.
\end{aligned}
$$

For the first two integrals we have (renaming ℓ by m)

$$\iint \sum_{m=1}^{M} H_m(w)\sum_{n=1}^{M}|h_n(v)|(\langle v\rangle^2 + \langle w\rangle^2)|v-w|dwdv \tag{4.5.3}$$

while, using the fact that

$$|h\psi_\varepsilon(h) - |h|| \leq |h|\chi_\varepsilon(h),$$

the third integral can be bounded above by

$$\iint \sum_{m=1}^{M} H_m(w)\sum_{n=1}^{M}\left[-|h_n(v)| + |h_n|(v)\chi_\varepsilon(h_n(v))\right]\langle v\rangle^2\,|v-w|dwdv \tag{4.5.4}$$

while for the fourth, by the elementary inequality $|v-w| \leq \langle v\rangle\langle w\rangle$, the moment bound Lemma 4.2.5, $|\psi_\varepsilon(h_m)| \leq 1$, is bounded above by

$$C_M \iint \sum_{m=1}^{M} H_m(w)\,\langle w\rangle^3 \sum_{n=1}^{M}|h_n|(v)\,\langle v\rangle\,dwdv \leq C\int \sum_{n=1}^{M}|h_n|(v)\,\langle v\rangle^2\,dv.$$

We get the upper bound on A_3^M by adding everything together and noting a cancellation in (4.5.3)-(4.5.4) that eliminates any higher moments in v,

$$A_3^M \leq C_M \iint \sum_{m=1}^{M} H_m(w) \sum_{n=1}^{M} |h_n(v)| \langle v \rangle \langle w \rangle^3 \, dvdw$$
$$+ \int \sum_{m=1}^{M} H_m(w) \sum_{n=1}^{M} \int_{\{|h_n(v)|<\varepsilon\}} |h_n(v)||v-w| dv \langle w \rangle^2 \, dw + C \int \sum_{n=1}^{M} |h_n|(v) \langle v \rangle^2 \, dv.$$

Now taking the limit as $\varepsilon \to 0$ we have

$$\limsup_{\varepsilon \to 0} A_3^M \leq C \iint \sum_{m=1}^{M} H_m(w) \sum_{n=1}^{M} |h_n(v)| \langle v \rangle \langle w \rangle^3 \, dvdw + \int \sum_{n=1}^{M} |h_n|(v) \langle v \rangle^2 \, dv$$

Consider now all the quantities together after passing to the limit, using again the moment bounds, we have

$$\frac{d}{dt} \sum_{m=1}^{M} \int |h_m(v)| \langle v \rangle^2 \, dv \leq C \int \sum_{m=1}^{M} |h_m(v)| \langle v \rangle^2 \, dv.$$

Now we can apply Gronwall's lemma and get that $\|f-g\|_{L^1_M(\langle v \rangle^2 dv)} = 0$, concluding the uniqueness. □

Appendix A

A Mean field limit for tracer particles

In this appendix we are going to show a scaling limit of interacting particle system to a random PDE close, in suitable sense, to a random Smoluchowski coagulation equation for the spatial-volumetric density of tracer particles in atmosphere

$$\partial_t \rho_t(x,v) + \sum_{j\in H} \left(\sigma_j(x,v)\cdot \nabla_x \rho_t(x,v)\right)\xi_t^j = \varepsilon \Delta_x \rho_t(x,v) + Q_v(\rho_t(x,\cdot)) \tag{A.0.1}$$

where Q_v is the non linear operator representing coagulation of different volume particles in the classic regime [83, 70, 2, 3], i.e.

$$\begin{aligned} Q_v(\rho_t(x,\cdot)) :=& \frac{1}{2}\int_0^v \rho_t(x,w)\rho_t(x,v-w)f(w,v-w)dw \\ &- \int_{\mathbb{R}_+} \rho_t(x,v)\rho_t(x,w)f(v,w)dw \end{aligned}$$

Although Coagulation equations with diffusion are already being studied (e.g. [2]) both in discrete [47, 8] and continuous setting [47, 9], as limit of particle system [92, 46, 5]) or as regularity of its solution [18]. Little is know about the counterpart $(A.0.1)$ which capture in detail the more complex motion of rain droplet in the atmosphere and is object of this study. Here a diffusion term and a random field act on the cloud density taking account of the macro-scale process, such as fluid motion, acting on the formation.

The airflow in which they interact, solution of Navier-Stokes equation, is thus replaced with a random field with finite correlation time, depending on an environmental random noise produced by Ornstein-Uhlenbeck processes. This choice stems from the idea of Stochastic Model Reduction [63] and can be replaced in future work with different approximations.

The reason for such a scaling limit is not only to have a rigorous computation to continue along the line of modelling fluid velocity with realistic noise as in [37, 48], but also to obtain an equation for which, in future work, one can apply a rigorous limit of the fluctuating velocity field in the sense of Galeati [42], obtaining a limiting PDE to study displacement of particles and their collisions property as done numerically in Chapter 1 for hard sphere swarm particles.

With this in mind, in Section A.1, we rigorously define a particle system dynamics that, in addition to being easier to simulate, approximate our key Smoluchowski equation (A.0.1).

Warm clouds and rain consist of large number of water droplets with broad range of radius from micrometers to several millimeters. Several sorts of aerosol particles are also floating in the atmosphere, which can be a seed of a cloud droplet.
Let N be the number of such individuals (rain droplets and dust particles) in the considered region, each particle is characterized by its position and volume: $\left(X_t^{i,N}, V_t^{i,N}\right)$, $i = 1, .., N$.
To describe the dynamics we see how particle acts on observable F of the system, using the infinitesimal generator $\mathcal{L}$ of the dynamical process.

$$\mathcal{L}F(\eta) = \mathcal{L}_D F(\eta) + \mathcal{L}_C F(\eta).$$

The first term on the r.h.s. represents the diffusion and random field acting on the particles

$$\mathcal{L}_D F(\eta) := \sum_i \varepsilon \Delta_{x_i} F(\eta) + \sum_i \mathcal{U}_t(x_i) \cdot \nabla_{x_i} F(\eta).$$

While the second term, representing the coalescence of the particle, is a mean field counterpart of the classic coagulation interaction term:

$$\mathcal{L}_C F(\eta) := \sum_{i,j} T_N(i,j) \left[\frac{1}{2}\mathbb{I}_{i,j} F(\eta^{i,j}) + \frac{1}{2}\mathbb{I}_{j,i} F(\eta^{j,i}) - F(\eta)\right]$$
$$\mathbb{I}_{i,j} := \mathbb{I}_{(v_i >= v_j)},\ \mathbb{I}_{j,i} := \mathbb{I}_{(v_j > v_i)};$$
$$T_N^\delta(i,j) := \frac{1}{2} N^{-1} \delta^{-3} \mathbb{I}_{B_{x_i}(\delta f(v_i,v_j))}(x_j) k(v_i, v_j)$$

Defining $\mu_t(x,v) := \frac{1}{N}\sum_{i=1}^N \delta_{(x_t^i, v_t^i)}$ as the empirical measure of the system and coupling it with the random noise ξ_t^h, $h \in H$ we are able to obtain convergence (i.e. Thm. (A.1.1) of the approximating particle dynamics to a solution of the non local Random Smoluchowski equation, parameterized by $\delta \in \mathbb{R}$

$$\partial_t \rho_t^\delta(x,v) + \sum_{j\in H} \left(\sigma_j(x,v) \cdot \nabla_x \rho_t^\delta(x,v)\right) \xi_t^j = \varepsilon \Delta_x \rho_t^\delta(x,v) + Q_v^\delta(\rho_t^\delta(x,\cdot)) \quad \text{(A.0.2)}$$

where Q^δ is the non local coagulation kernel, interpreted in a weak sense, closely related to equation (A.0.1) as shown in Section A.2.

There, a formal study of the mean field limit equation (A.0.2) is carried out heuristically, under regularity hypothesis, showing that, as in [16, 60], we can show proximity of our solution to the coagulation-position system (A.0.1). This result is summarized in Proposition 3.1 as a local convergence in the volume variable

$$\sup_{t\in[0,T]} \|\rho_t - \rho_t^\delta\|_{L_x^2(\mathbb{R}^d) L_v^1(0,R)} \to 0,\ as\ \delta \to 0,\ \forall\, R > 0, \mathbb{P} - a.s.$$

Justifying the use of the approximating particle system to compute meaningful quantities of the system of interest and recover information on the effect of the random field on coagulation of droplet in the the region of space considered.

A.1 Particle System Model

The microscopic model that we study in this appendix consists of a large number of tracer particles, in the space $\mathbb{R}^d,\ d \geq 3$, which move according to independent Brownian motions and a random field acting as the wind on the particles.

$$\begin{aligned} dX_t^i &= \mathcal{U}_t(X_t^i, \omega)dt + \varepsilon dB_t^i \\ \mathcal{U}_t(x) &:= \sum_{k\in K} \sigma_k(x)\xi_t^k \\ d\xi_t &= -\lambda\xi_t dt + \lambda dW_t^i,\ \xi_0 = 0. \end{aligned}$$

This velocity field $\mathcal{U} := \mathcal{U}^\lambda, \lambda > 1$, with finite correlation time, is of the following form:

$$\mathcal{U}^\lambda(t,x) = \sum_{h\in H} \sigma_h(x)\,\xi_t^{h,\lambda}$$

where H is a set of index with finite cardinality, $\{\sigma_h\}_h$ is a suitable family of time independent vector field and $\{\xi_t^{h,\lambda}\}_h$ is a family of stationary i.i.d. Ornstein-Uhlenbeck processes with covariance $cov(\xi_t^{h,\lambda}, \xi_s^{h,\lambda}) = \frac{\lambda}{2}exp(\lambda|t-s|)$, solution of

$$d\xi_t^h = -\lambda\xi_t^h dt + \sigma dW_t^h, \quad \xi_0^h = 0,\ k = 1, ..., K.$$

For a family of i.i.d. Brownian motions $\{W_t^h\}_{h\in H}$ on a probability space $\left(\Omega, \{\mathcal{F}_t\}_{t\in[0,T]}, \mathbb{P}\right)$. Up to changing the filtration, we also have an explicit formula for the solution of such object

$$\xi_t^{h,\lambda} = \lambda\int_0^t e^{-\lambda(t-s)}dW_s^h,\ t \in [0,T]$$

During our work we select smooth vector fields $\{\sigma_h\}_h$, ideally as smooth approximation of the Biot-Savart Kernel, such that fixing point $x_h \in \mathbb{R}^2$ is defined as

$$\sigma_h(x) \sim \frac{1}{2\pi}\frac{(x-x_h)^\perp}{|x-x_h|^2},\ (a,b)^\perp := (b,-a)$$

This choice, admittedly phenomenological, come from the idea that one would like to take $\mathcal{U}_t(x) \equiv U(x)$, the solution of the Navier-Stokes equations for the wind velocity, or a slight modification, and the use of this "vortex like structure" was the proposed approximation.

To each particle we attach a value $v \in (0,\infty)$ which represent the volume or mass of the particle (we assume that mass and volume are around the same and can be recovered from one and another). In the mean field model any pair of particles that approach to within a certain range of interaction are liable to coagulate, at which time they disappear from the system, to be replaced by a particle whose volume is equal to the sum of the volumes of the colliding particles, and whose location is a specific point in the vicinity of the location of the coagulation.

As a matter of convenience, we introduce the microscopic model, where the number of particles is initially deterministic. We define a sequence of microscopic models,indexed

by a positive integer N. A countable set $I := \mathbb{N}, ...$ of symbols is provided. A configuration η is an $\mathbb{R}^d \times (0,\infty) - valued$ function on a finite subset $I_\eta \subset I$. For any $i \in I_\eta$, the component $\eta(i)$ may be written as (x_i, v_i). The particle labelled by i has volume v_i and location x_i.
To describe this dynamics we need to see how the particle acts on observable of the system.
Let $F : (\mathbb{R}^d \times \mathbb{R}^0_+)^N \to \mathbb{R}$ denote a function such that $F : (\mathbb{R}^d \times \mathbb{R}_+)^N \to \mathbb{R}$ is smooth, and $F(x,0) = 0, \forall x \in \mathbb{R}^d$. The action on F of the infinitesimal generator $\mathcal{L}$ is given by

$$\mathcal{L}F(\eta) = \mathcal{L}_D F(\eta) + \mathcal{L}_C F(\eta).$$

The first term on the r.h.s. represents the diffusion and random field acting on the particles

$$\mathcal{L}_D F(\eta) := \sum_i \varepsilon \Delta_{x_i} F(\eta) + \sum_i \mathcal{U}_t(x_i) \cdot \nabla_{x_i} F(\eta).$$

While for the second term, representing the coalescence of the particle we have:

$$\mathcal{L}_C F(\eta) := \sum_{i,j} T_N(i,j) \left[\mathbb{I}_{i,j} F(\eta^{i,j}) + \mathbb{I}_{j,i} F(\eta^{j,i}) - F(\eta) \right]$$
$$\mathbb{I}_{i,j} := \mathbb{I}_{(v_i >= v_j)},\ \mathbb{I}_{j,i} := \mathbb{I}_{(v_j > v_i)};$$
$$T^\delta_N(i,j) := \frac{1}{2} N^{-1} \delta^{-3} \mathbb{I}_{B_{x_i}(\delta f(v_i,v_j))}(x_j) k(v_i, v_j)$$

here we have indicated

$$\eta^{i,j}_k = \begin{cases} \eta(k), & \text{if } k \neq i,j \\ (x_i, v_i + v_j), & \text{if } k = i \\ (x_i, 0), & \text{if } k = j. \end{cases}$$

We note here, as one can see from $\mathcal{L}_C$, that the coalescence generator is as such that two particles interact if they are close in the space depending not only on the radius, but also on some fixed scaling quantities δ.
This is done to obtain a scaling limit in the mean field regime for the system. As such, we needed to scale the T interaction Kernel with a factor $1/N$, that take into account the interaction with the particle as N grows.
In particular, as N grows the particle are nearer, with mean distance $N^{-1/d}$, and so when we consider the T function we should make a rescale in the position: two particles interact if $|X^{i,N}_t - X^{j,N}_t| \leq N^{-1/d}$, and since in our case the interaction depends also on the volume of each raindrop, we would like to have

$$|X^{i,N}_t - X^{j,N}_t| \leq N^{-1/d} f(V^{i,N}_t, V^{j,N}_t))$$

and thus making it a local problem. This is out of our capacity for now, so we select a rescaling parameter δ such that T is substituted whit T^δ of the form

$$\delta^\alpha \mathbb{I}_{B_x(\delta f(v,w)} g(v,w)$$

where α depend on the system (in particular the dimension) and δ depends on N.

We note that $(x_i(t), v_i(t)) \in C([0,T], R^d) \times \mathcal{D}([0,T], R_+)$, we consider now for each N the empirical measure associated to the particles

$$\mu_t^N := \frac{1}{N}\sum_{i=1}^{N} \delta_{(X_i^N(t), V_i^N(t))} \in \mathcal{D}([0,T], \mathcal{M}_1(\mathbb{R}^d \times \mathbb{R}_+)$$

As in the other setting we consider the pair $(\mu_t^N, \xi_t) \in \mathcal{D}([0,T], \mathcal{M}_1(\mathbb{R}^d \times \mathbb{R}_+)) \times C([0,T], \mathbb{R})$. If we consider now $\phi \in C_b^{1,2}$, $\phi(x,0) = 0$, non necessarily continuous in $v = 0$. we can compute the infinitesimal generator acting on $\langle \mu_t^N, \phi \rangle$ and we have

$$\begin{aligned}\langle \mu_t^N, \phi \rangle = \langle \mu_0^N, \phi \rangle + \int_0^t \varepsilon \langle \mu_s^N, \Delta\phi \rangle ds + \int_0^t \langle \mu_s^N, \mathcal{U}_s \cdot \nabla\phi \rangle ds + \\ + \int_0^t \left\langle \mu_t^N, \left\langle \mu_t^N, T^\delta(x,v,y,w) J^\phi(x,v,y,w) \right\rangle \right\rangle ds + \tilde{M}_t\end{aligned}$$

where

$$\begin{aligned}T^\delta(x,v,y,w) &:= \frac{1}{2}\delta^{-3} \mathbb{I}_{B_x(\delta f(v,w))}(y) k(v,w); \\ J^\phi(x,v,y,w) &:= \left[\mathbb{I}_{(v>=w)}\phi(x, v+w) + \mathbb{I}_{v<w}\phi(y, v+w) - \phi(x,v) - \phi(y,w)\right]\end{aligned}$$

$\tilde{M}_t$ is a martingale and we can compute is quadratic variation:

$$\mathbb{E}\left[\tilde{M}_t^2\right] = \mathbb{E}\left[\int_0^t \left(\mathcal{L}\langle \mu_s^N, \phi \rangle^2 - 2\langle \mu_s^N, \phi \rangle \mathcal{L}\langle \mu_s^N, \phi \rangle ds\right)\right]$$

which we can compute in two parts $M_D,\ M_C$ such that:

$$\begin{aligned}\langle M_D \rangle :&= \mathbb{E}\left[\int_0^t N^{-1} \langle \mu_t^N, |\nabla\phi|^2 \rangle ds\right] \\ \langle M_C \rangle :&= \mathbb{E}\left[\int_0^t \frac{1}{N^3}\sum_{i,j} T_t^\delta(i,j) J_t^\phi(i,j)^2 ds\right] \\ &= \mathbb{E}\left[\int_0^t N^{-1} \left\langle \mu_s^N, \left\langle \mu_s^N, T^\delta(x,v,y,w) J^\phi(x,v,y,w)^2 \right\rangle \right\rangle ds\right]\end{aligned}$$

The last computation is a very tedious one, but not difficult.

Our result is the following

Theorem A.1.1. *Assuming that (μ, ξ) realise a limiting law of the sequence (μ^N, ξ). Then μ is a continuous process taking values in $\mathcal{M}_1(\mathbb{R}^d \times \mathbb{R}_+)$ and satisfies the limit random PDE:*

$$\begin{aligned}\langle \mu_t, \phi \rangle - \langle \mu_0, \phi \rangle = \int_0^t \left\langle \mu_s, \frac{\varepsilon_x^2}{2}\Delta_x\phi \right\rangle ds + \int_0^t \sum_{j\in J} \langle \mu_s, \sigma_j(x,v) \cdot \nabla_x\phi \rangle \xi_s^j ds \\ + \int_0^t \left\langle \mu_s, \left\langle \mu_s, T^\delta J^\phi \right\rangle_{y,w} \right\rangle_{x,v} ds\end{aligned}$$

for every $t \in [0,T]$ and $\phi \in C_{test}$, with probability 1. Here:

$$T^{\delta}(x,v,y,w) := \frac{1}{2}\delta^{-3}\mathbb{I}_{B_x(\delta f(v,w))}(y)k(v,w);$$
$$J^{\phi}(x,v,y,w) := \left[\mathbb{I}_{(v>=w)}\phi(x,v+w) + \mathbb{I}_{v<w}\phi(y,v+w) - \phi(x,v) - \phi(y,w)\right].$$

Moreover, if μ_0 has finite volume of the particle, also μ_t does and we have:

$$\sup_{t\leq T}\int_{\mathbb{R}^d\times\mathbb{R}_+} v\mu_t(dx,dv) \leq \int_{\mathbb{R}^d\times\mathbb{R}_+} v\mu_0(dx,dv)$$

Later we'll show under suitable hypothesis how to pass to the limit as $\delta \to 0$ and retrieve that $\mu_t^{\delta} \to \mu_t$ where μ_t is a solution in the sense of weak formulation for the Random Smoluchowski equation, justifying our particle system approximation scheme:

Definition A.1.2. *A continuous family of measure $\mu_t \in C([0,T], \mathcal{M}_1(\mathbb{R}^d \times \mathbb{R})$, given ξ_t as before, is a weak solution of the RSPDE if*

$$\langle \mu_t, \phi\rangle - \langle \mu_0, \phi\rangle = \int_0^t \left\langle \mu_s, \frac{\varepsilon_x^2}{2}\Delta_x\phi \right\rangle ds + \int_0^t \sum_{j\in J} \langle \mu_s, \sigma_j(x,v)\cdot\nabla_x\phi\rangle\, \xi_s^j ds$$
$$+ \int_0^t \left\langle \mu_s, \left\langle \mu_s, k(v,w)T(v,w)J^{\phi}_{x,v,w}\right\rangle_{x,w}\right\rangle_{x,v} ds$$

for every $t \in [0,T]$ and $\phi \in C_{test}$, with probability 1. Here:

$$K(v,w)T(v,w) := \frac{\pi}{2}\left(v^{1/3}+w^{1/3}\right)^3 E(v,w),\ with\ E \in C_b^0;$$
$$J^{\phi}(x,v,w) := \left[\phi(x,v+w) - \phi(x,v) - \phi(x,w)\right].$$

A.1.1 Scaling Limit: Uniform Estimates and Compactness

Since ξ does not change in the sequence (μ^N, ξ), to prove tightness for law $Q^N := \mathcal{L}(\mu^N, \xi)$ we need to prove it just for the marginal μ_t^N, which is done in the following computation.
Suppose that the initial condition $(X_0^{i,N}, V_0^{i,N})$ of the system are i.i.d from a probability distribution with law μ_0 and $\mathcal{F}_0 - measurable$, suppose also that:

$a)$ $\sup_{i,N}\mathbb{E}\left[|X_0^{i,N}| + |V_0^{i,N}|\right] < \infty$;
$b)$ $\exists \mu_0 \in Pr_1(\mathbb{R}^d\times\mathbb{R}_+)$ such that $\langle \mu_0^N, \phi\rangle \to_{\mathbb{P}} \langle \mu_0, \phi\rangle$, for every $\phi \in C^{\infty}(\mathbb{R}^d\times\mathbb{R}_+)$.
$c)$ $\int_{\mathbb{R}^d} v\mu_0(dx,dv) < \infty$;

This is true under the particular assumption made in the introduction: $(X_0^{i,N}, V_0^{i,N}) = (X_0^i, V_0^i)$, where $\{X_0^i, V_0^i\}_{i\in\mathbb{N}}$ is a sequence of i.i.d. $\mathcal{F}_0-$measurable r.v.'s with common law $\mu_0 \in Pr_1(\mathbb{R}^d\times\mathbb{R}_+)$.
We also assume the following on system (3.1):

$c)$ $\mathcal{U}_t(x,v,\omega)$ is of the form $\sum_{h\in H}\sigma_h(x)D_h(v)\xi_t^h(\omega),\ |H|<\infty$, where σ_h is regular $\forall h, \|\sigma_h\|_\infty \le K_\sigma < \infty$, and D_h is smooth and bounded with a constant K_D;
$d)$ the interacting kernel for the volume of the particle is defined as

$$T^\delta := \delta^{-3}\mathbb{1}_{B_x(\delta f(v,w)}(y)k(v,w).$$

Here k represents the efficiency collision and is such that $k\in C_b^0,\ \|k\|_\infty<\infty$, and f is as usual.
We'll derive a real interaction kernel at the limit of $\delta\to 0$ later in the next chapter.

The crucial step in the proof of tightness is to establish suitable uniform bounds for the increments of the process μ_t^N.

Proposition A.1.3. *Let $T\ge 0$ and $\phi\in C^1,2$ be fixed. There exists a constant $C>0$ depending only on $T,\phi,\xi,K_\sigma,\delta$ such that for all $N\in\mathbb{N}$, any bounded stopping time $\tau\le T$ with respect to the filtration of μ^N, and $\vartheta>0$, it holds*

$$\mathbb{E}\left[|\left\langle \mu^N_{\tau+\vartheta}-\mu^N_\tau,\phi\right\rangle|^2\right]\le C\vartheta.$$

The proof of the latter shall be divided in two parts, corresponding to the generator part and the stochastic (martingale) part of the dynamics of μ^N. Indeed, we can always expand the above increments as

$$\left\langle \mu^N_{\tau+\vartheta}-\mu^N_\tau,\phi\right\rangle = \int_\tau^{\tau+\vartheta}\mathcal{L}_s\left\langle\mu_s^N,\phi\right\rangle ds + \left(\tilde{M}^{\phi,N}_{\tau+\vartheta}-\tilde{M}^{N,\phi}_\tau\right).$$

where $\tilde{M}$ is a martingale and we know the quadratic variation. Thus we can reduce ourselves to bound separately the first and second summands in the right-hand side of the expression above.

Lemma A.1.4. *In the notation above, it holds*

$$\mathbb{E}\left[\left|\int_\tau^{\tau+\vartheta}\mathcal{L}\left\langle\mu_t^N,\phi\right\rangle dt\right|^2\right]\le C\vartheta$$

where the constant $C>0$ only depends on ξ,ϕ,T,K_σ.

Proof. Consider the integrating function $\mathcal{L}\left\langle\mu_s^N,\phi\right\rangle$ we can explicitly bound

$$\begin{aligned}|\mathcal{L}\left\langle\mu_s^N,\phi\right\rangle| &\le |\mathcal{L}_D\left\langle\mu_s^N,\phi\right\rangle| + |\mathcal{L}_C\left\langle\mu_s^N,\phi\right\rangle| \le |\left\langle\mu_s^N,\frac{\varepsilon^2}{2}\Delta\phi\right\rangle| + |\left\langle\mu_s^N,\xi_s\sigma\cdot\nabla_x\phi\right\rangle| + \\ &+ |\left\langle\mu_s^N,\left\langle\mu_s^N,T^\delta J^\phi\right\rangle\right\rangle| \\ &\le \frac{\varepsilon^2}{2}\|\phi\|_{1,2} + K_\sigma\sup_{t\in[0,T]}|\xi_t|\|\phi\|_{1,2} + 2\delta^{-3}\|k\|_\infty\|\phi\|_\infty.\end{aligned}$$

Passing to the square, using Jensen inequality we get

$$\mathbb{E}\left[\left|\int_\tau^{\tau+\vartheta}\mathcal{L}\left\langle\mu_t^N,\phi\right\rangle dt\right|^2\right]\le C^2_{\xi,\phi,\sigma,k,\delta}\,\vartheta.$$

□

Lemma A.1.5. *In the notation above, it holds*

$$\mathbb{E}\left[\left(\tilde{M}^N_{\tau+\vartheta} - \tilde{M}^N_\tau\right)^2\right] \leq \frac{C\vartheta}{N},$$

where the constant $C > 0$ only depends on ϕ, T, δ.

Proof. Using the fact that τ is a stopping time for μ^N and $\tilde{M}$ is a martingale, follows

$$\begin{aligned}\mathbb{E}\left[\left(\tilde{M}^N_{\tau+\vartheta} - \tilde{M}^N_\tau\right)^2\right] &\leq \mathbb{E}\left[\left|\int_\tau^{\tau+\vartheta} \mathcal{L}\left\langle\mu^N_t,\phi\right\rangle^2 - 2\left\langle\mu^N_t,\phi\right\rangle\mathcal{L}\left\langle\mu^N_t,\phi\right\rangle dt\right|\right]\\ &\leq \vartheta\mathbb{E}\left[\sup_t\left(\mathcal{L}\left\langle\mu^N_t,\phi\right\rangle^2 - 2\left\langle\mu^N_t,\phi\right\rangle\mathcal{L}\left\langle\mu^N_t,\phi\right\rangle\right)\right].\end{aligned}$$

From the definition of the two martingale (the diffusive one and coagulation one) we have:

$$\begin{aligned}\langle M_D\rangle &:= \mathbb{E}\left[N^{-1}\left\langle\mu^N_t, |\nabla\phi|^2\right\rangle\right] \leq N^{-1}\|\phi\|_{1,2}\\ \langle M_C\rangle &:= \mathbb{E}\left[\frac{1}{N^3}\sum_{i,j} T^\delta_t(i,j)J^\phi_t(i,j)^2\right] \leq N^{-1}2\|\phi\|_\infty\delta^{-3}\|k\|_\infty.\end{aligned}$$

Which concludes the proof. □

The combination of Lemma 2.4 and Lemma 2.5 proves Proposition 2.3, from which we immediately deduce the following tightness result

Proposition A.1.6. *Under the hypothesis of the previous lemmas, $\{Q^N\}_{N\in\mathbb{N}}$ the law of $\{\mu^N_\cdot\}_{N\in\mathbb{N}}$ on $\mathcal{D}([0,T],\mathcal{M}_1(\mathbb{R}^d\times\mathbb{R}_+))$ is relatively compact.*
As a consequence the law of $(\mu^N,\xi)\in\mathcal{D}([0,T],\mathcal{M}_1(\mathbb{R}^d\times\mathbb{R}_+))\times C([0,T],\mathbb{R})$ is tight and there exist a sub sequence such that $(\mu^N_k,\xi)\ \to_{\mathcal{L}}\ Q$ a law in $\mathcal{D}([0,T],\mathcal{M}_1(\mathbb{R}^d\times\mathbb{R}_+))\times C([0,T],\mathbb{R})$.

Proof. it suffices to show that the laws of couplings$\left\langle\mu^N_t,\phi\right\rangle$ is tight on $\mathcal{D}([0,T],\mathbb{R})$ for any fixed ϕ in a dense subset of C^0 including the constant $\phi\equiv 1$. Such tightness is in turn verified if:

- for any $t\in[0,T]$ the sequence of random variables $\left\langle\mu^N_t,\phi\right\rangle$ is tight;
- for any $\overline{\delta}>0$ it holds

$$\lim_{\varepsilon\to 0}\limsup_{N\in\mathbb{N}}\sup_{\tau\in\mathcal{T}^N_T}\sup_{\vartheta\leq\varepsilon} Q^N(|\left\langle\mu^N_{\tau+\vartheta}-\mu^N_\tau,\phi\right\rangle|>\delta) = 0$$

  where $\mathcal{T}^N_T$ denotes the family of stopping times with respect to the filtration of μ^N_t bounded by T, that is $\tau\leq T$ almost surely;

The former condition is an easy consequence since $|\mu^N_t|\leq 1$, the collection $(\left\langle\phi,\mu^N_t\right\rangle)_{N\in\mathbb{N}}$ for fixed t is automatically tight because $\left\langle\phi,\mu^N_t\right\rangle\leq\|\phi\|_\infty$. The second condition, follows immediately from the previous proposition and Markov inequality. □

A.1.2 Passing to the Limit

As a consequence of proposition (2.6) the law of $(\mu^N, \xi) \in C([0,T], Pr_1(\mathbb{R}^d \times \mathbb{R}_+)) \times C([0,T], \mathbb{R})$ is tight and we can extract a subsequence, whcich we still denote Q^N, such that converges weakly to a law Q in $C([0,T], Pr_1(\mathbb{R}^d \times \mathbb{R}_+)) \times C([0,T], \mathbb{R})$.
Let us now consider (μ_t, ξ), a process such that its law is equal to Q and such that

$$(\mu_t^{N_k}, \xi) \to_{\mathcal{L}} (\mu_t, \xi).$$

Theorem A.1.7. *If (μ, ξ) realise the law of a weak limit point of a subsequence of $\{Q^N\}_{N\in\mathbb{N}}$, then μ solves the RPDE with probability 1 over test function.*

Proof. We consider the functional

$$\Psi_\phi(\nu_\cdot, f_\cdot) := \sup_{t\in[0,T]} \Big| \langle \nu_t, \phi\rangle - \langle \nu_0, \phi\rangle - \int_0^t \left\langle \nu_s, \frac{\varepsilon_x^2}{2}\Delta_x \phi \right\rangle ds \\ - \int_0^t \langle \nu_s, \sigma(x,v)\cdot\nabla_x\phi\rangle\, f_s\, ds - \int_0^t \left\langle \nu_s, \left\langle \nu_s, T^\delta J^\phi \right\rangle \right\rangle ds \Big|$$

defined for every $\phi \in C_b^{1,2}(\mathbb{R}^d \times \mathbb{R})$.
It is continuous on $\mathcal{D}([0.T], Pr_1(\mathbb{R}^d \times \mathbb{R})) \times C([0,T], \mathbb{R})$.
Hence, if $(\mu_t^{N_k}, \xi) \to_{\mathcal{L}} (\mu_t, \xi)$ is a subsequence which weakly converges to (μ, ξ), by Portmanteau theorem we have

$$\mathbb{P}(\Psi_\phi(\mu_\cdot, \xi_\cdot) > \delta) \le \liminf_{k\to\infty} \mathbb{P}\left(\Psi_\phi(\mu_\cdot^{N_k}, \xi_\cdot) > \tilde{\delta}\right).$$

Using the definition of the functional and the identity satisfied by (μ_t^N, ξ) in $lemma\ (3.3)$, the r.h.s. is equal to

$$= \mathbb{P}\left(\sup_{t\in[0,T]} |\left\langle \mu_0^{N_k}, \phi\right\rangle - \langle \mu_0, \phi\rangle + M_t^{\phi,N_k,x} + M_t^{\phi,N_k,v}| > \tilde{\delta}\right).$$

Using the hypothesis on the initial condition, regularity of the velocity field and interaction kernel, standard computation for the martingale part gives us

$$\mathbb{P}(\Psi_\phi(\mu_\cdot, \xi_\cdot) > \tilde{\delta}) \le \liminf_{k\to\infty} \mathbb{P}\left(\Psi_\phi(\mu_\cdot^{N_k}, \xi_\cdot) > \tilde{\delta}\right) = 0.$$

Since this hold true for every $\tilde{\delta} > 0$, we deduce that

$$\mathbb{P}(\Psi_\phi(\mu_\cdot, \xi_\cdot) > \tilde{\delta}) = 1.$$

Hence $\forall \phi \in C_b^{1,2}(\mathbb{R}^d \times \mathbb{R})$:

$$\langle \mu_t, \phi\rangle - \langle \mu_0, \phi\rangle = \int_0^t \left\langle \mu_s, \frac{\varepsilon_x^2}{2}\Delta_x\phi \right\rangle ds \\ + \int_0^t \langle \mu_s, \sigma(x,v)\cdot\nabla_x\phi\rangle\, \xi_s ds + \int_0^t \left\langle \nu_s, \left\langle \nu_s, T^\delta J^\phi \right\rangle \right\rangle ds$$

$\forall t \in [0,T]$, with probability 1. □

We now can conclude the proof of Theorem (2.1)

Proof. What we need to prove to conclude the theorem is that we can swap the quantifiers on $\phi \in \mathcal{D}(R^{d+1})$.
Since this space is separable we can work on a infinite countable dense subset and we have

$$\mathbb{P}(\forall \phi \ \Psi_\phi(\mu, \xi) = 0) = \mathbb{P}(\forall \phi_n \ \Psi_{\phi_n}(\mu, \xi) = 0) = 1.$$

And so we have that:

$$\begin{aligned}\langle \mu_t, \phi \rangle - \langle \mu_0, \phi \rangle = &\int_0^t \left\langle \mu_s, \frac{\varepsilon_x^2}{2} \Delta_x \phi \right\rangle ds \\ &+ \int_0^t \langle \mu_s, \sigma(x,v) \cdot \nabla_x \phi \rangle \, \xi_s ds + \int_0^t \left\langle \mu_s, \left\langle \mu_s, T^\delta J^\phi \right\rangle \right\rangle ds\end{aligned}$$

for every $t \in [0,T]$ and $\phi \in C_{test}$, with probability 1.
The continuity of μ follows from the fact that every element in the r.h.s. is continuous. □

What we have now is that any process realizing the limiting law is a solution of the random evolution equation in the sense above. What we need to conclude now is:

1. Prove uniqueness of solutions for this equation.
2. Conclude all limiting laws agree, and hence that we have convergence in law.

Theorem A.1.8. *If $(\mu, \xi),\ (\nu, \xi)$ are two processes such that μ, ν satisfy the weak formulation as in $Thm.\ 8.3$, $\mathbb{P} - a.s.$, then:*

$$\|\mu_t - \nu_t\| = 0, \ \forall t \in [0,T], \ \mathbb{P} - a.s.$$

Proof. Existence in the weak sense has been proved above. Let us prove uniqueness. To shorten the expressions we set $\varepsilon_x = \varepsilon_v = 1$ and $|H| = 1$.
Let μ and ν be two solutions. Using as test functions the heat kernel multiplied by a test function we have that both satisfy

$$\begin{aligned}\langle \mu_t - \nu_t, \phi \rangle = &\int_0^t \left\langle \mu_s - \nu_s, \sigma(x,v) \cdot \nabla_x (e^{(t-s)\Delta} \phi) \right\rangle \xi_s ds \\ &+ \int_0^t \left\langle \mu_s, \left\langle \mu_s, T^\delta J^{(e^{(t-s)\Delta}\phi)} \right\rangle \right\rangle ds \\ &- \int_0^t \left\langle \nu_s, \left\langle \nu_s, T^\delta J^{(e^{(t-s)\Delta}\phi)} \right\rangle \right\rangle ds\end{aligned}$$

We pass to the module and we estimate for $\mathbb{P} - a.s.$

$$\begin{aligned}|\langle \mu_t - \nu_t, \phi \rangle| \leq &\int_0^t \left| \left\langle \mu_s - \nu_s, \sigma(x,v) \cdot \nabla_x (e^{(t-s)\Delta} \phi) \right\rangle \right| ds \|\xi\|_{L_t^\infty} \\ &+ \int_0^t \left| \left\langle \mu_s - \nu_s, \left\langle \mu_s, T^\delta J^{(e^{(t-s)\Delta}\phi)} \right\rangle \right\rangle \right| ds \\ &+ \int_0^t \left| \left\langle \nu_s, \left\langle \mu_s - \nu_s, T^\delta J^{(e^{(t-s)\Delta}\phi)} \right\rangle \right\rangle \right| ds\end{aligned}$$

We the first term in the r.h.s. we have $\mathbb{P}-a.s.$

$$\begin{aligned}
&\int_0^t |\left\langle \mu_s-\nu_s, \sigma(x,v)\cdot\nabla_x(e^{(t-s)\Delta}\phi)\right\rangle| ds\|\xi\|_{L_t^\infty}\\
&\leq \int_0^t K_\sigma\|\phi\|_\infty\|\nabla e^{(t-s)\Delta}\|\|\mu_s-\nu_s\|ds\|\xi\|_{L_t^\infty}\\
&\leq \int_0^t \frac{C(\xi,\phi,\sigma)}{\sqrt{t-s}}\|\mu_s-\nu_s\|ds.
\end{aligned}$$

For the second term in the r.h.s we have

$$\int_0^t |\left\langle \mu_s-\nu_s, \left\langle \mu_s, T^\delta J^{(e^{(t-s)\Delta}\phi)}\right\rangle\right\rangle| ds \leq \int_0^t \left\langle \mu_s-\nu_s, 2\delta^{-3}\|\phi\|_\infty\|K\|_\infty\right\rangle ds$$

where we have used the fact that

$$\begin{aligned}
|T^\delta J^{e^{(t-s)\Delta}\phi}| &= |\int \frac{1}{2}\delta^{-3}\mathbb{I}_{B_x(\delta f(v,w))}k(v,w)4|e^{(t-s)\Delta}\phi|d\mu_s^N|\\
&\leq 2\delta^{-3}\int d\mu_s^N(dx,dv)\|\phi\|_\infty\|k\|_\infty \leq 2\delta^{-3}\|\phi\|_\infty\|K\|_\infty<\infty.
\end{aligned}$$

putting all together we have

$$\int_0^t \|\left\langle \mu_s-\nu_s, \left\langle \mu_s, T^\delta J^{(e^{(t-s)\Delta}\phi)}\right\rangle\right\rangle| ds \leq \int_0^t C(\delta,k,\phi)\|\mu_s-\nu_s\|ds.$$

For the last term we have

$$\int_0^t |\left\langle \nu_s, \left\langle \mu_s-\nu_s, T^\delta J^{(e^{(t-s)\Delta}\phi)}\right\rangle\right\rangle| ds \leq C(k,\delta,\phi)\int_0^t \|\mu_s-\nu_s\|ds$$

If we combine all the inequality we get, over the sup on the test function with $\|\phi\|=1$

$$\|\mu_t-\nu_t\| \leq C(\xi,k,\sigma,T,\delta)\int_0^t \frac{\sqrt{t-s}+1}{\sqrt{t-s}}\|\mu_s-\nu_s\|ds$$

and with a modification of a standard lemma we are able to conclude that $\|\mu_t-\nu_t\|=0$. □

Corollary A.1.9. *The family $\{Q^N\}_{N\in\mathbb{N}}$ of laws of the processes $(\mu_\cdot^N,\xi_\cdot)$ weakly converge to Q where $\mu\in C([0,T],\mathcal{M}_1(\mathbb{R}^d\times\mathbb{R}_+))$.*

Proof. What we have now is that every subsequence of $\{Q^N\}_{N\in\mathbb{N}}$ admit a limit measure Q such that every (μ,ξ) realizing the law solves $\mathbb{P}-a.s.$ the weak formulation of (2.2). From the previous theorem we now that any process ν_t that solves the same identity is such that $\mu_t=\nu_t,\ \mathbb{P}-a.s.$.
So any process realizing any limiting law are $\mathbb{P}-a.s.$ equal and so they have the same law. □

A.2 Conjecture on PDE-PDE Limit: Local Interaction

Before analyzing numerically our particle system and retrieve useful insight on turbulence and coagulation formation; In this section we show formally, how we can relate the limiting equation of our particle system to the Smoluchowski Coagulation random PDE (1.1), objective of this paper.
We also conjecture the convergence of a sequence of solution ρ_t^δ of the random Smulochovski PDE, as $\delta \to 0$, in the interaction kernel for the volume.
First of all, following the result of ([3],[9],[60]), we suppose that our system admits a measure valued solution with density $\rho_t(x,v) \in C([0,T], L^2(\mathbb{R}^d \times \mathbb{R}_+)) \cap L^1(\Omega, C([0,T], L^2(\mathbb{R}^d \times \mathbb{R}_+))$.

Approximation of the Local Interaction Kernel

The rescaled interaction Kernel considered for the volume exchange between particles is of the form

$$T^\delta(x,v,y,w) := \delta^{-3} \mathbb{I}_{B_x(\delta f(v,w))}\, k(v,w),$$

where we have defined:

$$\begin{aligned} &B_x(\delta f(v,w)) := \{y \in \mathbb{R}^d \,:\, |x-y|_d \le \delta f(v,w)\}, \forall \delta, v, w \in \mathbb{R}; \\ &f(v,w) := \left(v^{1/3} + w^{1/3}\right)\left(\frac{3}{4\pi}\right)^{1/3}; \\ &k(v,w) \in C_b^0, \text{ collision coefficient.} \end{aligned}$$

Fix $d = 3$, we consider now the definition of the mean field equation in weak form, when μ_t has a density ρ_t, for a fixed ω, ϕ:

$$\begin{aligned} \langle \rho_t, \phi\rangle - \langle \rho_0, \phi\rangle = &\int_0^t \left\langle \rho_s, \frac{\varepsilon_x^2}{2}\Delta_x \phi \right\rangle ds + \int_0^t \langle \rho_s, \sigma(x,v)\cdot \nabla_x \phi\rangle\, \xi_s ds \\ &+ \int_0^t \left\langle \rho_s, \left\langle \rho_s, T^\delta J^\phi \right\rangle_{y,w} \right\rangle_{x,v} ds \end{aligned} \tag{A.2.1}$$

where the bracket are to be intend as a L^2 product. We see that the only complicated term is the one involving T^δ

$$\begin{aligned} &\left(\left\langle \rho_s, T^\delta J^\phi \right\rangle_{y,w}\right)(x,v) := \\ &= \int \delta^{-3} \mathbb{I}_{B_x(\delta f(v,w))}\, k(v,w) \\ &\left(\int \underbrace{\left[\mathbb{I}_{(v>=w)}\phi(x,v+w) + \mathbb{I}_{v<w}\phi(y,v+w) - \phi(x,v) - \phi(y,w)\right]}_{J^\phi_{x,v,y,w}} \rho\,(y,w)\, dw \right) dy \\ &= \int_{\mathbb{R}_+} \left(\delta^{-3} \int_{B_x(\delta f(v,w))} J^\phi_{x,v,y,w} \rho_t(y,w) dy \right) k(v,w) dw \end{aligned}$$

Heuristically, if ρ is regular enough in w, since ϕ is a test function and therefor regular, we can use a Lebesgue differentiation theorem, and if we take the mean of the integral over the ball as $\delta \to 0$, we have $a.e.\ x \in \mathbb{R}^d$:

$$\left((\delta f(v,w))^{-3} \int_{B_x(\delta f(v,w))} J^{\phi}_{x,v,y,w} \rho_t(y,w) dy \right) \to J^{\phi}_{x,v,w} \rho_t(x,w),\ as\ \delta \to 0,$$

$\forall\, w \in \mathbb{R}$, where

$$J^{\phi}(x,v,w) = \left[\phi(x, v+w) - \phi(x,v) - \phi(x,w) \right],$$

and so the convergence of "$T^{\delta} * \rho$" to the new kernel:

$$\begin{aligned}
&\left(\left\langle \rho_s, T^{\delta} J^{\phi} \right\rangle_{y,w} \right)(x,v) := \\
&= \int_{\mathbb{R}} (f(v,w))^3 \left((\delta f(v,w))^{-3} \int_{B_x(\delta f(v,w))} J^{\phi}_{x,v,y,w} \rho_t(y,w) dy \right) k(v,w) dw \\
&\to \int_{\mathbb{R}} f(v,w)^3\, k(v,w) J^{\phi}(x,v,w) \rho_t(x,w) dw,\ a.e. x \in \mathbb{R}^d,\ \forall\, v \in \mathbb{R}_+.
\end{aligned}$$

Resulting in the Random Smoluchowski Coagulation PDE with a turbulence field as in definition 2.2:

$$\begin{aligned}
\langle \rho_t, \phi \rangle - \langle \rho_0, \phi \rangle = &\int_0^t \left\langle \rho_s, \frac{\varepsilon_x^2}{2} \Delta_x \phi \right\rangle ds + \int_0^t \langle \rho_s, \sigma(x,v) \cdot \nabla_x \phi \rangle\, \xi_s ds \\
&+ \int_0^t \left\langle \rho_s, \left\langle \rho_s, k(v,w) (f(v,w))^3 J^{\phi}(x,v,w) \right\rangle_{x,w} \right\rangle_{x,v} ds
\end{aligned} \tag{A.2.2}$$

Conjecture: Converge to Random Smoluchowski Equation

To conclude, in this section we give a brief idea of a possible convergence of sequence of solution under some additional assumption on the regularity of the random PDE. Consider again the candidate limiting equation in weak form:

$$\begin{aligned}
\langle \rho_t, \phi \rangle - \langle \rho_0, \phi \rangle = &\int_0^t \left\langle \rho_s, \frac{\varepsilon_x^2}{2} \Delta_x \phi \right\rangle ds + \int_0^t \langle \rho_s, \sigma(x,v) \cdot \nabla_x \phi \rangle\, \xi_s ds \\
&+ \int_0^t \left\langle \rho_s, \left\langle \rho_s, k(v,w) (f(v,w))^3 J^{\phi}(x,v,w) \right\rangle_{x,w} \right\rangle_{x,v} ds
\end{aligned} \tag{A.2.3}$$

And the approximate sequence of solutions ρ_t^{δ} that solves in weak sense:

$$\begin{aligned}
\langle \rho_t, \phi \rangle - \langle \rho_0, \phi \rangle = &\int_0^t \left\langle \rho_s, \frac{\varepsilon_x^2}{2} \Delta_x \phi \right\rangle ds + \int_0^t \langle \rho_s, \sigma(x,v) \cdot \nabla_x \phi \rangle\, \xi_s ds \\
&+ \int_0^t \left\langle \rho_s, \left\langle \rho_s, T^{\delta} J^{\phi} \right\rangle_{y,w} \right\rangle_{x,v} ds
\end{aligned} \tag{A.2.4}$$

Proposition A.2.1 (Limit δ). *Let $\rho_t(x,v) \in C([0,T], L^1 \cap L^2(\mathbb{R}^d \times \mathbb{R}_+)) \cap L^1(\Omega, C([0,T], L^1 \cap L^2(\mathbb{R}^d \times \mathbb{R}_+))$ be a weak solution of (1.1). Suppose that μ_0 has density ρ_0 that satisfy hypothesis (a,b,c) as in section.A.1. Suppose also that the kernel is symmetric and $K(v,w)f(v,w)^3 \leq v^\alpha$, with $\alpha \leq 1$.*
Let $\{\rho_t^\delta\}_\delta$ solutions of the equation with kernel T^δ, then we have

$$\sup_{t\in[0,T]} \|\rho_t - \rho_t^\delta\|_{L^2(\Omega\times(0,R))} \to 0,\ as\ \delta \to 0,\ \forall\, R>0,\ \forall \Omega \subset\subset \mathbb{R},\ \mathbb{P}-a.s.$$

Proof. Let's consider a test function ϕ and the difference between $\rho_t^\delta,\ \rho_t$ in the weak formulation:

$$\begin{aligned}\left\langle \rho_t - \rho_t^\delta, \phi \right\rangle = &\int_0^t \left\langle \rho_t - \rho_s^\delta, \mathcal{U}_s(x,v)\cdot\nabla_x(\phi)\right\rangle ds + \int_0^t \left\langle \rho_t - \rho_s^\delta, \Delta_x(\phi)\right\rangle ds \\ &+ F_{x,v}^{\phi,\delta}(\rho_t^\delta) - F_{x,v}^\delta(\rho_t).\end{aligned}$$

where the non linear term are

$$\begin{aligned}F_{x,v}^\phi(\rho_t) &= \int_0^t \left\langle \rho_s, \left\langle \rho_s, T(v,w) J^{\left(e^{(t-s)A}\phi\right)}\right\rangle_x \right\rangle ds \\ F_{x,v}^{\phi,\delta}(\rho_t^\delta) &= \int_0^t \left\langle \rho_s^\delta, \left\langle \rho_s^\delta, T^\delta J_y^{\left(e^{(t-s)A}\phi\right)}\right\rangle \right\rangle ds.\end{aligned}$$

Consider now the modulus and then, term by term, $\mathbb{P}-a.s.$

$$\begin{aligned}&\int_0^t |\left\langle \rho_t - \rho_s^\delta, \mathcal{U}_s(x,v)\cdot\nabla_x(\phi)\right\rangle| ds \leq \|\xi\|_{L^\infty} \int_0^t C_{\varepsilon,T}^\phi K_\sigma \|\rho_t - \rho_s^\delta\|_2^2 ds \\ &\int_0^t |\left\langle \rho_t - \rho_s^\delta, \Delta_x(\phi)\right\rangle| ds \leq \int_0^t C_T^\phi \|\rho_t - \rho_s^\delta\|_2^2 ds\end{aligned}$$

while for the other terms we need to add an subtract to get

$$\begin{aligned}&F_{x,v}^{\phi,\delta}(\rho_t^\delta - \rho_t) - (F_{x,v}^{\phi,\delta} - F_{x,v}^\phi)(\rho_t) := \\ &= |\int_0^t \left\langle \rho_s^\delta - \rho_s, \left\langle \rho_s^\delta, T^\delta(v,w) J^{(\phi)}\right\rangle\right\rangle ds + \\ &\quad + \int_0^t \left\langle \rho_s, \left\langle \rho_s^\delta - \rho_s, T^\delta(v,w) J^{(\phi)}\right\rangle\right\rangle ds - (F_{x,v}^{\phi,\delta} - F_{x,v}^\phi)(\rho_t)| \\ &\leq \left(\sup_t \|\rho_s^\delta\|_1 + \sup_t \|\rho_s\|_1\right) \int_0^t C_{\Omega,R}^\phi \|\rho_s^\delta - \rho_s\|_2^2 ds + |(F_{x,v}^{\phi,\delta} - F_{x,v}^\phi)(\rho_t)|\end{aligned}$$

For the last term we have

$$\begin{aligned}&(F_{x,v}^{\phi,\delta} - F_{x,v}^\phi)(\rho_t) = \\ &= \int_0^t |\left\langle \rho_s, \left\langle \rho_s, T^\delta\ J^{(\phi)}\right\rangle - \left\langle \rho_s, TJ^{(\phi)}\right\rangle_x\right\rangle| ds \\ &\leq \int_0^t |\left\langle \rho_s, \int_0^R k(v,w)\left(\int_\Omega \rho_t T^\delta \tilde{J}^\phi dy - \rho_s T J^{(\phi)}\right) dw\right\rangle| ds\end{aligned}$$

$$\leq C^{\phi} \int_0^t | \left\langle \rho_s, \int_0^R k(v,w) L d^{\delta}(\rho_t T J^{\phi}) dw \right\rangle ds$$

Where

$$L d^{\delta}(\rho_t T J^{\phi}) := \left(\int_{\Omega} \rho_t T^{\delta} \tilde{J}^{\phi} dy - \rho_s T J^{(\phi)} \right) \to 0, \ in \ L^{\infty}_v L^1_x, \ as \ \delta \to 0$$

thanks to Lebesgue differentiation theorem and bound on the volume component of the density. Putting all together we have:

$$\begin{aligned} & C^{\phi} \int_0^t | \left\langle \rho_s, \int_0^R k(v,w) L d^{\delta}(\rho_t T J^{\phi}) dw \right\rangle ds \\ & \leq \int_0^t c^{\phi} M_1(v \rho_t) \sup_{w \in (0,R)} \| L d^{\delta}(\rho_t T) \| \\ & \leq c^{\phi} M_1(v \rho_0) \sup_{w \in (0,R)} \| L d^{\delta}(\rho_t T) \| ds := \int_0^t A_{\delta} C^{\phi}_{R, \rho_0, \Omega} ds \end{aligned}$$

where the last inequality follows from the bound on the microscopic kernel k. If we put all the estimate together, taking the sup over all test functions with L^2 norm equal 1, we obtain with Gronwall the following

$$\sup_t \| \rho^{\delta}_t - \rho_t \|^2_2 \leq \left(\sup_t (A_{\delta}) T \right) \exp(C^{\phi}_{R, \Omega, \rho_0}) \to 0, \ as \ \delta \to 0.$$

With this we conclude the proof. □

Bibliography

[1] J Abrahamson. “Collision rates of small particles in a vigorously turbulent fluid”. In: *Chemical Engineering Science* 30.11 (1975), pp. 1371–1379.

[2] David J. Aldous. “Deterministic and Stochastic Models for Coalescence (Aggregation and Coagulation): A Review of the Mean-Field Theory for Probabilists”. In: *Bernoulli* 5.1 (1999), pp. 3–48.

[3] Herbert Amann and Christoph Walker. “Local and global strong solutions to continuous coagulation–fragmentation equations with diffusion”. In: *Journal of Differential Equations* 218 (Nov. 2005), pp. 159–186.

[4] Francesca Anceschi and Sergio Polidoro. “A survey on the classical theory for Kolmogorov equation”. In: *arXiv: Analysis of PDEs* 75 (2019), pp. 221–258.

[5] Inés Armendáriz. “Brownian coagulation and a version of Smoluchowski’s equation on the circle”. In: *Annals of Applied Probability* 20 (Sept. 2010).

[6] Anton Arnold et al. “Sharpening of Decay Rates in Fourier Based Hypocoercivity Methods”. In: *Recent Advances in Kinetic Equations and Applications*. Ed. by Francesco Salvarani. Cham: Springer International Publishing, 2021, pp. 1–50.

[7] Orlando Ayala et al. “Effects of turbulence on the geometric collision rate of sedimenting droplets. Part 1. Results from direct numerical simulation”. In: *New Journal of Physics* 10.7 (2008), p. 075015.

[8] John M Ball and Jack Carr. “The discrete coagulation-fragmentation equations: existence, uniqueness, and density conservation”. In: *Journal of Statistical Physics* 61.1 (1990), pp. 203–234.

[9] Jacek Banasiak. “Global solutions of continuous coagulation–fragmentation equations with unbounded coefficients”. In: *Discrete & Continuous Dynamical Systems - S* 13.12 (2020), pp. 3319–3334.

[10] J Bec, M Cencini, and R Hillerbrand. “Clustering of heavy particles in random self-similar flow”. In: *Physical Review E* 75.2 (2007), p. 025301.

[11] J Bec et al. “Spatial and velocity statistics of inertial particles in turbulent flows”. In: *Journal of Physics: Conference Series*. Vol. 333. 1. IOP Publishing. 2011, p. 012003.

[12] Jérémie Bec et al. “Heavy Particle Clustering in Turbulent Flows”. In: *IUTAM Symposium on Computational Physics and New Perspectives in Turbulence*. Ed. by Yukio Kaneda. Dordrecht: Springer Netherlands, 2008, pp. 79–84.

[13] Jacob Bedrossian and Stavros Papathanasiou. “The Vlasov-Poisson and Vlasov-Poisson-Fokker-Planck systems in stochastic electromagnetic fields: local well-posedness”. In: *arXiv preprint arXiv:2211.03336* (2022).

[14] Birnstiel, T., Dullemond, C. P., and Brauer, F. “Gas- and dust evolution in protoplanetary disks”. In: *A&A* 513 (2010), A79.

[15] Joseph Boussinesq. *Essai sur la théorie des eaux courantes*. Impr. nationale, 1877.

[16] Maxime Breden, Laurent Desvillettes, and Klemens Fellner. “Smoothness of moments of the solutions of discrete coagulation equations with diffusion”. In: *Monatshefte für Mathematik* 183 (July 2017), pp. 437–463.

[17] M. Briant and E. S. Daus. “The Boltzmann equation for a multi-species mixture close to global equilibrium”. In: *Arch. Ration. Mech. Anal.* 222.3 (2016), pp. 1367–1443.

[18] J.A. Cañizo, L. Desvillettes, and K. Fellner. “Regularity and mass conservation for discrete coagulation–fragmentation equations with diffusion”. en. In: *Annales de l’I.H.P. Analyse non linéaire* 27.2 (2010), pp. 639–654.

[19] Jaehun Chun et al. “Clustering of aerosol particles in isotropic turbulence”. In: *Journal of Fluid Mechanics* 536 (2005), pp. 219–251.

[20] BJ Devenish et al. “Droplet growth in warm turbulent clouds”. In: *Quarterly Journal of the Royal Meteorological Society* 138.667 (2012), pp. 1401–1429.

[21] Zhongwang Dou et al. “Effects of Reynolds number and Stokes number on particle-pair relative velocity in isotropic turbulence: a systematic experimental study”. In: *Journal of Fluid Mechanics* 839 (2018), pp. 271–292.

[22] Dorian Dupuy, Adrien Toutant, and Françoise Bataille. “Effect of the Reynolds number on turbulence kinetic energy exchanges in flows with highly variable fluid properties”. In: *Physics of Fluids* 31.1 (2019), p. 015104.

[23] Jens Eggers and Marco A Fontelos. “The role of self-similarity in singularities of partial differential equations”. In: *Nonlinearity* 22.1 (2008), R1.

[24] S. Elghobashi and G. C. Truesdell. “Direct simulation of particle dispersion in a decaying isotropic turbulence”. In: *Journal of Fluid Mechanics* 242 (1992), pp. 655–700.

[25] Gregory Falkovich, A Fouxon, and MG Stepanov. “Acceleration of rain initiation by cloud turbulence”. In: *Nature* 419.6903 (2002), pp. 151–154.

[26] Gregory Falkovich and Alain Pumir. “Sling effect in collisions of water droplets in turbulent clouds”. In: *Journal of the Atmospheric Sciences* 64.12 (2007), pp. 4497–4505.

[27] Ennio Fedrizzi et al. “Regularity of stochastic kinetic equations”. In: (2017).

[28] Charles L. Fefferman and Antonio Sanchez-Calle. “Fundamental Solutions for Second Order Subelliptic Operators”. In: *Annals of Mathematics* 124.2 (1986), pp. 247–272.

[29] F. Flandoli, M. Gubinelli, and E. Priola. “Full well-posedness of point vortex dynamics corresponding to stochastic 2D Euler equations”. In: *Stochastic Process. Appl.* 121.7 (2011), pp. 1445–1463.

[30] F. Flandoli and R. Huang. “Coagulation dynamics under environmental noise: scaling limit to SPDE”. In: *arXiv preprint arXiv:2111.10859* (2021).

[31] F. Flandoli, R. Huang, and A. Papini. “Turbulence enhancement of raindrop formation: the role of eddy diffusion in velocity”. In: *arXiv preprint arXiv:2209.14387* (2022).

[32] Franco Flandoli, Lucio Galeati, and Dejun Luo. “Delayed blow-up by transport noise”. In: *Communications in Partial Differential Equations* 46.9 (2021), pp. 1757–1788.

[33] Franco Flandoli, Lucio Galeati, and Dejun Luo. “Eddy heat exchange at the boundary under white noise turbulence”. In: *Philosophical Transactions of the Royal Society A* 380.2219 (2022), p. 20210096.

[34] Franco Flandoli, Lucio Galeati, and Dejun Luo. “Mixing, dissipation enhancement and convergence rates for scaling limit of SPDEs with transport noise”. In: *arXiv preprint arXiv:2104.01740* (2021).

[35] Franco Flandoli, Lucio Galeati, and Dejun Luo. “Scaling limit of stochastic 2D Euler equations with transport noises to the deterministic Navier–Stokes equations”. In: *Journal of Evolution Equations* 21.1 (2021), pp. 567–600.

[36] Franco Flandoli and Ruojun Huang. “Coagulation dynamics under environmental noise: scaling limit to SPDE”. In: *ALEA, Lat. Am. J. Probab. Math. Stat* 19 (2022), pp. 1241–1292.

[37] Franco Flandoli and Ruojun Huang. “The KPP equation as a scaling limit of locally interacting Brownian particles”. In: *Journal of Differential Equations* 303 (2021), pp. 608–644.

[38] Franco Flandoli and Dejun Luo. “Convergence of transport noise to Ornstein–Uhlenbeck for 2D Euler equations under the enstrophy measure”. In: *The Annals of Probability* 48.1 (2020), pp. 264–295.

[39] Franco Flandoli and Eliseo Luongo. “The Dissipation Properties of Transport Noise”. In: *Stochastic Transport in Upper Ocean Dynamics*. Ed. by Bertrand Chapron et al. Cham: Springer International Publishing, 2023, pp. 69–85.

[40] Franco Flandoli, Silvia Morlacchi, and Andrea Papini. “Effect of Transport Noise on Kelvin-Helmholtz instability”. In: *arXiv preprint arXiv:2303.00033* (2023).

[41] Graziano Frungieri et al. “Heavy and light inertial particle aggregates in homogeneous isotropic turbulence: A study on breakup and stress statistics”. In: *Computers & Fluids* 263 (2023), p. 105944.

[42] L. Galeati. “On the convergence of stochastic transport equations to a deterministic parabolic one”. In: *Stoch. Partial Differ. Equ. Anal. Comput.* 8.4 (2020), pp. 833–868.

[43] I. M. Gamba, V. Panferov, and C. Villani. “On the Boltzmann equation for diffusively excited granular media”. In: *Comm. Math. Phys.* 246.3 (2004), pp. 503–541.

[44] Benjamin Gess and Ivan Yaroslavtsev. “Stabilization by transport noise and enhanced dissipation in the Kraichnan model”. In: *arXiv preprint arXiv:2104.03949* (2021).

[45] Wojciech W Grabowski and Lian-Ping Wang. “Growth of cloud droplets in a turbulent environment”. In: *Annual review of fluid mechanics* 45.1 (2013), pp. 293–324.

[46] A. Hammond and F. Rezakhanlou. “Kinetic limit for a system of coagulating planar Brownian particles”. In: *Journal of statistical physics* 124.2 (2006), pp. 997–1040.

[47] Alan Hammond. “Coagulation and diffusion: A probabilistic perspective on the Smoluchowski PDE”. In: *Probability Surveys* 14 (Jan. 2014).

[48] Alan Hammond and Fraydoun Rezakhanlou. “The kinetic limit of a system of coagulating Brownian particles”. In: *Archive for rational mechanics and analysis* 185.1 (2007), pp. 1–67.

[49] Matthias Hieber et al. “Global properties of generalized Ornstein–Uhlenbeck operators on Lp (RN, RN) with more than linearly growing coefficients”. In: *Journal of mathematical analysis and applications* 350.1 (2009), pp. 100–121.

[50] Lars Hörmander. “Hypoelliptic second order differential equations”. In: *Acta Mathematica* 119 (1967), pp. 147–171.

[51] Ruojun Huang. “Scaling limit for a second-order particle system with local annihilation”. In: *arXiv preprint arXiv:2205.07312* (2022).

[52] PR Jonas. “Turbulence and cloud microphysics”. In: *Atmospheric research* 40.2-4 (1996), pp. 283–306.

[53] AP Kazantsev. “Enhancement of a magnetic field by a conducting fluid”. In: *Sov. Phys. JETP* 26.5 (1968), pp. 1031–1034.

[54] Claude Kipnis and Claudio Landim. *Scaling limits of interacting particle systems*. Vol. 320. Springer Science & Business Media, 1998.

[55] A. Kolmogoroff. “Zufallige Bewegungen (Zur Theorie der Brownschen Bewegung)”. In: *Annals of Mathematics* 35 (1934), p. 116.

[56] Robert H Kraichnan. “Anomalous scaling of a randomly advected passive scalar”. In: *Physical review letters* 72.7 (1994), p. 1016.

[57] Robert H Kraichnan. “Inertial ranges in two-dimensional turbulence”. In: *The Physics of Fluids* 10.7 (1967), pp. 1417–1423.

[58] Robert H Kraichnan. “Small-scale structure of a scalar field convected by turbulence”. In: *The Physics of Fluids* 11.5 (1968), pp. 945–953.

[59] Johannes GM Kuerten and AW Vreman. “Collision frequency and radial distribution function in particle-laden turbulent channel flow”. In: *International journal of multiphase flow* 87 (2016), pp. 66–79.

[60] Philippe Laurençot and Stéphane Mischler. “The Continuous Coagulation-Fragmentation Equations with Diffusion”. In: *Arch Ration Mech Anal* 162 (Mar. 2002), pp. 45–99.

[61] Xiang-Yu Li et al. “Eulerian and Lagrangian approaches to multidimensional condensation and collection”. In: *Journal of Advances in Modeling Earth Systems* 9.2 (2017), pp. 1116–1137.

[62] Bertrand Lods. “Semigroup generation propertiesof streaming operators with noncontractive boundary conditions”. In: *Mathematical and Computer Modelling* 42.13 (2005), pp. 1441–1462.

[63] Andrew J. Majda, Ilya Timofeyev, and Eric Vanden Eijnden. “A mathematical framework for stochastic climate models”. In: *Communications on Pure and Applied Mathematics* 54.8 (2001), pp. 891–974.

[64] Bernhard Mehlig, Ville Uski, and Michael Wilkinson. “Colliding particles in highly turbulent flows”. In: *Physics of Fluids* 19.9 (2007), p. 098107.

[65] Jan Meibohm, Kristian Gustavsson, and Bernhard Mehlig. “Caustics in turbulent aerosols form along the Vieillefosse line at weak particle inertia”. In: *Phys. Rev. Fluids* 8 (2 Feb. 2023), p. 024305.

[66] G. Metafune, D. Pallara, and V. Vespri. “L^p-estimates for a class of elliptic operators with unbounded coefficients in $\mathbf{R}^N$”. In: *Houston J. Math.* 31.2 (2005), pp. 605–620.

[67] S. Mischler and B. Wennberg. “On the spatially homogeneous Boltzmann equation”. In: *Ann. Inst. H. Poincaré C Anal. Non Linéaire* 16.4 (1999), pp. 467–501.

[68] Sylvain De Moor, Luis Miguel Rodrigues, and Julien Vovelle. *Invariant measures for a stochastic Fokker-Planck equation*. 2018.

[69] Alexander Nagel, Elias M. Stein, and Stephen Wainger. “Balls and metrics defined by vector fields I: Basic properties”. In: *Acta Mathematica* 155.none (1985), pp. 103–147.

[70] James R. Norris. “Smoluchowski’s coagulation equation: uniqueness, nonuniqueness and a hydrodynamic limit for the stochastic coalescent”. In: *The Annals of Applied Probability* 9.1 (1999), pp. 78–109.

[71] D. Nualart. *The Malliavin Calculus and Related Topics*. Probability and Its Applications. Springer Berlin Heidelberg, 2006.

[72] Ormel, C. W. and Cuzzi, J. N. “Closed-form expressions for particle relative velocities induced by turbulence”. In: *A&A* 466.2 (2007), pp. 413–420.

[73] A. Papini. “Coagulation dynamics under random field: turbulence effects on rain”. In: *arXiv preprint arXiv:2111.12584* (2021).

[74] Radu Precup and Paola Rubbioni. “Stationary Solutions of Fokker-Planck Equations with Nonlinear Reaction Terms in Bounded Domains”. In: *Potential Analysis* (2022), pp. 1–19.

[75] Alain Pumir and Michael Wilkinson. “Collisional aggregation due to turbulence”. In: *Annual Review of Condensed Matter Physics* 7 (2016), pp. 141–170.

[76] Walter C Reade and Lance R Collins. “A numerical study of the particle size distribution of an aerosol undergoing turbulent coagulation”. In: *Journal of Fluid Mechanics* 415 (2000), pp. 45–64.

[77] Linda Preiss Rothschild and E. M. Stein. “Hypoelliptic differential operators and nilpotent groups”. In: *Acta Mathematica* 137.none (1976), pp. 247–320.

[78] PGF Saffman and JS Turner. “On the collision of drops in turbulent clouds”. In: *Journal of Fluid Mechanics* 1.1 (1956), pp. 16–30.

[79] Antonio Sánchez-Calle. “Fundamental solutions and geometry of the sum of squares of vector fields.” In: *Inventiones mathematicae* 78 (1984), pp. 143–160.

[80] R. A. Shaw. “Particle-turbulence interactions in atmospheric clouds”. In: *Annual Review of Fluid Mechanics* 35.1 (2003), pp. 183–227.

[81] Shin-ichiro Shima et al. “The super-droplet method for the numerical simulation of clouds and precipitation: A particle-based and probabilistic microphysics model coupled with a non-hydrostatic model”. In: *Quarterly Journal of the Royal Meteorological Society: A journal of the atmospheric sciences, applied meteorology and physical oceanography* 135.642 (2009), pp. 1307–1320.

[82] J. Simon. “Compact sets in the space $L^p(0,T;B)$”. In: *Ann. Mat. Pura Appl. (4)* 146 (1987), pp. 65–96.

[83] M. v. Smoluchowski. “Drei vortrage uber diffusion, brownsche bewegung und koagulation von kolloidteilchen”. In: *Zeitschrift fur Physik* 17 (1916), pp. 557–585.

[84] Shivshankar Sundaram and Lance R Collins. “Numerical considerations in simulating a turbulent suspension of finite-volume particles”. In: *Journal of Computational Physics* 124.2 (1996), pp. 337–350.

[85] Harold Dean Victory Jr and Brian P O’Dwyer. “On classical solutions of Vlasov-Poisson Fokker-Planck systems”. In: *Indiana University mathematics journal* (1990), pp. 105–156.

[86] C. Villani. “A review of mathematical topics in collisional kinetic theory”. In: *Handbook of mathematical fluid dynamics, Vol. I*. North-Holland, Amsterdam, 2002, pp. 71–305.

[87] Michel Voßkuhle et al. “Collision rate for suspensions at large Stokes numbers – comparing Navier–Stokes and synthetic turbulence”. In: *Journal of Turbulence* 16.1 (2015), pp. 15–25. eprint: https://doi.org/10.1080/14685248.2014.948628.

[88] Lian-Ping Wang et al. “Theoretical formulation of collision rate and collision efficiency of hydrodynamically interacting cloud droplets in turbulent atmosphere”. In: *Journal of the atmospheric sciences* 62.7 (2005), pp. 2433–2450.

[89] M Wilkinson and Bernhard Mehlig. “Caustics in turbulent aerosols”. In: *Europhysics Letters* 71.2 (2005), p. 186.

[90] Michael Wilkinson, Bernhard Mehlig, and Vlad Bezuglyy. “Caustic activation of rain showers”. In: *Physical review letters* 97.4 (2006), p. 048501.

[91] Eugene Wong and Moshe Zakai. “On the convergence of ordinary integrals to stochastic integrals”. In: *The Annals of Mathematical Statistics* 36.5 (1965), pp. 1560–1564.

[92] Mohammad Reza Yaghouti, Fraydoun Rezakhanlou, and Alan Hammond. “Coagulation, diffusion and the continuous Smoluchowski equation”. In: *Stochastic Processes and their Applications* 119.9 (2009), pp. 3042–3080.

[93] PK Yeung and SB Pope. “An algorithm for tracking fluid particles in numerical simulations of homogeneous turbulence”. In: *Journal of computational physics* 79.2 (1988), pp. 373–416.